Performance Analysis of an Urban Stormwater Best Management Practice Retrofit

Andrew Simko

Thesis submitted to the faculty of the Virginia Polytechnic Institute and State University in partial fulfillment of the requirements for the degree of

Master of Science
in
Environmental Engineering

Thomas J. Grizzard, Chair
Adil N. Godrej
Glenn E. Moglen

August 8, 2014
Manassas, Virginia

Keywords: Best management practice, Event Mean Concentration, Summation of Loads Method, Effluent Probability Method

Performance Analysis of an Urban Stormwater Best Management Practice Retrofit

Andrew Simko

ABSTRACT

Historically, the primary objective of traditional stormwater best management practices (BMPs) was to attenuate peak runoff discharges from urban areas. There has been growing demand to construct BMPs that improve stormwater runoff quality to reduce pollutant loading into downstream water bodies. A BMP located in Herndon, Virginia was retrofitted in 2009. Previously a dry detention pond, the new BMP design contains permanent wet pools as well as elements of Low Impact Development practices. A performance analysis was conducted on the retrofit to determine if the BMP was removing pollutants from stormwater runoff. Two mass-based methods were utilized for the performance analysis: the Summation of Loads Method and Effluent Probability Method. The Kaplan-Meier method and Robust Regression on ordered statistics (ROS) were used to make it possible to include censored datasets in the analysis. Analysis with the SOL method showed removal of suspended sediment, nitrogen, iron, and copper. Export of dissolved solids, phosphorus, organic carbon, and manganese was observed. The results of the Effluent Probability Method showed statistically significant reductions of sediment, iron, and copper across the entire range of monitored storm event sizes (p-value$\leq$0.05). There was no statistical difference between the influent and effluent loads of nitrogen. Negative performance of dissolved solids, phosphorus, organic carbon, and manganese were observed for the entire range of monitored storm event sizes. The results of both methods indicated that the BMP retrofit is effectively removing sediment but failing to achieve significant nutrient reductions. This may be due to the creation of anoxic conditions from the oxygen demand of the micropool sediments and microbial degradation of vegetation within the BMP. Removal of the sediment bed and harvesting of the vegetation would likely improve the performance of the BMP.

Acknowledgements

I would like to express my thanks and gratitude to my advisor Dr. Thomas J. Grizzard for his support and mentorship during my time at Virginia Tech and the Occoquan Lab. I would also like to thank Dr. Adil N. Godrej and Dr. Glenn E. Moglen for their support towards this research project and my academic development. Working for the lab and attending your classes has helped grow as an engineer.

Special thanks go to the Fairfax County Department of Public Works and Environmental Services who provided the funding for this research. I would also like to extend my gratitude to the Occoquan lab staff who were instrumental in providing the lab analysis and field work necessary for this project.

I want to thank Justin Bartlett, Paul Le Bel, Mehdy Amirkhanzadeh Barandouz, Saurav Kumar, and Francisco Cubas for their friendship. I appreciate all the help you have given me in my school work and research.

I want to thank my parents, Rob and Joyce, and my sister, Katherine. Your love and support makes it possible for me to achieve my dreams and to continue to strive for excellence.

Finally, I would like to thank my friends who have supported me throughout the years.

TABLE OF CONTENTS

List of Figures

List of Tables

1 INTRODUCTION

The Chesapeake Bay watershed is the one of the largest and most complex in the United States. It spans six states and the District of Columbia. The Chesapeake Bay serves a number of economical and recreational purposes for Virginia and Maryland, as well as for other mid-Atlantic states. The water quality of the Bay has been deteriorating due to urbanization and nonpoint source pollution as well as point sources (EPA 2010a). Undeveloped lands produce less runoff because precipitation during storm events can infiltrate into the pervious soils. During urbanization, pervious land surfaces are replaced with impervious surfaces such as roads and buildings. This results in changes to the hydrologic cycle such as increases in peak runoff flow rates, flow volumes, and pollutant exportation. Human activity in urban areas such as construction or the application of road salts can also increase the amount of pollutants that are transported during runoff. (McCuen 2005; Davis 2008).

In 2010, the United States Environmental Protection Agency (EPA) established a total maximum daily load (TMDL) for the Chesapeake Bay, the largest in the history of the agency. The TMDL encompasses the states of Delaware, Maryland, New York, Pennsylvania, Virginia, West Virginia, and the District of Columbia. It aims to restore the Chesapeake Bay by 2025 through the reduction of sediments, nitrogen, and phosphorus loads into the Bay. (Environmental Protection Agency 2010a). The TMDL sets limits of 185.9 million pounds of nitrogen, 12.5 million pounds of phosphorus, and 6.45 billion pounds of sediment as the annual maximum loads entering the bay (Environmental Protection Agency 2010a). Approximately 58% of the Commonwealth of Virginia is located within the Chesapeake Bay watershed (Wallace, Benham et al. 2012), and the state accounts for 27% of the nitrogen, 43% of the phosphorus, and 41% sediment of the total loads entering the Bay annually. Stormwater runoff has been reported to be the leading source of pollutants entering the Bay, and 33% of the nitrogen, 50% of the phosphorus, and 39% of the sediment originates from Virginia (Environmental Protection Agency 2010b).

Much of the TMDL targets nonpoint source pollution from urban stormwater runoff, which is one of the leading causes of impairments of natural water bodies in the United States (Environmental Protection Agency 1992). Stormwater management facilities such as best

management practices (BMP) and low impact development (LID) practices are being built across the country to comply with TMDLs (Li and Davis 2009; Pomeroy, Strecker et al. 2012). BMPs and LID practices improve stormwater runoff quality through physical, chemical, and biological processes, including settling, evapotranspiration, soil infiltration, media adsorption, and plant uptake (Davis and Hsieh 2004; Minton 2005; Hunt, Davis et al. 2012).

In 2009, the Fairfax County Department of Public Works and Environmental Services (DPWES) retrofitted a stormwater detention basin in Herndon, Virginia to improve stormwater runoff quality. Originally the stormwater facility served as a peak shaving dry pond for 11.17 acres of roads, residential homes, and wooded areas. The BMP now has characteristics of traditional BMP design as well as LID attributes. The retrofit design includes a series of four wet micropools separated by rip-rap weirs and sand seeps that increase storage and detention time. This project was intended to provide DPWES with valuable information to develop future retrofit projects and improve stormwater management practices.

DPWES commissioned the Virginia Tech Occoquan Watershed Monitoring Laboratory (OWML) to conduct a performance analysis of the BMP retrofit. Automated monitoring equipment was installed at the primary inlets and outlet by OWML in October, 2012. Area velocity flow modules and sensors measured instantaneous flow velocities, flow rates, and flow volumes at the primary inlets and outlet. In addition, the monitoring equipment collected flow-weighted sample aliquots during storm events. A tipping bucket rain gage was also installed to measure rainfall at the site. The sample aliquots were collected after each storm event to measure the event mean concentration of constituents such as sediment, phosphorus, nitrogen, organic carbon, and trace metals. In addition, grab samples of the micropools were collected on a regular basis to measure the water quality within the BMP system. Continuous monitoring of the BMP facility by OWML took place from October, 2012 to March, 2014. A total of 39 storm events with hydrologic and constituent data were monitored during the study period.

A performance analysis of the facility was conducted using three different methods. Comparative boxplots provided a graphical comparison of the influent, effluent, and micropool grab sample concentrations. However, this method neglects hydrologic data. Certain types of BMPs reduce pollutants through reductions in stormwater runoff from infiltration and storage. Runoff reductions are not reflected when comparing influent and effluent EMCs. In addition, all EMCs

are weighted equally regardless of storm event size. Thus, comparisons of constituent loads are a better approach to measuring BMP performance. The water quality data and hydrologic data were used to calculate pollutant loads for the constituents of concern. The Summation of Loads (SOL) method is based on a comparison of the ratio of total effluent loads and total influent loads for the entire study period. (Minton 2005; Chen, Lin et al. 2009; Geosyntec Consultants and Wright Water Engineers 2009). The Effluent Probability Method (EPM) is a nonparametric graphical approach for comparing influent and effluent datasets (Quigley, Urbonas et al. 2002; Geosyntec Consultants and Wright Water Engineers 2009). The influent and effluent constituent loads are ranked and then plotted on a probability plot. This makes it possible to compare influent and effluent loads for individual storm events and it provided a way to quickly determine how BMP performance changes as a function of storm event size.

References

Chen, C.-F., J.-Y. Lin, C.-H. Huang, W.-L. Chen and N.-L. Chueh, 2009. Performance evaluation of a full-scale natural treatment system for nonpoint source and point source pollution removal. *Environ Monit Assess* **157**:391-406.

Davis, A., 2008. Field Performance of Bioretention: Hydrology Impacts. *Journal of Hydrologic Engineering* **13**:90-95.

Davis, A. P. and C.-h. Hsieh, 2004. Evaluation of Bioretention for Treatment of Urban Storm Water Runoff. *In*: *World Water & Environmental Resources Congress 2003.* pp. 1-8.

Environmental Protection Agency, 1992. Environmental Impacts of Stormwater Discharges.

Environmental Protection Agency, 2010a. Chesapeake Bay Total Maximum Daily Load for Nitrogen, Phosphorus and Sediment, Environmental Protection Agency.

Environmental Protection Agency, 2010b. Sources of Nitrogen, Phosphorus, and Sediment to the Chesapeake Bay, Environmental Protection Agency.

Geosyntec Consultants and Wright Water Engineers, 2009. Urban stormwater BMP performance monitoring.

Hunt, W., A. Davis and R. Traver, 2012. Meeting Hydrologic and Water Quality Goals through Targeted Bioretention Design. *Journal of Environmental Engineering* **138**:698-707.

Li, H. and A. Davis, 2009. Water Quality Improvement through Reductions of Pollutant Loads Using Bioretention. *Journal of Environmental Engineering* **135**:567-576.

McCuen, R. H., 2005. *Hydrologic Analysis and Design*, Pearson Education, Inc.,

Minton, G., 2005. *Stormwater Treatment-Biological, Chemical, and Engineering Principles*, Sheridan Books, Inc.

Pomeroy, C., E. Strecker, C. Rowney, M. Leisenring, A. Poresky, L. Roesner and M. Barrett, 2012. BMP Performance Algorithms for the BMP Selection/Receiving Water Protection Toolbox. *In*: *World Environmental and Water Resources Congress 2012.* pp. 3523-3532.

Quigley, M. M., B. Urbonas and E. W. Strecker, 2002. Overview of the Urban Stormwater BMP Performance Monitoring: A Guidance Manual for Meeting the National Stormwater BMP Database Requirements. *In*: *Global Solutions for Urban Drainage.* pp. 1-14.

Wallace, C., B. Benham, G. Yagow, B. Zeckoski and K. Kline, 2012. Developing TMDLs for Local Impairments Consistent with the Regional Chesapeake Bay TMDL. *In*: *World Environmental and Water Resources Congress 2012.* pp. 3800-3810.

2 LITERATURE REVIEW

2.1 Urbanization

The process of urbanization is most often characterized by the replacement of natural land with pavement, building roofs and other less pervious surfaces. As communities and cities expand, urban uses will continue to represent an increasing fraction of the land uses globally. Urbanization has a profound effect on the hydrologic cycle, in that less rainfall is infiltrated and stored in the soil, and more is converted to surface runoff. The increase in runoff leads to increased runoff volumes, higher peak discharges, and greater runoff duration, all of which, in turn, may lead to increased flooding and channel erosion (McCuen 2005; Davis 2008). Another consequence of urbanization is that baseflow is reduced due to the decrease of groundwater recharge from infiltration (Hollis 1975).

In addition to the hydrologic effects, urbanization also has negative impacts on water quality. Pollutants that have accumulated on impervious surfaces are washed off during storm events and are more quickly discharged into nearby aquatic systems (Schueler 2001). Stormwater from urban areas may transport increased loads of sediments, oxygen demanding substances, nutrients, bacteria, and metals (Environmental Protection Agency 1992). Pollutants from stormwater discharges have also been linked to decreased fish populations and impaired aquatic community diversity (Wang, Lyons et al. 2001).

There is a growing need to reduce the impacts of urbanization. Between one-third and two-thirds of the impairments in waters of the United States are due to stormwater and other nonpoint sources (Environmental Protection Agency 1992). In a 2004 report to Congress, the EPA determined that of all the water bodies included in their study, 44% of rivers, 39% of lakes, and 29% of bays and estuaries were impaired in some way (Environmental Protection Agency 2009).

2.2 Water Quality Constituents of Interest

2.2.1 Solids and Sediments

The amount of solids in water is often used as an indicator of overall water quality. Suspended solids include sand, clays, silt, and organic particles. Solid materials can absorb sunlight which may increase the water temperature and decrease photosynthetically available radiation. The

latter may result in decreased dissolved oxygen concentrations in the water column. In addition, suspended solids may clog fish gills and the filtering systems of other aquatic life. (Burton and Pitt 2002; Environmental Protection Agency 2012c). Suspended material may also carry other constituents of concern such nutrients, metals, organic compounds and toxins. For this reason, the removals of some constituents are closely associated with solids reductions (Sansalone, Liu et al. 2002).

There are two standard methods for measuring suspended particulate matter: total suspended solids (TSS) and suspended sediment concentration (SSC). Although they are often used interchangeably, there are important differences. The EPA "shake-and-pour" method for measuring TSS requires a 100 mL aliquot sample to be shaken and poured through a filter. Once the sample is oven dried, the mass of solids left in the filter is divided by the sample volume to calculate TSS in mg/L (Environmental Protection Agency 1971). Because of the difficulty in maintain all solids in suspension when pouring an aliquot from a vessel; it is likely that the method fails to capture some larger particles. For this reason, the TSS measurement may be biased low for some of the larger particles found in stormwater. The SSC method was developed at the United States Geological Survey (USGS), and is designed to measure the particulate solids in a whole water sample, thereby including the larger particles that may be excluded from the TSS method (Clark and Sui 2008). TSS and SSC measurements have been found to be generally equivalent for particles finer than 62 μm. For particles greater than 62 μm, SSC measurements tend to be greater than TSS (Gray, Glysson et al. 2000). Although SSC gives a more accurate total suspended solids concentration, many investigators still see TSS as a viable measurement because the larger solids included in SSC are generally too heavy for stormwater to transport (Clark and Sui 2008).

The primary mechanism for removal of suspended solids is settling, and efficiency is dependent on particle size, density, water velocity, and retention time within storage (Qizhong Guo 2005). Larger and denser particles have higher terminal settling velocities, and may be removed more quickly compared to particles that are smaller and less dense. Higher removal efficiencies may be achieved through altering flow rates and increasing retention times. In stormwater management practices, this may be achieved by reducing water velocity through the use of vegetation and by lengthening flow paths (Minton 2005).

Total dissolved solids (TDS) are operationally defined as the solids that pass through a 1.5 μm laboratory filter. The nominal filter pore size that sets the size exclusion range may allow some small particulates and colloidal material to pass the filter, and therefore, may result in an overestimation of TDS. TDS is a measure both the ionic and nonionic dissolved species in water (Benjamin 2002). Species included in the TDS measurement may include nutrients, toxicants, and organic matter. Included species may also have an effect on buffering capacity, salinity, and dissolved oxygen solubility (Burton and Pitt 2002).

The water balances of the cells of aquatic organisms are also affected by the ambient water concentrations of TDS. In aquatic environments with low concentrations of TDS, water will tend to move into the cells of aquatic organisms. Conversely, if TDS concentrations are high, then the water inside cells will tend to leave the cell. This water transfer may affect the ability of an organism to maintain the proper cell density, and may cause organisms to either sink or float to water depths to which they are not adapted (Environmental Protection Agency 2012c).

TDS are principally composed of dissolved anions and cations, which in natural waters generally include, among others, sodium (Na^{+}), potassium (K^{+}), calcium (Ca^{2+}), magnesium (Mg^{2+}), chlorine (Cl^{-}), sulfate (SO_4^{2+}), silicate (SiO_3^{2-}), nitrate (NO_3^{-}), fluoride (F) and alkalinity. Alkalinity is defined as the capacity of water to resist pH change when acidic species are added. The dominate species of alkalinity in natural water systems are carbonate (CO_3^{-}) and bicarbonate (HCO_3^{-}), but other acid neutralizing species contribute to the pH buffering capacity as well. The summation of the dissolved cations and anion may be used to estimate TDS. Generally, the measured TDS value is higher than the value calculated from ionic species concentrations, because the measured TDS will likely include other ions as well (Burton and Pitt 2002; Rice, Baird et al. 2012).

Effective TDS removal may be achieved through a number of processes that principally include adsorption, precipitation, and redox reactions. Removal efficiencies have shown to be very low and there may even be increases in TDS when leaving most systems designed to treat stormwater. Little removal of is expected unless there are redox potential and pH changes within the BMP system (Burton and Pitt 2002).

2.2.2 Organic Carbon

The amount of organic matter in water is principally characterized either by measurements of oxygen demand or direct measurements of organic carbon. Biochemical oxygen demand (BOD) and chemical oxygen (COD) tests are used to estimate the oxygen consumption resulting from the degradation of organic constituents. However, these tests may also include oxygen consumption by inorganics. Total organic carbon (TOC) is a more direct approach as it only includes the target species. (Benjamin 2002; Chang, Chiang et al. 2005; Minton 2005; Rice, Baird et al. 2012). Major sources of TOC and DOC include microorganisms, terrestrial runoff sources, and from the decay and decomposition of various organic matter (Wetzel 1983; Burton and Pitt 2002).

Degradation of TOC may cause decreases of ambient water dissolved oxygen (DO), and negative correlations have been reported between DO and TOC (Deng and Zhang ; Lee and Schwartz 2004). The theoretical COD:TOC is 2.66, but in practice, the true ratio is usually higher because not all oxygen consuming species contributing to COD are organic. Taken together, the two measurements can provide a better understanding of the organic content of a water (Garlepy 2002; Rice, Baird et al. 2012).

2.2.3 Nutrients

Phosphorus and nitrogen are essential nutrients for all living organisms. Both phosphorus and nitrogen are components of deoxyribonucleic acid (DNA) and ribonucleic acid (RNA). Phosphorus is also a component of cell membranes and adenosine triphosphate (ATP). Nitrogen is a component of amino acids, proteins and enzymes. Despite their importance to all life, at high concentrations, nitrogen and phosphorus may cause water quality problems by spurring the rapid growth of invasive plants and algae. Algal blooms can reduce light penetration, consume dissolved oxygen in the absence of sunlight, and stress or cause the death of other aquatic species. The microbial degradation of algal blooms also consumes oxygen, and may result in zones of hypoxia in the water column. Some algae produce toxins that are toxic to both aquatic and terrestrial life. There are many reported instances of health issues occurring in people that come into contact with them. (Wetzel 1983; Environmental Protection Agency 2012a). Because of the oversupply of nutrients entering the Chesapeake Bay, the US EPA established a TMDL which aims to reduce phosphorus and nitrogen loads to levels that can limit the growth of algae.

Phosphorus is often the limiting nutrient in aquatic systems because it is the least abundant, relative to need, of the major nutrients. It comes from many sources, including soils, atmospheric deposition, living and dead organisms, motor vehicles, and both industrial and domestic wastewaters. Orthophosphate (PO_4^{3-}) is the principal phosphorus-containing species in fresh water systems. (Wetzel 1983; Ma, Lenhart et al. 2011). In aquatic environments, phosphorus exists in both organic and inorganic forms. Plants uptake the inorganic phosphorus and convert it to organic phosphorus. Organic phosphorus is released into the water system from plant die-off and animal excretion. Bacterial decomposition coverts the organic phosphorus back into its inorganic forms and the cycle repeats (Wetzel 1983; Minton 2005).

Methods to remove phosphorus include precipitation with metal complexes in soil media, settling with suspended material, and uptake by vegetation (Erickson, Gulliver et al. 2007; Ng, Eheart et al. 2007; Vacca and Wadzuk 2012). Phosphorus interactions with iron are important to the removal of phosphorus through media adsorption and settling. Under aerobic conditions (high dissolved oxygen concentrations, high redox potential), insoluble iron reacts with phosphorus to form ferric hydroxide/phosphate complexes. These complexes can then settle along with the suspended sediment material. Maintaining aerobic conditions is necessary to prevent phosphorus from being released back into the water. Under anoxic conditions (low concentrations of free oxygen but relatively high oxidation-reduction potential), iron is reduced to its soluble form and phosphorus is released (Wetzel 1983; Minton 2005). In addition, media type and soil composition are important factors. At $pH < 6$, phosphorus precipitation is dominated by iron and aluminum. At $pH > 6$, precipitation with calcium is more prevalent. The ability of the media to retain and adsorb phosphorus will diminish as phosphorus loads increase. (Minton 2005; Erickson, Gulliver et al. 2007; Lucas and Greenway 2011; Ma, Lenhart et al. 2011). Vegetation may also aid in the removal of phosphorus by providing phosphorus uptake and extending the sorption capacity of the media. Plant harvesting and removal of saturated soil layers are the only ways to permanently remove phosphorus from the water system (Minton 2005; Geosyntec Consultants and Wright Water Engineers 2009).

Nitrogen (N) exists in water in many forms, including dissolved gaseous N_2, organically bound N in proteins and amino acids, ammonia (NH_3^+), ammonium (NH_4^+), nitrite (NO_2^-), and nitrate (NO_3^-). Common sources of nitrogen in the urban environment include fertilizers, fossil fuels,

wastewater, atmospheric deposition, and leaching from soils (Wetzel 1983; Environmental Protection Agency 2012b). In stormwater, most nitrogen is organically bound with smaller concentrations in the ammonia form (Minton 2005).

The aquatic nitrogen cycle is very important for the removal of nitrogen. Nitrogen forms and transformations are largely dependent on the redox potential of the aquatic system. Microbial processes convert organic nitrogen to ammonia/ammonium in a process called ammonification. Ammonification can occur in either the aerobic or anoxic soil surface layers. Assimilation is the conversion of ammonia nitrogen to organic nitrogen by plant uptake. In aerobic environments, the ammonia nitrogen forms can then be microbially converted to oxidized nitrogen forms through nitrification. Under anoxic conditions, oxidized nitrogen is converted to N_2 gas by denitrifying bacteria. The release of N_2 to the atmosphere is one method of removing nitrogen permanently from the water system (Wetzel 1983; Minton 2005; Grady, Daigger et al. 2011). Stormwater facilities can be engineered to form anoxic zones to promote denitrification. Anoxia can also occur from the degradation of organic matter located within the water system (Hunt, Jarrett et al. 2006; Li and Davis 2009)

Volatilization and fixation are two other processes that should be considered when discussing nitrogen removal. Ammonium can volatilize to ammonia gas and be released into the atmosphere. Volatilization occurs in environments with high pH and temperature conditions that favor evaporation. The rate of volatilization increases with increasing wind speed and decreasing water depths (Minton 2005). Fixation is the process of converting N_2 gas to nitrate. Certain types of bacteria and aquatic plant life are capable of fixation (Wetzel 1983; Minton 2005). The two most common fixing bacteria species are *Azotobacter* and *Clostridium pasteuianum*. Nearly all photosynthetic bacteria are also capable of fixation (Wetzel 1983). Fixation typically only occurs under extreme anaerobic conditions and a deficiency of other forms of nitrogen (Wetzel 1983; Minton 2005).

2.2.4 Trace Metals

Trace metals are cationic micronutrients that are vital for life. They aid in endocrine system activity, oxygen transport, and enzyme functions (Jensen 2003). Very low concentrations of trace metals can lead to nutrient deficiency (Driscoll, Otton et al. 1994; Jensen 2003). Trace metals

include chromium, copper, aluminum, iron, manganese and more (Driscoll, Otton et al. 1994; Karlsson and Viklander 2008). In the aquatic environment, the principal sources of trace metals are fertilizers, soils, plants, and animal excretions. Even though trace metals are vital for life, they are generally only beneficial at small concentrations. High concentrations of many trace metals may be toxic and cause detrimental health effects to a range of living systems (Driscoll, Otton et al. 1994).

The concentration and transport of trace metals in aquatic systems are generally correlated with sediments. Some metals such as copper, lead, and zinc interact with suspended particles, sediments, and soils through adsorption and desorption. Trace metals may also associate with ligands to form solid complexes (Driscoll, Otton et al. 1994). Concentrations of trace metals tend to be much higher in suspended solids and in the top few centimeters of soil compared to concentrations found in the water column (United States Geological Survey 1985; Karlsson and Viklander 2008).

Trace metals associated with small particles present a major challenge if removal is required. Smaller particles may remain suspended in water for longer periods of time, with the result that such particles, and associated trace metals will travel greater distances and require longer detention times to be removed by sedimentation (Characklis and Wiesner 1997). Sorbing trace metals to soil media may be one effective treatment technique. However, there is the possibility that the trace metals can remobilize and re-enter the water column due to changes in pH or redox potential (Driscoll, Otton et al. 1994; Karlsson and Viklander 2008; Young, Chen et al. 2010). Organic matter may also be used to form strong complexes with trace metals to help prevent remobilization from the soil (Igloria, Hathhorn et al. 1997; Young, Chen et al. 2010).

2.3 Best Management Practices

2.3.1 Introduction

To reduce the hydrologic and environmental effects of urbanization, a range of techniques, known collectively as best management practices (BMPs), have been developed. Stormwater BMPs can either be non-structural (such as developing landscaping and construction practices that reduce pollutant washoff) or structural (such as ponds or bioretention systems). For the purposes of this study, a BMP will be referred to as an engineered and constructed facility

designed to remove pollutants from stormwater and attenuate stormwater runoff. Common types of BMPs include, but are not limited to, detention basins, retention basins, bioretention systems, wetlands, and green roofs. Since the promulgation of the Chesapeake Bay TMDL, local governments have been heavily investing in the construction, retrofit, and monitoring of stormwater BMPs. These facilities are a primary method of mitigating stormwater runoff and nonpoint source pollution in urban areas. Selection of a BMP type will depend on the local meteorology, land use, construction and maintenance costs, and water quality constituents of interest.

2.3.2 Detention Basins

Detention basins (dry ponds) are among the most widely used BMPs (McCuen 2005). Their primary purpose is to reduce the peak design storm discharge to pre-development values, but they may also be designed to reduce total runoff volume, and have also been enhanced to achieve pollutant removal (Water Environment Federation and American Society of Civil Engineers 1998; Woo 2008). The design of a detention basin is dependent on the watershed area and the storm return period it is designed to control. Most basins are designed around the 2-, 10-, 25-, 50-, and 100-year storm events (Water Environment Federation and American Society of Civil Engineers 1998; McCuen 2005). Designing for a specific storm event may have the unintended consequence of providing undercontrol or overcontrol for other storm events. A detention basin outlet designed to control the 2-yr storm event may overcontrol the 100-yr storm event so that the 100-yr post-development discharge is actually less than the 100-yr predevelopment discharge. Likewise, an outlet designed to control the 100-yr storm may allow the 2-yr post-development discharge to be greater than the predevelopment 2-yr discharge. This has led to many detention basins having two-stage riser outlets so that multiple design storms can be adequately controlled (McCuen 2005).

Historically, detention basins were only designed to address the issue of peak storm discharge, but runoff volume reduction and groundwater recharge are emerging as important factors in improving in hydrologic performance (Emerson and Traver 2008). In recent years, extended detention basins have been built to provide the dual functions of reduction of runoff peaks and removal of pollutants. Extended detention basins have greater storage volume and longer detention times compared to standard detention basins, and allow for infiltration of water into the

soil media and the settling of suspended sediment. It has been recommended that extended detention basins be 20% larger than standard basins to allow for increased detention times for particle settling (Water Environment Federation and American Society of Civil Engineers 1998).

There is debate about the effectiveness of detention basins in reducing peak discharges. Detention basins located near the outlet of a watershed may possibly increase the peak runoff by delaying the time to peak of downstream runoff. This may cause the peak upstream discharge to occur at the same time as the downstream peak, thereby leading to an overall increase in peak watershed discharge (Emerson, Welty et al. 2005; McCuen 2005). Most detention basins are designed to control the 2-yr, 10-yr and 50-yr events. However, the design events account for only a small fraction of the overall rainfall in a year, so detention basins may not properly attenuate peak discharges for the majority of rainfall events (Emerson, Welty et al. 2005).

With regards to water quality benefits, studies have shown that detention basins have lower efficiency removals compared to other BMPs. BMPs with permanent pools more effectively support biological processes that reduce nutrient concentrations (Woo 2008; Poresky, Jones et al. 2011). Detention basins have also been shown to have little effect on bacteria in stormwater (Poresky, Jones et al. 2011).

2.3.3 Retention Basins

Unlike detention basins, retention basins (wet ponds) maintain a permanent pool between storm events. Retention basins are a design refinement that has more emphasis on water quality than water quantity. The permanent pool increases the detention time for physical, chemical and biological removal processes to take place (Water Environment Federation and American Society of Civil Engineers 1998; Woo 2008). Because water remains in the pond until it is displaced by the next storm event, there is increased time for sediments to settle and biological processes to achieve enhanced removal of nutrients (Water Environment Federation and American Society of Civil Engineers 1998).

Algae and aquatic plants that require permanent pools can play a significant role in the uptake of nutrients. Retention basins may also achieve high removal rates of sediment and nutrients if properly designed and maintained (Water Environment Federation and American Society of Civil Engineers 1998).

Pond depth should be sufficient to prevent sediments from resuspending as a result of hydrodynamic mixing at the sediment-water interface, and also to keep algal growth to a minimum. Ponds should also be shallow enough to support the aerobic conditions needed for nutrient removal and to reduce the occurrence of thermal stratification (Water Environment Federation and American Society of Civil Engineers 1998; Minton 2005). Photosynthetic processes are also dependent on the water depth. A mean depth between 3 to 10 feet will allow for algal photosynthesis to take place (Water Environment Federation and American Society of Civil Engineers 1998).

The volume of the pool may not be an important factor. Permanent pools that are larger than the volume of the design stormwater event have been shown to have little effect on several effluent pollutant concentrations such as phosphorus, nitrogen, and metals. Permanent pools volume should be designed so that the settling and biological process can effectively take place. Designing pool volumes that larger than required will not improve performance (Barrett 2004).

The benefits of building retentions basins instead of detention basins come at a price. Retention basins require two to seven times the volume of an extended detention basin, and require more land and excavation. Total construction costs of a retention basin can be 50 to 150% greater than the construction of a detention basin (Water Environment Federation and American Society of Civil Engineers 1998). Operation and maintenance costs are also much higher compared to other BMPs. For example, in California, over \$450 per m^3 are required in annual O&M costs. Other BMPs have annual O&M costs below \$100 per m^3. In addition to costs, a survey showed that retention basins are among the most difficult for workers to maintain (Buechter, Linkous et al. 2012).

2.3.4 Wetlands

A wetland is a saturated land area that can support vegetation. Wetlands remain saturated even when there are extended periods with no rainfall (Water Environment Federation and American Society of Civil Engineers 1998; Minton 2005). Stormwater wetlands are designed to treat smaller storm events through the provision of extended detention times and contact with vegetation (Traver 2001).

Increasing the stormwater contact time with the wetland area is the primary goal when designing a wetland (Water Environment Federation and American Society of Civil Engineers 1998). This can be achieved by designing an appropriate shape for the wetland. The length-to-width ratio of the wetland surface should not be less than 3. Much like other BMPs, the inlets and outlets should be located at opposite ends of the wetland in order to maximize the flow path length (Water Environment Federation and American Society of Civil Engineers 1998). Meandering flow paths may also be constructed to further increase the detention time (Traver 2002).

Wetland vegetation remove nutrients from the stormwater flow, and also add to the aesthetics values of the wetland. Plants should be selected for their ability to survive in wide ranges of water levels, temperatures, salt content and pH (Water Environment Federation and American Society of Civil Engineers 1998; Minton 2005). Plant harvesting may be necessary to permanently remove nutrients from the system. However, harvesting may disturb the soil and cause resuspension of sediments (Water Environment Federation and American Society of Civil Engineers 1998). A survey by Buechter, Linkous (2012) of BMP operation and maintenance practices revealed that wetlands are among the most expensive and most difficult BMPs to properly maintain.

2.3.5 Bioretention

Biorentention cells mainly utilize infiltration and vegetation practices to treat stormwater runoff (Davis and He 2009). Common bioretention cells are rain gardens and small basins. Compared to larger stormwater facilities, Bioretention cells are designed to treat smaller land areas such as parking lots, or small developed catchments. Bioretention cells are typically composed of a porous media layer, vegetation, and a mulch top layer (Davis and Hsieh 2004). Ponding areas are installed to retain stormwater, and provide for increased time for filtration, media sorption, and sedimentation (Hsieh and Davis 2005; Davis and He 2009).

Infiltration, evapotranspiration, and plant uptake processes within bioretention cells can attenuate stormwater runoff (James and Dymond 2012). These processes promote groundwater recharge and reduce runoff volume. Bioretention cells require shallow depths which may hinder the ability to reduce peak runoff (Hunt, Davis et al. 2012). It may be necessary to pair bioretention cells with other BMPs to achieve pre-development peak runoff (James and Dymond 2012).

Selecting an appropriate soil is vital to the performance of a bioretention cell. Soil selection is dependent on soil infiltration rates, stability, and the pollutants a soil is capable of removing (Horst, Welker et al. 2011). Typically, bioretention cells are composed of porous media with a high hydraulic conductivity (Hsieh and Davis 2005). Removal of pollutants through soil filtration is both a physical and chemical process. As water infiltrates into the media, larger particles cannot pass through the smaller pores. The trapped particles remain in the soil until they are removed the by chemical and/or biological processes, or are mobilized by subsequent influent water (Clark and Pitt 2011). Pollutants may be expected to react and sorb differently with various soil types. In selecting a soil, consideration should be given both to the permeability and the chemical properties needed to achieve best removal efficiencies (Hsieh and Davis 2005). The soil media should be regularly maintained to prevent the pores from being clogged (Hunt and Brown 2011).

Vegetation within the cell can help aid in the treatment process through pollutant uptake and evapotranspiration. Plants have little impact on the reduction of sediments but are significant for nutrient reduction. Plant growth also helps maintain soil permeability and porosity (Li and Davis 2009). Recently, grass cover has been considered for inclusion in bioretention for aesthetic purposes and ease of maintenance. Grass cells showed high removal of nutrients and performed favorably compared to other types of vegetation (Smith and Hunt 2007; Passeport, Hunt et al. 2009).

2.4 Considerations for BMP Performance

2.4.1 First Flush

First flush is the term used to describe the phenomenon where the greatest mass of a given pollutant is washed off at the beginning of a runoff event. However, there has yet to be a definitive definition on what to consider first flush. It has been defined it as a percentage of the total rainfall (Minton 2005), but others consider it to be runoff resulting from the first 0.5 to 1 inches of runoff (Ahlfeld and Minihane 2004; Woo 2008). For the removal of constituents which exhibit the first flush effect, it has been recommended that BMP basins be designed to completely contain the first flush volume (Woo 2008).

The first flush phenomenon is more likely to occur in small watersheds with short times of travel. Larger watersheds will generally have longer times of travel, and early runoff may mix with later runoff before reaching the BMP (Khan, Lau et al. 2004; Minton 2005). Watersheds that experience high rainfall intensities are also more likely to experience the first flush effect (Minton 2005). Rainfall intensity, however, may also vary throughout a storm event; some regions experience higher intensities at the beginning of a storm whereas others experience the highest intensities in the middle of storm duration (Ahlfeld and Minihane 2004).

Even though there is no universal definition for first flush, the criteria for first flush should be clearly defined for a given BMP. Local meteorology and watershed characteristics play a role in defining first flush. First flush depth, location of a BMP, and return period all should be identified in any analysis of first flush (Ahlfeld and Minihane 2004; Woo 2008). Failure to clearly define first flush in an analysis can lead to improper BMP design and improper monitoring methods in performance assessments.

2.4.2 Media Type and Design

Selecting the appropriate media type and depth are necessary for achieving pollutant removal objectives in BMPs that utilize soil infiltration. The mass of pollutant removal is dependent on a number of physical and chemical properties of the media. Particulate associated pollutant reductions are achieved through infiltration by trapping in media pore spaces. The permanent removal of pollutants is achieved by subsequent chemical interactions between particulate and soluble species and the soil media. Thus, selection of the proper filtration media should be based on an assessment of the chemistry between the soil and the constituents of interest. (Clark and Pitt 2011).

The ease with which water travels through porous media is measured by the hydraulic conductivity. Hydraulic conductivity is both dependent on the soil and water characteristics. The hydraulic conductivity can be calculated with the equation below (Emerson and Traver 2008):

$$K = k\, x \frac{pg}{\mu}$$

Where K = hydraulic conductivity (cm/s), k = intrinsic permeability (cm^2), p = density of water (g/cm^3), g = acceleration due to gravity (cm/s^2), and μ = dynamic viscosity of water (g/cm-s). A

soil with high hydraulic conductivity should be used to infiltrate large volumes of water (Hsieh and Davis 2005), however, there may be disadvantages to having too high a value of K. Porosity and intrinsic permeability determine how quickly water will travel through the soil, and pollutants carried in water traveling at higher velocities will have shorter contact times with the media. Because sufficient contact time is required for the media to react with stormwater-borned pollutants (Clark and Pitt 2011; Hunt and Brown 2011), it is necessary to maintain a balance between having a high enough hydraulic conductivity to allow for high volumes of infiltration while also giving enough contact time for pollutants to be removed.

The removal of pollutants through chemical processes is dependent on the interactions with a given soil type. Important soil properties include cation exchange capacity (CEC), anion exchange capacity (AEC), and pH. In addition, the oxidation-reduction (Redox) potential of a system can dictate chemical reactions between the soils and constituents. CEC is the amount of cations that can be adsorbed by the soil, and AEC is the amount of anions that can be adsorbed the soil. Both these properties vary with pH. Some pollutants may be affected by redox reactions while traveling through the media. Pollutants at lower valence states are typically more soluble and are more easily retained and removed (Burton and Pitt 2002; Minton 2005; Clark and Pitt 2011).

Installing media is one of the most expensive parts in the construction of an infiltration based system so shallower depths are preferred to reduce costs (Brown and Hunt 2011). Most regulations require a minimum media depth of 2.5 ft and some require a minimum depth of 4 ft when shrubs or trees are planted (O'Neill and Davis 2009). Deeper media installations are capable of infiltrating larger volumes of water and supporting the plant life necessary for nutrient removal (O'Neill and Davis 2009; Brown and Hunt 2011). A study by Li and Davis (2008) found that most trace metal capture occurred in the top 10-20 cm layers of the soil, and they concluded that there were diminishing returns with increasing media depth.

2.4.3 Seasonal Variation

Season dependent variables may alter the performance of a BMP, including those related to the hydrologic cycle and the characteristics of water. Wet seasons experience more frequent and intense rainfall events. Climate and temperature changes also affect plant growth and aquatic

chemistry (Helsel and Hirch 2002; Emerson and Traver 2008; Roseen, Ballestero et al. 2009). Therefore, monitoring programs designed to characterize BMP performance should be conducted throughout the year.

Infiltration systems can experience lower performance during cold seasons. This is attributed to the freezing of the filter media (Wildey, Houle et al. 2006). Frost can penetrate and clog the pores of the media. Frozen media pores can increase the hydrologic lag time (Roseen, Ballestero et al. 2009). However, in some studies it was shown that frost penetration had little impact on infiltration performance. This was attributed to defrosting of the media from rainfall and snow melt. (Wildey, Houle et al. 2006; Roseen, Ballestero et al. 2009).

The physical properties of water also change with temperature. Water becomes more viscous as temperature decreases, and while changes in viscosity are often neglected in storm water practices, they may have profound effects on media infiltration. As shown in the equation in the previous section, hydraulic conductivity is dependent not only the properties of the soil but also the viscosity and density of the water. The viscosity of the water is nearly halved in the temperature range from 0 - 38°C which may result in reduced infiltration during cold period (Emerson and Traver 2008).

2.4.4 Construction and Maintenance

Construction can often deviate from design plans, and may result in poorer performance of BMPs (Woodworth and Hirschman 2010). Soil compaction from construction practices can significantly reduce infiltration rates (Pitt, Chen et al. 2008; Sileshi, Clark et al. 2012). Brown and Hunt (2010) conducted a study that compared rake and scoop soil excavation techniques for BMP construction. The rake method scarified the soil surface while the scoop method smeared and compressed the soil. The results showed that rake method produced greater infiltration rates because the soil was not compacted. The study also showed that excavation during wet conditions reduced infiltration rates so it was recommended that excavation should not occur after a rainfall event.

BMPs do not retain their maximum efficiencies throughout their lifespan and must be properly maintained on a regular time schedule. Over time, the pores in the filter media can be filled and reduce further infiltration. Removing the clogged soil layer once a year can increase the

infiltration rate by a factor of ten and double the amount of surface storage volume (Hunt and Brown 2011). The soil can also become saturated with pollutants and begin leaching those pollutants back into the water (Baker, Treese et al. 2010).

Vegetation also must be properly maintained. During the construction of a BMP, fertilizer is sometimes added to stimulate initial plant growth. Nutrients from the fertilizer can leach out, and result in poor nutrient removal during the initial months after construction (Hunt and Brown 2011). Vegetation can also degrade overtime because of weather, erosion, competition with other plant life, and failure to adapt to the local environment (Buechter, Linkous et al. 2012). When vegetation dies off, it will release nutrients removed back into the water system. Harvesting and re-planting of vegetation may be necessary to maintain BMP performance (Struck, Nietch et al. 2004; Li and Davis 2008; Davis, Hunt et al. 2009; Geosyntec Consultants and Wright Water Engineers 2009)

2.5 Measuring BMP Performance

2.5.1 Pollutant Concentrations and Loads

Water quality is often measured through the comparison of constituent concentrations to a regulatory criterion or standard. Regulatory agencies establish concentration limits of pollutants that can be harmful to human health, aquatic life, etc. When conducting a BMP performance study, the constituent concentrations coming in and out of the BMP need to be known. Concentrations can vary over the course of a storm event and with seasonal changes. The event mean concentration (EMC) is a flow-weighted concentration that is representative of the entire flow volume for individual storm events. The efficiency ratio, which is the ratio of the influent and effluent EMCs, is a common method for measuring BMP pollutant removal performance (Geosyntec Consultants and Wright Water Engineers 2009), but it is only applicable when there is conservation of flow mass between the influent and effluent.

Simple comparisons of influent and effluents concentrations alone for analysis can be misleading and give an inaccurate picture of the true performance of a BMP. Some BMPs can reduce pollutants through reductions in water volume from storage, infiltration, and evapotranspiration. These reductions are not reflected when hydrologic data are not included. Concentrations can be higher at the outlets for BMPs that significantly reduce water volume. Some pollutant removal

techniques are dependent on the concentrations coming into the BMP. If concentrations are low at the inlet, then there may not be a drastic change in concentrations at the outlet. (Geosyntec Consultants and Wright Water Engineers 2009).

A more appropriate method is to compare the influent and effluent pollutant loads. Pollutant loads are products of the EMCs and the total flow volume. By comparing the pollutant loads at the inlet and the outlet, the total mass of pollutants removed by the BMP can be calculated. This will give a more accurate representation on how well a BMP is removing pollutants from the water system (Kayhanian, Roseen et al. 2009; Li and Davis 2009; Pomeroy, Strecker et al. 2012). Determining the absolute pollutant loads is also more important than concentrations in the determining how much pollution is entering the downstream waters. The TDML program uses pollutant loads to establish guidelines for pollutant reductions. (Geosyntec Consultants and Wright Water Engineers 2009).

2.5.2 Effluent Probability Method

The Effluent Probability Method is a nonparametric graphical comparison of the influent and effluent pollutant EMCs or loads. Before any EPM graphical representations are made, two initial steps should be conducted:

- A test for distributional adherence must be performed to determine the best transformation to be applied to the inflow and outflow EMCs or loads;
- A statistical test must be performed to determine if observed differences between influent and effluent EMCs or loads are statistically significant (Geosyntec Consultants and Wright Water Engineers 2009; Kayhanian, Roseen et al. 2009).

If significant difference is established, then influent and effluent datasets can be plotted, typically with a standard parallel probability plot. The Effluent Probability Method provides a simple and clear approach to determine the BMP performance for individual storm events (Strecker, Quigley et al. 2001; Chen, Lin et al. 2009; Geosyntec Consultants and Wright Water Engineers 2009).

2.5.3 Summation of Loads

The Summation of Loads (SOL) method for evaluating BMP performance uses the ratio of the sum of the effluent loads over the sum of the influent loads (Minton 2005; Chen, Lin et al. 2009; Geosyntec Consultants and Wright Water Engineers 2009):

$$SOL = 1 - \frac{sum\ of\ the\ outlet\ loads}{sum\ of\ the\ inlet\ loads}$$

There are several assumptions to be made when using the SOL method:

- Removal of pollutants over the entire time period of the analysis is most important;
- Monitored storm events represent the entire pollutant load over the analyzed time period;
- Storm events that were not measured are assumed to have ratio of inlet to outlet loads that are similar to monitored storm events.

The SOL value is the fraction of the constituent remaining. To express the performance number as a fraction removed, the SOL value is then subtracted from unity. A percent reduction value can then be calculated as the product of the SOL value and one hundred. The SOL method should also be supplemented with appropriate statistical tests to determine if the difference between the inlet loads and outlet loads are statistically significant. The SOL method is convenient because it provides a single percent reduction value to compare with other BMPs or studies. However, it is not recommended that the SOL method be used as a stand-alone method of measuring BMP performance, because results may be dominated by larger storm events and performance for individual storm event sizes is not discernable with the method (Strecker, Quigley et al. 2001; Geosyntec Consultants and Wright Water Engineers 2009).

2.6 Censored Data

Censored data may result from the occurrence of values that are below or above an analytical or measurement reporting limit. Reporting limits vary depending on monitoring methods, equipment, and laboratory tests used. In environmental datasets, censored data are typically low-level concentrations (left-censored). The true value is only known be between 0 and the reporting limit, but the measuring methods are too imprecise to give a single value. Although censored data may seem inconsequential, ignoring the data can cause the analytical statistics to be biased.

Censored data should be including in any analysis and reporting to more accurately represent the conditions of the monitoring site (Helsel and Hirch 2002; Geosyntec Consultants and Wright Water Engineers 2009; Helsel 2012).

Simple substitution approaches have been used to replace censored values with a constant value. The values used are typically zero, half the detection limit, or the detection limit itself. Simple substitution is not based on any mathematical or theoretical basis, or knowledge of the underlying distribution, so it should be avoided. The measures of central tendency (e.g., mean or median) tend to be biased either high or low when simple substitution is used. If simple substitution must be used, then using half the detection is the only suitable option to lessen bias (Helsel and Hirch 2002; Geosyntec Consultants and Wright Water Engineers 2009). Helsel (2012) recommends three alternative approaches for including censored data: (1) use nonparametric methods after censoring at the highest reporting limit; (2) use maximum likelihood estimation; (3) and using nonparametric survival analysis procedures.

Distribution methods assume that the censored data follow a particular distribution, such as a lognormal distribution (Helsel and Hirch 2002; Geosyntec Consultants and Wright Water Engineers 2009). Summary statistics are estimated to best match the observed data and the percentage of data below the detection limit. Two common distribution methods are the maximum likelihood estimator method (MLE) and probability plotting. Both methods may have biased estimates when the data do not exactly match the assumed distribution. If a lognormal distribution is assumed, MLE can provide a good estimate of the percentiles of environmental data distribution, but it has difficulty estimating the mean and standard deviation. This is due to the mean and standard deviation being very sensitive to the largest observed values in a normal distribution and because there is a transformation bias when estimating the mean and standard deviation (Helsel and Hirch 2002; Helsel 2012).

Robust methods use both the observed data above the reporting limit and values below the reporting limit to calculate estimations of summary statistics. The first step is to determine a distribution that best fits the data above the detection limit by either using MLE or probability plot procedures. Values below the detection limit can then be extrapolated using the distribution of the uncensored data. Robust methods are not sensitive to the largest values and do not have a transformation bias (Helsel and Hirch 2002). Two types of robust methods include regression

ordered on statistics (ROS) and Kaplan-Meir (K-M). Using ROS, values above and below the detection limit are ranked independently. The uncensored values are plotted on a probability plot and a regression equation is calculated to best fit the data. This regression equation is then used along with the plotting of positions of the uncensored data to estimate values below the detection limit. The K-M method is also a ranked-based method that estimates survival probabilities. The survival probability is the probability that a data point will be below the next incremental concentration. Originally this method was developed for right-censored data sets but it has been adapted for left-censored data. The data are "flipped" by subtracting the observed value from an assigned value that is greater than the maximum (Geosyntec Consultants and Wright Water Engineers 2009).

It is recommended that either distributional MLE or robust probability plot procedures be used to estimate values below the detection limit. Simple substitution should not be used in order to minimize estimation errors (Helsel and Hirch 2002). The K-M method is the most robust method but cannot be used when censored data account for over 50% of the dataset, and it typically estimates high mean values. ROS is the preferred robust method since is fairly accurate, simple to use, and does not require a large sample size (Geosyntec Consultants and Wright Water Engineers 2009).

2.7 Parametric and Nonparametric Tests

In pollutant reduction assessments in BMPs, it is essential to determine whether differences in datasets are statistically significant. This is especially important when comparing the influent and effluent pollution loads and concentrations. The first step is determining whether the untransformed data fit a specific statistical distribution. A distribution can be determined by either using graphical means or by using a goodness-of-fit test such as the chi-square test; Kolmogorov-Smirnov (K-S) test; the modified Lilliefors test; the Shapiro-Wilk test; or the probability plot correlation coefficient (PPCC) test. Environmental data are typically positively skewed so the distribution is often lognormal. Parameters of the distribution can then be calculated using the method of moments; the method of maximum likelihood; or the method of L-moments (Helsel and Hirch 2002; Geosyntec Consultants and Wright Water Engineers 2009).

In water resources, data rarely follow a well-defined statistical distribution. Nonparametric statistics are rank-based and do not require the data to follow a particular distribution. Nonparametric statistics are resistant to the effects of extreme values since the rank-based systems are not dependent on the magnitude of the data. Statistics on pollutant concentrations tend to be skewed because of extreme values and outliers. When computing summary statistics for EMC datasets, calculating the mean value may not be appropriate since it is greatly affected by extreme values. In nonparametric statistics, the data are ranked and median value is determined where half the data are below and half the data are above. Using the median to represent the central tendency of EMC datasets may be a better approach since it is not affected by the magnitude of the data or skewed by outliers (Geosyntec Consultants and Wright Water Engineers 2009).

2.8 Hypothesis Tests

To employ hypothesis testing, the scale of the data must be determined and the objective of the test must be established. Hypothesis tests can be either parametric or nonparametric. As discussed earlier, parametric tests assume the data the follow a particular distribution. Nonparametric tests do not assume an underlying distribution for the data, and are rank-based systems. It must also be established if the test will be comparing paired data tests, two independent data sets, more than two independent data sets or more than two dependent data sets.

Once an appropriate test has been selected, the null and alternate hypotheses must be established. The null hypothesis (H_0) is what is being assumed to be true. The alternate hypothesis (H_1) is assumed to be true if evidence shows that the null hypothesis is likely false. In BMP performance analysis, the null hypothesis is typically assumes that the BMP is providing treatment and the BMP is not providing treatment is the alternate hypothesis. Most tests in water resources are two-sided tests where evidence either positive or negative causes the null hypothesis to be rejected (Helsel and Hirch 2002).

The probability of incorrectly rejecting null hypothesis is the significance level (α-value). It is standard practice to set a value of 0.05 (5%) for α, but other values may be used. A type I error is when the null hypothesis is incorrectly rejected when it is actually true. A Type II error (β) is

failing to reject the null hypothesis when it is actually false. To avoid the possibility of having a Type II error, the sample size n can be increased or a test procedure with the greatest power can be used (Helsel and Hirch 2002).

Once the α-value has been established, it must be decided whether or not to reject the null hypothesis while avoiding either the Type I error or Type II error. This can be accomplished by determining a p-value. The p-value can be used to decide whether or not to reject the null hypothesis. The p-value is the probability of obtaining a computed test statistic when the null hypothesis is true. The smaller the p-value, the less likely the observed test statistic will be observed when the null hypothesis is true. Low p-values serve as evidence to reject the null hypothesis. If the p-value is less than the α-value, then the null hypothesis is rejected. A p-value that is greater than the α-value does not serve as proof that the null hypothesis is true. The null hypothesis is never accepted to be true and only assumed to be true since there is not sufficient evidence to prove it false (Helsel and Hirch 2002).

2.9 Graphical Presentation

Interpreting statistical data through just numbers and tables can be difficult. Graphical presentations are an effective way to quickly and easily present statistical data to an audience. However, graphs should be simple to interpret and clearly show important concepts and conclusions from the results. Selecting an appropriate graph is dependent the types of data that is being presented and what type of conclusions the audience should see (Helsel and Hirch 2002).

2.9.1 Histograms

Histograms represent data through a series of bars. Each bar or bin represents a category or certain range of values. The height of each bar is the number of values that fall within that range. Histograms are common and be very useful in determining the shape, symmetry, or skew of the data. The major downside to using histograms is that the bars are dependent on number of categories that are being presented (Helsel and Hirch 2002; Geosyntec Consultants and Wright Water Engineers 2009)

2.9.2 Scatter Plots

Scatter plots are used to compare paired data sets. Two or more data sets can be plotted against each other along a common independent variable. Basic scatters plots can be used to perform a preliminary analysis of the data and observe any possible trends. If a more thorough analysis is needed, the standard structure of scatter plots can be used to create other statistical plots such as quantile plots and probability plots (Geosyntec Consultants and Wright Water Engineers 2009).

2.9.3 Hydrographs

A hydrograph is a common representation in water resources studies, and shows flow rate (discharge) versus time. Hydrographs display much useful information including: peak discharges, time to peak, duration of discharge, and lag time between rainfall and runoff. The integration of a hydrograph gives the total volume of water that has passed during that time period (McCuen 2005). This integration is vital in determining the total runoff and total pollutant load during a storm event (Geosyntec Consultants and Wright Water Engineers 2009). Hydrographs are often paired with hyetographs which show the distribution of rainfall over time. By graphing the discharge and rainfall on the same time scale, it is possible to see how changes in rainfall alter the runoff. Since many BMPs are designed to reduce water volume and peak discharges, it is beneficial to plot the influent and effluent hydrographs on common time axes (McCuen 2005).

2.9.4 Quantile and Probability Plots

Quantile plots clearly illustrate the median value, and some key components of the data distribution. Unlike histograms, there is no need to create arbitrary categories of data and all the data are represented on the graph. Quantile plots that compare two sets of data are known as Q-Q plots. To create a quantile plot, the data must first be ranked from smallest to largest. The smallest data receives a rank of 1 and the highest receives a rank of n, where n is the total number of data points. The dependent variable on the y-axis is the plotting position. There are a number of methods to calculate plotting position such as the Wiebull and Cunnane methods. However, common variable is plotting position formulas are the rank (i) and number of data points (n). Once the plotting positions are calculated, they can be plotted against the dependent variable. A quantile plot is a cumulative distribution function (cdf) where the y-axis is the

probability of i/n being less than or equal to the observation (Helsel and Hirch 2002; Geosyntec Consultants and Wright Water Engineers 2009).

Unlike quantile plots which show the cdf, probability plots present the actual data against the quantiles of a specific probability distribution. Probability plots are useful in determining if the data follows a particular distribution such as the normal or log-normal distribution. If the data points generally follow the theoretical straight line, then the data likely follows that particular distribution. Other goodness-of-fit tests such as the K-S test and the chi-squared test should be performed to supplement the findings from the probability plots (Geosyntec Consultants and Wright Water Engineers 2009).

2.9.5 Box Plots

Box plots are used to summarize the distribution of data. A box plot is composed of two boxes, two lines, and possible outlying data points. The lower box displays the range from the 1st quartile (Q1) to the 2nd quartile (median). The upper box displays the range from the median to the 3rd quartile. The total height (Q3-Q1) of the two boxes is the interquartile range (IRQ). A line extends from each box. The lower line extends from the 1st quartile to Q1-1.5IQR. The upper line extends from the 3rd quartile to Q3+1.5IQR. Outliers are represented with asterisks or other point symbols. Two or more box plots can be plotted together for easy comparison. In environmental engineering, often the concentrations or pollutant loads of the influent and effluent are plotted against each other to determine whether or not treatment is occurring within the BMP (Helsel and Hirch 2002; Geosyntec Consultants and Wright Water Engineers 2009).

References

Ahlfeld, D. and M. Minihane, 2004. Storm Flow from First-Flush Precipitation in Stormwater Design. *Journal of Irrigation and Drainage Engineering* **130**:269-276.

Baker, K. H., D. P. Treese and S. E. Clark, 2010. Nutrient Leaching from Disturbed Soil Horizons. *In*: *World Environmental and Water Resources Congress 2010.* pp. 2927-2938.

Barrett, M. E., 2004. Retention Pond Performance: Examples from the International Stormwater BMP Database. *In*: *Critical Transitions in Water and Environmental Resources Management.* pp. 1-10.

Benjamin, M. M., 2002. *Water Chemistry*, McGraw-Hill,

Brown, R. and W. Hunt, 2010. Impacts of Construction Activity on Bioretention Performance. *Journal of Hydrologic Engineering* **15**:386-394.

Brown, R. and W. Hunt, 2011. Impacts of Media Depth on Effluent Water Quality and Hydrologic Performance of Undersized Bioretention Cells. *Journal of Irrigation and Drainage Engineering* **137**:132-143.

Buechter, M. T., B. W. Linkous and K. M. Flynn, 2012. Operation and Maintenance Assessment for Structural Stormwater BMPs. *In*: *World Environmental and Water Resources Congress 2012.* pp. 3662-3673.

Burton, A. and R. E. Pitt, 2002. *Stormwater Effects Handbook,* Lewis Publishers.

Chang, E., P. Chiang, Y. Lin and H. Tsai, 2005. Evaluation of Source Water Quality Standards for Total Coliforms, TOC, and COD in Taiwan. *Practice Periodical of Hazardous, Toxic, and Radioactive Waste Management* **9**:193-203.

Characklis, G. W. and M. R. Wiesner, 1997. Particles, Metals, and Water Quality in Runoff from Large Urban Watershed. *Journal of Environmental Engineering* **123**:753-759.

Chen, C.-F., J.-Y. Lin, C.-H. Huang, W.-L. Chen and N.-L. Chueh, 2009. Performance evaluation of a full-scale natural treatment system for nonpoint source and point source pollution removal. *Environ Monit Assess* **157**:391-406.

Clark, S. E. and R. Pitt, 2011. Filtered Metals Control in Stormwater Using Engineered Media. *In*: *World Environmental and Water Resources Congress 2011.* pp. 415-427.

Clark, S. E. and C. Y. S. Sui, 2008. Measuring Solids Concentration in Stormwater Runoff: Comparison of Analytical Methods. *Environmental Science Technology* **42**:511-516.

Davis, A., 2008. Field Performance of Bioretention: Hydrology Impacts. *Journal of Hydrologic Engineering* **13**:90-95.

Davis, A., W. Hunt, R. Traver and M. Clar, 2009. Bioretention Technology: Overview of Current Practice and Future Needs. *Journal of Environmental Engineering* **135**:109-117.

Davis, A. P. and Z. He, 2009. Unit Process Modeling of Stormwater Flow and Pollutant Sorption in a Bioretention Cell. *In*: *World Environmental and Water Resources Congress 2009.* pp. 1-9.

Davis, A. P. and C.-h. Hsieh, 2004. Evaluation of Bioretention for Treatment of Urban Storm Water Runoff. *In*: *World Water & Environmental Resources Congress 2003.* pp. 1-8.

Deng, Z.-Q. and Z. Zhang, Dissolved Oxygen Impairment and BMP Effectiveness in Mermentau River Basin. *In*: *World Environmental and Water Resources Congress 2010.* pp. 3952-3960.

Driscoll, C. T., J. K. Otton and A. Iverfeldt, 1994. Trace Metals Speciation and Cycling. *Biogeochemistry of Small Catchments: A Tool for Environmental Research*.

Emerson, C. and R. Traver, 2008. Multiyear and Seasonal Variation of Infiltration from Storm-Water Best Management Practices. *Journal of Irrigation and Drainage Engineering* **134**:598-605.

Emerson, C., C. Welty and R. Traver, 2005. Watershed-Scale Evaluation of a System of Storm Water Detention Basins. *Journal of Hydrologic Engineering* **10**:237-242.

Environmental Protection Agency, 1971. Residue, Non-Filterable (Gravimetric, Dried at 103-105°C), Environmental Protection Agency.

Environmental Protection Agency, 1992. Environmental Impacts of Stormwater Discharges.

Environmental Protection Agency, 2009. National Water Quality Inventory: Report to Congress-2004 Reporting Cycle.

Environmental Protection Agency, 2012a. National Nutrient Strategy.

Environmental Protection Agency, 2012b. Sources and Solutions: Stormwater.

Environmental Protection Agency, 2012c. Total Solids.

Erickson, A., J. Gulliver and P. Weiss, 2007. Enhanced Sand Filtration for Storm Water Phosphorus Removal. *Journal of Environmental Engineering* **133**:485-497.

Garlepy, D., 2002. TOC and BOD5 Correlations for Biodegradable Organic Matter in the Pulp and Paper Industry. *In*: *TAPPI Environmental Conference.*

Geosyntec Consultants and Wright Water Engineers, 2009. Urban stormwater BMP performance monitoring.

Grady, C. P. L., G. T. Daigger, N. G. Love and C. D. M. Filipe, 2011. *Biological Wastewater Treatment*, IWA Publishing.

Gray, J. R., D. Glysson, L. M. Turcios and G. E. Schqarz, 2000. Comparability of Suspended-Sediment Concentration and Total Suspended Solids Data, United States Geological Survey.

Helsel, D. R., 2012. *Statistis for Censored Environmental Data Using Minitab and R*,

Helsel, D. R. and R. M. Hirch, 2002. Statistical Methods in Water Resources United States Geological Survey.

Hollis, G. E., 1975. The Effect of Urbanization on Floods of Different Recurrence Interval. *Water Resources Research* **2**:431-435.

Horst, M., A. Welker and R. Traver, 2011. Multiyear Performance of a Pervious Concrete Infiltration Basin BMP. *Journal of Irrigation and Drainage Engineering* **137**:352-358.

Hsieh, C.-h. and A. P. Davis, 2005. Evaluation and Optimization of Bioretention Media for Treatment of Urban Storm Water Runoff. *Journal of Environmental Engineering* **131**:1521-1530.

Hunt, W., A. Davis and R. Traver, 2012. Meeting Hydrologic and Water Quality Goals through Targeted Bioretention Design. *Journal of Environmental Engineering* **138**:698-707.

Hunt, W., A. Jarrett, J. Smith and L. Sharkey, 2006. Evaluating Bioretention Hydrology and Nutrient Removal at Three Field Sites in North Carolina. *Journal of Irrigation and Drainage Engineering* **132**:600-608.

Hunt, W. F. and R. A. Brown, 2011. Evaluating Media Depth, Surface Storage Volume, and Presence of an Internal Water Storage Zone on Four Sets of Bioretention Cells in North Carolina. *In*: *World Environmental and Water Resources Congress 2011.* pp. 405-414.

Igloria, R., W. Hathhorn and D. Yonge, 1997. NOM and Trace Metal Attenuation During Storm-Water Infiltration. *Journal of Hydrologic Engineering* **2**:120-127.

James, M. and R. Dymond, 2012. Bioretention Hydrologic Performance in an Urban Stormwater Network. *Journal of Hydrologic Engineering* **17**:431-436.

Jensen, J. N., 2003. *A Problem-Solving Approach to Aquatic Chemistry*. 111 River Street, Hoboken, NJ 07230, John Wiley and Sons, Inc. ,

Karlsson, K. and M. Viklander, 2008. Trace Metal Composition in Water and Sediment from Catch Basins. *Journal of Environmental Engineering* **134**:870-878.

Kayhanian, M., R. Roseen, J. Lenhart and G. Williams, 2009. Potential Data Analysis Methodology to Evaluate the Performance of Manufactured BMPs. *In*: *World Environmental and Water Resources Congress 2009.* pp. 1-10.

Khan, S., S.-L. Lau, S. Ha, L.-H. Kim, M. Kayhanian, Y.-X. Li, M. K. Stenstrom and J.-S. Ma, 2004. First Flush Phenomena for Highways: How It Can Be Meaningfully Defined. *In*: *Global Solutions for Urban Drainage.* pp. 1-11.

Lee, S. and F. W. Schwartz, 2004. Storm-Induced DOC Loading from an Urban Parking Lot. *In*: *Bridging the Gap.* pp. 1-11.

Li, H. and A. Davis, 2009. Water Quality Improvement through Reductions of Pollutant Loads Using Bioretention. *Journal of Environmental Engineering* **135**:567-576.

Li, H. and A. P. Davis, 2008. Heavy Metal Capture and Accumulation in Bioretention Media. *Environmental Science Technology* **42**.

Lucas, W. and M. Greenway, 2011. Phosphorus Retention by Bioretention Mesocosms Using Media Formulated for Phosphorus Sorption: Response to Accelerated Loads. *Journal of Irrigation and Drainage Engineering* **137**:144-153.

Ma, J., J. Lenhart and K. Tracy, 2011. Orthophosphate Adsorption Equilibrium and Breakthrough on Filtration Media for Storm-Water Runoff Treatment. *Journal of Irrigation and Drainage Engineering* **137**:244-250.

McCuen, R. H., 2005. *Hydrologic Analysis and Design*, Pearson Education, Inc.,

Minton, G., 2005. *Stormwater Treatment-Biological, Chemical, and Engineering Principles*, Sheridan Books, Inc.,

Ng, T. L., J. W. Eheart and X. Hu, 2007. Discharge Trading Programs Based on Constructed Wetlands for Nutrient Trading. *In*: *World Environmental and Water Resources Congress 2007.* pp. 1-8.

O'Neill, S. W. and A. P. Davis, 2009. Analysis of Bioretention Media Specifications and Relationships to Overall Performance. *In*: *World Environmental and Water Resources Congress 2009.* pp. 1-9.

Passeport, E., W. Hunt, D. Line, R. Smith and R. Brown, 2009. Field Study of the Ability of Two Grassed Bioretention Cells to Reduce Storm-Water Runoff Pollution. *Journal of Irrigation and Drainage Engineering* **135**:505-510.

Pitt, R., S. Chen, S. Clark, J. Swenson and C. Ong, 2008. Compaction's Impacts on Urban Storm-Water Infiltration. *Journal of Irrigation and Drainage Engineering* **134**:652-658.

Pomeroy, C., E. Strecker, C. Rowney, M. Leisenring, A. Poresky, L. Roesner and M. Barrett, 2012. BMP Performance Algorithms for the BMP Selection/Receiving Water Protection Toolbox. *In*: *World Environmental and Water Resources Congress 2012.* pp. 3523-3532.

Poresky, A., J. Jones, M. Leisenring, A. Earles and J. Clary, 2011. BMP Performance Analysis Results for the International Stormwater BMP Database. *In*: *World Environmental and Water Resources Congress 2011.* pp. 441-449.

Qizhong Guo, P. E., Ph.D., 2005. Development of Adjustment and Scaling Factors for Measured Suspended Solids Removal Performance of Stormwater Hydrodynamic Treatment Devices. *In*: *Impacts of Global Climate Change.* pp. 1-10.

Rice, E. W., R. B. Baird, A. D. Eaton and L. S. Clesceri, 2012. *Standard Methods For the Examination of Water and Wastewater*, American Public Health Assocation, American Water Works Association, Water Environment Federation,

Roseen, R., T. Ballestero, J. Houle, P. Avellaneda, J. Briggs, G. Fowler and R. Wildey, 2009. Seasonal Performance Variations for Storm-Water Management Systems in Cold Climate Conditions. *Journal of Environmental Engineering* **135**:128-137.

Sansalone, J., D. Liu and I. Donald Glenn, 2002. Influence of Chemistry, Hydrology and Suspended Solids on Partitioning of Heavy Metals to Particles - Considerations for In-Situ Control of Urban Stormwater Quality. *In*: *Global Solutions for Urban Drainage.* pp. 1-14.

Schueler, T., 2001. The Importance of Imperviousness. *Watershed Protection Techniques* **1**:100-111.

Sileshi, R., S. Clark and R. Pitt, 2012. Assessing the Impact of Soil Media Characteristics on Stormwater Bioinfiltration Device Performance. *In*: *World Environmental and Water Resources Congress 2012.* pp. 3505-3516.

Smith, R. A. and W. F. Hunt, 2007. Pollutant Removal in Bioretention Cells with Grass Cover. *In*: *World Environmental and Water Resources Congress 2007.* pp. 1-11.

Strecker, E., M. Quigley, B. Urbonas, J. Jones and J. Clary, 2001. Determining Urban Storm Water BMP Effectiveness. *Journal of Water Resources Planning and Management* **127**:144-149.

Struck, S., C. Nietch and M. Borst, 2004. Constructed Wetlands vs. Retention Pond BMPs: Mesocosm Studies for Improved Pollutant Management in Urban Stormwater Treatment. *In*: *Critical Transitions in Water and Environmental Resources Management.* pp. 1-13.

Traver, R. G., 2001. Routing through a Wetlands Best Management Practice—A Validation. *In*: *Bridging the Gap.* pp. 1-8.

Traver, R. G., 2002. Comparison of Routing Techniques in a Stormwater Wetlands BMP. *In*: *Global Solutions for Urban Drainage.* pp. 1-9.

United States Geological Survey, 1985. A Primer on Trace Metal-Sediment Chemistry, U. S. G. Survey (U. S. G. Survey)U. S. G. Surveys). 604 South Pickett, Alexandria, VA 223044.

Vacca, K. and B. Wadzuk, 2012. An Analysis of Soluble Reactive Phosphorus Removal Mechanisms in Surface-Flow Constructed Stormwater Wetlands. *In*: *World Environmental and Water Resources Congress 2012.* pp. 3475-3483.

Wang, L., J. Lyons and P. Kanehl, 2001. Impacts of Urbanization on Steam Habitat and Fish Across Spatial Scales. *Environmental Management* **28**:255-266.

Water Environment Federation and American Society of Civil Engineers, 1998. *Urban Runoff Quality Management*. 601 Wythe Street, Alexandria, VA 223144-1994.

Wetzel, R. G., 1983. *Limnology*, Saunders College Publishing, ISBN 0-03-057913-9

Wildey, R., J. J. Houle, R. M. Roseen, T. P. Ballestero, P. Avelleneda and J. Briggs, 2006. An Examination of Cold Climate Performance of Low Impact Development Stormwater BMPs in a Northern Climate. *In*: *Current Practices in Cold Regions Engineering.* pp. 1-13.

Woo, M. H., 2008. Design Criteria for the Water Quality Volume of Stormwater Ponds. *In*: *World Environmental and Water Resources Congress 2008.* pp. 1-10.

Woodworth, L. and D. J. Hirschman, 2010. Design, Construction, and Maintenance of LID Practices: Results from a Field Assessment in Virginia's James River Watershed. *In*: *Low Impact Development 2010.* pp. 1075-1088.

Young, C. B., X. Chen, J. Saadi and E. Peltier, 2010. Metal Sequestration and Remobilization in Bioretention Media. *In*: *World Environmental and Water Resources Congress 2010.* pp. 3028-3037.

3 MANUSCRIPT I: "PERFORMANCE ANALYSIS OF AN URBAN STORMWATER BEST MANAGEMENT PRACTICE RETROFIT USING THE SUMMATION OF LOADS AND EFFLUENT PROBABILITY METHODS"

3.1 Abstract

Historically, the primary objective of traditional stormwater best management practices (BMPs) has been to attenuate stormwater peak runoff. In recent years, however, there has been growing demand to install BMPs that improve stormwater runoff quality. A BMP located in Herndon, Virginia was retrofitted by the Fairfax County Department of Public Works and Environmental Services in 2009. Previously a dry detention pond, the new BMP design contains permanent micropools as well as other elements of Low Impact Development (LID) practices. A 1.5 year long performance assessment was conducted on the retrofit to determine the pollutant removal performance from stormwater runoff. Two mass-based methods were utilized for the performance analysis: the Summation of Loads (SOL) Method and the Effluent Probability Method (EPM). The Kaplan-Meier (KM) method and Robust Regression on Ordered Statistics (ROS) were used so that censored datasets might be included in the analysis. The SOL method showed removal of suspended sediment, nitrogen, iron, and copper, but exports of dissolved solids, phosphorus, organic carbon, and manganese. The results of the EPM showed statistically significant reductions of sediment, iron, and copper across the entire range of monitored storm events. No significant difference was observed between the influent and effluent loads of nitrogen and iron. Export of dissolved solids, phosphorus, organic carbon, and manganese was determined for the entire range of monitored storm events. The results of both methods indicate that the BMP retrofit was effectively removing sediment, but failing in its primary goal of achieving significant nutrient reductions. This may have been due to the oxygen demand of micropool sediments and microbial degradation of vegetation within the BMP which facilitated the release of sediment-bound pollutants under anoxic conditions. Removal of the sediment bed and harvesting vegetation may improve the performance of the BMP.

3.2 Introduction

3.2.1 Urbanization and Nonpoint Pollution

The process of urbanization replaces previously pervious land such as forests and pastures with impervious surfaces such as roads, buildings, sidewalks, and parking lots. This change has a profound effect on the hydrologic cycle. Urbanized watersheds exhibit increased runoff flow rates and volumes compared to their pre-development conditions (McCuen 2005; Davis 2008; Hawkins, Ward et al. 2009). In addition, nonpoint source pollution from urban stormwater runoff is one of the leading causes of impairment of natural water bodies in the United States (EPA 1992).

Nonpoint source pollution from urban development has contributed to the deterioration of water quality in the Chesapeake Bay, a major estuary on the east coast of the United States. The Chesapeake Bay watershed encompasses six states and the District of Columbia, and water quality within the Bay has been in decline for many decades (EPA 2010a). In an effort to restore the system, the US Environmental Protection Agency (EPA) established a total maximum daily load (TMDL) for the Chesapeake Bay in 2010, and it is the largest TMDL program in the history of the agency. The TMDL sets annual limits of 185.9 million pounds of nitrogen, 12.5 million pounds of phosphorus, and 6.45 billion pounds of sediment entering the bay, and requires each state in the watershed to contribute to meeting the limits (EPA 2010a). Virginia accounts for 27% of the nitrogen, 43% of the phosphorus, and 41% of the sediment loads entering the Bay annually (EPA 2010b).

Reduction of nonpoint source pollution from urban stormwater runoff is a major goal of the TMDL program. Most traditional stormwater best management practice (BMP) facilities only address the hydrologic component of watershed management by attenuating peak flow rates produced during storm events. Recently, there has been a shift to develop BMPs that can also improve stormwater runoff quality by employing physical, chemical, and biological processes to reduce pollutant concentrations and loads. (Davis and Hsieh 2004; Minton 2005; Davis 2007; Hunt, Davis et al. 2012; Pomeroy, Strecker et al. 2012) .

3.2.2 Cinnamon Oaks Best Management Practice Retrofit Monitoring Project

The Cinnamon Oaks best management practice is located in Herndon, Virginia at the intersection of Ashburton Avenue and Saffron Drive. The facility serves a total drainage area of 11.2 acres that include roads, residential homes, and grass-wooded areas. The catchment area also includes conventional curb and gutter, sidewalks, and a piped stormwater drainage system. Originally a peak shaving dry pond, the Fairfax County of Public Works and Environmental Services (DPWES) retrofitted the facility in 2009 to create a stormwater treatment system that combines some aspects of LID practices with traditional best management practices. The retrofit BMP contains four separate micropools, sand seeps, and rip-rap weirs that are designed to reduce stormwater runoff volume and increase detention time. The primary goals of the retrofit design are the reductions of sediments, phosphorus, and nitrogen.

DPWES commissioned the Virginia Tech Occoquan Watershed Monitoring Laboratory (OWML) of the Via Department of Civil and Environmental Engineering to conduct a performance assessment of the BMP retrofit. Automated monitoring equipment was installed at the primary inlets and outlet in October, 2012. The automated equipment was installed to measure rainfall and stormwater flows, and to construct flow-weighted composite samples during storm events. The composite samples were retrieved after each storm event, and analyzed to provide information on the event mean concentration (EMC) of constituents of interest, including sediment, phosphorus, nitrogen, organic carbon, and trace metals. In addition, grab samples of the micropools were collected on a regular basis to characterize water quality within the BMP system. Continuous monitoring of the BMP facility by OWML took place from October, 2012 to March, 2014. A total of 39 storm events with both hydrologic and constituent data were monitored during the study period.

The performance analysis was conducted using three different methods. Comparative boxplots provided a graphical comparison of the influent and effluent EMCs and micropool instantaneous concentrations. While this method provided some insights into EMC changes through the facility, and also allowed comparison to concentrations in the micropools, it did not allow assessment of the effects of the system hydrology. Comparisons of constituent loads on a mass basis were taken as a better approach for overall characterization of BMP performance. Flow and EMC data were used to calculate pollutant loads for the constituents of concern. The Summation

of Loads (SOL) method was used to compute a percent reduction value for the removal of each constituent for all paired storm events monitored during the study period. The Effluent Probability Method (EPM) is a graphical approach that allows for influent and effluent comparisons to be made over the entire range of storm event sizes, and was used to provide insights on the effect of storm size on performance. The SOL method and EPM plots were supported by the generalized Wilcoxon test which determined if the influent and effluent loads were statistically different. (Helsel and Hirch 2002; Geosyntec Consultants and Wright Water Engineers 2009; Helsel 2012)

3.3 Methods

3.3.1 Site Description

Figure 3-1 shows an aerial view of the Cinnamon Oaks BMP. There are two primary inlets to the retrofitted pond. The west inlet, which had a study designation of CO20, is a 24-inch reinforced concrete pipe (RCP). The east inlet, which had a study designation of CO30, is a 27-inch RCP. Both inlets were part of the original dry pond. CO20 serves a total drainage area of 3.0 acres that includes Ashburton Avenue, portions of West Ox Road, Saffron Drive, and residential lots along Ashburton Avenue. CO30 serves a drainage area of 5.5 acres that includes Tarragon Court, portions of Saffron Drive, and the majority of the associated residential lots. The remaining catchment area is the direct drainage of grassed and wooded areas around the pond and the pond area itself, with a total area of 2.7 acres. The pond outlet is a 24-inch RCP that is located on the southwest side adjacent to Ashburton Avenue and has a study designation of CO10. Stormwater leaving the pond at the outlet structure flows under Ashburton Avenue and eventually to a nearby stream.

The pond retrofit design included a number of features to improve stormwater runoff water quality. Four internal micropools were constructed, and were assigned designations of CO40, CO50, CO60, and CO70 for the study. CO70 is located on the west side of the facility and receives drainage from the CO20 inlet. CO60 is located on the east side and receives drainage from the CO30 inlet and from CO70. CO60 drains into CO50. CO40 is located on the west side and receives drainage from CO50.When the water level in CO40 reaches the elevation of the outlet structure weir at CO10, stormwater begins to flow from the facility. A schematic of the flow path is shown in Figure 3-2. The micropools are separated by natural material weirs

composed of rip-rap and sand. Stormwater can move between ponds either by slowly seeping through the weirs or overtopping them during larger storm events. Due to the serpentine nature of the flow path through the pond, there is increased retention time to promote settling of particulate matter, and infiltration into the sub-soils. The micropools have maintained a free water pool for the length of the study to date.

Other characteristics include a series of four sand seeps separated with rock weirs located between CO30 and CO60. The weirs reduce the flow velocity and create mini pools to allow for infiltration. Drainage from CO20 flows through a concrete channel before discharging into CO70. Throughout the study period, there was a thriving mix of vegetation both within and around the micropools that included trees, shrubs, and herbaceous rooted plants.

Figure 3-1. Aerial view of the Cinnamon Oaks urban detention basin post-retrofit (Google Maps, 2011). Used under fair use 2014.

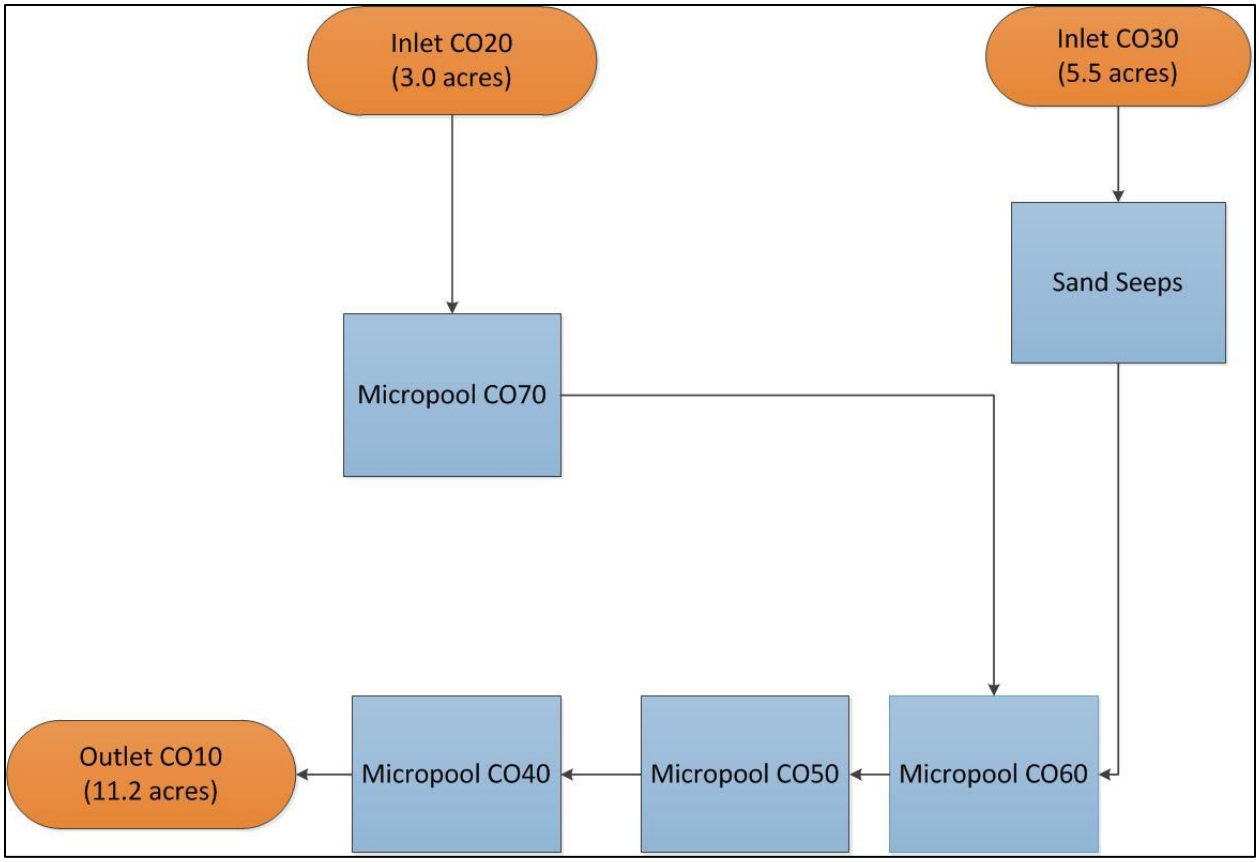

Figure 3-2. Flow schematic for Cinnamon Oaks site.

3.3.2 Instrumentation

3.3.2.1 Instrument Description

Instrumentation Specialties Company (ISCO) Model 2150 area velocity (AV) flow modules and sensors (Teledyne ISCO 2012a) and ISCO Glacier transportable samplers (Teledyne ISCO 2012b) were selected for installation at CO10, CO20, and CO30. Each monitoring station was designed to measure flow and to facilitate the collection of flow-weighted storm samples. The AV flow module included a sensor that was affixed to the invert of the stormwater conduit at each station. The sensor had an internal pressure transducer to measure static head of water inside the pipe and a pair of ultrasonic transducers to measure average water velocity in the conduit cross section. Using the conduit geometry, mean velocity, and depth of flow, instantaneous discharge was calculated as a product of the average velocity and wetted cross section area. Velocity, flow rate, and flow volume were calculated in one minute intervals and stored in flash memory at each station. Telecommunications access was provided via an onboard cellular modem, and enabled remote data acquisition.

The ISCO Glacier transportable sampler retrieved flow-weighted composite samples of stormwater flow at each of the instrumented stations. The AV modules were programmed to initiate sample collection at a pre-determined increments of total flow. When the samplers were activated, intakes installed at the invert of each station transported a 200 mL aliquot of stormwater to a storage vessel located in the sampler. Each sampler had storage capacity of 20 L and could take up to 76 samples before requiring a reset. The samplers maintained a refrigerated environment at 4°C until the samples were retrieved and transported to the laboratory for further analysis.

A tipping bucket rain gage was installed near the CO10 station and integrated with the flow metering system. The rain gage had a measurement sensitivity of 0.01 inches of rain, and a maximum intensity sensing capacity of 4 inches/hour. The precipitation data were stored (and retrieved) in the data logging system at CO10.

The instruments were sited in fiberglass shelters located at each station. The shelters were fastened to temporary wooden structures anchored to the ground. Conduits were installed between the shelters and the stormwater conveyance system at each site to allow sample intake hoses and sensor wiring to be protected from the elements. Three deep-cycle 12-volt marine batteries were wired in parallel at each site to provide adequate electrical power for flow metering, data logging, and to operate the refrigerated sampler. Solar panels on the roof of each housing provided additional power to the equipment.

3.3.2.2 Instrument Verification

Obtaining accurate hydrologic data is important to any stormwater BMP study. Since pollutant loads are calculated as the product of the EMCs and the runoff volumes, there needs to be confidence in the data provided by the flow-monitoring equipment. Poorly calibrated monitoring equipment may underestimate or overestimate the runoff volumes. This may result in pollutant removal efficiency calculations that are not truly representative of the actual BMP performance. To provide context for the precipitation data from the local rain gage, the Cinnamon Oaks data were compared to rainfall data from a National Weather Service gage at Dulles Airport (National Weather Service 2012-2014) reported during the study period. The Cinnamon Oaks BMP is

located 3.5 miles southeast of Dulles Airport. Due to their close proximity, it was anticipated that daily rainfall events at the two gages would be comparable in size.

Manual flow verification studies were also conducted to insure that the AV sensing system was accurately estimating flows *in situ*. Initially, manual flow measurements were made using a SonTek Flowtracker (SonTek YSI Incorporated 2009) at stations CO10, CO20, and CO3O during storm events.

An EPA SWMM model was also constructed for the system in order to provide further insights into the reported flows from the ISCO flow metering modules. The initial model was created using GIS analytical tools to map out the sub-catchments and land uses of the watershed. Survey data collected in the summer of 2013 was used to develop the micropool geometry for SWMM. The weir function in SWMM was used to simulate flow overtopping the micropool weirs but there was no SWMM function to simulate flow seeping through rip-rap. Instead, the model conduit function using high values of Manning's n (0.5-1) was used to simulate flow seeping through rip-rap. The storm event from October 28 – November 02, 2012 (Hurricane Sandy) was used to initially calibrate the model. Other monitored storm events were also modeled for further calibration and monitoring instrument verification.

3.3.3 Storm Event Monitoring and Sample Collection

Operationally, a storm event was defined to encompass the period between the onset of rainfall and the point at which flow at all stations had returned to zero. Prior to each storm event, acid cleaned storage vessels were placed in each sampler, and the on-site counter set to 0 of a possible 76 sample aliquots. During a storm event, the AV dataloggers in each station numerically integrated the cumulative flow volume under the storm hydrograph, and when pre-selected volume increments were reached, the instruments triggered the collection of a 200 mL sample aliquot. Because the sampler could only retrieve a total of 76 aliquots, the sample volume increments were altered depending on the anticipated size of the storm event. The flow increments were selected to provide a balance between collecting sufficient volume to support the analytical program for small storms, while insuring that the storage volume of the composite vessel was not exceeded for large storms. A minimum of 15 sample aliquots were required to test for all the constituents of concern. Using the drainage area, land use, and predicted storm event

rainfall, the SCS Curve Number Method (NRCS 1986) was used to estimate the total flow volume anticipated at each station. Using the predicted flow volume, the sample volume increments were set to obtain approximately 25 sample aliquots. This value was chosen as a compromise between the minimum sample requirements, while providing a buffer against sample vessel overflow if the event size was larger than predicted.

During a storm event, the instruments continuously recorded precipitation, water velocities, depths of flow, and computed flow volumes in one minute increments. Text messaging alert systems were programmed to notify OWML staff when rainfall was detected, when flow rates exceeded 0.5 and 1.0 cfs at the stations, and when negative flows were detected. The monitoring equipment recorded negative flow when it detected runoff moving opposite of the normal flow direction. This backwater flow was occasionally caused by sediment and debris buildup near the monitoring equipment. When activated, the sampler retrieved an aliquot and placed it in the composite vessel. In this way, the liquid in the sampler always represented a flow-weighted composite at any point throughout a stormwater runoff event. It follows, then that analysis of an aliquot from such a composite represented the Event Mean Concentration (EMC) for any constituent of interest for the total runoff event. If the equipment is programmed to retrieve a sample aliquot representing each sub-area, the protocol provides the opportunity to take many more samples than would be possible with other compositing or sequential-discrete collection methods, and thereby enhances the representativeness of the overall composite for each event.

Following the completion of a storm event, OWML staff visited the site to collect composite samples, service the station, and prepare the equipment for subsequent event. Sampler vessels were removed and placed over ice in an insulated cooler to reduce chemical reaction or bacterial growth during transport. Clean sample vessels were then installed in the samplers. A laptop computer was connected to the instrumentation modules to perform any setting changes and to calibrate the equipment. Following the end of an event, total flow volumes and sampler counts were reset to zero. The pressure transducers often required re-calibration. At the end of an event, if a standing pool was present in the conduits, the water depth was measured manually and compared to the depth reported by the pressure transducer. If the depths did not match within 0.05 ft., the operating protocol required that the transducer be re-calibrated. Battery state was

also examined at each site visit, and replacements installed if necessary. Following the completion of on-site servicing, samples were transported back to OWML for analysis.

3.3.4 Micropool Monitoring

The performance analysis also included monitoring of the CO40, CO50, and CO60 micropools. The CO70 pool was not included because, unlike the other micropools, it did not have a continuous standing pool after storm events. Alkalinity, pH, conductivity, and dissolved oxygen measurements were made on a weekly basis. Grab samples and chlorophyll-a measurements were taken for laboratory analysis on a monthly basis but this was changed to a weekly basis in late November, 2013. The micropool grab samples underwent the same laboratory analyses as the storm event samples.

3.3.5 Flow Balances

3.3.5.1 Water Budget

The ISCO monitoring equipment calculated and stored flow rate and flow volume information in 1-minute increments based on the conduit geometry and directly sensed water depth and velocity. Hyetographs, hydrographs and cumulative flow volumes were generated for each storm event for which water quality samples were collected. When the rain gage first detects precipitation marked the beginning time of each storm event. The end time for a storm event was when the flow rates at CO10 returned to zero. Total inflow volumes were taken to be the sum of the inflows from CO20 and CO30, estimates of ungaged runoff, and direct precipitation inputs to the micropools. Flow reductions through the facility micropools occurred due to storage, infiltration, and evapotranspiration. The measured discharges at CO10 represented the total outflow volume. The goal in constructing a water budget for the system was for total outflow volume to not differ from total inflow volume by more than 5 percent.

3.3.5.2 Estimating Direct Catchment and Storage

A survey of the micropools was conducted in summer, 2013. The goals of the survey were to estimate the direct catchment area and total possible storage of each micropool. A Leica TS06 total station (Leica Geosystems 2012) was used to obtain XY coordinates and elevations at Cinnamon Oaks. A total of 507 survey points were made both around the BMP area and in the micropools. A contour map of the BMP area was created using the survey data and ArcGIS

analytical tools. This contour map was then used to determine the maximum storage volumes and surface areas of each micropool. The maximum storage volumes were calculated using the following equation (Wetzel 1983):

$$V_{max} = \sum_{\Delta h=0}^{h_{max}} \left(\frac{\Delta h}{3}\right)(A_1 + A_2 + \sqrt{A_1 A_2})$$

Where:

A_1 = area of the upper surface

A_2 = area of the lower surface

Δh = vertical depth of the stratum

h_{max}= maximum height of the micropool = height to the top of the outflow weir

Direct catchment volumes during storm events were calculated as the product of the micropool area and total event rainfall depth. The amount of runoff stored in the ponds in each storm event was more difficult to quantify because there were standing pools in CO40, CO50, and CO60 throughout the entire study period. The depths of the pools varied and there was no instrumentation in place for continuous monitoring.

3.3.5.3 Estimating Ungaged Runoff

The grassed and wooded areas around the stormwater facility contributed ungaged runoff that did not pass through the monitoring stations. Because monitoring data were unavailable, the SCS Curve Number method outlined in TR-55 was used to estimate the total ungaged runoff.

The SCS Curve Number equation is given as (NRCS 1986):

$$Q = \frac{(P - I_a)^2}{(P - I_a) + S}$$

Where: Q = runoff (in), P = total rainfall (in), S = potential maximum retention (in), S= maximum retention (in), and I_a = initial abstraction (in).

S may be calculated by:

$$S = \frac{1000}{CN} - 10$$

The Curve Number (CN) depends on the land use, soil group, hydrologic conditions, and antecedent rainfall. Low CN values represent more pervious land use that produces less runoff. Higher CN values are associated with impervious land uses that produce more runoff. Initial abstraction is the amount of rainfall that falls before runoff begins and has been historically estimated by the following equation:

$$I_a = \lambda S$$

The recommendation in TR-55 is that λ=0.2 but new studies suggest that this value may be much lower. Hawkins et al. (2009) suggested that λ=0.05 is a more accurate representation of initial abstraction, and that value was used here. A constraint of the curve number method is that $P \geq I_a$. If $P < I_a$, then Q = 0. The method may only be used to estimate the total runoff during a storm event, and cannot be used to estimate the flow at a given time. Despite its limitations, the curve number method has been successfully used to estimate runoff for individual events when monitoring was not possible (Hawkins et al.2009).

The ungaged runoff area consisted of open grass land in fair condition around the BMP area and wooded areas in good condition between CO20 and CO30 and to the southeast. A soil survey map by Fairfax County (Fairfax County Department of Information Technology 2011) indicated that the grassy area and the wooded area between CO20 and CO30 were hydrologic soil group (HSG) A (CN=44), and the wooded area to the southeast was HSG D (CN=79). Based on these parameters, an area-weighted curve number of 65 was calculated for the entire ungaged area (NRCS 1986).

3.3.5.4 Constituent EMC Analysis

Constituents analyzed for storm event samples included total suspended solids (TSS), suspended sediment concentration (SSC), total dissolved solids (TDS), total nitrogen (TN), oxidized nitrogen (OxN), ammonia nitrogen (NH_3N), total phosphorus (TP), orthophosphate phosphorus (OP), total organic carbon (TOC), dissolved organic carbon (DOC) and the trace metals iron (Fe), manganese (Mn), copper (Cu), cadmium (Cd), chromium (Cr), nickel (Ni), lead (Pb), and

Zinc (Zn). Analysis of the micropool grab samples included the same constituents as well as measurements for chlorophyll-a and alkalinity.

Upon return to the laboratory, storm event aliquots were poured through a churn splitter (Pickering 1978) and distributed to smaller containers for further preparation and analysis. Table 3-1 shows the analytical methods employed and the reporting limits of each constituent.

Table 3-1. Water quality parameters monitored for storm events.

Parameter	**Reporting Limit (mg/L)**	**Method**
Total Suspended Solids	1	SM 2540 D
Suspended Sediment Concentration	1	ASTM D3977
Total Dissolved Solids	10	SM 2540 C
Total Phosphorus	0.01	SM 4500-P F, 4500 - P J
Orthophosphate Phosphorus	0.01	SM 4500-P F
Total Nitrogen	0.25	SM 4500 - P-J
Oxidized Nitrogen	0.01	SM 4500NH3-H
Ammonia Nitrogen	0.01	SM 4500NO3-H
Total Organic Carbon	1	SM 5130 A
Dissolved Organic Carbon	1	SM 5130 A
Parameter	**Reporting Limit (µg/L)**	**Method**
Iron	10	EPA 200.8
Manganese	10	EPA 200.8
Copper	3	EPA 200.8
Cadmium	1	EPA 200.8
Chromium	2	EPA 200.8
Lead	2	EPA 200.8
Nickel	10	EPA 200.8
Zinc	10	EPA 200.8

3.3.6 Accounting for Censored Data

Censored datasets result when constituent concentration measurements result in reporting values that are either too high (greater than a maximum measured value) or too low (generally less than a quality assurance reporting limit). In environmental datasets, censored values are typically low-level concentrations (left-censored). The true concentration is only known to exist between

zero and the equipment/laboratory reporting limit. It is common practice to substitute values below analytical detection limits with the detection limit, half the detection limit, or zero. None of these approaches are recommended because there are no mathematical or theoretical explanations for the practices. If substitution is used, then using half of the detection limit has been described as the only viable option because using zero or the detection limit may cause severe bias in the data (Helsel and Hirch 2002; Geosyntec Consultants and Wright Water Engineers 2009). Helsel (2002) provides three alternate approaches for the analysis of censored data: (1) using nonparametric methods after censoring at the highest reporting limit; (2) using maximum likelihood estimation; (3) and using nonparametric survival analysis procedures.

3.3.6.1 Regression on Ordered Statistics

Robust regression on ordered statistics (ROS) uses a least-squares regression on a probability plot to calculate summary statistics that include censored data. Summary statistics are calculated using the uncensored values. The summary statistics of the uncensored data are then used to estimate new values for the censored data. The plotting positions for both uncensored and censored data are calculated and ranked independently. Uncensored values are plotted on a probability plot and a regression equation is created to best-fit to the data. The regression equation is then used along with the normal scores of the censored data to extrapolate new values for the censored data. These new values are combined with the uncensored data to provide a new data set that can be used to produce summary statistics. It is not recommended that robust ROS be used for datasets with high levels (>80%) of censoring. (Helsel and Hirch 2002; Geosyntec Consultants and Wright Water Engineers 2009). Robust ROS was used to estimate censored data for the SOL method and also in the distributional adherence test for the Effluent Probability Method.

3.3.6.2 Kaplan-Meier Method

The Kaplan-Meier (KM) method is a nonparametric approach that uses ranks of the data to estimate “survival probabilities.” A survival probability is the probability that a data point will be at or below the next incremental data point. The method was originally developed for right-censored data (such as found in pharmaceutical trials), but has been adapted for use with left-censored data. The data are “flipped” by subtracting observed values from a value that is greater than the maximum value in the dataset. It has been recommended that the Kaplan-Meier method

not be used on datasets with greater than 50% censoring. The KM method was used to include censored data for the EPM plots (Helsel and Hirch 2002; Geosyntec Consultants and Wright Water Engineers 2009).

3.3.7 Measuring BMP Performance

3.3.7.1 Concentration Summary Statistics

When inflows and outflows can be assumed to be balanced, BMP performance is often measured by differences between influent and effluent concentrations. Boxplots were created for graphical nonparametric comparisons of the influent and effluent EMCs (Strecker, Quigley et al. 2001; Chen, Lin et al. 2009; Geosyntec Consultants and Wright Water Engineers 2009). ROS was used to include censored data (Helsel and Hirch 2002; Geosyntec Consultants and Wright Water Engineers 2009). Boxplots of the micropool grab samples were also made to analyze the changes in concentration within the BMP. In examining the box plots, however, it should be noted that the EMCs represented average concentrations for the entire duration of a storm, while the micropool concentrations were from surface grab samples taken at set time intervals with no regard for flow conditions.

3.3.7.2 Mass-based Analysis

Performance analyses based only on constituent concentrations may not accurately describe all the reductions occurring in a BMP. BMPs may also reduce constituent loads through reductions in water volume from storage, infiltration, and evapotranspiration, and such reductions are not represented when comparing inflow and outflow concentrations. Because constituent loads are the products of their respective EMCs and total flow volumes, assessments performed on a mass basis are preferred over concentration-based approaches when determining BMP performance (Kayhanian, Roseen et al. 2009; Li and Davis 2009; Environmental Protection Agency 2012; Pomeroy, Strecker et al. 2012). In addition, when conducting a mass-based performance assessment, it is important to maintain long-term monitoring that includes a wide range of event sizes and dry weather flows (Geosyntec Consultants and Wright Water Engineers 2009).

3.3.7.3 Calculating Inflow and Outflow Loads

Pollutant loads were computed by the multiplying constituent EMCs and total flow volumes for a particular storm event. Flow volume and EMC data at CO10, CO20, and CO30 were obtained

from the flow data and laboratory analytical results, respectively. Inflow loads to the facility were computed from the observed data at CO20 and CO30, and from load estimates from ungaged runoff and direct deposition. Effluent loads were computed from the observed data at CO10. The following equations describe the calculations for the outflow and inflow loads:

$$Effluent\ Loads = CO10_{EMC}\ X\ CO10_{Flow\ Volume}$$

$$Effluent\ Loads = CO10_{EMC}\ X\ CO10_{Flow\ Volume}$$

Where:

$CO10_{EMC}$ = Flow-weighted EMC for CO10

$CO10_{Flow\ Volume}$ = ISCO flow volume for CO10

$CO20_{EMC}$ = Flow-weighted EMC for CO20

$CO20_{Flow\ Volume}$ = ISCO flow volume for CO20

$CO30_{EMC}$ = Flow-weighted EMC for CO30

$CO30_{Flow\ Volume}$ = ISCO flow volume for CO30

$Ungaged_{EMC}$ = Ungaged runoff EMC from literature

$Ungaged_{Flow\ Volume}$ = Ungaged runoff volume estimates using SCS Curve Number Method

DR_{EMC} = direct rainfall concentration from literature

$DR_{Flow\ Volume}$ = Direct rainfall flow volume

Direct rainfall and ungaged runoff loads were estimated because no monitoring data were available to characterize them. EMCs and deposition concentrations were obtained from the literature, and a summary of sources is shown in Tables 3-2 and 3-3. Because the direct catchment and ungaged runoff volumes were small compared to the observed flow volumes at the inflow monitoring stations, the sources had minimal effects on the BMP performance calculations.

Table 3-2. Ungaged runoff and direct deposition EMCs selected from the literature.

	Ungaged Runoff EMC		Direct Deposition	
Constituent	(mg/L)	Source	(mg/L)	Source
TSS	19	CH2M Hill (2000)	0	
SSC	23	CH2M Hill (2000)	0	
TDS	52	CH2M Hill (2000)	10	NADP (2009)
TP	0.15	CH2M Hill (2000)	0.023[3]	Virginia Tech (1983)
OP	0.02	CH2M Hill (2000)	0.010	Virginia Tech (1983)
TN	1.1	CH2M Hill (2000)	0.90-2.46[4]	NADP (2009)
OXN	0.4	CH2M Hill (2000)	0.81-2.46[4]	NADP (2009)
NH_3N	0.1	CH2M Hill (2000)	0.14-0.54[4]	NADP (2009)
TOC	11.05[1]	CH2M Hill (2000)	3.76[5]	Virginia Tech (1983)
DOC	11.05[2]	CH2M Hill (2000)	3.76[2]	Virginia Tech (1983)
	Ungaged Runoff EMC		Direct Deposition	
Constituent	(µg/L)	Source	(µg/L)	Source
Iron	220	Minton (2005)	34	Conko, Rice et al. (2004)
Manganese	2.6	Conko, Rice et al. (2004)	2.6	Conko, Rice et al. (2004)
Copper	5.3	CH2M Hill (2000)	0.95	Conko, Rice et al. (2004)
Cadmium	0.5	CH2M Hill (2000)	0.06	Conko, Rice et al. (2004)
Chromium	2.8	CH2M Hill (2000)	0.25	Conko, Rice et al. (2004)
Nickel	4.7	CH2M Hill (2000)	0.35	Conko, Rice et al. (2004)
Lead	3.0	CH2M Hill (2000)	0.54	Conko, Rice et al. (2004)
Zinc	22.9	CH2M Hill (2000)	5.5	Conko, Rice et al. (2004)

[1]The source provide a chemical oxygen demand (COD) EMC of 29.4 mg/L. Using the theoretical COD/TOC=2.66, a TOC EMC was calculate by multiplying the COD/TOC with the COD EMC.

[2]Assumed DOC composed most of TOC therefore DOC=TOC.

[3]Used median EMC of values that range between 0.150 – 0.03 mg/L.

[4]Used monthly averages based on data from January, 2004 – December, 2008.

[5]The source provide a chemical oxygen demand (COD) EMC of 10 mg/L. Using the theoretical COD/TOC=2.66, a TOC EMC was calculate by multiplying the COD/TOC with the COD EMC.

3.3.7.4 Summation of Loads Method

The Summation of Loads (SOL) method is based on a comparison of the ratio of the sum of the effluent loads and the sum of the influent loads (Minton 2005; Chen, Lin et al. 2009; Geosyntec Consultants and Wright Water Engineers 2009; Kayhanian, Roseen et al. 2009):

$$\text{SOL} = 1 - \frac{\sum \text{Effluent Loads}}{\sum \text{Influent Loads}}$$

The resulting value of SOL, of course, is the fraction of constituent remaining, and in order to express the performance number as the fraction removed, it must be subtracted from unity. A percent reduction value can be calculated as the product of the SOL value and one hundred. The method is based on the assumptions that constituent removal over the entire period of observation is the best measure of performance, that significant storms that were not monitored have inlet to outlet load ratios that are similar to the monitored events, that both inflow and outflow loads are available for all events included, and that no constituent materials were exported from the BMP during dry periods (Geosyntec Consultants and Wright Water Engineers 2009). Because paired data sets were required for the analysis, only those storm events having complete data from CO10, CO20, and CO30 were used in the SOL method. The SOL method provides a convenient way to quickly compare removal efficiencies of different BMPs. However, it is not recommended as a stand-alone method of measuring BMP performance and should be supplemented with an appropriate test to determine if the differences in loads are statistically significant. This method does not show the performance of individual storm events. Knowing how performance changes between individual storm events promotes further understanding of the removal mechanisms occurring within a BMP (Strecker, Quigley et al. 2001; Geosyntec Consultants and Wright Water Engineers 2009).

Results from the SOL method can be dominated by very large events, and for that reason, outliers in the EMC datasets were removed from the SOL analysis to prevent skewing of the final results. Identification of outliers can be determined using numerical or graphical approaches (Helsel and Hirch 2002). For the purposes of this study, it was decided that EMCs that were greater than three standard deviations above the mean would be excluded from the SOL method. This boundary was selected because for normally distributed datasets, 99.73% of values lie within three standard deviations of the mean. Also, EMCs that exceeded three standard

deviations above the mean were clearly separated from rest of the EMCs as shown on the boxplots and the Q-Q plots.

3.3.7.5 Effluent Probability Method

The Effluent Probability Method is based on a graphical comparison of rank-ordered influent and effluent EMCs or loads. Two initial steps are required, however, in the application of the method:

- A test for distributional adherence must be performed to determine the best transformation to be applied to the inflow and outflow EMC or load datasets;
- An appropriate test must be performed to determine if observed differences between influent and effluent EMCs or loads are statistically significant (Geosyntec Consultants and Wright Water Engineers 2009; Kayhanian, Roseen et al. 2009).

Following the steps above, BMP performance for a given constituent may then be characterized by plotting both the transformed inflow and outflow data on a normal probability axis. Because the method is based on characterizing both the influent and effluent load datasets over the entire range of storm event sizes, the method does not require the exclusion of non-synoptic storm event data. The resulting cumulative probability plots make it possible to draw inferences about changes in constituent removal as a function of storm event size (Strecker, Quigley et al. 2001; Chen, Lin et al. 2009; Geosyntec Consultants and Wright Water Engineers 2009; Kayhanian, Roseen et al. 2009).

In conducting the distributional adherence test for this study, the Robust ROS method was used so that censored data could be used for analysis (Strecker, Quigley et al. 2001; Geosyntec Consultants and Wright Water Engineers 2009). Even though the method allowed the use of unpaired influent and effluent data, influent loads could only be computed where data from both CO20 and CO30 were available.

3.3.7.6 Testing for Significant Differences Between Influent and Effluent Loads

Both the Summation of Loads Method and Effluent Probability Method should be accompanied with an appropriate test to determine if the influent and effluent loads are significantly different.

Selection of the 95 percent confidence interval (α=0.05) has been recommended (Geosyntec Consultants and Wright Water Engineers 2009). The generalized Wilcoxon signed-ranked test is a nonparametric statistical test that determines if two or more datasets significantly differ. A 1-sided test can be used if one dataset is expected to be larger than the other. A 2-sided test, which was used in this study, simply determines if two datasets are significantly different. Both uncensored values and Kaplan-Meier censored values may be used to estimate the percentiles of the distribution function of the data (Helsel and Hirch 2002).

In computing the generalized Wilcoxon test statistic W_{rs}, the first step is to calculate the difference between paired values, D_i, which may be positive or negative. The D_i values are then assigned a rank, R_i, based on their absolute magnitudes. The smallest D_i is assigned a rank of 1 and the largest D_i is assigned a rank of n. The R_i values are then assigned + or – based on whether the corresponding D_i was positive or negative. The R_i values are then separated into positive and negative groups. The equation for W is given below:

$$W_{rs} = \ sum\ of\ the\ ranks\ for\ the\ group\ with\ the\ smaller\ sample\ size = \sum_{1}^{n} R_i$$

W_{rs} may then be used to determine a p-value. For datasets with less than 10 samples, a precise p-value must be calculated. For datasets with more 10 samples or greater, the distribution W_{rs} closely approximates a normal distribution. An approximated p-value can be determined using the following equations:

$$\mu_w = \frac{n * (N+1)}{2}$$

$$\Theta_w = \sqrt{n * m * \left(\frac{N+1}{12}\right)}$$

$$Z = \frac{\left(W_{rs} - \left(\frac{d}{2}\right) - \Theta_w\right)}{\mu_w} \ if\ W_{rs} > \Theta_w$$

$$Z = \frac{\left(W_{rs} + \left(\frac{d}{2}\right) - \Theta_w\right)}{\mu_w} \ if\ W_{rs} < \Theta_w$$

Where n = sample size of the smaller group, m = sample size of the larger group, N = n + m, d = minimum difference between possible values of the test statistic (d =1for the rank-sum test), and Z = standard normal statistic. Once Z is computed, a probability, p can be determined using a standard normal table. For a 2-sided rank sum test, the p-value is simply 2*p. This approach is common in many statistical software programs (Helsel and Hirch 2002; Helsel 2012). For this study, p-values were determined using the large sample approximation, and built-in standard normal tables in the R statistical programming software (The R Core Team 2012). At the 95 percent confidence interval, a p-value less than 0.05 indicates that the influent loads and effluent loads likely do differ (Helsel and Hirch 2002; Helsel 2012).

3.4 Results

3.4.1 Assessment of Monitoring Equipment

3.4.1.1 Rain Gage Verification

The rain gage used in this study was not heated, and on occasion, freezing rain or snow accumulation affected the accuracy of the data. In order to obtain usable rainfall data during such events, daily and monthly rainfall comparisons between the Cinnamon Oaks gage and a reference gage were sought. The National Weather Service gage at Dulles Airport (National Weather Service 2012-2014) is located approximately three miles northwest of the Cinnamon Oaks site, and the comparison is shown for monthly and daily rainfalls in Figures 3-3 and 3-4, respectively. As may be seen from the figures, the daily and monthly rainfall data matched well, giving confidence that the Dulles gage data could be used for the limited number events for which Cinnamon Oaks rainfall data were not available. Daily precipitation data for the two gages in the summer could sometimes differ significantly due to flashy storm events that were concentrated over smaller areas. However, the Dulles gage data were not required as a replacement for missing Cinnamon Oaks gage data for any summer events. Using the Dulles gage daily data to synthesize event data was possible only for those days where a single event occurred. In those cases, the daily data also represented the event data.

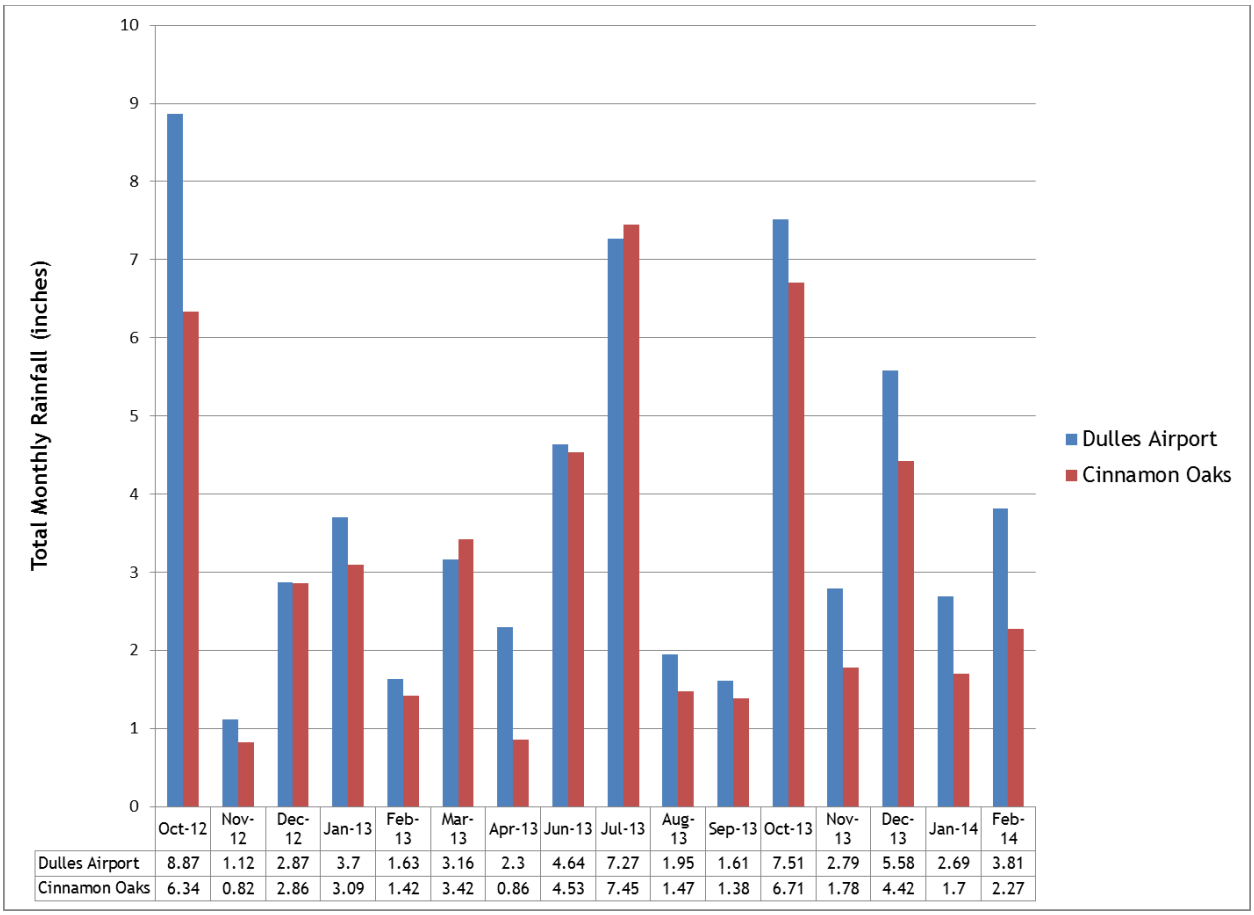

	Oct-12	Nov-12	Dec-12	Jan-13	Feb-13	Mar-13	Apr-13	Jun-13	Jul-13	Aug-13	Sep-13	Oct-13	Nov-13	Dec-13	Jan-14	Feb-14
Dulles Airport	8.87	1.12	2.87	3.7	1.63	3.16	2.3	4.64	7.27	1.95	1.61	7.51	2.79	5.58	2.69	3.81
Cinnamon Oaks	6.34	0.82	2.86	3.09	1.42	3.42	0.86	4.53	7.45	1.47	1.38	6.71	1.78	4.42	1.7	2.27

Figure 3-3. Total Monthly Rainfall at Cinnamon Oaks and Dulles Airport rain gages.

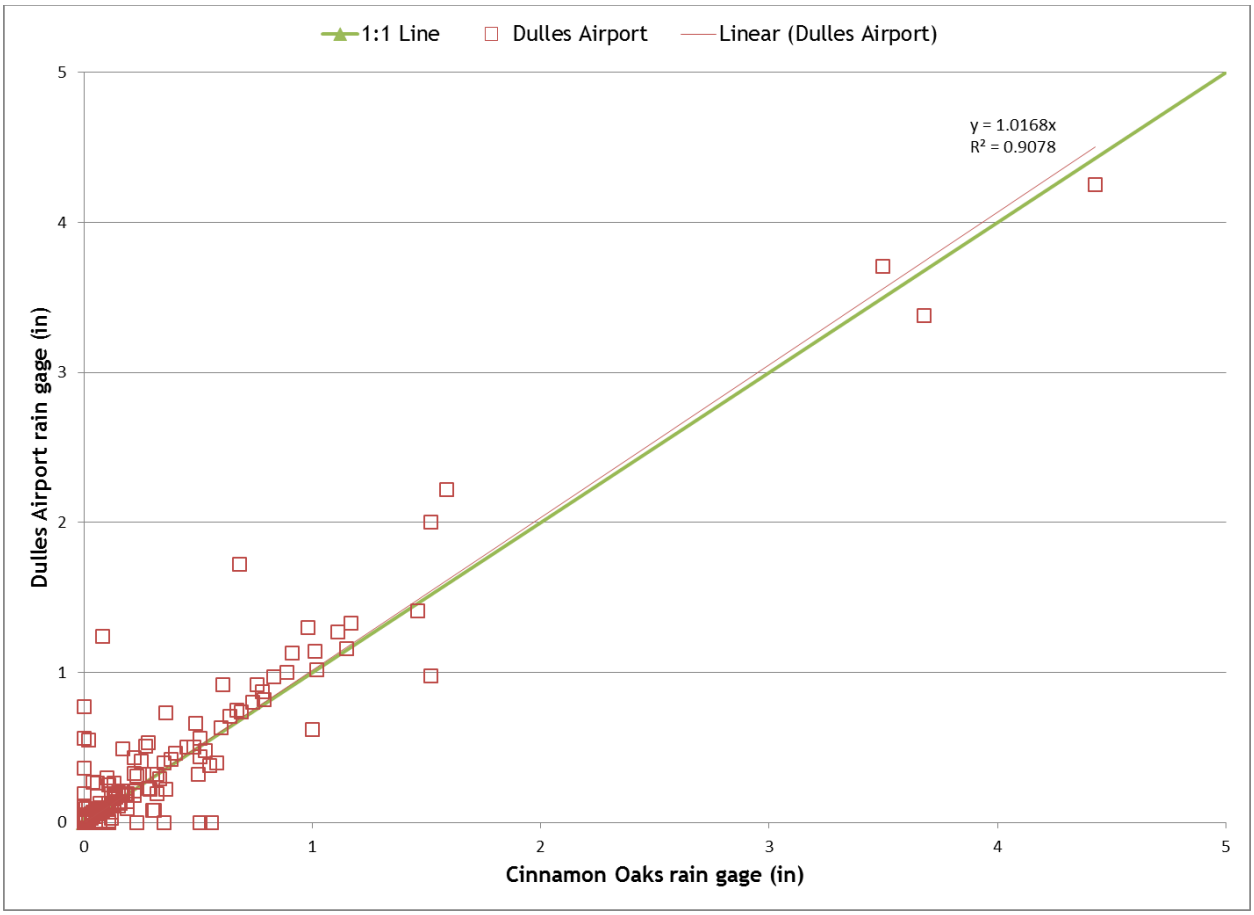

Figure 3-4. Comparison of 24-hour rainfall depth at Cinnamon Oaks and Dulles Airport, rain gages.

3.4.1.2 Flow Meter Verification

Although the flow measurements at stations CO10, CO20, and CO30 were made with a direct area-velocity method, efforts were also made to verify the recorded flows by making comparative manual measurements in the field. The results are illustrated in Figure 3-5. Manual measurements were made with a hand-held Sontek Flowtracker Model (SonTek YSI Incorporated 2009). Unlike the relatively rapid readings from the ISCO flow modules, measurements with the Flowtracker took between 30 seconds to several minutes to complete. Due to the flashiness of the storm events, this limitation made comparing flow rates difficult. Additional comparison data were obtained by arranging for controlled hydrant releases by Fairfax Water near CO20 and CO30 in summer, 2013. Flows from this source gave more consistent and stable flows from which to make manual measurements. At the maximum hydrant release rate, stable flows above 1 cfs could not be achieved. Because of the long detention times within the BMP, a hydrant release for CO10 was not possible. The manually gaged flow

measurements suggested that, for the range of flows available, the AV equipment at CO20 and CO30 were both overestimating flow. The AV equipment readings at CO10, however, were reasonably accurate. However, applying correction factors based on manual flow measurements to the AV flow readings at CO20 and CO30 was found to significantly alter the water budget. Based on the best-fit lines from Figure 3-5, correction factors of 0.75 and 0.5 would have been applied to flow rates of CO20 and CO30, respectively. There would be no correction factor for CO10. This would have resulted in much lower total inflow estimations. With the corrections applied, total outflow volumes were found to exceed total inflow volumes by more than 5% for the majority of the monitored storm events. In retrospect, it was concluded that the manual methods were themselves prone to error. Manual measurements could take up to several minutes to complete, and steady flows greater than 1 cfs and flow depths greater than one inch rarely occurred for sufficient lengths of time. As a result, the direct comparisons of manual flow measurements and the AV equipment indicated flows were inconclusive.

Results from the application of the EPA SWMM model were more conclusive. Hydrographs produced by the model for a number of monitored storm events are shown in Figures F-1 - Figure F-4 in Appendix F. In general, SWMM flow measurements at CO20, and CO30 matched well with the morphology of the hydrographs produced by the ISCO flow meters. For CO10, the SWMM model and ISCO equipment matched well with large events but hydrographs for the smaller storm events were noticeably different. The differences may due to errors in trying to use a closed conduit to simulate seepage through rip-rap and due to not knowing the exact water volumes within the BMP before storm events. During large events, the water flow through CO10 was dominated by new runoff coming into the BMP and water overtopping the weirs. In smaller events, water already within the BMP and seepage through the rip-rap had a more pronounced effect on the discharge through CO10. Despite these issues, the SWMM model results gave more confidence that the AV equipment were accurately measuring flows.

Calibration problems with the AV equipment pressure transducers and other site conditions were found to be the main source of inaccurate flow measurements from the AV equipment at CO20 and CO30. These issues were resolved by recalibrating the pressure transducers during each site visit. For the limited number of events where calibration issues affected the flow measurements, correction factors were applied to CO20 and CO30 measurements. The correction factors were

based on the ratio of the AV pressure transducer depth readings to the manual onsite field measurements. Negative flows were periodically reported by the AV monitoring equipment during some of the larger storm events. The negative flows were found to be the result of backwater flows caused by sand and leaf buildup at the stations. In these cases, flow predictions from the SWMM model were used as substitutes for the negative flow values.

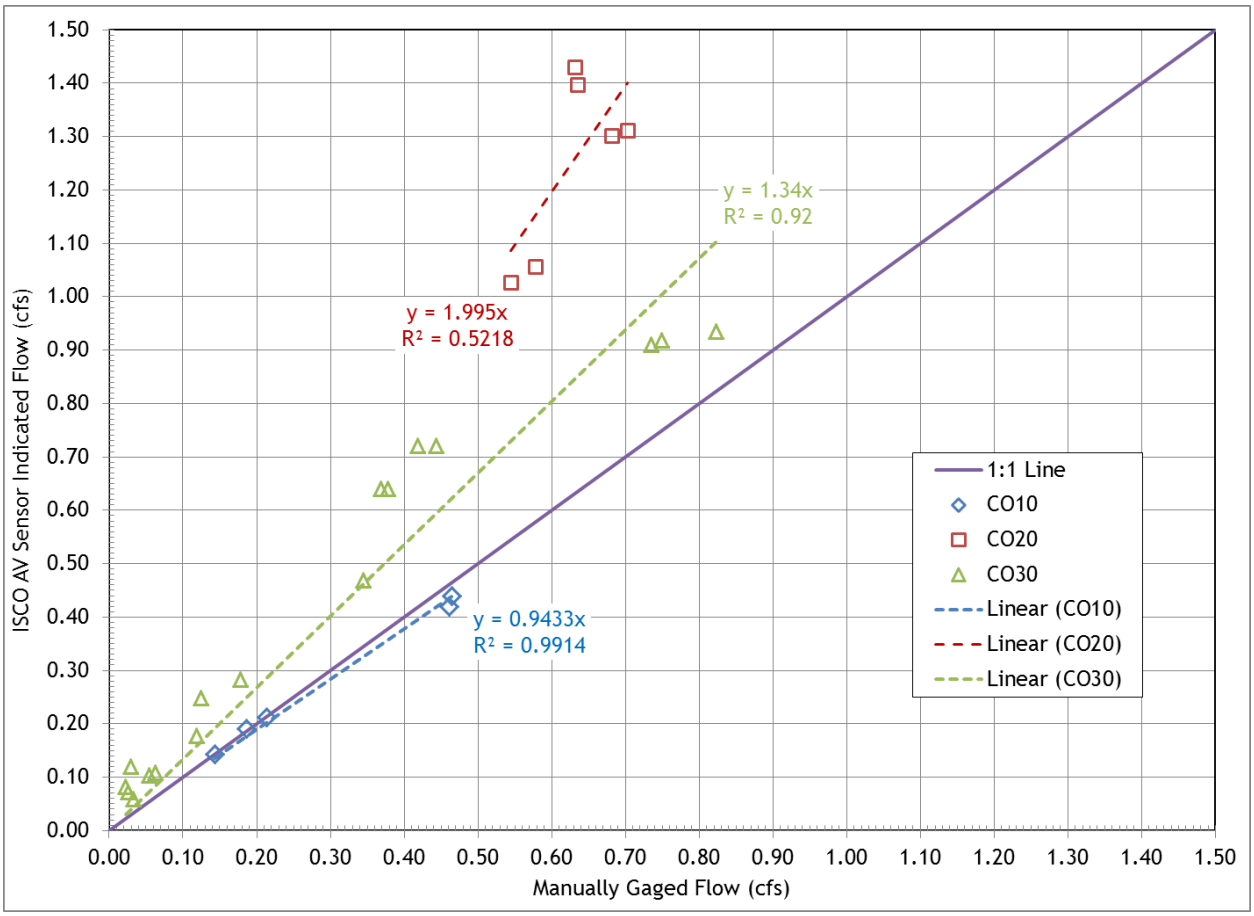

Figure 3-5. Comparison of AV sensor indicated flows and manually gaged flows.

3.4.1.3 Sampler Performance

In general, the sampling equipment functioned as intended and provided representative sample aliquots of storm events. Sampling equipment malfunctions did, however, occur on occasion during the study period. The range of sampler malfunctions included failure to retrieve samples when activated, taking samples when not activated, and failure to retrieve samples due to clogging of the intake. Water quality data for a storm event were considered unusable if the equipment failed to sample for more than 10% of the indicated activations.

3.4.2 Hydrologic Data

3.4.2.1 Pond Storage

The site survey data were used to generate the contour map of the Cinnamon Oaks BMP shown in Figure 3-6. Table 3-3 presents the computed maximum storage volumes of the Cinnamon Oaks micropools using data from the OWML site survey and DPWES pre-construction calculations.

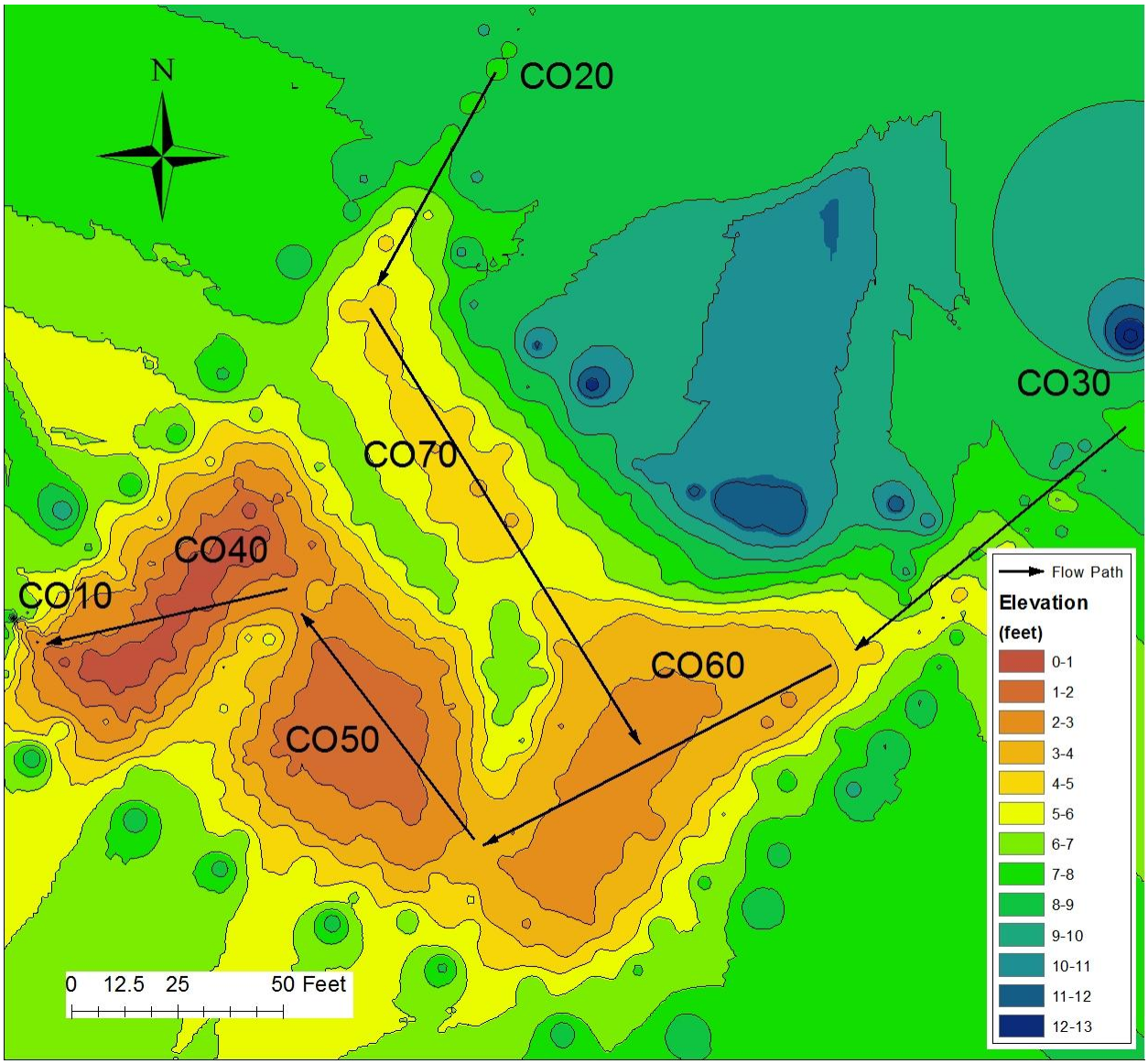

Figure 3-6. Contour map of Cinnamon Oaks Best Management Practice retrofit.

Table 3-3. Maximum Storage Estimations of Cinnamon Oaks Micropools

Micropool ID	OWML Survey (cf)	DPWES (cf)
CO70	2054	2493
CO60	3143	4791
CO50	1812	3649
CO40	1497	1792
Total	8506	12725

CO70 was the only micropool observed to return to a dry condition after storm events. CO40, CO50, and CO60 remained wet throughout the entire study period, and storage generally remained near capacity. Observed differences in pond volumes between the OWML survey and DPWES design estimations were likely due to sediment deposition and plant growth since the construction was completed in 2009. CO60, in particular, contained deposits of sediment, vegetation, and mud that occupied much of the total available storage.

3.4.2.2 Monitored Storm Events

Summaries of the rainfall and runoff data for the Cinnamon Oaks BMP retrofit are shown in Table 3-4. A total of 39 storms with complete water quality data were monitored during the study period. The rainfall for the monitored storm events ranged from 0.18 to 5.76 inches with a median event size of 0.91 inches. Using the survey data and GIS, it was determined that the micropool surface area was 0.3 acres and the ungaged area was 2.15 acres. These values were used to estimate inflow runoff that did not pass through the monitoring equipment at CO20 and CO30. As noted in Section 3.5.1, the goal of the water budget was for total outflow volume to not exceed total inflow volume by more than 5%.

Hydrographs and flow volume time series plots were created for each monitored event. Flow rates, flow volumes, and rainfall intensity for the October 28 – November 02, 2012 storm event

are shown in Figure 3-7 as an example. Hydrographs and flow volume time series plots for all the monitored events may be found in Figures A-1 through A-39 in Appendix A.

Table 3-4.Hydrology data for monitored storm event at Cinnamon Oaks best management practice.

			Total Flow Volumes								Peak Flow Rates		
Event Date	Total Rain	Total Rainfall Volume	CO30	CO20	CO20 + CO30	Direct Catchment	Ungaged Runoff	Total In	CO10	Inflow/Outflow Difference	C30	CO20	CO10
	(in)	(cf)	(cf)	(cf)	(cf)	(cf)	(cf)	(cf)	(cf)	(%)	(cfs)	(cfs)	(cfs)
10/18/12	0.48	19515	1600	4071	5671	523	62	6256	106	98	1.1	2.1	0.1
10/28/12	5.68	230926	53028	58925	111952	6175	21165	139292	139656	0	1.2	1.2	3.0
11/13/12	0.79	32118	3283	5063	8346	849	358	9554	4370	54	0.2	0.7	0.2
12/20/12	0.86	34964	2130	5373	7503	937	456	8896	7218	19	0.5	1.1	0.5
12/26/12	1.65	67082	16439	20952	37391	1797	2199	41387	41520	0	1.1	1.7	1.9
01/14/13	1.04	42282	5639	8542	14181	1133	753	16067	14743	8	0.3	0.4	0.5
01/30/13	1.82	73994	15095	24269	39365	2178	2706	44249	43438	2	2.4	3.3	4.5
02/13/13	0.32	13010	1492	2577	4069	348	4	4421	1850	58	0.1	0.3	0.1
02/26/13	0.71	28866	4225	7509	11734	773	260	12768	6264	51	0.4	0.8	0.4
03/06/13	1.28	52040	12231	13201	25432	1383	1247	28062	29390	-5	0.3	0.4	0.5
04/12/13	0.51	20735	1624	2608	4233	555	80	4868	4007	18	0.6	0.8	0.2
04/19/13	1.20[1]	48787	6823	7743	14566	1307	1071	16943	17587	-4	1.7	2.1	1.3
05/07/13	1.55	63017	7776	9934	17709	1688	1921	21318	18154	15	1.9	2.5	0.7
06/02/13	0.57	23174	1819	2688	4506	621	124	5251	2956	44	1.5	2.2	0.2
06/06/13	1.29	52446	7857	11841	19698	1405	1270	22372	16005	28	0.6	0.9	0.8
06/09/13	1.74	70741	15124	16116	31239	1884	2463	35586	38415	-8	6.6	6.6	4.0
06/13/13	0.23	9351	609	997	1606	240	0	1846	1922	-4	1.6	1.3	0.1
06/23/13	0.18	7318	392	957	1349	196	0	1545	34	98	0.2	0.4	0.0
06/28/13	0.32	13010	952	1775	2727	338	4	3068	523	83	1.3	1.4	0.1
06/30/13	0.33	13416	885	1698	2583	348	5	2937	1250	57	1.1	1.9	0.1
07/03/13	1.00	40656	6748	7163	13911	1078	682	15670	14077	10	2.7	2.9	1.1
07/07/13	0.43	17482	1049	1301	2350	436	36	2822	1177	58	1.1	1.2	0.1
07/10/13	0.33	13416	1023	1480	2503	338	5	2846	2533	11	0.0	2.4	0.2
07/27/13	0.61	24800	2099	3837	5935	653	158	6747	5085	25	1.7	2.5	0.3

[1]Spiderweb blocked rain gage tipping bucket. Dulles Airport rainfall data was used to substitute for this value.

Table 3-4. Hydrology data for monitored storm event at Cinnamon Oaks best management practice (Continued).

			Total Flow Volumes								Peak Flow Rates		
Event Date	**Total Rain**	**Total Rainfall Volume**	**CO30**	**CO20**	**CO20 + CO30**	**Direct Catchment**	**Ungaged**	**Total In**	**CO10**	**Inflow/Outflow Difference**	**C30**	**CO20**	**CO10**
	(in)	**(cf)**	**(cf)**	**(cf)**	**(cf)**	**(cf)**	**(cf)**	**(cf)**	**(cf)**	**(%)**	**(cfs)**	**(cfs)**	**(cfs)**
08/13/13	0.67	27240	2508	2848	5356	730	217	6302	4686	26	1.7	1.9	0.3
08/23/13	0.25	10164	675	1476	2151	272	0	2423	209	91	0.3	0.6	0.0
09/01/13	0.29	11790	767	1131	1898	316	1	2214	21	99	0.7	1.0	0.0
09/21/13	0.99	40249	3750	4734	8484	1078	664	10226	7122	30	1.2	1.5	0.5
10/07/13	0.91	36997	4371	6140	10512	991	532	12035	3638	70	1.8	2.9	0.3
10/09/13	5.76	234179	67265	66942	134207	6273	17001	157480	155048	2	3.7	3.6	5.5
11/26/13	2.22[2]	90256	13980	15534	29514	1209	4049	34772	35419	-2	0.6	0.7	1.6
12/06/13	1.02[3]	41469	9331	10369	19700	1111	717	21528	17445	19	0.7	0.9	0.7
12/08/13	1.50[3]	60984	18184	11499	29683	348	1787	31819	31741	0	0.4	0.4	0.6
12/14/13	0.85	34558	5592	2765	8356	926	441	9723	8652	11	0.4	0.4	0.3
12/22/13	1.01	41063	14115	11032	25147	1100	699	26946	28197	-5	0.8	1.0	1.1
12/29/13	1.11	45128	14160	13872	28033	1220	886	30138	29687	1	1.5	1.3	2.5
02/03/14	1.17	47568	13412	15382	28793	1274	1007	31075	28127	9	1.1	0.8	1.4
02/05/14	0.55[3]	22361	8095	9397	17493	33	109	17634	14706	17	0.7	0.8	0.4
02/18/14	1.82[3]	73994	31412	30440	61852	240	2706	64798	56084	13	1.8	1.3	0.7

[2]Malfunction occurred at rain gage. Dulles Airport rainfall data was used to substitute for this value.

[3]Snow event that prevented tipping of rain gage. Dulles Airport rainfall data was used to substitute for this value.

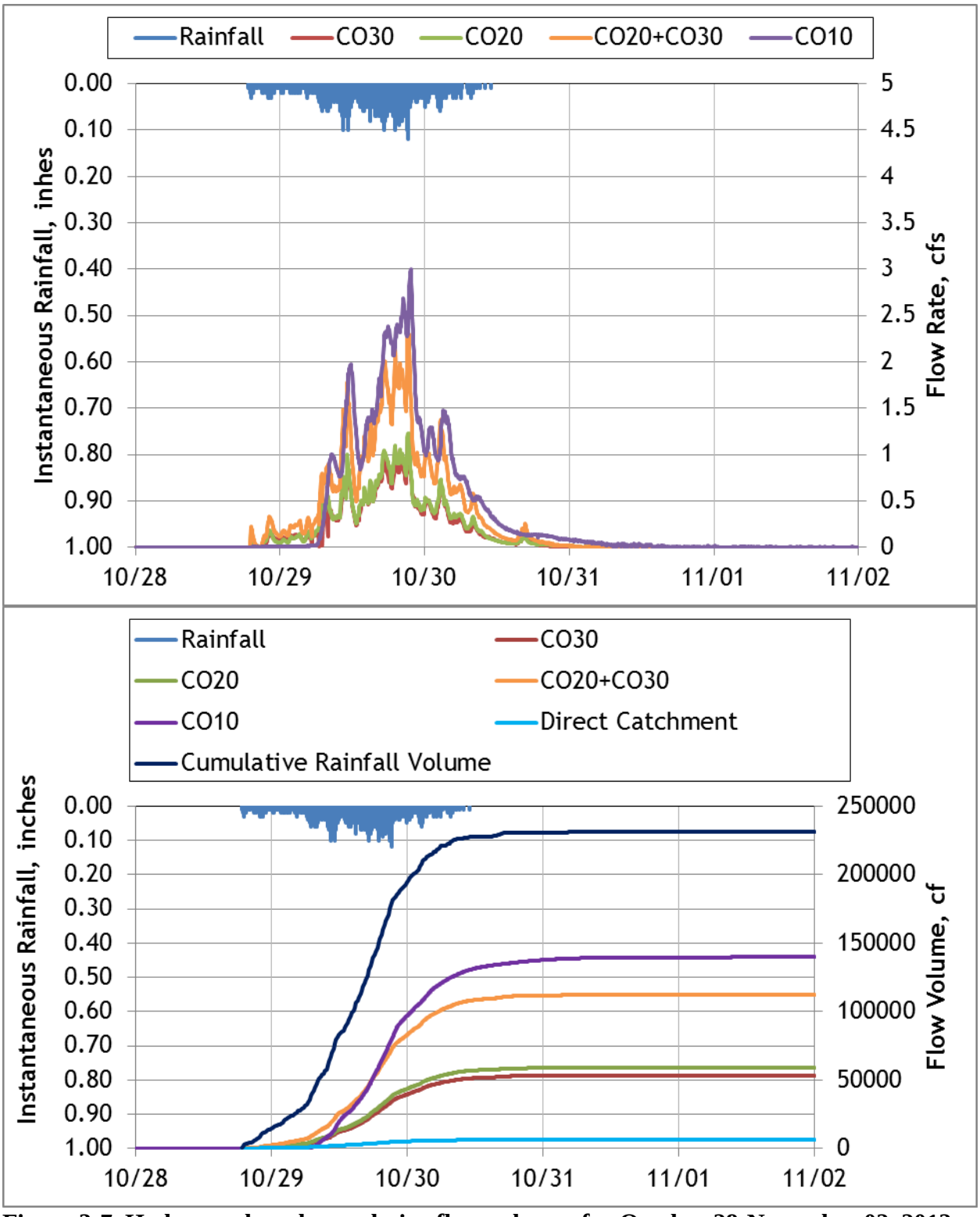

Figure 3-7. Hydrograph and cumulative flow volumes for October 28-November 02, 2012

3.4.3 Storm Event Mean Concentrations and Micropool Grab Samples

Computed event mean concentrations (EMCs) for monitored constituents for each storm event are presented in Tables 3-5 through 3-11. Tables 3-12 through 3-18 present constituent concentrations of the micropool grab samples. Temperature, dissolved oxygen, pH, and alkalinity measurements taken at the micropools are displayed in Table 3-19. Comparative boxplots of EMCs and pond grab samples for each constituent may be found in in Appendix B. Boxplots for TSS are shown in Figure 3-8 as an example. Time series plots of storm event EMCs and micropool grab sample concentrations may be found in Appendix C. The boxplots display how the distribution of constituent concentrations changed along the longitudinal gradient from inlet(s) to outlet. It must be remembered, however, that EMCs computed from the station monitoring equipment are representative of storm events, while the micropool grab samples were representative of instantaneous concentrations at the water surface. However, comparison of concentrations along the distance gradient did provide some insights into constituent removal within the BMP, and where deficiencies may have been occurring.

Table 3-5. Event Mean Concentrations of solids for monitored events.

Event Date	Event Mean Concentration (mg/L)														
	Total Suspended Solids (mg/L)			Suspended Sediment Concentration (mg/L)			Total Dissolved Solids (mg/L)			Specific Conductance (µmhos/cm@25°C)			Turbidity (NTU)		
	CO30	CO20	CO10	CO30	CO20	CO10	CO30	CO20	CO10	CO30	CO20	CO10	CO30	CO20	CO10
10/18/12	51.9	51.6						24.0							
10/28/12	266.0	14.8	8.4	313.8	18.7	7.4	69.0	52.0	64.0				15.1	15.1	15.6
11/13/12	4.0	8.0	3.2			3.2		51.0	118.0	43.1	44.7	163.2			
12/20/12	158.0	30.4	8.0		76.1	4.3	67.4	49.0	110.0						
12/26/12		21.6	9.5		24.8	9.4		341.0	234.0					24.1	16.3
01/14/13	30.4	16.8	6.0	31.7	13.2	6.6	67.0	50.0	112.0	67.0	52.0	111.0			
01/30/13	409.0	84.0	32.4	939.1	93.4	35.5				70.0	291.0	180.0			
02/13/13		14.8	11.6		14.6			213.0	177.0		365.0	276.0			
02/26/13	60.8	32.0	19.2	97.1	42.7	9.9	51.0	91.0	126.0	71.0	160.0	214.0	31.9	13.2	33.6
03/06/13	11.2	10.4	17.6	19.4	18.2	19.3	59.0	348.0	199.0	75.0	620.0	331.0	16.7	18.6	30.5
04/12/13		89.6	12.8		108.3	10.0		73.0	274.0		120.0	416.0		35.9	13.9
04/19/13	86.4	57.6	16.0	145.1	63.2	16.1	40.0	52.0	101.0	41.0	73.0	136.0	26.6	20.4	21.0
05/07/13	70.0	50.0	12.8	60.4	42.1	15.7	42.0	64.0	84.0	48.0	81.0	199.0	9.4	12.1	13.7
06/02/13	67.2	80.0	22.0	97.7	129.4	24.4	104.0	162.0	6.0				11.4	20.1	10.6
06/06/13	10.8	12.4	12.0	11.8	14.6	10.8	48.0	44.0	86.0	189.0	132.0	185.0	7.4	8.8	10.6
06/09/13	12.8	24.0	12.8	239.1		12.1	57.0	48.0	76.0	64.0	79.0	108.0	43.0	37.1	10.0
06/13/13	24.0	42.7	11.0	15.7	44.4	15.2	6.7	69.0	103.0	43.0	118.0	162.0	16.7	23.0	11.8
06/23/13	13.0	18.0	56.0	17.5	453.3	49.1	27.5	41.1	108.0	52.0	59.0	182.0			
06/28/13	114.0	104.0	41.0	124.4	156.5	42.0	22.0	36.0	133.0	53.0	58.0	201.0	18.5	23.6	20.8
06/30/13	43.6	46.4	15.2	59.0	63.6	20.3	35.0	42.0	117.0	39.0	93.0	186.0	16.1	9.5	9.7
07/03/13	32.4	5.2	9.2	10.5	61.9	34.4	29.0	46.0	64.0	97.0	43.0	66.0	8.4	7.8	17.7
07/07/13	27.2	6.5	23.6	6.6	7.9	20.0	47.0	52.0	87.0	56.0	103.0	120.0	6.6	4.6	11.6
07/10/13	32.8	48.4	14.7	35.7	24.3	16.4	27.0	27.0	93.0	34.0	48.0	142.0			
07/27/13	50.4	34.0	9.6	71.9	56.0	8.3	45.0	38.0	153.0	55.0	49.0	223.0	16.1	11.1	5.0

Blank cells denote where water quality data were not obtained for a constituent.

Table 3-5. Event Mean Concentrations of solids for monitored events (continued).

Event Date	Event Mean Concentration														
	Total Suspended Solids (mg/L)			Suspended Sediment Concentration (mg/L)			Total Dissolved Solids (mg/L)			Specific Conductance (µmhos/cm@25°C)			Turbidity (NTU)		
	CO30	CO20	CO10	CO30	CO20	CO10	CO30	CO20	CO10	CO30	CO20	CO10	CO30	CO20	CO10
08/13/13	76.0	41.6	15.3	124.4	61.4	17.3	28.0	19.0	104.0	34.0	150.0	149.9	32.8	9.1	8.7
08/23/13	12.8	21.6		9.4	31.8		38.0	30.0		46.0	46.0		1.9	4.6	
09/01/13	26.4	37.6		32.0	59.3		30.0	33.0		33.0	37.0		4.5	5.8	
09/21/13	38.4	49.2	20.4	46.6	63.6	25.0	39.0	34.0	108.0	43.0	40.0	163.0	8.1	14.2	10.7
10/07/13	28.8	31.2	27.2	33.6	35.1	48.0	49.0	38.0	84.0	55.0	40.0	110.0			
10/09/13	22.8	14.8	23.2	22.9	17.2	25.4	55.0	49.0	62.0	65.0	58.0	72.0			
11/26/13	12.4	16.4	4.8	16.4	17.3	6.7	21.0	24.0	47.0	55.0	51.0	81.0	9.1	13.9	8.9
12/06/13	7.6	13.6	2.8	7.4	14.2	2.1	108.0	52.0	77.0	101.0	61.0	105.0			
12/09/13	3.6	18.0	1.6	2.5	13.1		219.0	952.0	498.0				9.3	48.2	14.3
12/14/13	15.2	35.2	3.6	16.7	34.3	2.5	99.0	145.0	297.0	142.0	246.0	531.0	14.3	37.5	10.7
12/22/13	25.3	50.0	7.3	60.9	294.4	10.8	90.0	93.0	140.0	109.0	132.0	206.0			
12/29/13	57.3	30.7	20.0	67.1	178.0	34.4	40.0	45.0	64.0	68.0	76.0	107.0	46.4	41.1	30.9
02/03/14	54.0	58.4	15.2	71.3	57.9	11.7	132.0	721.0	276.0	190.0	1340.0	491.0	32.9	56.2	32.3
02/05/14	17.6	24.0	5.6	20.8	32.3	3.1	137.0	709.0	294.0	217.0	1320.0	491.0	21.1	26.6	17.4
02/18/14	22.8	16.8	8.0	22.9	15.3	5.9				106.0	670.0	375.0	20.7	24.8	18.1

Blank cells denote where water quality data were not obtained for a constituent.

Table 3-6. Event Mean Concentrations of nutrients for monitored events

Event Date	Event Mean Concentration														
	Total Phosphorus (mg/L)			Orthophosphate Phosphorus (mg/L)			Total Nitrogen (mg/L)			Oxidized Nitrogen (mg/L)			Ammonia Nitrogen (mg/L)		
	CO30	CO20	CO10	CO30	CO20	CO10	CO30	CO20	CO10	CO30	CO20	CO10	CO30	CO20	CO10
10/18/12	0.16	0.10		0.04	0.04		1.27	0.88		0.30	0.22		0.17	0.18	
10/28/12	2.93	0.12	0.23	0.14	0.08	0.17	32.60	1.99	2.45	1.41	1.15	1.33	0.26	0.13	0.07
11/13/12	0.07	0.05	0.10	0.03	0.02	0.06	1.28	1.06	1.17	0.43	0.30	0.20	0.29	0.06	0.03
12/20/12	0.20	0.08	0.13	0.09	0.04	0.10	3.45	0.72	1.49	0.88	0.20	0.70	0.21	0.12	0.05
12/26/12		0.10	0.14		0.05	0.10		1.65	1.35		1.01	0.64		0.14	0.10
01/14/13	0.13	0.07	0.10	0.03	0.02	0.05	2.14	1.17	1.18	0.99	0.49	0.42	0.06	0.11	0.04
01/30/13	0.57	0.18	0.22	0.07	0.06	0.11	5.21	1.86	1.93	0.43	0.68	0.57	0.07	0.14	0.08
02/13/13		0.04	0.08		0.02	0.02		1.23	0.98		0.60	0.01		0.29	0.01
02/26/13	0.30	0.16	0.14	0.06	0.03	0.04	2.59	1.98	1.32	0.50	0.46	0.31	0.24	0.12	0.04
03/06/13	0.09	0.06	0.14	0.03	0.04	0.05	1.26	1.24	1.51	0.69	0.62	0.43	0.05	0.16	0.03
04/12/13		0.24	0.30		0.06	0.13		1.87	1.84		0.25	0.05		0.32	0.11
04/19/13	0.27	0.22	0.28	0.06	0.03	0.12	2.73	1.96	1.63	0.40	0.30	0.26	0.22	0.18	0.13
05/07/13	0.19	0.20	0.28	0.04	0.04	0.17	1.30	1.73	1.36	0.33	0.31	0.12	0.07	0.15	0.06
06/02/13	0.14	0.14		0.07	0.05	0.13	2.11	1.01	1.78	0.50	0.33	0.01	0.24	0.16	0.07
06/06/13	0.10	0.04	0.27	0.05	0.02	0.10	1.34	0.94	1.47	0.38	0.34	0.12	0.07	0.12	0.06
06/09/13		0.07	0.29		0.02	0.10	2.66	1.12	1.48			0.05	0.10		0.02
06/13/13			0.29	1.06	0.54	0.17	1.60	1.86	2.26	0.30	0.46	0.02	0.28	0.29	0.05
06/23/13	0.22	0.11	0.71	0.17	0.06	0.15	1.77	1.56	3.57	0.63	0.31	0.03	0.21	0.19	0.04
06/28/13	0.28	0.18	0.72	0.08	0.05	0.22	2.83	1.96	3.45	0.49	0.32	0.02	0.45	0.40	0.06
06/30/13	0.26	0.12	0.37	0.08	0.05	0.16	2.46	1.13	1.87	0.38	0.31	0.02	0.24	0.23	0.05
07/03/13	0.25	0.07	0.30	0.10	0.02	0.10	1.42	0.70	2.19	0.46	0.17	0.24	0.12	0.05	0.05
07/07/13	0.27	0.15	0.51	0.12	0.15	0.13	1.60	0.98	2.47	0.50	0.28	<0.01	0.13	0.21	0.02
07/10/13	0.14	0.10	0.38	0.07	0.04	0.14	1.66	1.24	1.77	0.44	0.32	<0.01	0.27	0.27	0.04
07/27/13	0.11	0.07	0.29	0.08	0.03	0.14	2.29	1.21	1.13	0.68	0.39	0.05	0.33	0.30	0.07

Blank cells denote where water quality data were not obtained for a constituent.

Table 3-6. Event Mean Concentrations of nutrients for monitored events (continued).

Event Date	Event Mean Concentration														
	Total Phosphorus (mg/L)			Orthophosphate Phosphorus (mg/L)			Total Nitrogen (mg/L)			Oxidized Nitrogen (mg/L)			Ammonia Nitrogen (mg/L)		
	CO30	CO20	CO10	CO30	CO20	CO10	CO30	CO20	CO10	CO30	CO20	CO10	CO30	CO20	CO10
08/13/13	0.14	0.10	0.35	0.07	0.03	0.16	1.33	1.21	1.62	0.39	0.21	0.12	0.23	0.23	0.07
08/23/13	0.13	0.10		0.06	0.02		1.56	1.51		0.58	0.39		0.19	0.23	
09/01/13	0.14	0.16		0.09	0.06		2.24	2.63		0.48	0.37		0.38	0.37	
09/21/13	0.14	0.15	0.45	0.07	0.07	0.19	1.62	1.64	2.01	0.66	0.20	0.38	0.15	0.30	0.02
10/07/13	0.19	0.12	0.48	0.14	0.08	0.24	1.54	1.00	2.77	0.69	0.26	0.41	0.21	0.20	0.04
10/09/13	0.16	0.09	0.26	0.11	0.06	0.16	1.94	1.88	2.20	1.13	1.23	0.86	0.08	0.10	0.07
11/26/13	0.10	0.09	0.16	0.07	0.06	0.13	1.75	1.45	1.60	1.03	0.95	0.88	0.09	<0.01	<0.01
12/06/13	0.12	0.08	0.12	0.06	0.04	0.06	4.51	1.67	1.96	2.11	0.86	0.80	0.89	0.10	0.15
12/09/13	0.08	0.10	0.10	0.05	0.03	0.06	3.18	1.86	2.37	2.18	1.11	1.47	0.23	0.18	0.10
12/14/13	0.09	0.09	0.10	0.04	0.03	0.06	5.04	1.77	2.47	2.55	1.02	1.50	0.17	0.11	0.06
12/22/13	0.16	0.15	0.17	0.05	0.04	0.06	3.37	2.00	2.21	1.65	0.79	0.74	0.09	0.06	0.05
12/29/13	0.18	0.12	0.17	0.08	0.06	0.10	2.19	1.34	1.56	1.05	0.58	0.66	0.09	0.06	0.05
02/03/14	0.16	0.16	0.15	0.07	0.04	0.09	2.28	2.45	1.78	1.22	1.26	0.92	0.16	0.31	0.18
02/05/14	0.11	0.07	0.08	0.05	0.03	0.05	2.83	1.87	2.11	1.67	1.39	1.41	0.14	0.20	0.17
02/18/14	0.11	0.08	0.12	0.05	0.04	0.07	1.74	1.53	1.42	0.88	1.00	0.80	0.10	0.14	0.08

Blank cells denote where water quality data were not obtained for a constituent.

Table 3-7. Event Mean Concentrations of organic carbon for monitored events.

Event Date	Event Mean Concentration					
	Total Organic Carbon (mg/L)			Dissolved Organic Carbon (mg/L)		
	CO30	CO20	CO10	CO30	CO20	CO10
10/18/12	3.0	3.4			3.4	
10/28/12	20.2	6.3	9.5	8.8	5.7	8.8
11/13/12	8.9	9.7	15.1	<8.9	9.7	11.4
12/20/12	10.2	6.7	9.8	9.7	6.4	9.3
12/26/12		5.8	7.8		5.5	<7.8
01/14/13	6.7	4.5	7.8	6.2	4.1	7.6
01/30/13	10.5	6.7	9.8	7.9	6.3	9.4
02/13/13		3.9	9.4		<4.2	8.3
02/26/13	6.6	4.2	7.3	6.3	4.1	7.2
03/06/13	5.8	4.5	8.2	5.7	4.4	7.7
04/12/13		6.6	12.5		5.7	11.7
04/19/13	9.4	5.7	10.7	8.8	<5.7	9.7
05/07/13	9.7	6.9	10.0	9.2	6.9	<10.2
06/02/13	6.8	7.3	13.3	6.3	7.2	12.3
06/06/13	5.8	5.0	9.4	<5.8	<5.0	8.1
06/09/13	10.3		10.5	9.8		9.5
06/13/13	9.3	9.5	17.7	9.0	<9.5	16.1
06/23/13	6.9	10.4	20.8	<6.9	<10.4	18.4
06/28/13	8.3	8.8	16.1	7.6	8.2	<16.1
06/30/13	8.1	8.8	15.8	<8.1	8.1	15.1
07/03/13	8.0	4.4	10.1	<8.0	<4.4	9.4
07/07/13	10.4		15.6	<10.4		14.4
07/10/13	8.8	9.2	16.0	8.1	9.1	
07/27/13	8.3	7.7	9.1	8.1	7.4	8.2

Blank cells denote where water quality data was not obtained for that constituent.

Table 3-7. Event Mean Concentrations of organic carbon for monitored events (continued).

Event Date	Event Mean Concentration (mg/L)					
	Total Organic Carbon (mg/L)			Dissolved Organic Carbon (mg/L)		
	CO30	CO20	CO10	CO30	CO20	CO10
08/13/13	6.0	6.0	11.4	5.6	5.6	<11.4
08/23/13	7.5	7.0		6.7	<7.0	
09/01/13	8.3	9.2		8.0	8.7	
09/21/13	4.6	4.7	11.0	4.5	4.6	10.6
10/07/13	12.5	6.5	12.3	7.9	6.4	11.0
10/09/13	7.3	5.0	8.7	6.7	5.5	8.6
11/26/13	5.0	5.8	8.7	<5.0	5.7	8.5
12/06/13	9.4	5.9	9.1	9.3	5.7	9.0
12/09/13	5.8	4.7	8.2	<5.8	<4.7	<8.2
12/14/13	6.8	5.3	7.7	<6.8	<5.3	7.5
12/22/13	10.1	7.4	10.2	9.8	<7.4	<10.2
12/29/13	6.7	5.1	7.7	6.7	5.1	7.3
02/03/14	7.6	6.3	7.0	7.0		7.1
02/05/14	6.9	5.3	7.1	7.1	6.3	7.0
02/18/14				6.9	5.1	7.1

Blank cells denote where water quality data were not obtained for a constituent.

Table 3-8. Event Mean Concentrations of iron and manganese for monitored events.

Event Date	Event Mean Concentration											
	Total Iron (ug/L)			Soluble Iron (ug/L)			Total Manganese (ug/L)			Soluble Manganese (ug/L)		
	CO30	CO20	CO10	CO30	CO20	CO10	CO30	CO20	CO10	CO30	CO20	CO10
10/18/12					<10						<10.0	
10/28/12				42.4	31.4	88.8				21.2	<10.0	10.5
11/13/12			156			<10			43.5	<10.0	<10.0	<10.0
12/20/12		362	200	28.6	<10	12.4		53.3	46.2	<10.0	<10.0	<10.0
12/26/12		678	292		94.6	32.4		40.6	65.1	<10.0	<10.0	<10.0
01/14/13	461	346	303	60.1	57.7	303.0	57.1	24.1	74.3	<10.0	<10.0	74.3
01/30/13	4180	2100	738	103.0	109.0	126.0	394	88.3	76.7	19.5	10.6	<10.0
02/13/13		341			<10			28.5			<10.0	
02/26/13	939	602	640	37.5	76.9	14.0	94.5	41	141	<10.0	<10.0	<10.0
03/06/13	348	345	571	141.0	90.8	108.0	24.5	19.4	139	<10.0	<10.0	<10.0
04/12/13		1330	791	337.0	204.0	57.9		74.7	792		<10.0	26
04/19/13	962	949	846		67.7	222.0	81.1	35	391	<10.0	<10.0	18.9
05/07/13	1040	1120	904	53.5	25.4	316.0	89	41.9	416	<10.0	<10.0	10.0
06/02/13	1020	200	2070	26.6	25.2	294.0	95.1	13.7	1990	<10.0	<10.0	124
06/06/13	153	197	908	10.0	24.6	140.0	11.3	<10.0	494	<10.0	<10.0	144
06/09/13	960	469	296	70.1	25.5	409.00	65.4	22.7	160	<10.0	<10.0	76.4
06/13/13				111.0	35.4	202.0						
06/23/13	192	258	1400				31.4	18.4	813	<10.0	<10.0	35.4
06/28/13	811	538	2180	16.6	46.5	79.5	66.2	32.8	1320	<10.0	<10.0	27.5
06/30/13	456	309	1880	24.1	14.6	156.0	58.4	25.5	1290	11.9	12.8	294
07/03/13	545	303	723	17.8	35.3	320	37.3	33.5	313	<10.0	10.0	140
07/07/13	250		2060	15.4		319	19.8		1080	<10.0		105
07/10/13	436	799	1790	<10.0	59.6	246	31.4	37.4	960	<10.0	<10.0	<10.0
07/27/13	760	20	768	32.6	<10.0		60.6	<10.0	482	<10.0	<10.0	

Blank cells denote where water quality data were not obtained for a constituent.

Table 3-8. Event Mean Concentrations of iron and manganese for monitored events (continued).

Event Date	Event Mean Concentration											
	Total Iron (ug/L)			Soluble Iron (ug/L)			Total Manganese (ug/L)			Soluble Manganese (ug/L)		
	CO30	CO20	CO10	CO30	CO20	CO10	CO30	CO20	CO10	CO30	CO20	CO10
08/13/13	2600	726	214	55	38	336	552	101	15.4	14.4	<10.0	24.2
08/23/13		684			17.1			39.9			<10.0	
09/01/13		847			52			138			<10.0	
09/21/13	587	2560	2210	20.2	39.5	103	158	296	780	<10.0	<10.0	34.4
10/07/13	1140	323	765	35.2	39.1	376	423	56.6	79.3	<10.0	<10.0	63.8
10/09/13	196	251	190	41.4	27.6	93.1	12.6	13.2	48.5	<10.0	<10.0	22.7
11/26/13	199	278	198	67.2	122	145	29.6	26.6	63	30.9	27.9	68.5
12/06/13	161	317	240	93.7	116	185	13.4	17	38.9	<10.0	<10.0	22.4
12/09/13	196	1340	333	72.8	136	165	26.1	44	53.5	13.8	27.1	38.9
12/14/13	124	820	164	48.4	97	106	15.1	42.2	45	<10.0	<10.0	32.5
12/22/13	448	826	308	70	99.5	97.3	33.2	39.6	63.9	<10.0	<10.0	<10.0
12/29/13		565	415		119	109		24	64.4		<10.0	<10.0
02/03/14				40.6	52.5	77.6				<10.0	<10.0	23.3
02/05/14				12.8	65.1	68.1				<10.0	<10.0	27.4
02/18/14				59.9	94.2	83.1				<10.0	<10.0	23.9

Blank cells denote where water quality data were not obtained for a constituent.

Table 3-9. Event Mean Concentrations of copper and cadmium for monitored events.

Event Date	Event Mean Concentration											
	Total Copper (ug/L)			Soluble Copper (ug/L)			Total Cadmium (ug/L)			Soluble Cadmium (ug/L)		
	CO30	CO20	CO10	CO30	CO20	CO10	CO30	CO20	CO10	CO30	CO20	CO10
10/18/12					<3.0						<1.0	
10/28/12				5.5	7.1	5.3				<1.0	<1.0	<1.0
11/13/12			<3.0			3.1			<1.0			<1.0
12/20/12		9.6	<3.0	3.0	<3.0	3.0		<1.0	<1.0	<1.0	<1.0	<1.0
12/26/12		8.9	<3.0		<3.0	4.6		<1.0	<1.0		<1.0	<1.0
01/14/13	6.8	7	<3.0	<3.0	<3.0	3.0	<1.0	<1.0	<1.0	<1.0	<1.0	<1.0
01/30/13	18.8	13.7	5.2	<3.0	5.4	3.0	<1.0	<1.0	<1.0	<1.0	<1.0	<1.0
02/13/13		7.3	<3.0		<3.0			<1.0	<1.0		<1.0	
02/26/13	10.9	10.6	3.9	3.2	3.1	<3.0	<1.0	<1.0	<1.0	<1.0	<1.0	<1.0
03/06/13	6.8	8	4.4	<3.0	4.3	<3.0	<1.0	<1.0	<1.0	<1.0	<1.0	<1.0
04/12/13		15.4	<3.0		5.7	<3.0		<1.0	<1.0		<1.0	<1.0
04/19/13	10.1	11.1	4.3	5.7	5.5	3.5	<1.0	<1.0	<1.0	<1.0	<1.0	<1.0
05/07/13	11.7	14.3	3.6	5.4	8.0	<3.0	<1.0	<1.0	<1.0	<1.0	<1.0	<1.0
06/02/13				4.3	5.1	<3.0				<1.0	<1.0	<1.0
06/06/13	14.8	4.3	<3.0	6.1	5.8	<3.0	<1.0	<1.0	<1.0	<1.0	<1.0	<1.0
06/09/13	5.5	<3.0	<3.0	7.4	8.6	<3.0	<1.0	<1.0	<1.0	<1.0	<1.0	<1.0
06/13/13	9.3	10.4	<3.0				<1.0	<1.0	<1.0			
06/23/13	7.2	10.3	6.2	6.6	7.7	5.0	<1.0	<1.0	<1.0	<1.0	<1.0	<1.0
06/28/13	9.9	9.5	<3.0	4.0	5.4	<3.0	<1.0	<1.0	<1.0	<1.0	<1.0	<1.0
06/30/13	6.5	7.1	<3.0	4.5	4.9	<3.0	<1.0	1.6	<1.0	<1.0	<1.0	<1.0
07/03/13	6.3	5.7	<3.0	<3.0	4.8	4.5	<1.0	<1.0	<1.0	<1.0	<1.0	<1.0
07/07/13	8.4		<3.0	7.3		<3.0	<1.0		<1.0	<1.0		<1.0
07/10/13	6.4	9.1	<3.0	4.0	4.5	<3.0		<1.0	<1.0	<1.0	<1.0	<1.0
07/27/13	7.1	<3.0	<3.0	4.2	4.1		<1.0	<1.0	<1.0	<1.0	<1.0	

Blank cells denote where water quality data were not obtained for a constituent.

Table 3-9. Event Mean Concentrations of copper and cadmium for monitored events (continued).

Event Date	Event Mean Concentration											
	Total Copper (ug/L)			Soluble Copper (ug/L)			Total Cadmium (ug/L)			Soluble Cadmium (ug/L)		
	CO30	CO20	CO10	CO30	CO20	CO10	CO30	CO20	CO10	CO30	CO20	CO10
08/13/13	<3.0	5.4	7.5	4.4	4	<3.0	<1.0	<1.0	<1.0	<1.0	<1.0	<1.0
08/23/13		9.4			5			<1.0			<1.0	
09/01/13		8.0			5.7			<1.0			<1.0	
09/21/13	<3.0	6.0	<3.0	3.1	<3.0	<3.0	<1.0	<1.0	<1.0	<1.0	<1.0	<1.0
10/07/13	3.9	8.5	7.8	4.7	4.5	3.0	<1.0	<1.0	<1.0	<1.0	<1.0	<1.0
10/09/13	5.4	8.1	4.4	4.7	7.5	4.2	<1.0	<1.0	<1.0	<1.0	<1.0	<1.0
11/26/13	4.6	8.4	3.1	4.9	9.6	3.7	<1.0	<1.0	<1.0	<1.0	<1.0	<1.0
12/06/13	6.5	10.5	4.4	6.9	10.4	4.8	<1.0	<1.0	<1.0	<1.0	<1.0	<1.0
12/09/13	4.5	8.6	4.9	4.6	7.8	4.6	<1.0	<1.0	<1.0	<1.0	<1.0	<1.0
12/14/13	4.9	10.2	3.6	5.4	7.6	3.9	<1.0	<1.0	<1.0	<1.0	<1.0	<1.0
12/22/13	7.3	12.4	5.2	6.4	10.4	5.1		<1.0	<1.0	<1.0	<1.0	<1.0
12/29/13		7.3	4.1		6.7	3.9					<1.0	<1.0
02/03/14				5.0	7.6	4.4				<1.0	<1.0	<1.0
02/05/14				5.2	7.2	3.8				<1.0	<1.0	<1.0
02/18/14				5.3	7.5	4.3				<1.0	<1.0	<1.0

Blank cells denote where water quality data were not obtained for a constituent.

Table 3-10. Event Mean Concentrations of chromium and lead for monitored events.

Event Date	Event Mean Concentration											
	Total Chromium (ug/L)			Soluble Chromium (ug/L)			Total Lead (ug/L)			Soluble Lead (ug/L)		
	CO30	CO20	CO10	CO30	CO20	CO10	CO30	CO20	CO10	CO30	CO20	CO10
10/18/12					<2.0						<2.0	
10/28/12				<2.0	2.7	<2.0				<2.0	<2.0	<2.0
11/13/12			<2.0			<2.0			<2.0			<2.0
12/20/12		<2.0	<2.0	<2.0	<2.0	<2.0		<2.0	<2.0	<2.0	<2.0	<2.0
12/26/12		6.8	<2.0		<2.0	<2.0		<2.0	<2.0		<2.0	<2.0
01/14/13	<2.0	<2.0	<2.0	<2.0	<2.0	<2.0	2.0	<2.0	<2.0	<2.0	<2.0	<2.0
01/30/13	6.5	4.9	<2.0	<2.0	<2.0	<2.0	8.1	3	<2.0	<2.0	<2.0	<2.0
02/13/13		2.0	<2.0		<2.0			<2.0			<2.0	
02/26/13	<2.0	2.0	<2.0	<2.0	<2.0	<2.0	<2.0	<2.0	<2.0	<2.0	<2.0	<2.0
03/06/13	<2.0	4.1	<2.0	<2.0	<2.0	<2.0	<2.0	3.3	2.2	<2.0	<2.0	<2.0
04/12/13		4.7	<2.0		<2.0	<2.0		2.3	<2.0		<2.0	2.2
04/19/13	2.1	3.3	<2.0	<2.0	<2.0	<2.0	<2.0	<2.0	<2.0	<2.0	<2.0	<2.0
05/07/13	<2.0	2.4	<2.0	<2.0	<2.0	<2.0	<2.0	<2.0	<2.0	<2.0	<2.0	<2.0
06/02/13				<2.0	<2.0	<2.0	<2.0	<2.0	<2.0	<2.0	<2.0	<2.0
06/06/13	<2.0	<2.0	<2.0	<2.0	<2.0	<2.0	<2.0	<2.0	<2.0	<2.0	<2.0	<2.0
06/09/13	2.2	<2.0	<2.0	<2.0	<2.0	<2.0	<2.0	<2.0	<2.0	<2.0	<2.0	<2.0
06/13/13	<2.0	<2.0	<2.0				<2.0	<2.0	<2.0			
06/23/13	<2.0	<2.0	4.2	<2.0	<2.0		<2.0	<2.0	<2.0	<2.0	<2.0	<2.0
06/28/13	<2.0	<2.0	<2.0	<2.0	<2.0		<2.0	<2.0	<2.0	2.5	<2.0	2.2
06/30/13	<2.0	1.6	3.4	<2.0	<2.0	<2.0	<2.0	<2.0	<2.0	3.4	<2.0	2.2
07/03/13	2.5	2.2	<2.0	<2.0	<2.0	<2.0	<2.0	<2.0	<2.0	2.2	<2.0	<2.0
07/07/13	<2.0		<2.0	<2.0		<2.0	<2.0		<2.0	<2.0		<2.0
07/10/13	<2.0	2.4	<2.0	<2.0	<2.0	<2.0	<2.0	<2.0	<2.0	<2.0	<2.0	<2.0
07/27/13	<2.0	<2.0	<2.0	<2.0	<2.0		2.2	<2.0	<2.0	<2.0	<2.0	

Blank cells denote where water quality data were not obtained for a constituent.

Table 3-10. Event Mean Concentrations of chromium and lead for monitored events (continued).

Event Date	Event Mean Concentration											
	Total Chromium (ug/L)			Soluble Chromium (ug/L)			Total Lead (ug/L)			Soluble Lead (ug/L)		
	CO30	CO20	CO10	CO30	CO20	CO10	CO30	CO20	CO10	CO30	CO20	CO10
08/13/13	<2.0	2.8	<2.0	<2.0	<2.0	<2.0	<2.0	<2.0	<2.0	<2.0	<2.0	<2.0
08/23/13		<2.0			<2.0			2.3			<2.0	
09/01/13		<2.0			<2.0			2.6			<2.0	
09/21/13	<2.0	2.6	2.0	<2.0	<2.0	<2.0	<2.0	4.4	3	<2.0	<2.0	<2.0
10/07/13	<2.0	<2.0	3.1	<2.0	<2.0	<2.0		8.5	2.9	<2.0	<2.0	<2.0
10/09/13	<2.0	5.1	<2.0	<2.0	<2.0	<2.0	<2.0	<2.0	<2.0	<2.0	<2.0	<2.0
11/26/13	<2.0	<2.0	<2.0	<2.0	<2.0	<2.0	<2.0	<2.0	<2.0	<2.0	<2.0	<2.0
12/06/13	<2.0	<2.0	<2.0	<2.0	<2.0	<2.0	<2.0	<2.0	<2.0	<2.0	<2.0	<2.0
12/09/13	<2.0	<2.0	<2.0	<2.0	<2.0	<2.0	<2.0	<2.0	<2.0	<2.0	<2.0	<2.0
12/14/13	<2.0	2.5	<2.0	<2.0	<2.0	<2.0	<2.0	<2.0	<2.0	<2.0	<2.0	<2.0
12/22/13	<2.0	2.5	<2.0	<2.0	<2.0	<2.0	<2.0	<2.0	<2.0	<2.0	<2.0	<2.0
12/29/13	<2.0	<2.0	<2.0		<2.0	<2.0		<2.0	<2.0		<2.0	<2.0
02/03/14				<2.0	<2.0	<2.0				<2.0	<2.0	<2.0
02/05/14				<2.0	<2.0	<2.0				<2.0	<2.0	<2.0
02/18/14				<2.0	<2.0	<2.0				<2.0	<2.0	<2.0

Blank cells denote where water quality data were not obtained for a constituent.

Table 3-11. Event Mean Concentrations of nickel and zinc for monitored events.

Event Date	Event Mean Concentration											
	Total Nickel (ug/L)			Soluble Nickel (ug/L)			Total Zinc (ug/L)			Soluble Zinc (ug/L)		
	CO30	CO20	CO10	CO30	CO20	CO10	CO30	CO20	CO10	CO30	CO20	CO10
10/18/12					<2.0						14.2	
10/28/12				<2.0	<2.0	<2.0				<10.0	<10.0	<10.0
11/13/12			<2.0			<2.0			<10.0			<10.0
12/20/12		<2.0	<2.0	<2.0	<2.0	<2.0		35.9	<10.0	<10.0	16.7	<10.0
12/26/12		2.5	<2.0		<2.0	<2.0		23.3	<10.0		<10.0	13.8
01/14/13	2.6	<2.0	<2.0	<2.0	<2.0	<2.0	20.6	15.9	<10.0	11.6	<10.0	<10.0
01/30/13	7.8	4.3	<2.0	<2.0	<2.0	<2.0	55.9	43.4	12.3	<10.0	10.4	<10.0
02/13/13		<2.0	<2.0		<2.0			25.5			13.4	
02/26/13	3.3	<2.0	<2.0	<2.0	<2.0	<2.0	30.7	23.9	<10.0	<10.0	<10.0	<10.0
03/06/13	<2.0	<2.0	<2.0	2.4	<2.0	<2.0	<10.0	14.2	<10.0	<10.0	11.1	<10.0
04/12/13		2.5	2.7		<2.0	2.2		65.1	<10.0		31.8	<10.0
04/19/13	3.3	<2.0	<2.0	<2.0	<2.0	<2.0	24.1	35.0	<10.0	10.4	15.1	<10.0
05/07/13	2.5	2.1	<2.0	<2.0	<2.0	<2.0	<10.0	29.1	<10.0	18.8	13.8	<10.0
06/02/13	2.6	<2.0	2.1	<2.0	<2.0	<2.0	35.8	12.5	<10.0	<10.0	18.3	<10.0
06/06/13	<2.0	<2.0	<2.0	<2.0	<2.0	<2.0	<10.0	<10.0	<10.0	<10.0	<10.0	<10.0
06/09/13	3.4	<2.0	<2.0	2.7	3.0	<2.0	11.7	<10.0	<10.0	<10.0	<10.0	<10.0
06/13/13	<2.0	<2.0	2.6				<10.0	<10.0	<10.0			
06/23/13	<2.0	<2.0	<2.0	<2.0	<2.0	<2.0	10.5	23.9	13.3	<10.0	16.5	<10.0
06/28/13	3.5	<2.0	<2.0	2.5	<2.0	2.2	55.8	53.3	11.5	25.9	35.9	<10.0
06/30/13	3.9	<2.0	<2.0	3.4	<2.0	2.2	17.7	36.9	<10.0	15.2	32.8	<10.0
07/03/13	<2.0	<2.0	<2.0	2.2	<2.0	<2.0	11.6	14.1	<10.0	<10.0	<10.0	<10.0
07/07/13	<2.0		<2.0	<2.0		<2.0	16.3		<10.0	10.9		<10.0
07/10/13	2.5	2.5	<2.0	<2.0	<2.0	<2.0	17.0	50.4	<10.0	<10.0	27.2	<10.0
07/27/13	3.1	<2.0	2.6	<2.0	<2.0		28.3	13.8	37.6	<10.0	14.7	

Blank cells denote where water quality data were not obtained for a constituent.

Table 3-11. Event Mean Concentrations of nickel and zinc for monitored events (continued).

Event Date	Event Mean Concentration											
	Total Nickel (ug/L)			Soluble Nickel (ug/L)			Total Zinc (ug/L)			Soluble Zinc (ug/L)		
	CO30	CO20	CO10	CO30	CO20	CO10	CO30	CO20	CO10	CO30	CO20	CO10
08/13/13	<2.0	<2.0	<2.0	<2.0	2.1	<2.0	<10.0	<10.0	28.4	<10.0	15.8	<10.0
08/23/13		6.0			<2.0			45.6			13.8	
09/01/13		4.0			<2.0			28.5			15.4	
09/21/13	<2.0	4.0	<2.0	3.4	<2.0	<2.0	<10.0	25.2	<10.0	18.6	<10.0	<10.0
10/07/13	2.2	8.5	2.9	4.2	<2.0	<2.0	<10.0	27.8	36.8	<10.0	<10.0	<10.0
10/09/13	<2.0	<2.0	<2.0	<2.0	<2.0	<2.0	<10.0	11.8	<10.0	<10.0	<10.0	<10.0
11/26/13	<2.0	<2.0	<2.0	<2.0	<2.0	<2.0	<10.0		<10.0	10.3	14.1	<10.0
12/06/13	<2.0	2.8	<2.0	<2.0	<2.0	<2.0	<10.0	10.8	<10.0	<10.0	10.6	<10.0
12/09/13	<2.0	<2.0	<2.0	<2.0	<2.0	<2.0	<10.0	23.1	<10.0	<10.0	18.4	<10.0
12/14/13	2.1	<2.0	<2.0	<2.0	<2.0	<2.0	<10.0	22	<10.0	<10.0	<10.0	<10.0
12/22/13	2.1	<2.0	<2.0	<2.0	<2.0	<2.0	<10.0	23	<10.0	<10.0	18.4	<10.0
12/29/13		<2.0	<2.0		<2.0	<2.0		13.8	<10.0		<10.0	<10.0
02/03/14				<2.0	<2.0	<2.0				<10.0	10.1	<10.0
02/05/14				<2.0	<2.0	<2.0				<10.0	<10.0	<10.0
02/18/14				<2.0	<2.0	<2.0				<10.0	<10.0	<10.0

Blank cells denote where water quality data were not obtained for a constituent.

Table 3-12. Micropool concentrations for solids.

Collection Date	Concentration														
	Total Suspended Solids (mg/L)			Suspended Sediment Concentration (mg/L)			Total Dissolved Solids (mg/L)			Specific Conductance (µmhos/cm@25°C)			Turbidity (NTU)		
	CO60	CO50	CO40	CO60	CO50	CO40	CO60	CO50	CO40	CO60	CO50	CO40	CO60	CO50	CO40
11/28/12	2.0	<1.0	<1.0	3.8	0.5	2.2	151.0	86.0	70.0	295	177	145	6.0	0.7	0.8
12/17/12	33.6	<1.0	1.2	11.6	<1.0	0.4	181.0	137.0	101.0	380	265	203	10.3	1.0	0.9
01/14/13	124.0	8.4	2.4	130.9	7.7	3.4	197.0	179.0	188.0	348	316	334			
02/11/13	4.0	5.2	2.4	7.7	6.8	3.2	311.0	186.0	170.0	25	295	267	4.9	9.7	3.6
03/11/13	182.0	42.8	8.4	201.8	24.4	9.6	189.0	191.0	195.0	315	308	311	212.0	45.5	20.7
04/08/13	208.0	8.0	26.7	206.6	22.4	8.5	223.0	320.0	283.0	341	443	511	202.0	28.6	6.8
05/13/13	65.2	5.2	15.6	46.1	10.1	12.4	133.0	94.0	87.0	211	139	131	27.4	10.4	7.7
06/18/13	212.0	19.3	25.0	207.9	14.7	15.7	143.0	140.0	124.0	204	189	184	134.0	26.6	28.6
07/02/13	5340.0	86.7	19.0	20956.6	77.4	23.7	84.0	78.0	100.0	150	139	171		24.4	9.6
08/14/13	212.0	68.7	246.0	260.3	28.0	46.0	71.0	69.0	91.0	233	161	147	23.2	9.5	3.3
09/17/13		2490.0	131.0		2504.0	149.2		131.0	115.0		166	166		680.0	27.5
10/17/13	166.0	24.7	52.0	444.6	16.0	49.0	148.0	121.0	117.0	217	152	154	40.4	4.9	4.3
11/14/13		518.0	3.6		160.0	121.0		160.0	121.0		234	168			
11/26/13	1140.0	26.0	25.2	114.0	129.0	107.0	114.0	129.0	107.0	225	201	192	353.0	7.0	1.7
11/27/13	36.8	32.0	6.4	77.0	52.0	90.0	77.0	52.0	90.0				28.9	18.4	17.9
12/05/13	28.8	7.0	3.0							123	151	146		6.7	4.1
12/11/13	60.4	89.3	17.2	150.0	14.3	3.7	333.0	299.0	331.0	496	508	582	30.1	47.2	26.9
12/19/13	12.0	<1.0	1.2	32.0	0.5	<1.0	111.0	205.0	191.0	149	368	251	11.0	7.0	7.8
01/02/14	2.4	14.4	<1.0	3.8	2.6	<1.0	155.0	118.0	115.0	298	188	193	3.7	12.1	9.6
01/09/14	206.0	7.6	4.4	175.8	1.9	2.1	123.0	573.0	391.0	184	110	792	30.0	9.0	6.7
01/15/14	26.4	6.4	1.6	7.5	5.3	2.6	108.0	155.0	164.0	159	261	267	22.3	10.1	8.3
02/20/14	8.0	1.6	<1.0	1.3	4.4	0.9	117.0	227.0	210.0	341	418	359	13.0	13.8	15.4

Blank cells denote where water quality data were not obtained for a constituent.

Table 3-13. Micropool concentrations for nutrients.

Collection Date	Concentration														
	Total Phosphorus (mg/L)			Orthosphophate Phosphorus (mg/L)			Total Nitrogen (mg/L)			Oxidized Nitrogen (mg/L)			Ammonia Nitrogen (mg/L)		
	CO60	CO50	CO40	CO60	CO50	CO40	CO60	CO50	CO40	CO60	CO50	CO40	CO60	CO50	CO40
11/28/12	0.07	0.03	0.05	0.02	0.01	0.02	1.54	0.6	0.6	0.73	0.01	<0.01	0.16	0.03	0.02
12/17/12	0.13	0.04	0.06	0.05	0.01	0.02	1.59	0.68	0.77	0.01	<0.01	<0.01	0.03	0.02	0.02
01/14/13	0.56	0.09	0.05	0.02	0.01	0.01	5.14	0.93	0.67	0.03	<0.01	<0.01	0.09	0.02	0.02
02/11/13	0.04	0.06	0.05	0.03	0.02	0.02	0.78	0.88	0.74	0.38	0.13	0.03	0.02	0.01	0.01
03/11/13	0.7	0.34	0.13	0.02	0.03	0.03	6.38	3.19	1.29	0.54	0.4	0.22	0.19	0.02	0.02
04/08/13	0.96	0.18	0.28	0.02	0.06	0.03	7.29	1.29	2.18	<0.01	<0.01	<0.01	0.03	0.08	0.02
05/13/13	0.26	0.78	0.45	0.07	0.22	0.24	2.41	1.55	1.8	<0.01	<0.01	<0.01	0.09	0.07	0.06
06/18/13	0.46	0.36	0.53	0.04	0.08	0.11	4.33	2.18	2.5	0.02	0.01	0.01	0.04	0.16	0.02
07/02/13		0.63	0.43	0.05	0.1	0.17		4.81	2.24	<0.01	<0.01	<0.01	0.11	0.04	0.06
08/14/13	0.51	0.48	0.75	0.21	0.14	0.13	4.58	3.26	5.31	0.01	<0.01	<0.01	0.11	0.05	0.03
09/17/13		0.5	0.4		0.06	0.12		5.65	4.78		<0.01	<0.01		0.08	0.04
10/17/13	0.94	0.28	0.5	0.13	0.09	0.13	5.05	1.87	2.79	<0.01	<0.01	<0.01	0.02	0.03	0.04
11/14/13		1.35	0.06		0.04	0.04		7.28	0.85		<0.01	0.02		0.07	0.02
11/26/13		0.21	0.27	0.04	0.1	0.18	17.5	1.57	1.51	0.02	0.01	0.01	<0.01	<0.01	<0.01
11/27/13	0.27	0.3	0.31	0.17	0.17	0.21	3.8	2.94	31.7	2.08	1.65	1.54	<0.01	<0.01	<0.01
12/05/13	0.61	0.12	0.09	0.06	0.03	0.04	2.92	2.51	1.75	<0.01	1.18	0.62	0.02	0.05	0.04
12/11/13	0.38	0.3	0.2	0.14	0.08	0.06	2.85	3.29	2.98	1.47	0.33	1.13	0.04	0.03	0.03
12/19/13	0.22	0.04	0.13	0.07	0.03	0.03	0.81	2.8	2.19	0.05	2.06	1.11	0.03	0.02	0.02
01/02/14	0.06	0.08	0.07	0.03	0.03	0.04	2.62	1.86	1.79	1.8	0.99	0.87	0.03	0.02	0.03
01/09/14	0.53	0.08	0.05	0.02	0.02	0.02	6.88	2.76	1.11	1.92	1.71	0.22	<0.01	<0.01	0.03
01/15/14	0.29	0.07	0.05	0.09	0.03	0.03	1.35	1.88	1.8	0.07	1.19	1.16	<0.01	<0.01	<0.01
02/20/14	0.12	0.09	0.08	0.07	0.06	0.05	2.09	2.23	1.87	1.32	1.48	1.21	0.09	0.06	0.08

Blank cells denote where water quality data were not obtained for a constituent.

Table 3-14. Micropool concentrations for organic carbon.

Collection Date	Concentration					
	Total Organic Carbon (mg/L)			Dissolved Organic Carbon (mg/L)		
	CO60	CO50	CO40	CO60	CO50	CO40
11/28/12	5.7	7.2	7.3	5.4	7.1	7
12/17/12	6.4	7.2	7.6		7.2	7.5
01/14/13	8.1	7.8	7.8	7.2	7.1	7.6
02/11/13	6.1	7.7	8.7	5.4	7.4	8.4
03/11/13	8	11.2	9.9	7.6	8	8.9
04/08/13	10.4	10.6	10.4	10.1	10	9.3
05/13/13	14.4	14.7	14.3	13.7	13.8	13.7
06/18/13	13.6	16.7	15.6	13.2	15.9	14.2
07/02/13	32.5	18.2	14.2	10.4	15.4	13.6
08/14/13	12.7	11.5	10.9	9	8.7	8.9
09/17/13		43.7	17.3		15.7	13.7
10/17/13	16.6	13.7	13.3	13.2	13.5	11.4
11/14/13		22.9	14.8		20.1	12.4
11/26/13	22		16.8	15.9	13.4	13.2
11/27/13	16.9	11.9	16.6	14.9	12.5	18.8
12/05/13	16.8	11.5	10.9	12.5	10.2	10.6
12/11/13	12.2	12.6	7	<12.2	<12.6	6.9
12/19/13	9.9	8	10.4	6.7	<8	9.6
01/02/14	6.7	10.2	10.6	6.7	<10.2	10.7
01/09/14	8.2	9.9	9.4	7.8	9.3	<9.4
01/15/14	10.2	7	7.1	9.7	6.8	6.5
02/20/14						

Blank cells denote where water quality data were not obtained for a constituent.

Table 3-15. Micropool concentrations for iron and manganese.

Collection Date	Concentration											
	Total Iron (ug/L)			Soluble Iron (ug/L)			Total Manganese (ug/L)			Soluble Manganese (ug/L)		
	CO60	CO50	CO40	CO60	CO50	CO40	CO60	CO50	CO40	CO60	CO50	CO40
11/28/12	367	14.4	41.8	125	<10	<10	172	<10	<10	<10	<10	<10
12/17/12	660	60	37.9	22.6	12.9	<10	113	<10	<10	<10	<10	<10
01/14/13	3120	294	181	3120	124	50.1	1150	95.7	29.8	1150	75.3	26.7
02/11/13	88	262	142	33.2	151	89.2	28.4	61.1	46.6	22.9	41.8	42.1
03/11/13	3320	965	497	483	185	158	674	183	107	321	76	46.7
04/08/13	3710	1000	604	419	330	174	451	254	401	42	63.1	103
05/13/13	1240	1680	1360	775	1440	1130	229	369	350	165	191	224
06/18/13	5750	1420		656	963	650	289	1260	<10	142	982	1210
07/02/13			2330	740	86	259	4190		1350	559	51.7	109
08/14/13	2040	1500	2380			573	250	481	567	<10	13.7	37.1
09/17/13		667	1240		1510	484		39.2	701		276	36.9
10/17/13	3940	558	1310	31.1	138	57.9	889	162	720	11.6	47.1	28.3
11/14/13		182	293		28.7	76.1		93.6	110		12.2	25.1
11/26/13	3180	397	132	1610	27.1	52	815	135	83.3	80.8	<10	25
11/27/13	279	289	248		188	110	30.5	80.8	20.5		87.6	<10
12/05/13												
12/11/13	1580	761	629	803	245	258	483	98.2	116	493	77.1	106
12/19/13	1530	96.5	378	768	79.7	81.1	436	22.8	31.2	21.9	<10	<10
01/02/14				49.6	142	88.5				<10	<10	<10
01/09/14				997	113	116				270	18.2	<10
01/15/14				651	167	222				182	16.2	45.1
02/20/14												

Blank cells denote where water quality data were not obtained for a constituent.

Table 3-16. Micropool concentrations for copper and cadmium.

Collection Date	Concentration											
	Total Copper (ug/L)			Soluble Copper (ug/L)			Total Cadmium (ug/L)			Soluble Cadmium (ug/L)		
	CO60	CO50	CO40	CO60	CO50	CO40	CO60	CO50	CO40	CO60	CO50	CO40
11/28/12	<3.0	<3.0	<3.0	<3.0	<3.0	<3.0	<1.0	<1.0	<1.0	<1.0	<1.0	<1.0
12/17/12	<3.0	<3.0	<3.0	<3.0	<3.0	<3.0	<1.0	<1.0	<1.0	<1.0	<1.0	<1.0
01/14/13	5.6	<3.0	<3.0	5.6	<3.0	<3.0	<1.0	<1.0	<1.0	<1.0	<1.0	<1.0
02/11/13	<3.0	<3.0	5.0	<3.0	<3.0	<3.0	<1.0	<1.0	<1.0	<1.0	<1.0	<1.0
03/11/13	7.4	4.2	3.4	<3.0	<3.0	<3.0	<1.0	<1.0	<1.0	<1.0	<1.0	<1.0
04/08/13	7.0	<3.0	<3.0	<3.0	<3.0	<3.0	<1.0	<1.0	<1.0	<1.0	<1.0	<1.0
05/13/13	8.5	3.1	<3.0	3.1	<3.0	<3.0	<1.0	<1.0	<1.0	<1.0	<1.0	<1.0
06/18/13	4.8	<3.0	<3.0	<3.0	<3.0	<3.0	<1.0	<1.0	<1.0	<1.0	<1.0	<1.0
07/02/13			<3.0	4.5	<3.0	<3.0	2.4		<1.0	<1.0	<1.0	<1.0
08/14/13	8.1	3.1	<3.0	<3.0	<3.0	<3.0	<1.0	<1.0	<1.0	<1.0	<1.0	<1.0
09/17/13		10.4	<3.0	<3.0	<3.0	<3.0	<1.0	<1.0	<1.0		<1.0	<1.0
10/17/13	13	3.6	10	<3.0	3.4	<3.0		<1.0	<1.0	<1.0	<1.0	<1.0
11/14/13		<3.0	<3.0		<3.0	<3.0	<1.0	<1.0	<1.0		<1.0	<1.0
11/26/13	<3.0	<3.0	<3.0	<3.0	<3.0	<3.0		<1.0	<1.0	<1.0	<1.0	<1.0
11/27/13	5	6.4	5.2	9.3	5.3	5.5	<1.0	<1.0	<1.0	<1.0	<1.0	
12/05/13							<1.0	<1.0	<1.0			<1.0
12/11/13	4.1	5.5	4.5	<3.0	5.1	4.5				<1.0	<1.0	<1.0
12/19/13	<3.0	3.5	44.7	<3.0	3.7	3.8	<1.0	<1.0	<1.0	<1.0	<1.0	<1.0
01/02/14				<3.0	4.3	4.7	<1.0	<1.0	<1.0	<1.0	<1.0	<1.0
01/09/14				<3.0	4.2	3.4				<1.0	<1.0	<1.0
01/15/14				<3.0	3.3	3.6				<1.0	<1.0	
02/20/14												

Blank cells denote where water quality data were not obtained for a constituent.

Table 3-17. Micropool concentrations for chromium and lead.

Collection Date	Concentration											
	Total Chromium (ug/L)			Soluble Chromium (ug/L)			Total Lead (ug/L)			Soluble Lead (ug/L)		
	CO60	CO50	CO40	CO60	CO50	CO40	CO60	CO50	CO40	CO60	CO50	CO40
11/28/12	<2.0	<2.0	<2.0	<2.0	<2.0	<2.0	<2.0	<2.0	<2.0	<2.0	<2.0	<2.0
12/17/12	<2.0	<2.0	<2.0	<2.0	<2.0	<2.0	<2.0	<2.0	<2.0	<2.0	<2.0	<2.0
01/14/13	2.8	<2.0	<2.0	2.8	<2.0	<2.0	3.6	<2.0	<2.0	3.6	<2.0	<2.0
02/11/13	<2.0	<2.0	<2.0	<2.0	<2.0	<2.0	<2.0	<2.0	<2.0	<2.0	<2.0	<2.0
03/11/13	4.4	<2.0	<2.0	<2.0	<2.0	<2.0	4	<2.0	<2.0	<2.0	<2.0	<2.0
04/08/13	3.5	<2.0	<2.0	<2.0	<2.0	<2.0	4.7	<2.0	<2.0	<2.0	<2.0	<2.0
05/13/13	<2.0	<2.0	<2.0	<2.0	<2.0	<2.0	<2.0	<2.0	<2.0	<2.0	<2.0	<2.0
06/18/13	4.8	<2.0	<2.0	<2.0	<2.0	<2.0	3.8	<2.0	<2.0	<2.0	<2.0	<2.0
07/02/13			<2.0			<2.0			<2.0	<2.0	<2.0	<2.0
08/14/13	3.7	<2.0	<2.0	<2.0	<2.0	<2.0	4.4	<2.0	<2.0	<2.0	<2.0	<2.0
09/17/13		<2.0	<2.0		<2.0	<2.0		<2.0	<2.0		<2.0	<2.0
10/17/13	4.6	<2.0	<2.0	<2.0	<2.0	<2.0	7	<2.0	<2.0	<2.0	<2.0	<2.0
11/14/13		<2.0	<2.0		<2.0	<2.0		<2.0	<2.0		<2.0	<2.0
11/26/13	<2.0	<2.0	<2.0	<2.0	<2.0	<2.0	<2.0	<2.0	<2.0	<2.0	<2.0	<2.0
11/27/13	<2.0	<2.0	<2.0	<2.0	<2.0	<2.0	<2.0	<2.0	<2.0	<2.0	<2.0	<2.0
12/05/13				<2.0	<2.0	<2.0						
12/11/13	<2.0	<2.0	<2.0	<2.0	<2.0	<2.0	<2.0	<2.0	<2.0	<2.0	<2.0	<2.0
12/19/13	<2.0	<2.0	<2.0	<2.0	<2.0	<2.0	<2.0	<2.0	5.6	<2.0	<2.0	<2.0
01/02/14				<2.0	<2.0	<2.0				<2.0	<2.0	<2.0
01/09/14				<2.0	<2.0	<2.0				<2.0	<2.0	<2.0
01/15/14				<2.0	<2.0	<2.0				<2.0	<2.0	<2.0
02/20/14				<2.0	<2.0	<2.0				<2.0	<2.0	<2.0

Blank cells denote where water quality data were not obtained for a constituent.

Table 3-18. Micropool concentrations for nickel and zinc.

Collection Date	Concentration											
	Total Nickel (ug/L)			Soluble Nickel(ug/L)			Total Zinc (ug/L)			Soluble Zinc (ug/L)		
	CO60	CO50	CO40	CO60	CO50	CO40	CO60	CO50	CO40	CO60	CO50	CO40
11/28/12	<2.0	<2.0	<2.0	<2.0	<2.0	<2.0	<10.0	<10.0	<10.0	<10.0	<10.0	<10.0
12/17/12	<2.0	<2.0	<2.0	<2.0	<2.0	<2.0	<10.0	<10.0	<10.0	<10.0	<10.0	<10.0
01/14/13	2.3	<2.0	<2.0	<2.0	<2.0	<2.0	19.6	<10.0	<10.0	19.6	<10.0	<10.0
02/11/13	<2.0	<2.0	<2.0	<2.0	<2.0	<2.0	<10.0	<10.0	<10.0	<10.0	<10.0	<10.0
03/11/13	<2.0	<2.0	<2.0	<2.0	<2.0	<2.0	<10.0	<10.0	<10.0	<10.0	<10.0	<10.0
04/08/13	3	<2.0	<2.0	<2.0	<2.0	<2.0	19.8	<10.0	<10.0	<10.0	<10.0	<10.0
05/13/13	3.7	<2.0	<2.0	<2.0	<2.0	<2.0	<10.0	<10.0	<10.0	<10.0	<10.0	<10.0
06/18/13	3.6	<2.0	<2.0	<2.0	<2.0	<2.0	13	<10.0	<10.0	13	<10.0	<10.0
07/02/13	75.9		<2.0	<2.0	<2.0	<2.0		<10.0			<10.0	
08/14/13	3.5	<2.0	<2.0	<2.0	<2.0	<2.0	23.3	<10.0	<10.0	<10.0	<10.0	<10.0
09/17/13		<2.0	<2.0		<2.0	<2.0	<10.0	55.8	<10.0	<10.0	<10.0	<10.0
10/17/13	5.2	<2.0	4.2	<2.0	<2.0	<2.0	45.3	<10.0	22.9	<10.0	<10.0	<10.0
11/14/13		<2.0	<2.0		<2.0	<2.0		<10.0	<10.0		<10.0	<10.0
11/26/13	<2.0	2.8	<2.0	<2.0	<2.0	<2.0	13.6	<10.0	<10.0	<10.0	<10.0	<10.0
11/27/13	<2.0	<2.0	<2.0	<2.0	<2.0	<2.0	<10.0	11.3	<10.0	15.6	<10.0	<10.0
12/05/13												
12/11/13	2.1	2.7	<2.0	<2.0	<2.0	<2.0	<10.0	<10.0	<10.0	<10.0	<10.0	<10.0
12/19/13	<2.0	3.2	2.5	<2.0	<2.0	<2.0	<10.0	<10.0	40.4	<10.0	<10.0	<10.0
01/02/14				<2.0	<2.0	<2.0				<10.0	<10.0	<10.0
01/09/14				8.8	<2.0	<2.0				<10.0	<10.0	<10.0
01/15/14				<2.0	<2.0	<2.0				<10.0	<10.0	<10.0
02/20/14				2.1	<2.0	<2.0						

Blank cells denote where water quality data were not obtained for a constituent.

Table 3-19. Micropool field data.

Collection Date	Temperature (°C)			Dissolved Oxygen (mg/l)			Specific Conductance (µmhos/cm@25°C)			pH			Alkalinity (mg/l CaCO3)		
	CO60	CO50	CO40	CO60	CO50	CO40	CO60	CO50	CO40	CO60	CO50	CO40	CO60	CO50	CO40
11/7/2012	4.7	4.9	5.7	10.3	12.9	12.7	263	204	177	6.7	6.8	6.9	55.7	43.9	40.9
11/14/2012	6.5	6.7	7.5	3.0	9.1	9.0	112	91	122	7.2	7.1	6.5	34.2	33.6	60.5
11/20/2012	8.7	7.3	7.4	8.5	16.0	13.8	235	130	118	6.8	7.4	6.9	50.7	36.0	34.7
11/28/2012	5.5	5.8	5.7	9.8	16.8	11.6	295	177	145	6.7	7.5	7.2	53.1	43.5	42.6
12/5/2012	10.1	9.7	9.6	11.7	11.8	9.4	361	226	176	6.6	6.6	6.7	59.1	46.9	42.7
12/11/2012	10.3	10.2	9.9	15.2	11.2	8.5	339	235	176	7.4	7.4	7.1	67.8	55.6	50.1
12/17/2012	8.4	7.5	7.1	10.6	11.1	9.2	380	265	203	6.8	6.6	6.3	58.6	55.0	49.7
1/8/2013	4.8	4.5	4.3	11.2	19.4	16.7	329	337	335	6.3	6.5	6.6	53.6	48.8	45.5
1/14/2013	10.9	9.3	8.2	4.6	14.8	14.2	348	316	334	6.6	6.6	6.6	64.0	49.3	47.4
1/23/2013	2.4	2.4	2.4	19.2	18.3	16.6	348	244	216	6.9	7.1	7.2	67.6	54.9	49.1
1/28/2013	0.4	0.3	0.7	15.4	14.9	18.1	195	161	246	6.5	6.7	6.7	30.4	32.1	50.1
2/5/2013	2.7	2.9	3.3	15.7	19.1	17.5	336	304	268	6.3	6.5	6.8	39.6	38.0	36.2
2/11/2013	5.6	4.5	5.2	10.4	17.7	17.0	25	295	267	7.1	7.1	7.2	50.9	39.2	38.6
2/19/2013	2.8	3.1	4.3	17.3	19.3	18.1	311	347	351	7.5	7.9	7.5	28.1	34.6	32.3
2/25/2013	4.2	4.3	5.3	9.7	14.5	14.3	418	320	338	7.1	7.3	7.4	48.1	40.7	39.8
3/4/2013	9.1	5.8	7.5	14.7	16.8	15.8	292	238	225	7.1	7.7	7.6	51.2	41.8	40.6
3/11/2013	8.6	8.7	8.7	5.9	13.4	11.5	315	308	311	6.7	7.3	7.1	45.3	40.8	41.8
3/25/2013	5.1	5.5	6.4	8.6	13.3	10.5	549	360	346	7.0	7.2	7.0	42.1	39.6	38.5
4/1/2013	10.1	10.4	10.7	4.0	14.3	13.6	455	635	653	6.9	7.6	7.3	54.9	43.4	43.0
4/8/2013	13.5	15.7	15.4	8.2	12.6	7.9	341	443	511	7.0	7.6	7.0	53.8	47.6	54.2
4/15/2013	16.1	17.0	16.7	13.8	7.8	4.5	233	233	359	6.9	6.6	6.4	70.2	70.2	56.9

Blank cells denote where water quality data were not obtained for a constituent.

Table 3-19. Micropool field data (continued).

Collection Date	Temperature (°C)			Dissolved Oxygen (mg/l)			Specific Conductance (µmhos/cm@25°C)			pH			Alkalinity (mg/l CaCO3)		
	CO60	CO50	CO40	CO60	CO50	CO40	CO60	CO50	CO40	CO60	CO50	CO40	CO60	CO50	CO40
4/22/2013	9.9	13.1	13.3	4.8	5.0	4.6	163	123	118	6.6	6.8	6.7	44.7	36.3	36.4
4/30/2013	16.1	15.7	16.0	1.1	1.8	3.6	269	208	211	6.8	6.8	6.8	70.5	60.1	68.1
5/6/2013	17.5	16.5	17.5	1.5	2.7	3.2	336	223	224	6.7	6.8	6.9	117.7	65.6	68.8
5/13/2013	16.5	18.4	18.2	2.5	2.5	5.2	211	139	131	6.5	6.6	6.6	53.1	42.6	40.1
5/20/2013	22.4	21.6	20.7	0.6	0.3	2.9	245	261	185	6.5	6.6	6.4	121.1	86.2	50.2
6/3/2013	20.3	21.1	21.4	2.0	1.9	2.2	190	170	170	6.1	6.1	6.1	53.2	54.3	54.3
6/18/2013	21.6	21.9	21.9	0.4	0.3	0.5	204	189	184	6.6	6.3	6.4	65.5	57.5	59.3
6/24/2013	26.1	26.4	26.2	1.1	2.0	2.8	254	207	213	6.7	6.7	6.6	68.6	62.3	64.5
6/28/2013	26.0	24.2	23.6	3.5	4.0	4.4	336	477	218	6.6	6.6	6.7	90.3	68.2	74.9
7/1/2013	23.6	24.0	23.5	0.3	0.8	1.4	116	155	182	6.1	6.2	6.4	21.1	37.1	54.1
7/2/2013	25.0	24.7	24.3	0.1	0.4	0.3	150	139	171	6.3	6.3	6.4	80.6	38.2	49.2
7/8/2013	26.7	24.7	24.2	2.0	0.2	1.0	145	129	119	6.2	6.2	6.2	67.3	57.4	52.1
7/15/2013	30.2	30.2	25.9	0.1	0.4	1.2	232	172	162	6.4	6.4	6.4	46.7	46.7	38.9
7/23/2013	27.8	26.7	27.6	2.7	0.3	1.2	165	237	216	6.3	6.3	6.5	45.7	54.7	45.4
7/29/2013	26.3	26.1	27.1	4.3	1.4	0.1	147	112	157	6.5	6.4	6.4	52.3	37.4	45.2
8/14/2013	26.9	29.4	31.2	0.1	0.4	0.1	233	161	147	6.5	6.3	6.6	56.3	58.4	50.1
8/19/2013	19.5	19.9	20.4	0.1	0.4	0.7	206	115	133	6.4	6.2	6.5			
8/26/2013	23.9	24.1	27.5	0.3	0.3	1.7	190	144	120	6.4	6.1	6.2	48.6	41.5	43.6
9/5/2013	25.7	27.6	25.6	0.1	1.6	0.6	180	137	160	6.9	6.4	6.3	54.2	49.8	60.0

Blank cells denote where water quality data were not obtained for a constituent.

Table 3-19. Micropool field data (continued).

Collection Date	Temperature (°C)			Dissolved Oxygen (mg/l)			Specific Conductance (µmhos/cm@25°C)			pH			Alkalinity (mg/l CaCO3)		
	CO60	CO50	CO40	CO60	CO50	CO40	CO60	CO50	CO40	CO60	CO50	CO40	CO60	CO50	CO40
9/12/2013		25.1	24.3		0.7	0.1		175	163		6.4	6.4		50.1	57.6
9/17/2013		16.8	16.2		0.1	1.0		166	166		6.5	6.5		60.9	58.5
9/26/2013	14.2	16.1	15.7		1.0	0.9	340	122	112	7.2	6.3	6.2	36.2	31.6	36.5
10/3/2013		18.4	16.6		1.34	0.37		153	130		6.4	6.2		51.2	45.9
10/17/2013	16.4	16.4	17.1	2.66	0.79	0.67	217	152	154	6.8	6.8	6.5	51.6	45.4	42.3
10/24/2013	5.8	8.3	10.8	4.68	0.18	8.91	270	178	155	6.9	6.5	6.6	54.7	54.7	58.3
10/31/2013		12.2	13.3		0.5	2.18		191	163		6.5	7			
11/7/2013	12.6	11.7	13.5	1.71	1.42	0.32	306	199	162	6.9	6.7	6.6	75.2	63.8	66.8
11/14/2013		1.7	6.3		0.21	0.17		234	168		6.7	6.7		53.6	53.6
11/21/2013	4.2	5.3	6.5	2.14	0.11	2.01	191	185	183	6.9	6.5	6.7	43.5	47.8	59.2
11/26/2013	0.8	1.9	2.7	0.21	0.24	1.18	225	201	192	6.5	6.8	6.6	60.2	55.7	55.3
12/5/2013	13.8	9.0	10.1	14.2	5.45	11.0	123	151	146	6.7	6.5	7	29.9	33.6	47.5
12/11/2013	0.6	3.1	4.3	8.45	9.76	10.3	496	508	582	6.8	6.6	6.9	42.6	40.1	37.7
12/19/2013	5.2	3.5	5.5	5.21	11.5	13.2	149	368	251	6.2	6.9	6.8	35	49.1	41.6
1/2/2014	2.2	3.6	3.6	10.3	12.4	13.6	298	188	193	6.4	6.6	6.7	35.6	38.3	37.8
1/9/2014	4.3	1.9	2.5	8.82	15.9	17.1	184	110	792	5.3	6.9	7.1	38.2	43.4	43.4
1/15/2014	6.4	4	6.4	6.73	10.7	9.3	159	261	267	6.4	6.4	6.7	26.4	32	38.4
2/20/2014	3.0	3.0	2.2	9.72	11.1	11.4	341	418	359	6.3	6.5	6	21.6	25.8	25.4

Blank cells denote where water quality data was not obtained for a constituent.

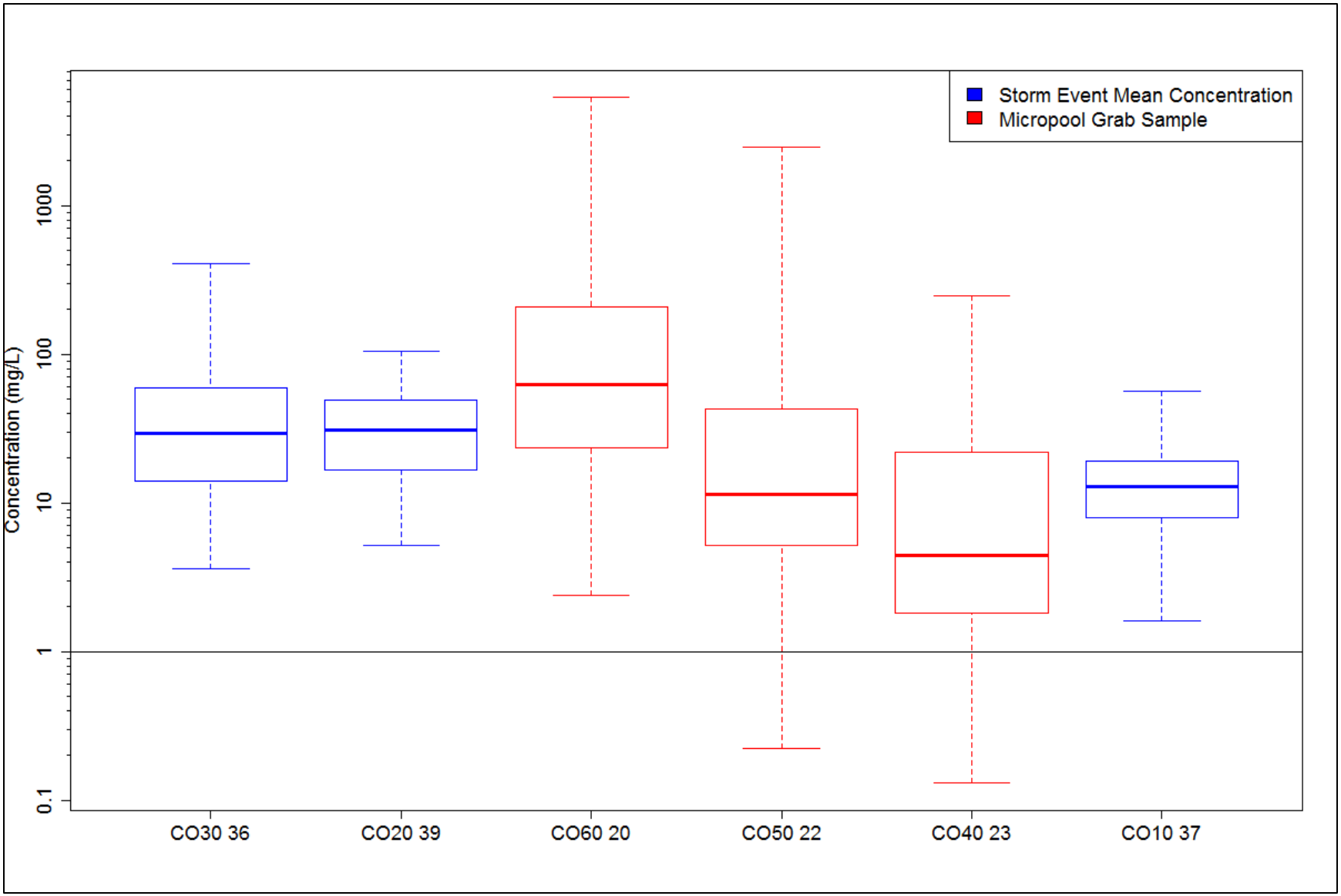

Figure 3-8. Boxplots of influent and effluent event mean concentrations and micropool grab samples for TSS.

3.4.4 Water Quality Pollutant Loads Analysis

3.4.4.1 Storm Event Constituent Loads

A summary of the calculated constituent loads is presented in Tables 3-20 through 3-25. The calculated influent and effluent load data sets were used in assessments of BMP performance with both the Effluent Probability Method and Summation of Loads methods.

3.4.4.2 Influent and Effluent Distributional Adherence Tests

Determining the underlying distribution of the loading datasets is the first important to step to using the Effluent Probability Method. Figure 3-9 and Figure 3-10 show ROS Q-Q plots of influent and effluent loads TSS, respectively. The Q-Q plot on the left displays the untransformed dataset against a theoretical normal distribution line. If the dataset closely follows the normal distribution line, then it may be assumed that data are normally distributed. The Q-Q plot on the right displays the log transformed data against a theoretical lognormal distribution line. If the dataset is closely approximated with the log-normal line, then it can be assumed that dataset has a log-normal distribution.

As shown in the Q-Q plots for TSS, influent and effluent loads fit well with the log-normal transformation. The log-normal transformation was also found to be satisfactory for the other monitored constituents as well. Therefore, the EPM analysis was conducted with log transformations for all constituents. Q-Q plots for all constituents may be found in Appendix E.

3.4.4.3 Summation of Loads Results

A summary of constituent removals using the Summation of Loads method is shown in Table 3-26. Only storm events with data from all three monitoring stations were used for this analysis. Positive % removal values indicate a net decrease of pollutant loads. Negative % removal values indicate a net increase of pollutant loads.

3.4.4.4 Effluent Probability Method Plots

EPM plots for all constituents are displayed in Appendix D. The EPM plot for TSS is shown in Figure 3-11. If the effluent data are to the left of the influent data, then the BMP reduced constituent loads at the given percentile. If the effluent data are to the right of the influent data, then the BMP exported constituent loads at the given percentile. Table 3-27 displays the results

of the generalized Wilcoxon test. A p-value less than 0.05 indicates that the influent and effluent loads are statistically significantly different. Table 3-28 displays a summary of the load reductions at the minimum, 10^{th}, 30^{th}, 50^{th}, 70^{th}, 90^{th}, and maximum percentiles from the EPM plots.

Table 3-20. Solids loads for monitored storm events.

Date	Pollutant Loads (lbs)																	
	Total Suspended Solids						Suspended Sediment Concentration						Total Dissolved Solids					
	CO30	CO20	Direct Catch	Ungaged	Total In	CO10	CO30	CO20	Direct Catch	Ungaged	Total In	CO10	CO30	CO20	Direct Catch.	Ungaged	Total In	CO10
10/18/12	5.17	13.07	--	0.07	18.31				--	0.09			0.00	6.08	0.33	0.20		
10/28/12	877.46	54.25	--	25.02	956.73	72.98	1035.11	68.55	--	30.28	1133.93	64.20	227.61	190.61	3.84	68.47	418.22	556.01
11/13/12	0.82	2.52	--	0.42	3.76	0.87			--	0.51		0.88	0.00	16.06	0.53	1.16		32.08
12/20/12	20.94	10.16	--	0.54	31.64	3.59		25.43	--	0.65		1.91	8.93	16.38	0.70	1.47	25.31	49.39
12/26/12		28.15	--	2.60		24.54		32.31	--	3.15		24.18	0.00	444.44	1.34	7.11		604.39
01/14/13	10.66	8.93	--	0.89	20.48	5.50	11.12	7.00	--	1.08	19.20	6.06	23.50	26.57	0.77	2.44	50.07	102.72
01/30/13	384.07	126.82	--	3.20	514.08	87.55	881.88	141.04	--	3.87	1026.79	96.01			1.49	8.75		
02/13/13		2.37	--	0.00		1.33	0.00	2.34	--	0.01				34.14	0.30	0.01		20.37
02/26/13	15.98	14.95	--	0.31	31.24	7.48	25.53	19.96	--	0.37	45.86	3.86	13.40	42.51	0.67	0.84	55.91	49.10
03/06/13	8.52	8.54	--	1.47	18.54	32.18	14.72	14.93	--	1.78	31.44	35.32	44.89	285.78	1.46	4.03	330.67	363.83
04/12/13		14.54	--	0.10		3.19		17.57	--	0.12		2.49		11.85	0.45	0.26		68.29
04/19/13	36.67	27.74	--	1.27	65.68	17.51	61.58	30.46	--	1.53	93.58	17.65	16.98	25.05	1.06	3.46	42.02	110.50
05/07/13	33.86	30.90	--	2.27	67.03	14.46	29.24	26.00	--	2.75	57.98	17.67	20.32	39.55	1.47	6.21	59.86	94.86
06/02/13	7.60	13.37	--	0.15	21.12	4.05	11.05	21.64	--	0.18	32.86	4.48	11.77	27.08	0.46	0.40	38.85	1.10
06/06/13	5.28	9.13	--	1.50	15.91	11.95	5.75	10.76	--	1.82	18.33	10.72	23.46	32.41	1.05	4.11	55.87	85.63
06/09/13	12.04	24.06	--	2.91	39.01	30.59	224.91		--	3.52		28.84	53.63	48.12	1.41	7.97	101.75	181.62
06/13/13	0.91	2.65	--	0.00	3.56	1.31	0.59	2.75	--	0.00	3.34	1.82	0.25	4.28	0.18	0.00	4.53	12.31
06/23/13	0.32	1.07	--	0.00	1.39	0.12	0.43	26.99	--	0.00	27.41	0.10	0.67	2.45	0.15	0.00	3.12	0.23
06/28/13	6.75	11.49	--	0.00	18.24	1.33	7.36	17.29	--	0.01	24.65	1.37	1.30	3.98	0.25	0.01	5.28	4.33
06/30/13	2.40	4.90	--	0.01	7.31	1.18	3.25	6.72	--	0.01	9.98	1.58	1.93	4.44	0.26	0.02	6.36	9.10
07/03/13	13.60	2.32	--	0.81	16.72	8.06	4.42	27.56	--	0.98	32.96	30.11	12.17	20.50	0.94	2.20	32.67	56.04
07/07/13	1.78	0.53	--	0.04	2.35	1.73	0.43	0.64	--	0.05	1.12	1.46	3.07	4.21	0.38	0.12	7.28	6.37
07/10/13	2.09	4.46	--	0.01	6.55	2.32	2.27	2.24	--	0.01	4.52	2.58	1.72	2.49	0.29	0.02	4.20	14.66
07/27/13	6.58	8.12	--	0.19	14.88	3.04	9.39	13.37	--	0.23	22.98	2.64	5.87	9.07	0.57	0.51	14.94	48.40

Blank cells denote incomplete datasets. Total In values are computed only if water quality data are present at both CO20 and CO30.

Table 3-20. Solids loads for monitored storm events (continued).

Event Date	Pollutant Loads (lbs)																	
	Total Suspended Solids						Suspended Sediment Concentration						Total Dissolved Solids					
	CO30	CO20	Direct Catch.	Ungaged	Total In	CO10	CO30	CO20	Direct Catch.	Ungaged	Total In	CO10	CO30	CO20	Direct Catchment	Ungaged	Total In	CO10
08/13/13	11.86	7.37	--	0.26	19.48	4.46	19.40	10.87	--	0.31	30.58	5.05	4.37	3.37	0.86	0.70	7.73	30.32
08/23/13	0.54	1.98	--		2.52		0.40	2.92	--	0.00	3.32		1.59	2.75	0.32	0.00	4.35	
09/01/13	1.26	2.64	--		3.91		1.53	4.17	--	0.00	5.70		1.43	2.32	0.18	0.00	3.75	
09/21/13	8.96	14.49	--	0.78	24.23	9.04	10.87	18.74	--	0.95	30.56	11.08	9.10	10.01	0.60	2.15	19.11	47.85
10/07/13	7.83	11.92	--	0.63	20.38	6.16	9.12	13.40	--	0.76	23.28	10.86	13.32	14.52	0.62	1.72	27.84	19.01
10/09/13	95.40	61.63	--	20.09	177.13	223.77	95.65	71.58	--	24.32	191.56	245.0	230.14	204.05	3.90	55.00	434.19	598.00
11/26/13	10.78	15.85	--	4.79	31.42	10.58	14.25	16.68	--	5.79	36.72	14.81	18.26	23.19	0.75	13.10	41.46	103.56
12/06/13	4.41	8.77	--	0.85	14.03	3.04	4.27	9.17	--	1.03	14.46	2.24	62.69	33.54	0.83	2.32	96.23	83.56
12/08/13	4.07	12.88	--	2.11	19.06	3.16	2.79	9.37	--	2.56	14.72		247.73	680.99	0.26	5.78	928.72	983.32
12/14/13	5.29	6.05	--	0.52	11.86	1.94	5.80	5.91	--	0.63	12.34	1.35	34.44	24.94	0.69	1.43	59.37	159.86
12/22/13	22.22	34.31	--	0.83	57.36	12.80	53.51	202.04	--	1.00	256.55	19.01	79.03	63.82	0.82	2.26	142.85	245.57
12/29/13	50.47	26.49	--	1.05	78.01	36.93	59.12	153.61	--	1.27	213.99	63.60	35.24	38.83	0.91	2.87	74.07	118.19
02/03/14	45.05	55.88	--	1.19	102.12	26.60	59.49	55.39	--	1.44	116.33	20.42	110.13	689.90	0.95	3.26	800.03	482.93
02/05/14	8.86	14.03	--	0.13	23.02	5.12	10.46	18.86	--	0.16	29.47	2.85	68.99	414.47	0.02	0.35	483.46	268.96
02/18/14	44.55	31.81	--	3.20	79.56	27.91	44.73	29.03	--	3.87	77.63	20.51	148.51	645.71	0.18	8.75	803.16	748.99

Blank cells denote incomplete datasets. Total In values are computed only if water quality data are present at both CO20 and CO30.

Table 3-21. Phosphorus loads for monitored storm events.

	Pollutant Loads (lbs)											
	Total Phosphorus						Orthophosphate Phosphorus					
Event Date	CO30	CO20	Direct Catch.	Ungaged	Total In	CO10	CO30	CO20	Direct Catch.	Ungaged	Total In	CO10
10/18/12	0.0159	0.0253	0.0007	0.0006	0.0426		0.0040	0.0101	0.0003	0.0001	0.0145	
10/28/12	9.6653	0.4399	0.0088	0.1975	10.3115	1.9982	0.4618	0.2932	0.0038	0.0263	0.7852	1.4769
11/13/12	0.0143	0.0157	0.0012	0.0033	0.0346	0.0272	0.0061	0.0063	0.0005	0.0004	0.0134	0.0163
12/20/12	0.0265	0.0267	0.0013	0.0043	0.0588	0.0584	0.0119	0.0134	0.0006	0.0006	0.0264	0.0449
12/26/12		0.1303	0.0026	0.0205		0.3616		0.0652	0.0011	0.0027		0.2583
01/14/13	0.0456	0.0372	0.0016	0.0070	0.0914	0.0917	0.0105	0.0106	0.0007	0.0009	0.0228	0.0459
01/30/13	0.5353	0.2718	0.0031	0.0253	0.8354	0.5945	0.0657	0.0906	0.0014	0.0034	0.1610	0.2972
02/13/13		0.0064	0.0005	0.0000		0.0092		0.0032	0.0002	0.0000		0.0023
02/26/13	0.0789	0.0747	0.0011	0.0024	0.1571	0.0546	0.0158	0.0140	0.0005	0.0003	0.0306	0.0156
03/06/13	0.0685	0.0493	0.0020	0.0116	0.1314	0.2560	0.0228	0.0328	0.0009	0.0016	0.0581	0.0914
04/12/13		0.0389	0.0008	0.0008		0.0748		0.0097	0.0003	0.0001		0.0324
04/19/13	0.1146	0.1060	0.0019	0.0100	0.2324	0.3063	0.0255	0.0145	0.0008	0.0013	0.0421	0.1313
05/07/13	0.0919	0.1236	0.0024	0.0179	0.2358	0.3162	0.0193	0.0247	0.0011	0.0024	0.0475	0.1920
06/02/13	0.0158	0.0234	0.0009	0.0012	0.0413		0.0079	0.0084	0.0004	0.0002	0.0168	0.0239
06/06/13	0.0489	0.0295	0.0020	0.0118	0.0922	0.2688	0.0244	0.0147	0.0009	0.0016	0.0416	0.0996
06/09/13		0.0702	0.0027	0.0230		0.6930		0.0201	0.0012	0.0031		0.2390
06/13/13			0.0003	0.0000		0.0347	0.0401	0.0335	0.0001	0.0000	0.0738	0.0203
06/23/13	0.0054	0.0065	0.0003	0.0000	0.0122	0.0015	0.0042	0.0036	0.0001	0.0000	0.0078	0.0003
06/28/13	0.0166	0.0199	0.0005	0.0000	0.0370	0.0234	0.0047	0.0055	0.0002	0.0000	0.0105	0.0072
06/30/13	0.0143	0.0127	0.0005	0.0000	0.0275	0.0288	0.0044	0.0053	0.0002	0.0000	0.0099	0.0124
07/03/13	0.1049	0.0312	0.0015	0.0064	0.1440	0.2627	0.0420	0.0089	0.0007	0.0008	0.0524	0.0876
07/07/13	0.0176	0.0121	0.0006	0.0003	0.0307	0.0373	0.0078	0.0121	0.0003	0.0000	0.0203	0.0095
07/10/13	0.0089	0.0092	0.0005	0.0000	0.0187	0.0599	0.0045	0.0037	0.0002	0.0000	0.0084	0.0221
07/27/13	0.0144	0.0167	0.0009	0.0015	0.0335	0.0917	0.0104	0.0072	0.0004	0.0002	0.0182	0.0443

Blank cells denote incomplete datasets. Total In values are computed only if water quality data are present at both CO20 and CO30.

Table 3-21. Phosphorus loads for monitored storm events (continued).

Event Date	Pollutant Loads (lbs)											
	Total Phosphorus						Orthophosphate Phosphorus					
	CO30	CO20	Direct Catch.	Ungaged	Total In	CO10	CO30	CO20	Direct Catch.	Ungaged	Total In	CO10
08/13/13	0.0218	0.0177	0.0010	0.0020	0.0426	0.1020	0.0109	0.0053	0.0005	0.0003	0.0170	0.0466
08/23/13	0.0055	0.0092	0.0004	0.0000	0.0150		0.0025	0.0018	0.0002	0.0000	0.0045	
09/01/13	0.0067	0.0113	0.0005	0.0000	0.0184		0.0043	0.0042	0.0002	0.0000	0.0087	
09/21/13	0.0327	0.0442	0.0015	0.0062	0.0846	0.1994	0.0163	0.0206	0.0007	0.0008	0.0384	0.0842
10/07/13	0.0517	0.0458	0.0014	0.0050	0.1039	0.1086	0.0381	0.0306	0.0006	0.0007	0.0699	0.0543
10/09/13	0.6695	0.3748	0.0090	0.1586	1.2119	2.5077	0.4603	0.2499	0.0039	0.0212	0.7352	1.5432
11/26/13	0.0870	0.0870	0.0017	0.0378	0.2134	0.3525	0.0609	0.0580	0.0008	0.0050	0.1246	0.2864
12/06/13	0.0697	0.0516	0.0016	0.0067	0.1295	0.1302	0.0348	0.0258	0.0007	0.0009	0.0622	0.0651
12/08/13	0.0905	0.0715	0.0005	0.0167	0.1792	0.1975	0.0566	0.0215	0.0002	0.0022	0.0805	0.1185
12/14/13	0.0313	0.0155	0.0013	0.0041	0.0522	0.0538	0.0139	0.0052	0.0006	0.0005	0.0202	0.0323
12/22/13	0.1405	0.1029	0.0016	0.0065	0.2515	0.2982	0.0439	0.0275	0.0007	0.0009	0.0729	0.1052
12/29/13	0.1586	0.1036	0.0017	0.0083	0.2721	0.3139	0.0705	0.0518	0.0008	0.0011	0.1241	0.1847
02/03/14	0.1335	0.1531	0.0018	0.0094	0.2978	0.2625	0.0584	0.0383	0.0008	0.0013	0.0987	0.1575
02/05/14	0.0554	0.0409	0.0000	0.0010	0.0974	0.0732	0.0252	0.0175	0.0000	0.0001	0.0429	0.0457
02/18/14	0.2149	0.1515	0.0003	0.0253	0.3920	0.4187	0.0977	0.0757	0.0001	0.0034	0.1770	0.2442

Blank cells denote incomplete datasets. Total In values are computed only if water quality data are present at both CO20 and CO30.

Table 3-22. Nitrogen loads for monitored storm events.

Event Date	Pollutant Loads (lbs)																	
	Total Nitrogen						Oxidized Nitrogen						Ammonia Nitrogen					
	CO30	CO20	Direct Catch.	Ungaged	Total In	CO10	CO30	CO20	Direct Catch.	Ungaged	Total In	CO10	CO30	CO20	Direct Catch.	Ungaged	Total In	CO10
10/18/12	0.13	0.22	0.03	0.00	0.39		0.03	0.06	0.03	0.00	0.11		0.02	0.05	0.00	0.00	0.07	
10/28/12	107.54	7.29	0.37	1.45	116.66	21.28	4.65	4.22	0.32	0.53	9.71	11.55	0.86	0.48	0.06	0.13	1.52	0.61
11/13/12	0.26	0.33	0.05	0.02	0.67	0.32	0.09	0.09	0.04	0.01	0.23	0.05	0.06	0.02	0.01	0.00	0.09	0.01
12/20/12	0.46	0.24	0.07	0.03	0.80	0.67	0.12	0.07	0.06	0.01	0.25	0.31	0.03	0.04	0.01	0.00	0.08	0.02
12/26/12		2.15	0.13	0.15		3.49		1.32	0.11	0.05		1.65		0.18	0.02	0.01		0.26
01/14/13	0.75	0.62	0.08	0.05	1.50	1.08	0.35	0.26	0.08	0.02	0.71	0.39	0.02	0.06	0.01	0.00	0.09	0.04
01/30/13	4.89	2.81	0.15	0.19	8.04	5.22	0.40	1.03	0.15	0.07	1.65	1.54	0.07	0.21	0.03	0.02	0.32	0.22
02/13/13	0.00	0.20	0.04	0.00		0.11		0.10	0.04	0.00		0.00		0.05	0.00	0.00		0.00
02/26/13	0.68	0.92	0.08	0.02	1.70	0.51	0.13	0.21	0.08	0.01	0.43	0.12	0.06	0.06	0.01	0.00	0.13	0.02
03/06/13	0.96	1.02	0.21	0.09	2.27	2.76	0.53	0.51	0.21	0.03	1.28	0.79	0.04	0.13	0.05	0.01	0.22	0.05
04/12/13		0.30	0.05	0.01		0.46	0.00	0.04	0.05	0.00		0.01		0.05	0.01	0.00		0.03
04/19/13	1.16	0.94	0.12	0.07	2.30	1.78	0.17	0.14	0.12	0.03	0.46	0.28	0.09	0.09	0.02	0.01	0.21	0.14
05/07/13	0.63	1.07	0.19	0.13	2.02	1.54	0.16	0.19	0.19	0.05	0.59	0.14	0.03	0.09	0.04	0.01	0.18	0.07
06/02/13	0.24	0.17	0.05	0.01	0.46	0.33	0.06	0.06	0.05	0.00	0.16	0.00	0.03	0.03	0.01	0.00	0.07	0.01
06/06/13	0.65	0.69	0.11	0.09	1.54	1.46	0.19	0.25	0.11	0.03	0.57	0.12	0.03	0.09	0.02	0.01	0.15	0.06
06/09/13	2.50	1.12	0.14	0.17	3.94	3.54			0.14	0.06		0.12	0.09		0.03	0.02		0.05
06/13/13	0.06	0.12	0.02	0.00	0.19	0.27	0.01	0.03	0.02	0.00	0.06	0.00	0.01	0.02	0.00	0.00	0.03	0.01
06/23/13	0.04	0.09	0.01	0.00	0.15	0.01	0.02	0.02	0.01	0.00	0.05	0.00	0.01	0.01	0.00	0.00	0.02	0.00
06/28/13	0.17	0.22	0.03	0.00	0.41	0.11	0.03	0.04	0.03	0.00	0.09	0.00	0.03	0.04	0.01	0.00	0.08	0.00
06/30/13	0.14	0.12	0.03	0.00	0.28	0.15	0.02	0.03	0.03	0.00	0.08	0.00	0.01	0.02	0.01	0.00	0.04	0.00
07/03/13	0.60	0.31	0.09	0.05	1.04	1.92	0.19	0.08	0.09	0.02	0.37	0.21	0.05	0.02	0.02	0.00	0.10	0.04
07/07/13	0.10	0.08	0.04	0.00	0.22	0.18	0.03	0.02	0.04	0.00	0.09	0.00	0.01	0.02	0.01	0.00	0.03	0.00
07/10/13	0.11	0.11	0.03	0.00	0.25	0.28	0.03	0.03	0.03	0.00	0.09	0.00	0.02	0.02	0.01	0.00	0.05	0.01
07/27/13	0.30	0.29	0.05	0.01	0.65	0.36	0.09	0.09	0.05	0.00	0.24	0.02	0.04	0.07	0.01	0.00	0.13	0.02

Blank cells denote incomplete datasets. Total In values are computed only if water quality data are present at both CO20 and CO30.

Table 3-22. Nitrogen loads for monitored storm events (continued).

Event Date	Pollutant Loads (lbs)																	
	Total Nitrogen						Oxidized Nitrogen						Ammonia Nitrogen					
	CO30	CO20	Direct Catch.	Ungaged	Total In	CO10	CO30	CO20	Direct Catch.	Ungaged	Total In	CO10	CO30	CO20	Direct Catch.	Ungaged	Total In	CO10
08/13/13	0.21	0.21	0.06	0.01	0.50	0.47	0.06	0.04	0.06	0.01	0.17	0.03	0.04	0.04	0.01	0.00	0.09	0.02
08/23/13	0.07	0.14	0.02	0.00	0.23		0.02	0.04	0.02	0.00	0.08		0.01	0.02	0.00	0.00	0.03	
09/01/13	0.11	0.18	0.02	0.00	0.31		0.02	0.03	0.02	0.00	0.07		0.02	0.03	0.00	0.00	0.05	
09/21/13	0.38	0.48	0.06	0.05	0.97	0.89	0.15	0.06	0.06	0.02	0.29	0.17	0.03	0.09	0.01	0.00	0.14	0.01
10/07/13	0.42	0.38	0.06	0.04	0.90	0.63	0.19	0.10	0.06	0.01	0.36	0.09	0.06	0.08	0.01	0.00	0.15	0.01
10/09/13	8.12	7.83	0.38	1.16	17.49	21.22	4.73	5.12	0.38	0.42	10.65	8.29	0.33	0.42	0.06	0.11	0.92	0.68
11/26/13	1.52	1.40	0.07	0.28	3.27	3.53	0.90	0.92	0.07	0.10	1.99	1.94	0.08	0.01	0.01	0.03	0.12	0.02
12/06/13	2.62	1.08	0.08	0.05	3.82	2.13	1.22	0.55	0.07	0.02	1.87	0.87	0.52	0.06	0.01	0.00	0.60	0.16
12/08/13	3.60	1.33	0.03	0.12	5.08	4.68	2.47	0.79	0.02	0.04	3.33	2.90	0.26	0.13	0.00	0.01	0.40	0.20
12/14/13	1.75	0.30	0.07	0.03	2.15	1.33	0.89	0.18	0.06	0.01	1.13	0.81	0.06	0.02	0.01	0.00	0.09	0.03
12/22/13	2.96	1.37	0.08	0.05	4.46	3.88	1.45	0.54	0.07	0.02	2.08	1.30	0.08	0.04	0.01	0.00	0.13	0.09
12/29/13	1.93	1.16	0.09	0.06	3.23	2.88	0.92	0.50	0.08	0.02	1.52	1.22	0.08	0.05	0.01	0.01	0.15	0.09
02/03/14	1.90	2.34	0.09	0.07	4.41	3.11	1.02	1.21	0.13	0.03	2.38	1.61	0.13	0.30	0.02	0.01	0.45	0.31
02/05/14	1.43	1.09	0.00	0.01	2.53	1.93	0.84	0.81	0.00	0.00	1.66	1.29	0.07	0.12	0.00	0.00	0.19	0.16
02/18/14	3.40	2.90	0.02	0.19	6.50	4.95	1.72	1.89	0.02	0.07	3.70	2.79	0.20	0.27	0.00	0.02	0.48	0.28

Blank cells denote incomplete datasets. Total In values are computed only if water quality data are present at both CO20 and CO30.

Table 3-23. Organic carbon loads for monitored storm events.

Event Date	Pollutant Loads (lbs)											
	Total Organic Carbon						Dissolved Organic Carbon					
	CO30	CO20	Direct Catch.	Ungaged	Total In	CO10	CO30	CO20	Direct Catch.	Ungaged	Total In	CO10
10/18/12	0.30	0.86	0.05	0.04	1.25		0.00	0.86	0.00	0.05		
10/28/12	66.63	23.09	0.53	14.55	104.81	82.53	29.03	20.89	76.45	0.53	65.01	76.45
11/13/12	1.82	3.05	0.07	0.25	5.19	4.10	1.82	3.05	3.10	0.07	5.19	3.10
12/20/12	1.35	2.24	0.08	0.31	3.99	4.40	1.29	2.14	4.18	0.08	3.82	4.18
12/26/12	0.00	7.56	0.16	1.51		20.15	0.00	7.17	20.15	0.16		20.15
01/14/13	2.35	2.39	0.10	0.52	5.36	7.15	2.17	2.18	6.97	0.10	4.97	6.97
01/30/13	9.86	10.12	0.19	1.86	22.02	26.48	7.42	9.51	25.40	0.19	18.98	25.40
02/13/13	0.00	0.63	0.03	0.00		1.08	0.00	0.67	0.96	0.03		0.96
02/26/13	1.73	1.96	0.07	0.18	3.94	2.84	1.66	1.92	2.81	0.07	3.82	2.81
03/06/13	4.41	3.70	0.12	0.86	9.09	14.99	4.34	3.61	14.08	0.12	8.93	14.08
04/12/13	0.00	1.07	0.05	0.06		3.12	0.00	0.92	2.92	0.05		2.92
04/19/13	3.99	2.75	0.11	0.74	7.58	11.71	3.73	2.79	10.61	0.11	7.38	10.61
05/07/13	4.69	4.26	0.15	1.32	10.42	11.29	4.45	4.26	11.52	0.15	10.18	11.52
06/02/13	0.77	1.22	0.05	0.09	2.13	2.45	0.71	1.20	2.26	0.05	2.06	2.26
06/06/13	2.83	3.68	0.12	0.87	7.51	9.36	2.83	3.68	8.06	0.12	7.51	8.06
06/09/13	9.69	0.00	0.16	1.69		25.09	9.22	0.00	22.70	0.16		22.70
06/13/13	0.35	0.59	0.02	0.00	0.96	2.12	0.34	0.59	1.92	0.02	0.95	1.92
06/23/13	0.17	0.62	0.02	0.00	0.80	0.04	0.17	0.62	0.04	0.02	0.80	0.04
06/28/13	0.49	0.97	0.03	0.00	1.49	0.52	0.45	0.91	0.52	0.03	1.39	0.52
06/30/13	0.45	0.93	0.03	0.00	1.41	1.23	0.45	0.86	1.17	0.03	1.34	1.17
07/03/13	3.36	1.96	0.09	0.47	5.88	8.84	3.36	1.96	8.23	0.09	5.88	8.23
07/07/13	0.68	0.00	0.04	0.03		1.14	0.68	0.00	1.05	0.04		1.05
07/10/13	0.56	0.85	0.03	0.00	1.44	2.52	0.52	0.84	0.00	0.03	1.39	
07/27/13	1.08	1.84	0.06	0.11	3.09	2.88	1.06	1.77	2.59	0.06	2.99	2.59

Blank cells denote incomplete datasets. Total In values are computed only if water quality data are present at both CO20 and CO30.

Table 3-23. Organic carbon loads for monitored storm events (continued).

	Pollutant Loads (lbs)											
	Total Organic Carbon						Dissolved Organic Carbon					
Event Date	CO30	CO20	Direct Catch.	Ungaged	Total In	CO10	CO30	CO20	Direct Catch.	Ungaged	Total In	CO10
08/13/13	0.94	1.06	0.06	0.15	2.21	3.32	0.87	0.99	0.06	0.15	2.08	3.32
08/23/13	0.31	0.64	0.02	0.00	0.98		0.28	0.64	0.02	0.00	0.95	
09/01/13	0.40	0.65	0.03	0.00	1.07		0.38	0.61	0.03	0.00	1.02	
09/21/13	1.07	1.38	0.09	0.46	3.01	4.87	1.05	1.35	0.09	0.46	2.95	4.70
10/07/13	3.40	2.48	0.09	0.37	6.33	2.78	2.15	2.44	0.09	0.37	5.04	2.49
10/09/13	30.55	20.82	0.54	11.69	63.60	83.91	28.04	22.90	0.54	11.69	63.17	82.95
11/26/13	4.35	5.60	0.10	2.78	12.84	19.17	4.35	5.51	0.10	2.78	12.74	18.73
12/06/13	5.46	3.81	0.10	0.49	9.85	9.88	5.40	3.68	0.10	0.49	9.66	9.77
12/08/13	6.56	3.36	0.03	1.23	11.18	16.19	6.56	3.36	0.03	1.23	11.18	16.19
12/14/13	2.37	0.91	0.08	0.30	3.66	4.14	2.37	0.91	0.08	0.30	3.66	4.04
12/22/13	8.87	5.08	0.10	0.48	14.52	17.89	8.61	5.08	0.10	0.48	14.26	17.89
12/29/13	5.90	4.40	0.11	0.61	11.02	14.22	5.90	4.40	0.11	0.61	11.02	13.48
02/03/14	6.34	6.03	0.11	0.69	13.17	12.25	5.84	6.03	0.11	0.69	12.67	12.42
02/05/14	3.47	3.10	0.00	0.07	6.65	6.50	3.58	3.10	0.00	0.07	6.75	6.31
02/18/14							0.00	0.00	0.02	1.86		

Blank cells denote incomplete datasets. Total In values are computed only if water quality data are present at both CO20 and CO30.

Table 3-24. Iron and Manganese loads for monitored storm events.

Event Date	Pollutant Loads (grams)																	
	Total Iron						Soluble Iron						Total Manganese					
	CO30	CO20	Direct Catch.	Ungaged	Total In	CO10	CO30	CO20	Direct Catch.	Ungaged	Total In	CO10	CO30	CO20	Direct Catch.	Ungaged	Total In	CO10
10/18/12			1.11	0.85				0.64	1.11	0.13					0.00	0.01		
10/28/12			13.06	289.66			63.44	52.21	13.06	44.77	173.5	349.93			0.00	3.42		
11/13/12			1.80	4.91		19.23			1.80	0.76		1.23			0.00	0.06		5.4
12/20/12		54.88	1.98	6.24		40.73	1.72	0.92	1.98	0.96	5.6	2.53		8.1	0.00	0.07		9.4
12/26/12		400.82	3.80	30.10		342.10	0.00	55.93	3.80	4.65		37.96		24.0	0.00	0.36		76.3
01/14/13	73.35	83.40	2.40	10.31	169.4	126.05	9.56	13.91	2.40	1.59	27.5	126.05	9.1	5.8	0.00	0.12	15.0	30.9
01/30/13	1780.43	1438.09	4.61	37.04	3260.2	904.55	43.87	74.64	4.61	5.72	128.8	154.44	167.8	60.5	0.00	0.44	228.7	94.0
02/13/13		24.79	0.74	0.05				0.30	0.74	0.01				2.1	0.00	0.00		
02/26/13	111.95	127.55	1.64	3.56	244.7	113.12	4.47	16.29	1.64	0.55	23.0	2.47	11.3	8.7	0.00	0.04	20.0	24.9
03/06/13	120.10	128.51	2.93	17.06	268.6	473.53	48.66	33.82	2.93	2.64	88.0	89.56	8.5	7.2	0.00	0.20	15.9	115.3
04/12/13		97.89	1.17	1.10		89.43	15.44	15.01	1.17	0.17	31.8	6.55		5.5	0.00	0.01		89.5
04/19/13	185.20	207.34	2.76	14.65	410.0	419.84	0.00	14.79	2.76	2.26		110.17	15.6	7.6	0.00	0.17	23.4	194.0
05/07/13	228.18	313.93	3.57	26.29	572.0	463.08	11.74	7.12	3.57	4.06	26.5	161.87	19.5	11.7	0.00	0.31	31.6	213.1
06/02/13	52.34	15.17	1.31	1.70	70.5	172.65	1.37	1.91	1.31	0.26	4.9	24.52	4.9	1.0	0.00	0.02	5.9	166.0
06/06/13	33.92	65.82	2.97	17.37	120.1	410.07	2.22	8.22	2.97	2.69	16.1	63.23	2.5	3.3	0.00	0.21	6.1	223.1
06/09/13	409.67	213.27	3.98	33.70	660.6	320.85	29.91	11.60	3.98	5.21	50.7	443.33	27.9	10.3	0.00	0.40	38.6	173.4
06/13/13			0.51	0.00			1.91	1.00	0.51	0.00	3.4	10.95			0.00	0.00		
06/23/13	2.13	6.97	0.41	0.00	9.5	1.33			0.41	0.00			0.3	0.5	0.00	0.00	0.8	0.8
06/28/13	21.78	26.95	0.71	0.05	49.5	32.20	0.45	2.33	0.71	0.01	3.5	1.17	1.8	1.6	0.00	0.00	3.4	19.5
06/30/13	11.39	14.80	0.74	0.07	27.0	66.29	0.60	0.70	0.74	0.01	2.0	5.50	1.5	1.2	0.00	0.00	2.7	45.5
07/03/13	103.77	61.24	2.28	9.33	176.6	287.18	3.39	7.13	2.28	1.44	14.2	127.11	7.1	6.8	0.00	0.11	14.0	124.3
07/07/13	7.40		0.92	0.50		68.42	0.46		0.92	0.08		10.60	0.6		0.00	0.01		35.9
07/10/13	12.59	33.37	0.71	0.07	46.7	127.95	0.15	2.49	0.71	0.01	3.4	17.58	0.9	1.6	0.00	0.00	2.5	68.6
07/27/13	45.00	2.17	1.38	2.17	50.7	110.20	1.93	1.23	1.38	0.33	4.9		3.6	1.1	0.00	0.03	4.7	69.2

Blank cells denote incomplete datasets. Total In values are computed only if water quality data are present at both CO20 and CO30.

Table 3-24. Iron and Manganese loads for monitored storm events (continued).

Event Date	Pollutant Loads (grams)																	
	Total Iron						Soluble Iron						Total Manganese					
	CO30	CO20	Direct Catch.	Ungaged	Total In	CO10	CO30	CO20	Direct Catch.	Ungaged	Total In	CO10	CO30	CO20	Direct Catch.	Ungaged	Total In	CO10
08/13/13	184.0	58.3	1.54	2.97	246.8	28.3	3.9	3.1	1.54	0.46	8.9	44.4	39.1	8.1	0.00	0.04	47.2	2.0
08/23/13		28.5	0.58				0.0	0.7	0.58	0.00		0.0	0.0	1.7	0.00	0.00		
09/01/13		27.0	0.67	0.01			0.0	1.7	0.67	0.00		0.0	0.0	4.4	0.00	0.00		
09/21/13	62.1	342.0	2.28	9.09	415.4	444.1	2.1	5.3	2.28	1.40	11.1	20.7	16.7	39.5	0.00	0.11	56.4	156.8
10/07/13	140.6	56.0	2.10	7.28	206.0	78.5	4.3	6.8	2.10	1.12	14.3	38.6	52.2	9.8	0.00	0.09	62.1	8.1
10/09/13	372.0	474.1	13.27	232.67	1092.1	831.2	78.6	52.1	13.27	35.96	179.9	407.3	52.2	9.8	0.16	0.09	52.6	212.2
11/26/13	78.5	121.9	2.56	55.41	258.3	197.9	26.5	53.5	2.56	8.56	91.1	144.9	23.9	24.9	1.01	2.75	24.2	63.0
12/06/13	42.4	92.8	2.35	9.81	147.3	118.1	24.7	33.9	2.35	1.52	62.5	91.1	11.7	11.7	0.20	0.65	8.8	19.1
12/09/13	100.6	434.8	0.74	24.46	560.5	298.2	37.4	44.1	0.74	3.78	86.0	147.8	3.5	5.0	0.18	0.12	28.0	47.9
12/14/13	19.6	64.0	1.96	6.04	91.5	40.0	7.6	7.6	1.96	0.93	18.1	25.9	13.4	14.3	0.06	0.29	5.9	11.0
12/22/13	178.4	257.1	2.33	9.57	447.5	245.1	27.9	31.0	2.33	1.48	62.7	77.4	2.4	3.3	0.15	0.07	25.8	50.8
12/29/13						347.6	0.0	46.6	2.58	1.87		91.3	13.2	12.3	0.18	0.11		53.9
02/03/14							15.4	22.8	2.69	2.13	43.0	61.6						
02/05/14							2.9	17.3	0.07	0.23	20.5	28.3						
02/18/14							53.1	80.9	0.51	5.72	140.2	131.5						

Table 3-25. Copper loads for monitored storm events.

	Pollutant Loads (grams)											
	Total Copper						Soluble Copper					
Event Date	CO30	CO20	Direct Catch.	Ungaged	Total In	CO10	CO30	CO20	Direct Catch.	Ungaged	Total In	CO10
10/18/12			0.03	0.02			0.00	0.17	0.03	0.02		
10/28/12			0.36	6.98			8.23	11.80	0.36	6.98	27.38	20.89
11/13/12			0.05	0.12		0.37			0.05	0.12		0.38
12/20/12		1.46	0.06	0.15		0.61	0.11	0.29	0.06	0.15	0.61	0.11
12/26/12		5.26	0.11	0.73		3.51		0.44	0.11	0.73		5.39
01/14/13	1.08	1.69	0.07	0.25	3.08	1.25	0.00	0.32	0.07	0.25		0.21
01/30/13	8.01	9.38	0.13	0.89	18.41	6.37	0.29	3.70	0.13	0.89	5.01	0.38
02/13/13		0.53	0.02	0.00		0.16		0.07	0.02	0.00		
02/26/13	1.30	2.25	0.05	0.09	3.68	0.69	0.38	0.66	0.05	0.09	1.17	0.19
03/06/13	2.35	2.98	0.08	0.41	5.82	3.65	0.22	1.60	0.08	0.41	2.32	0.32
04/12/13		1.13	0.03	0.03		0.34		0.42	0.03	0.03		0.07
04/19/13	1.94	2.43	0.08	0.35	4.80	2.13	1.10	1.20	0.08	0.35	2.73	1.74
05/07/13	2.57	4.01	0.10	0.63	7.31	1.84	1.18	2.24	0.10	0.63	4.16	0.21
06/02/13			0.04	0.04			0.22	0.39	0.04	0.04	0.69	0.15
06/06/13	3.28	1.44	0.08	0.42	5.22	1.35	1.35	1.94	0.08	0.42	3.79	0.21
06/09/13	2.35	1.36	0.11	0.81	4.63	3.25	3.16	3.91	0.11	0.81	7.99	0.32
06/13/13	0.16	0.29	0.01	0.00	0.47	0.16			0.01	0.00		
06/23/13	0.08	0.28	0.01	0.00	0.37	0.01	0.07	0.21	0.01	0.00	0.29	0.00
06/28/13	0.27	0.48	0.02	0.00	0.76	0.04	0.11	0.27	0.02	0.00	0.40	0.04
06/30/13	0.16	0.34	0.02	0.00	0.52	0.11	0.11	0.23	0.02	0.00	0.37	0.07
07/03/13	1.20	1.15	0.06	0.22	2.64	1.19	0.20	0.97	0.06	0.22	1.46	1.79
07/07/13	0.25		0.03	0.01		0.10	0.22	0.00	0.03	0.01		0.10
07/10/13	0.18	0.38	0.02	0.00	0.59	0.21	0.12	0.19	0.02	0.00	0.33	0.15
07/27/13	0.42	0.32	0.04	0.05	0.84	0.43	0.25	0.44	0.04	0.05	0.78	

Table 3-25. Copper loads for monitored storm events (continued).

	Pollutant Loads (grams)											
	Total Copper						Soluble Copper					
Event Date	CO30	CO20	Direct Catch.	Ungaged	Total In	CO10	CO30	CO20	Direct Catch.	Ungaged	Total In	CO10
08/13/13	0.21	0.43	0.04	0.07	0.76	0.99	0.31	0.32	0.04	0.07	0.75	0.40
08/23/13		0.39	0.02	0.00				0.21	0.02	0.00		
09/01/13		0.26	0.02	0.00				0.18	0.02	0.00		
09/21/13	0.32	0.80	0.06	0.22	1.40	0.60	0.33	0.40	0.06	0.22	1.01	0.30
10/07/13	0.48	1.47	0.06	0.18	2.19	0.80	0.58	0.78	0.06	0.18	1.59	0.29
10/09/13	10.2	15.3	0.37	5.61	31.5	19.2	8.92	14.17	0.37	5.61	29.06	18.37
11/26/13	1.8	3.7	0.07	1.33	6.9	3.1	1.93	4.21	0.07	1.33	7.55	3.70
12/06/13	1.7	3.1	0.07	0.24	5.1	2.2	1.82	3.04	0.07	0.24	5.16	2.36
12/09/13	2.3	2.8	0.02	0.59	5.7	4.4	2.36	2.53	0.02	0.59	5.50	4.12
12/14/13	0.8	0.8	0.05	0.15	1.8	0.9	0.85	0.59	0.05	0.15	1.65	0.95
12/22/13	2.9	3.9	0.07	0.23	7.1	4.1	2.55	3.24	0.07	0.23	6.08	4.06
12/29/13						3.4		2.62	0.07	0.29		3.27
02/03/14							1.89	3.30	0.08	0.33	5.60	3.49
02/05/14							1.19	1.91	0.00	0.04	3.13	1.58
02/18/14							4.70	6.44	0.01	0.89	12.05	6.80

Table 3-26. Cinnamon Oaks BMP retrofit pollutant removal results for Summation of Loads Method.

	TSS	SSC	TDS	TP	OP	TN	OxN	NH_3N	TOC	DOC
Number of Samples	33	29	30	29	32	33	32	32	30	29
Inflow Loads (lbs)	2514	3620	4592	5.5	3.1	83.7	48.2	7.5	355	262
Outflow Loads (lbs)	679	714	4887	7.5	5.7	75.6	38.8	3.4	391	372
% Removal	73	80	-6	-36	-83	10	19	55	-10	-42

Table 3-26. Cinnamon Oaks BMP retrofit pollutant removal results for Summation of Loads Method (continued).

	Total Fe	Soluble Fe	Total Mn	Total Cu	Soluble Cu
Number of Samples	23	28	24	18	28
Inflow Loads (grams)	6341	1341	727	63	138
Outflow Loads (grams)	5406	2806	2134	14	73
% Removal	15	-109	-193	79	47

Table 3-27.Generalized Wilcoxon results for Influent and Effluent Constituent Loads.

Water Quality Constituent	Sample	No. Samples	p-value	Statistically Different at 95% confidence level?
Total Suspended Solids	Influent	36	0.00122	Yes
	Effluent	36		
Suspended Sediment Concentration	Influent	32	0.000253	Yes
	Effluent	34		
Total Dissolved Solids	Influent	33	0.227	No
	Effluent	35		
Total Phosphorus	Influent	34	0.211	No
	Effluent	35		
Orthophosphate Phosphorus	Influent	35	0.0817	No
	Effluent	36		
Total Nitrogen	Influent	36	0.816	No
	Effluent	36		
Oxidized Nitrogen	Influent	35	0.0893	No
	Effluent	36		
Ammonia Nitrogen	Influent	35	0.000466	Yes
	Effluent	36		
Total Organic Carbon	Influent	33	0.425	No
	Effluent	35		

Table 3-27. Generalized Wilcoxon results for Influent and Effluent Constituent Loads (continued).

Water Quality Constituent	Sample	No. Samples	p-value	Statistically Different at 95% confidence level?
Dissolved Organic Carbon	Influent	32	0.486	No
	Effluent	34		
Total Iron	Influent	24	0.453	No
	Effluent	30		
Soluble Iron[1]	Influent	28	0.079	No
	Effluent	33		
Total Manganese	Influent	24	0.00283	Yes
	Effluent	30		
Total Copper	Influent	24	0.00191	Yes
	Effluent	30		
Soluble Copper	Influent	28	0.0127	Yes
	Effluent	33		

[1]. Even though the results of the generalized Wilcoxon test give a p-value greater than 0.05, the EPM plots and SOL method both show a large export of soluble iron out of the BMP.

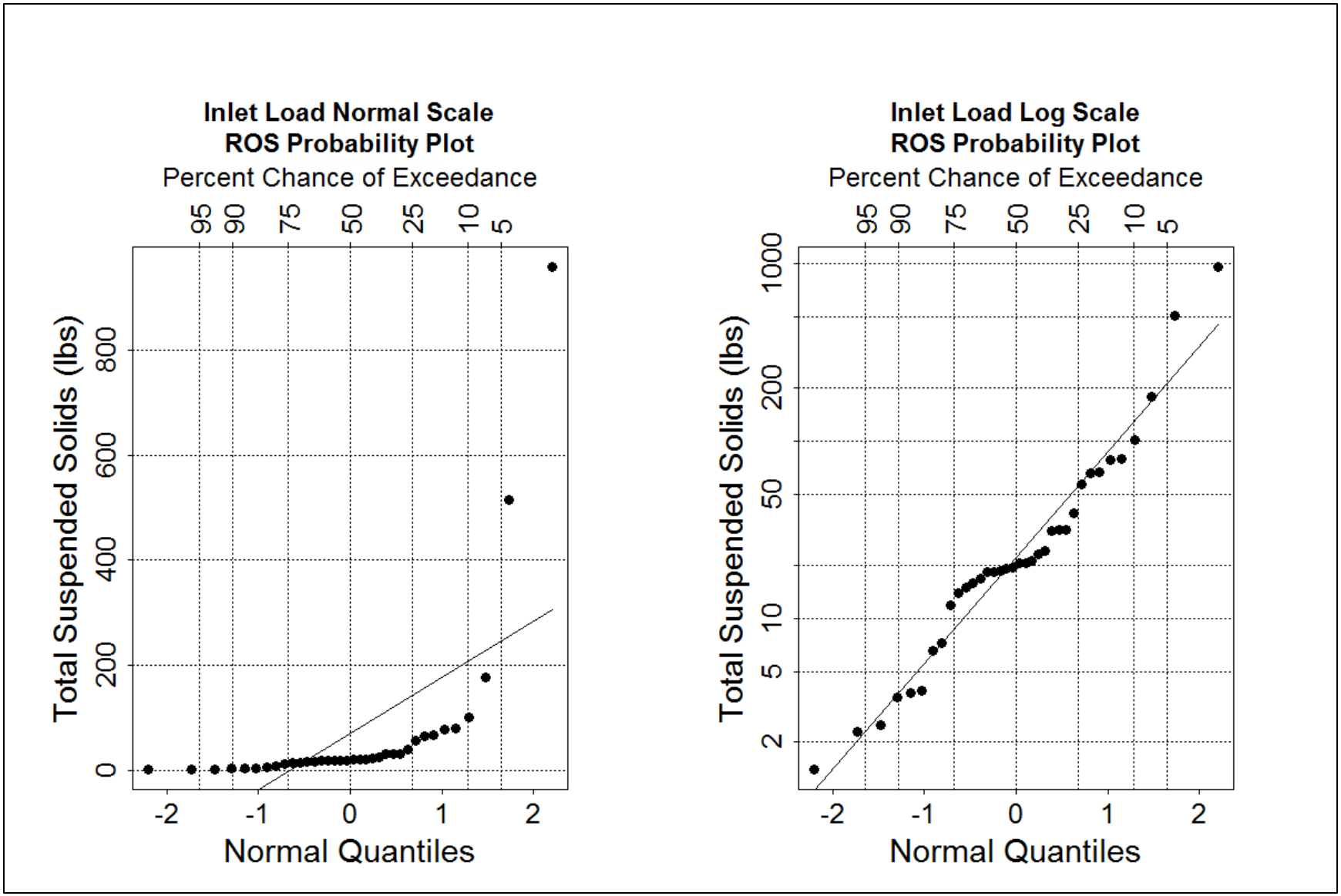

Figure 3-9. Q-Q plots of influent loads for total suspended solids.

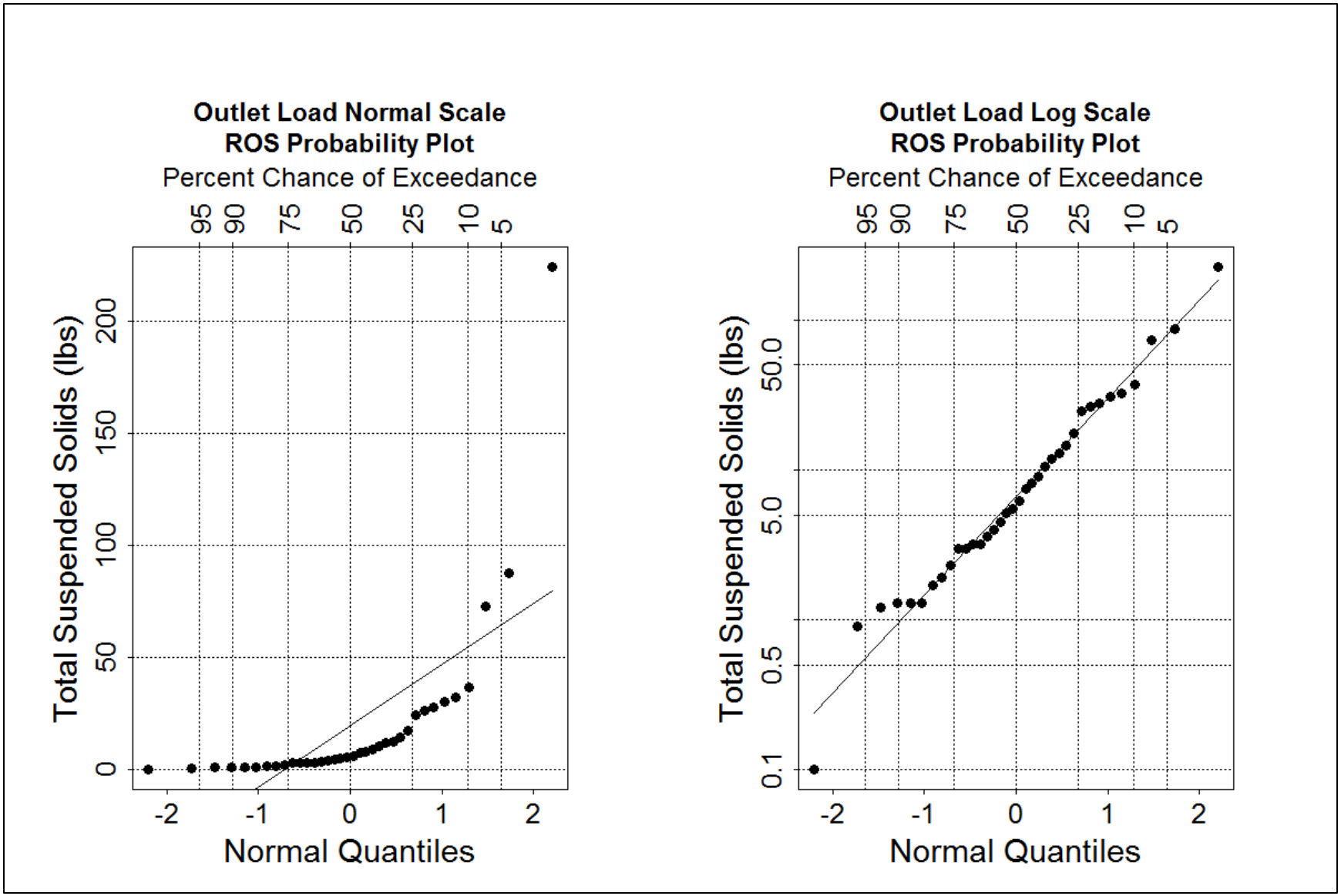

Figure 3-10. Q-Q plots of effluent loads for total suspended solids.

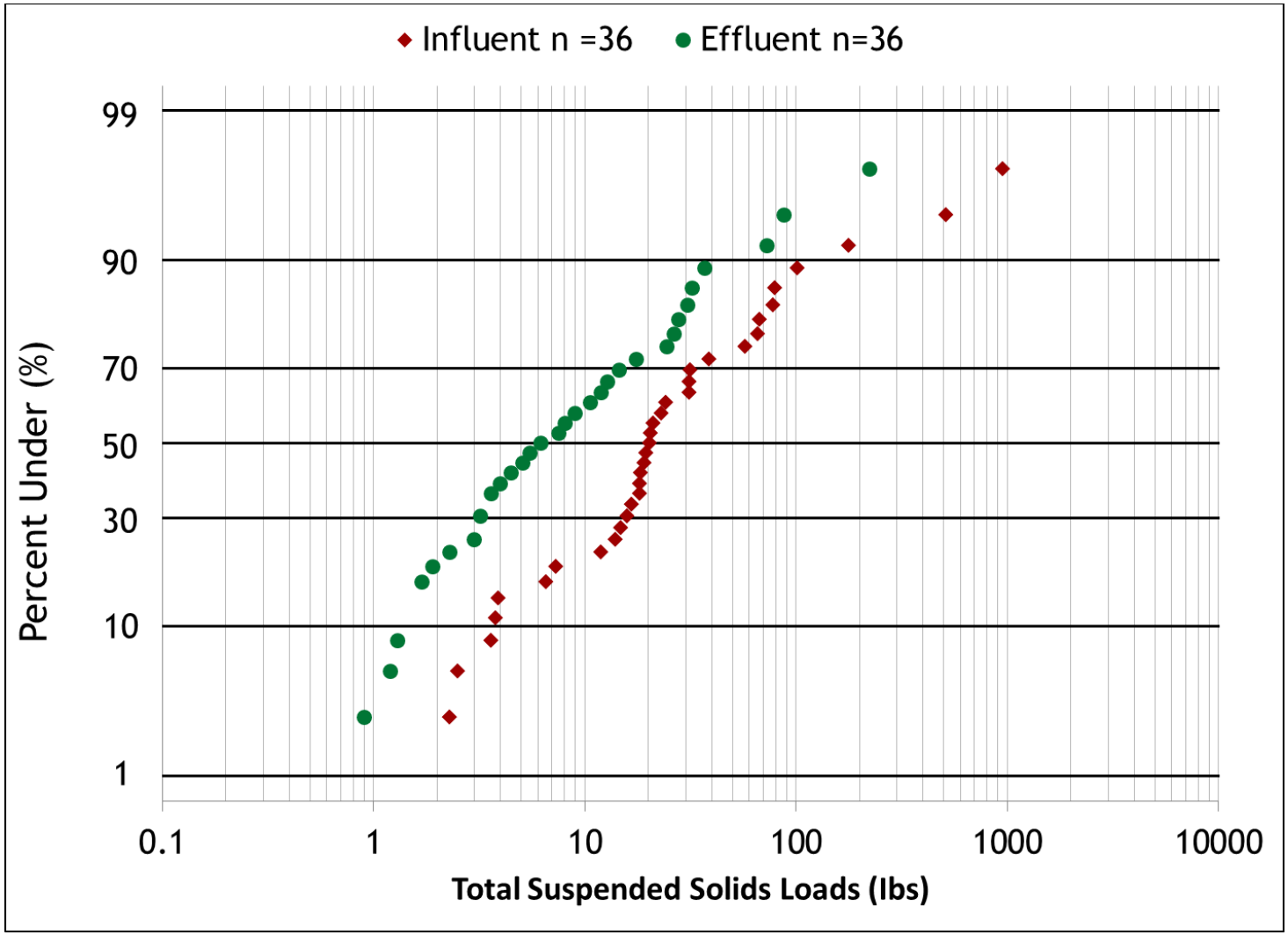

Figure 3-11. Effluent Probability Method plot for influent and effluent loads for total suspended solids.

Table 3-28. Quantile loads reductions from the Effluent Probability Method.

Percentile	Percent Reduction (%)									
	TSS	SSC	TDS	TP	OP	TN	OxN	NH_3N	TOC	DOC
Minimum	60	73	-1	50	75	35	99	96	48	27
10th	63	69	-49	0	-6.5	25	98	94	-6	-6
30th	80	86	-150	-55	-50	12	77	84	0	9
50th	70	65	-104	-100	-67	19	51	75	-10	-36
70th	54	65	-88	-48	-129	-47	20	49	-42	-37
90th	63	75	-24	-22	-70	60	21	35	-19	-32
Maximum	76	78	-6	76	-96	80	-9	56	21	-26

Table 3-28. Percentile loads reductions from the Effluent Probability Method (continued).

Percentile	Percent Reduction (%)				
	Total Fe	Soluble Fe	Total Mn	Total Cu[1]	Soluble Cu[1]
Minimum	26	24	17	-	-
10th	31	-66	-170	-	-
30th	26	-73	-390	-	-
50th	29	-121	-213	77	78
70th	18	-102	-260	68	56
90th	52	-150	-241	75	43
Maximum	75	-160	-269	39	28

[1]Load reductions could not be computed because the effluent datasets did not have data points below the 40th percentile.

3.5 Discussion

3.5.1 Suspended Solids

Removal of suspended solids in stormwater is primarily achieved through settling (Minton 2005; Qizhong Guo 2005). Figure 3-11 displays an EPM plot of the influent and effluent loads for TSS. As shown in the figure, removal of TSS was achieved throughout the entire range of monitored storm events. TSS removal efficiency was found to be 73% using the SOL method. As shown in Figure 3-11, TSS reductions sharply decreased for storm events above the 70th percentile. This was an expected result because the larger events minimize the effects of storage and also have reduced residence times. In the micropools, concentrations of TSS were observed to be highest in CO60 and lowest in CO40.

Solids removal based on the SSC method was found to be greater than for TSS. An EPM plot of the influent and effluent loads of SSC is shown in Figure D-2 in Appendix D. Using the SOL method, 80% removal of SSC was calculated. As with TSS, SSC removal decreased above the 70th percentile. Because the SSC analysis typically captures larger particles that are not well represented in the TSS measurement, the latter data may be assumed to be biased low (Clark and Sui 2008). That indicated removal of SSC was found to be greater than TSS was consistent with the relative bias of the analytical methods.

Boxplots for TSS and SSC are shown in Figures B-1 and B-2, respectively. As may be seen, concentrations of TSS and SSC decreased through the micropool series, but appeared to increase between CO40 and CO10. This was likely due to the shallow pond depth and vegetation growth at CO10. During dry periods, sediment and organic matter were observed to build up near CO10 and were then washed away in later storm events. Forebay sedimentation near the outlet is a common maintenance problem in BMPs (Lord and Hunt 2010). Overall, the Cinnamon Oaks BMP effectively reduces suspended solids. The results of the generalized Wilcoxon test show that influent and effluent loads were statistically significantly different for both TSS (p-value=0.00122) and SSC (p-value=0.000253). It is clear that the construction of the micropools and rip-rap weirs created sufficient settling time for the removal of suspended solids.

3.5.2 Total Dissolved Solids

The calculated removal efficiency of TDS using the SOL method was -5%, indicating that the BMP had little effect on dissolved constituents. Figure D-3 in Appendix D shows the EPM plot of influent and effluent loads for TDS which show a slight net export of TDS across the entire range of monitored storm events. Based on the generalized Wilcoxon test, there was no statistical significant difference between the influent and effluent loads for TDS (p-value=0.227). Figure C-5 in Appendix C displays a time series plot of the influent and effluent TDS concentrations and Figure C-6 displays a time series plot of TDS concentration within the ponds. TDS concentrations were highest in the winter and lowest in the summer, a result that was consistent with the application of deicing salts on roads in the winter months (Minton 2005).

Figure B-3 and Figure B-4 in Appendix B show comparative boxplots of TDS concentrations and specific conductance, respectively. It may be seen that there was an increase in TDS concentrations and conductance at CO60 compared to the EMCs of either CO20 or CO30. Concentrations of TDS then decreased in the succeeding micropools and at the outlet CO10. As will be discussed, the trend of increasing concentrations at CO60 and decreasing in the following micropools was observed for other constituents as well.

3.5.3 Phosphorus

EPM plots of the influent and effluent loads for TP and OP may be found in Figures D-4 and D-5 in Appendix D, respectively. SOL results for TP and OP were -36% and -83%, respectively. The EPM plots clearly demonstrate that TP and OP are being exported throughout the entire range of storm events with the exceptions of the highest and lowest percentiles represented. The top percentile represents the storm event for October 28 - November 12, 2012 (Hurricane Sandy) for which a TP reduction of 81% was computed. In examining the data, it was determined that the high efficiency was the result of an unusually high TP event mean concentration at CO20 (2.93 mg/L). It is not known why TP concentrations were so high for this event at CO20, but the removals for this single event should not be considered indicative of typical TP removal for a storm event. For this study, EMC data were excluded from the SOL analysis if they were above or below the mean by more than three standard deviations. The TP dataset for CO30 had a mean of 0.38 mg/L and a standard deviation of 0.48 mg/L. The 2.93 mg/L TP measured during Hurricane Sandy greatly exceeded three standard deviations. Therefore, this storm event was

removed from the SOL analysis for TP. If the Hurricane Sandy were included in the SOL analysis of TP, then the computed SOL removal efficiency would be 41%. This result indicates that the BMP was effective in reducing phosphorus loads, but this is not supported by the EPM plots which show exports of phosphorus throughout the entire range of storm events. This clearly demonstrates how large events can dominate the SOL method. The results of the generalized Wilcoxon test confirmed that the influent and effluent load datasets for TP ($p=0.211$) and OP ($p= 0.0817$) are not statistically significantly different.

Comparative boxplots of TP and OP of storm EMCs and pond grab samples are displayed in Figures B-6 and Figure B-7, respectively. The boxplots show a large increase of TP and OP in micropool CO60 compared to the inlet EMCS at CO20 and CO30. This suggests that CO60 is, in some manner, serving as a source of phosphorus. In any case, it is clear that the BMP is failing to remove phosphorus and is actually introducing more phosphorus into the stormwater runoff.

Phosphorus removal in BMPs is principally achieved through plant uptake and binding to soil media (Erickson, Gulliver et al. 2007; Ng, Eheart et al. 2007; Vacca and Wadzuk 2012). Phosphorus-sediment interactions are largely dependent on the oxidation-reduction (redox) conditions. Under aerobic conditions, phosphorus tends to bind iron which then settles with the rest of the suspended sediment material (Wetzel 1983; Minton 2005). Since high removal of suspended solids was achieved, it was expected that TP would behave similarly. Under anoxic conditions, particulate-bound phosphorus can disassociate within the soil media and suspend solids (Wetzel 1983; Minton 2005). The increase in phosphorus may suggest the presence of anoxic zones within the BMP, particularly in the micropool where CO60 was located.

3.5.4 Nitrogen

Total nitrogen (TN) is the sum of ammonia nitrogen (NH_3-N), oxidized nitrogen (Ox-N), and organic nitrogen (Org-N). Oxidized nitrogen is the sum of nitrite and nitrate (NO_2^--N + NO_3^--N). Ammonia nitrogen is the sum of ammonia and ammonium (NH_3-N + NH_4^+-N). The effective removal of nitrogen is dependent on the species present and their transformations within the BMP, and these in turn, strongly depend on the redox potential within the BMP system. Ammonia concentration reductions occur from either conversion to Org-N from biological uptake or conversion to oxidized nitrogen from nitrification under aerobic conditions. Ammonia

is generally the preferred form of nitrogen by plants. Under anoxic conditions, oxidized nitrogen is converted to N_2 through dissimilatory denitrification. Organic and inorganic nitrogen reductions may also occur through sedimentation of nitrogen bound compounds (Wetzel 1983; Minton 2005; Grady, Daigger et al. 2011). In order to avoid confusion where transformations may be mistaken for removal, BMP performance with respect to nitrogen is generally based on total N.

The EPM plot for influent and effluent TN loads is shown in Figure D-6 in Appendix D, and shows that there were no significant reductions of TN across most of the monitored storm events. As with TP, the exception was the top percentile (Hurricane Sandy) where the computed load reduction was 81%. High influent loads were calculated due to a high TN EMC at CO20 (32.6 mg/L as N). The causes for the high TN concentrations at CO20 for this event are not known. However, this was an extreme event and TN reductions during this event are not indicative of overall BMP performance. Like with TP, TN EMC data were excluded from the SOL analysis if they were above or below three standard deviations. The mean TN EMC at CO30 was 3.13 mg/L and the standard deviation was 5.15 mg/L. Thus, the 32.2 mg/L TN measured during the Hurricane Sandy event greatly exceeded three standard deviations. The removal efficiency of TN using the SOL method with the Hurricane Sandy event removed was 10%. The SOL method with Hurricane Sandy included was 53% which, as with total phosphorus, would have suggested that the BMP was achieving significant removal of nitrogen. Significant total nitrogen load reductions were not apparent with the EPM method. In addition, the results of the generalized Wilcoxon rank test show that there was no significant statistical difference between the influent and effluent TN loads (p=0.816). It also appeared there was no seasonal trend for TN EMCs at the CO10, CO20, and CO30 stations, as shown in the time series of Figure C-15 in Appendix C. Figure C-12 in Appendix C shows a time series plot of the micropool TN concentrations. TN concentrations in the micropools CO40 and CO50 showed a seasonal trend with concentrations increasing in the beginning of spring, reaching their peak in late summer, and then decreasing into the winter.

SOL results for OxN and NH_3N were 19% and 55%, respectively. EPM plots for OxN and NH_3N may be found in Figure D-7 to Figure D-8 in Appendix D. As noted previously, due to the many possible conversions of nitrogen forms, removal performance should be based on TN reductions.

The datasets for OxN and NH_3N, however, may give insight on the processes occurring with the BMP system. The results from the SOL method and generalized Wilcoxon test for NH_3N (p=0.0004466) indicated that the effluent loads were significantly less than the influent loads which may suggest that nitrification was occurring. The apparent decrease of OxN loads below the 30^{th} percentile may imply denitrification was occurring during smaller storm events. But the results of the generalized Wilcoxon test showed no significant statistical difference between the influent and effluent loads (p=0.0893). As such, there is not enough information available to make a conclusion about nitrogen reactions occurring with the BMP system. Based on the TN results, it was concluded that the BMP did not achieve significant reductions of nitrogen.

3.5.5 Organic Carbon

Organic carbon is a preferred measure of the organic content in water (Chang, Chiang et al. 2005; Minton 2005; Rice, Baird et al. 2012). The SOL load removal results for TOC and DOC were -10% and -0.42%, respectively. EPM plots for TOC and DOC are displayed in Figure D-9 and Figure D-10 in Appendix D, respectively. TOC effluent loads exceeded influents loads over the entire range of monitored events with the exceptions of the minimum and maximum events. The results of the Generalized Wilcoxon Test indicated that there was no statistical difference between the influent and effluent loads for either TOC (p-value=0.425) and DOC (p-value=0.486).

Low removal or export of organic carbon was not unexpected. Development of plant biomass within the BMP can result in increased concentrations of organic carbon (Li and Davis 2009). The Cinnamon Oaks BMP contained thriving growth in the spring and summer seasons. Duckweed, arrow heads, and other vegetation were observed within and around the micropools throughout the summer. This is supported by Figure C-21 and Figure C-23 in Appendix C which show the concentrations of TOC and DOC increasing in the summer. Times series plots and comparative boxplots of chlorophyll-a micropool concentrations may be found in Figure C-25 in Appendix C and Figure B-13 in Appendix B, respectively. Chlorophyll-a, which is used as an indirect measurement of algal activity, indicated that the Cinnamon Oaks BMP also periodically experienced high levels of algal growth. Vegetation die-off was observed to begin in early fall. Decaying vegetation was observed to accumulate within and around the BMP during the winter.

3.5.6 Trace Metals

Removal efficiency for total iron in the study period using the SOL method was found to be 15%. As with TP and TN, SOL analysis for total iron was heavily skewed by one storm event. The EMC for total iron event for January 31 – February 9, 2013 was 4180 μg/L at CO30. The mean iron EMC at CO30 was 767 μg/L and the standard deviation was 901 μg/L. Thus, the CO30 EMC for this event exceeded three standard deviations and was excluded from the SOL analysis. With the inclusion of this event in the SOL analysis, the calculated removal efficiency would be 34%. The EPM plot shown in Figure D-11 in Appendix D showed that there was little difference between the influent and effluent iron loads below the 80th percentile. This was supported by the results of the generalized Wilcoxon test that showed there was no statistical difference between the influent and effluent total iron loads (p-value=0.713). Figure D-12 in Appendix D and Figure B-15 in Appendix B display the EPM plot and comparative boxplots for soluble iron. The SOL load reduction result for soluble iron was -109%. Export of soluble iron occurred for the entire range of monitored storm event sizes.

The removal of total manganese using the SOL method was found to be -193%. The EPM plot shown in Figure D-13 in Appendix D, along with the results from the generalized Wilcoxon test (p=0.00283) showed a significant export of manganese for the entire range of storm event sizes. Influent datasets for soluble manganese were highly censored (>80%) and thus ROS could not be used to estimate censored values, calculate summary statistics, or calculate influent loads. Soluble manganese concentrations at CO10 were less censored (30%) and appeared to be greater than the concentrations at the CO20 and CO30. But the magnitude of the difference between the influent and effluent concentrations could not be calculated due to the high censoring of the influent datasets.

As with nitrogen and phosphorus, meaningful removal efficiencies for iron and manganese may only be calculated using total iron and total manganese datasets. However, analysis of soluble iron and soluble manganese can provide insight on the transformations occurring within the BMP. The significance of the increases in soluble iron and soluble manganese will be discussed in Section 3.5.8.

The removal of total copper using the SOL method was found to be 79% for the study period. The EPM plot and comparative boxplots for total copper are shown in Figure D-14 in Appendix D and Figure B-15 in Appendix B, respectively. Removal of copper was achieved throughout the entire range of monitored storm events. Removal rates above the 50^{th} percentile were between 40% and 70%. Performance sharply decreased between the 30^{th} and 50^{th} percentiles. The greatest load reductions (on a percent removal basis) appeared to occur below the 30^{th} percentile. However, due to the small number of observations, this conclusion cannot be definitely made. The results of the generalized Wilcoxon test showed that there was a significant difference between the influent and effluent loads (p=0.00191).

Datasets for chromium, cadmium, lead, nickel, and zinc had censoring above 80%, and therefore, removal analysis for these metals could not be computed (Helsel 2012).

3.5.7 Comparison to Fairfax County Projections

Table 3-28 shows the estimated pre- and post-retrofit annual loads from Fairfax DPWES for TSS, TP, and TN (DPWES 2012). Projection calculations were made using the Chesapeake Bay Program (CBP) Expert Panel Method (Bahr, Brown et al. 2012).

Due to sampling problems and the inability to obtain water quality data for events below 0.18 inches, not all storm events were included for the analysis between October 18, 2012 and October 18, 2013 (one full year of monitoring). Therefore, observed constituent loads within that time period are less than the project loading. However, total rainfall for the entire study period (with the exclusion of the Hurricane Sandy event) was 39.9 inches which is comparable to the 40 inches annual average of the Washington D.C. metropolitan area. Thus, the influent and effluent constituent loads of the entire study period between October, 2012 and March, 2014 were used as a reasonable surrogate of annual loadings. These values can be found in Table 3-29.

Table 3-29. Fairfax County Cinnamon Oaks Projections using the CBP Export Panel Method and measured Cinnamon Oaks loads from October 18, 2012 to October 18, 2013.

Expert Panel Method				
Constituent	Pre-retrofit (lb/yr)	Post-retrofit (lb/yr)	Net Load Removal (lb/yr)	Percent Reduction (%)
TSS	2335.34	1120.27	1215.06	52
TP	15.18	8.97	6.21	41
TN	108.59	80.34	28.25	26
Cinnamon Oaks Monitored Data				
Constituent	Influent Loads (lbs)	Effluent Loads (lbs)	Percent Reduction based on SOL method (%)	
TSS	1629	635.5	73	
TP	5.9	8.67	-36	
TN	87.69	78.17	10	

Although it appears that the CBP Expert Panel Method accurately projected post-retrofit TP and TN effluent loads, the method overestimated the sediment and nutrient loads entering the BMP. The percent reduction of TN was less than the Fairfax County projection. Since the performance analysis showed a net export of TP, is clear the BMP failed to meet the projected nutrient reductions.

3.5.8 Micropool CO60 as a Pollutant Source

The results of the Summation of Loads method and Effluent Probability Method analyses indicated that the Cinnamon Oaks BMP retrofit failed to have significant reductions of key constituents. Only TSS, SSC, NH_3N, and copper exhibited statistically significant positive performance. Negative constituent removal was exhibited for TP, OP, TOC, DOC, TDS, manganese, and soluble iron. An investigation of concentration changes within the BMP showed that constituent concentrations decreased in the downstream direction. Concentrations were highest at CO60 and lowest at CO40. Counterintuitively, however, the boxplots also showed that concentrations at CO60 were higher than the event mean concentrations measured at both CO20 and CO30 for TP, OP, TOC, DOC, TDS, iron and manganese.

BMPs with permanent pools enhance water quality benefits by increasing the time for physical, chemical, and biological processes to take place. However, proper maintenance of such stormwater facilities is required to insure that the desired performance takes place continuously

over time. In practices having some bioretention attributes, permanent nutrient removal through plant uptake can only be achieved by regular removal of plant biomass and replanting (Lucas and Greenway 2011). Nutrient saturated soils and sediments must also be removed to prevent possible leaching back into the stormwater (Baker, Treese et al. 2010).

The apparent export of phosphorus, orthophosphate, soluble iron, and soluble manganese suggests that anoxic zones existed within the BMP system. The cycling of these constituents are both dependent on the redox potential of the system, which in turn, is largely dependent on the amount of dissolved oxygen in the system. In aerobic conditions, insoluble iron precipitates with orthophosphate to form ferric hydroxide/phosphate complexes which settle along with manganese and other suspended materials. As long as aerobic conditions are maintained; iron, manganese, and phosphorus can remain trapped in the BMP sediments. Redox potential sharply decreases with the loss of dissolved oxygen. Under anoxic conditions, iron and manganese can be reduced to their soluble forms. Iron loses its bond with phosphorus and all three constituents may be released from the sediment bed and back into the water. The significant removal of copper but not iron and manganese also supports the idea that anoxia was occurring within the BMP system. Of the metal ions, iron and manganese are the dominate electron acceptors. Therefore, when anoxia occurs, copper is reduced at a slower rate than iron and manganese and it remains mostly in its insoluble form (Wetzel 1983; Minton 2005).

The formation of anoxic zones may occur from the high oxygen demand of sediment and the microbial degradation of dead organic matter. The rate of organic loading governs the rate of oxygen reduction (Wetzel 1983). Suspension of organic matter by wind or hydrodynamic mixing may also change the aerobic/anoxic conditions within a BMP (Minton 2005). Micropool CO60 contains large deposits of sediment and organic matter that take up the majority of the available storage volume. In comparison, CO40 and CO50 had less deposited sediment, and as a result, deeper water. In the summer, vegetative growth was especially heavy in CO60. The ensuing winter die-off, along with leaf fall, contributed to additional deposition of organic matter available to contribute to the internal system oxygen demand.

The increases of pollution concentrations may indicate that, at least at this time, CO60 has become an internal source for several constituents, as noted above. Despite only being retrofitted in 2009, CO60 has likely exceeded its pollutant removal capacity and is now leaching pollutants

back into the stormwater runoff. It is possible that the organic matter present within CO60 is depleting the dissolve oxygen to periodically form anoxic zones. A time series plot of the micropool field temperature and dissolved oxygen measurements are shown in Figure C-25 in Appendix C. Dissolved Oxygen concentrations were found to be below 1 mg/L during the summer months, which supports the notion that dissolved oxygen was being depleted within the micropool. Organic matter loading and low dissolved oxygen concentrations have been shown to have negative impacts on the nitrogen and phosphorus removal capacities of stormwater treatment facilities (Hunt, Jarrett et al. 2006; Li and Davis 2009). As noted previously, it is possible that anoxic zones facilitate the release of sediment bound phosphorus, iron, and manganese. The decaying organic matter may also explain the poor total nitrogen removal. As organic matter was broken down, nitrogen removed through plant uptake could be released back into the water as soluble organic nitrogen. The sediment bed and any pollutants in the interstitial water may have been mobilized during storm events due to increased mixing in the shallow micropool at the sediment-water interface. Because CO60 is the most upstream micropool to receive inflows from both primary inlets, it has experienced greater stormwater-borne pollutant loadings than the other micropools. The accumulated biomass and externally contributed organic matter (e.g., leaf litter) has resulted in a decrease in storage volume and a reduced time until impaired function. It is often recommended that plant harvesting be conducted on a regular (annual) basis to prevent these type of negative impacts from occurring (Geosyntec Consultants and Wright Water Engineers 2009).

Another possible explanation for the poor treatment performance would be the existence of an unknown contaminated influent water source. One speculation was that sewage was entering CO60 through groundwater flow. In speaking with the Fairfax County Department of Public Health, it was discovered that the property just south of the BMP had an underground septic tank. However, upon further investigation, it was found that the septic tank had been removed prior to the retrofit and the drain field flow was away from the Cinnamon Oaks pond. An investigation of the other properties within the BMP drainage area showed no other existing septic tanks. Total coliform and Escherichia coli (E. coli) measurements were made in micropools weekly from December to February. Total coliform counts ranged between 12.2 – 46100 MPN/100 ml. E. coli concentrations ranged between 6.3 – 199 MPN/100 ml. Fecal coliform concentrations in stormwater (a subset of E. coli) typically range between 0.2 – 1.9E6

MPN/100ml (Minton 2005). Based on these concentrations, it is unlikely that domestic sewage was entering the BMP.

3.5.9 Importance of Storage and Retention Time

As stated earlier, the wet micropools were designed to provide storage and increased retention time for the removal of pollutants both during and between storm events. Reductions of TSS, SSC, OxN, NH_3N, and copper were greater for smaller storm events because these events produced less runoff and longer potential retention times. For such events, the BMP was capable of providing sufficient retention time and storage to enhance the removal or conversion of these pollutants. Larger storm events produced more runoff and decreased retention times, with the result that there was less time for internal pollutant removal mechanisms to achieve greater reductions.

Based on the OWML survey data, the Cinnamon Oaks micropools could store a maximum of 0.21 inches of rainfall. Throughout the monitoring period, the micropools were observed to be near maximum capacity between storm events. The exception was during an extended dry period between August to September, 2013 which resulted in significant drawdowns of CO40 and CO50. In the same period, CO60 did not maintain a permanent pool. Near the beginning of each storm, the discharges through CO10 were primarily due to the displacement of water that was in the micropools prior to the events. As storm event size and duration increased, the total discharges through CO10 were increasingly dominated by runoff originating from the event.

Compared to the volumes estimates by the OWML survey, DPWES design estimates had a maximum storage volume of 0.31 inches. It is clear that at the time of this study, the Cinnamon Oaks BMP is under-designed to meet the storage objectives of the original DPWES plan. This may be due to sediment buildup in the micropools in the post-construction period. It would seem likely then that the removal of the sediment from the facility will increase storage volume, which may, in turn, improve constituent removal performance.

3.5.10 Comparison of Performance Analysis Methods

Performance analyses based on concentration reductions are common in the literature and many regulatory agencies establish concentration limits on pollutants. The concentration distribution display in boxplots provided a graphical illustration of changes in influent and effluent EMCs, as

well as the longitudinal change in concentrations within the BMP. However, the major flaw of using concentration changes alone is that they do not include the hydrologic data necessary to compute constituent mass. The need for an assessment method that accounts for mass is especially critical for BMPs that are designed to reduce stormwater runoff volume from storage and infiltration. This method also weighed all EMCs at all the monitoring stations equally regardless the storm event runoff that was measured at each station. However, the hydrologic data show that the catchment area for CO20 produced more runoff than the catchment area for CO30 during storm events. Without the hydrologic data, it was not possible to determine if concentration reductions were due to the BMP removing pollutants from the stormwater or if it was because of dilution from multiple runoff sources. Despites the limitations, boxplots of the EMCs did provide a means of comparison to the pond grab sample concentrations. In this way, it was possible to see how concentrations were changing within the BMP itself and where pollutant reductions or increases may have been occurring.

The Summation of Loads method is mass-based, and includes both water quality and hydrologic data in the performance analysis. It provided a single value that represented the BMP performance over the entire study period. This was useful for comparing pollutant removal efficiencies to other BMPs or LID practices. However, a major flaw of the Summation of Loads method was made clear in this study: the results may be heavily skewed by large events. Events were excluded from the SOL analysis if they contained EMCs that were three standard deviations above or below the mean. The storm event for October 28, 2012 (Hurricane Sandy) was removed from the Summation of Loads method for TP and TN because of its dramatic effect of skewing the results. If the event was used in the Summation of Loads method, then reductions of 53% for TN and 41% for TP. Similarly, the event on for January 31, 2013 contained EMC values for total iron above three standard deviations from the mean. If this event was included in the SOL analysis, a removal 34% for total iron would be computed. These high removal efficiencies were contradicted by the other performance assessment method used in this study. Without including the Hurricane Sandy event, load reductions were found to be 12% for TN, -36% for TP, and 2% for total iron.

Storm events of less than 0.18 inches of rain did not produce enough runoff volume for the sampling equipment to retrieve the minimum of five 200 mL aliquots required for analysis.

During the study period, 82 storm events that produced less than 0.18 inches of rain were measured at the site. These minor events totaled a sum of 5.59 inches of rain which accounted for 10% of the total measured rainfall at Cinnamon Oaks. Although the magnitudes were small, a large number of these events may have affected the overall results if they were included the Summation of Loads method. For this reason, it should be remembered that, although Summation of Loads method is assumed to represent the pollutant removal performance over an entire study period, it may not include all storm events in that period.

Instead of a using a single value to represent pollutant removal performance for all events as is done in the Summation of Loads method, the Effluent Probability Method provided a graphical analysis that gave greater understanding of performance across all monitored storm event sizes. Because it does not required paired storm events, all pollutant loads were available for use in this method. The EPM plots make it clear how removal performance increased or decreased as a function of storm event size. All influent and effluents loads were rank-ordered, thereby making it possible to remove the influence of extreme events on the performance analysis. Of the three methods used, the Effluent Probability Method gave the most thorough understanding of the BMP performance.

3.6 Conclusion

The primary goal of the Cinnamon Oaks BMP retrofit was to improve the removal of suspends solids, nitrogen, and phosphorus from stormwater runoff. For the 1.5 year long monitoring study, it was concluded that the retrofit only achieved significant removals of suspended sediment. There was no statistically significant removal of nitrogen, and in fact, a net export of phosphorus was observed during the study period. The BMP did remove pollutants between individual series of micropools as intended. However, possibly due an increased inventory of organic nutrient matter, CO60 was observed to be leaching nutrients and reducing the overall effectiveness of the BMP. While several theories were explored, it was not possible to determine a reason for the internal increases in nutrient concentrations in the facility. In any case, however, regular inspection and maintenance activities are required to prevent further significant impairment of BMP function. It is recommended that:

1. Because sediment forebay deposits at the outlet are a common problem in BMP maintenance (Lord and Hunt 2010), it is recommended that an increase in water depth near the outlet be used to reduce the buildup of sediment near the water surface.
2. An annual program of harvesting vegetation both within and around the BMP should be considered (Water Environment Federation and American Society of Civil Engineers 1998; Davis, Hunt et al. 2009; Geosyntec Consultants and Wright Water Engineers 2009). Harvesting should be done before the die-back season to prevent decaying vegetation from releasing nutrients back into the BMP. The harvesting of vegetation should help reduce episodes of micropool anoxia, and the associated release of nutrients from sediments and degrading organic matter. Such a program will also permanently remove nutrients from within the BMP system.
3. A regular program of dredging of the sediment and organic matter bed within the micropools should also be considered. While the data from this study do not suggest a frequency for this activity, it should be done on a regular basis, especially within CO60, to prevent pollutant saturated sediment from leaching pollutants back into the water (Baker, Treese et al. 2010).

Lastly, because of the difficulty in conducting a performance assessment not biased by the internal cycling observed, it is also recommended that monitoring and analysis of the BMP resume only after maintenance has been performed. This will promote further understanding of the retrofit design and provide valuable information on the effect of maintenance practices on long-term performance.

References

Bahr, R., T. Brown, L. Hansen, J. Kelly, J. Papacosma, V. Snead, B. Stack, R. Stack and S. Stewart, 2012. Recommendations of the Expert Panel to Define Removal Rates for Urban Stormwater Retrofit Projects.

Baker, K. H., D. P. Treese and S. E. Clark, 2010. Nutrient Leaching from Disturbed Soil Horizons. *In*: *World Environmental and Water Resources Congress 2010.* pp. 2927-2938.

CH2M Hill, 2000. Technical Memorandum 1, Urban Stormwater Assessment, prepared for North Carolina Department of Environment and Natural Resources.

Chang, E., P. Chiang, Y. Lin and H. Tsai, 2005. Evaluation of Source Water Quality Standards for Total Coliforms, TOC, and COD in Taiwan. *Practice Periodical of Hazardous, Toxic, and Radioactive Waste Management* **9**:193-203.

Chen, C.-F., J.-Y. Lin, C.-H. Huang, W.-L. Chen and N.-L. Chueh, 2009. Performance evaluation of a full-scale natural treatment system for nonpoint source and point source pollution removal. *Environ Monit Assess* **157**:391-406.

Clark, S. E. and C. Y. S. Sui, 2008. Measuring Solids Concentration in Stormwater Runoff: Comparison of Analytical Methods. *Environmental Science Technology* **42**:511-516.

Conko, K. M., K. C. Rice and M. M. Kennedy, 2004. Atmospheric wet deposition of trace elements to a suburban environment, Reston, Virginia, USA. *Atmospheric Environment* **38**:4025-4033.

Davis, A., 2008. Field Performance of Bioretention: Hydrology Impacts. *Journal of Hydrologic Engineering* **13**:90-95.

Davis, A., W. Hunt, R. Traver and M. Clar, 2009. Bioretention Technology: Overview of Current Practice and Future Needs. *Journal of Environmental Engineering* **135**:109-117.

Davis, A. P., 2007. Field Performance of Bioretention: Water Quality. *Environmental Engineering Science* **24**:1048-1064.

Davis, A. P. and C.-h. Hsieh, 2004. Evaluation of Bioretention for Treatment of Urban Storm Water Runoff. *In*: *World Water & Environmental Resources Congress 2003.* pp. 1-8.

Environmental Protection Agency, 1992. Environmental Impacts of Stormwater Discharges.

Environmental Protection Agency, 2010a. Chesapeake Bay Total Maximum Daily Load for Nitrogen, Phosphorus and Sediment, Environmental Protection Agency.

Environmental Protection Agency, 2010b. Sources of Nitrogen, Phosphorus, and Sediment to the Chesapeake Bay, Environmental Protection Agency.

Environmental Protection Agency, 2012. Three Keys to BMP Performance - Concentration, Volume and Total Load.

Erickson, A., J. Gulliver and P. Weiss, 2007. Enhanced Sand Filtration for Storm Water Phosphorus Removal. *Journal of Environmental Engineering* **133**:485-497.

Fairfax County Department of Information Technology, 2011. Soils Map 35-2. The County of Fairfax, Fairfax, Virginia.

Fairfax County Department of Public Works and Environmental Services, 2012. Fairfax County Cinnamon Oaks projections using the CBP Expert Panel Method.

Geosyntec Consultants and Wright Water Engineers, 2009. Urban stormwater BMP performance monitoring.

Grady, C. P. L., G. T. Daigger, N. G. Love and C. D. M. Filipe, 2011. *Biological Wastewater Treatment*, IWA Publishing,

Hawkins, R. H., T. J. Ward, D. E. Woodward and J. A. V. Mulluem, 2009. *Curve Number Hydrology: State of the Practice*. Reston, VA, American Society of Civil Engineers,

Helsel, D. R., 2012. *Statistis for Censored Environmental Data Using Minitab and R*,

Helsel, D. R. and R. M. Hirch, 2002. Statistical Methods in Water Resources United States Geological Survey (United States Geological Survey)United States Geological Surveys).

Hunt, W., A. Davis and R. Traver, 2012. Meeting Hydrologic and Water Quality Goals through Targeted Bioretention Design. *Journal of Environmental Engineering* **138**:698-707.

Hunt, W., A. Jarrett, J. Smith and L. Sharkey, 2006. Evaluating Bioretention Hydrology and Nutrient Removal at Three Field Sites in North Carolina. *Journal of Irrigation and Drainage Engineering* **132**:600-608.

Kayhanian, M., R. Roseen, J. Lenhart and G. Williams, 2009. Potential Data Analysis Methodology to Evaluate the Performance of Manufactured BMPs. *In*: *World Environmental and Water Resources Congress 2009.* pp. 1-10.

Leica Geosystems, 2012. *Leica FlexLine plus User Manual*. Heerbrugg, Switzerland, Leica Geosystems.

Li, H. and A. Davis, 2009. Water Quality Improvement through Reductions of Pollutant Loads Using Bioretention. *Journal of Environmental Engineering* **135**:567-576.

Lord, W. G. and W. F. Hunt, 2010. Stormwater BMP Inspection and Maintenance Program in North Carolina—A 3 Year Update. *In*: *Low Impact Development 2010.* pp. 612-618.

Lucas, W. and M. Greenway, 2011. Phosphorus Retention by Bioretention Mesocosms Using Media Formulated for Phosphorus Sorption: Response to Accelerated Loads. *Journal of Irrigation and Drainage Engineering* **137**:144-153.

McCuen, R. H., 2005. *Hydrologic Analysis and Design*, Pearson Education, Inc.,

Minton, G., 2005. *Stormwater Treatment-Biological, Chemical, and Engineering Principles*, Sheridan Books, Inc.

National Weather Service, 2012-2014. WFO Monthly/Daily Climate Data - Washington Dulles DC.

Ng, T. L., J. W. Eheart and X. Hu, 2007. Discharge Trading Programs Based on Constructed Wetlands for Nutrient Trading. *In*: *World Environmental and Water Resources Congress 2007*. pp. 1-8.

NRCS, 1986. Urban Hydrology for Small Watersheds TR-55.

Pickering, R. J., 1978. Equipment & Supplies -- Church Splitteres. United States Geological Survey.

Pomeroy, C., E. Strecker, C. Rowney, M. Leisenring, A. Poresky, L. Roesner and M. Barrett, 2012. BMP Performance Algorithms for the BMP Selection/Receiving Water Protection Toolbox. *In*: *World Environmental and Water Resources Congress 2012*. pp. 3523-3532.

Program, N. A. D., 2009. National Trends Network Data-Mason Neck Station (VA10) [online data]. NADP Program Office, Illinois State Water Survey, 2204 Griffith Dr., Champaign, IL 61820.

Qizhong Guo, P. E., Ph.D., 2005. Development of Adjustment and Scaling Factors for Measured Suspended Solids Removal Performance of Stormwater Hydrodynamic Treatment Devices. *In*: *Impacts of Global Climate Change.* pp. 1-10.

Rice, E. W., R. B. Baird, A. D. Eaton and L. S. Clesceri, 2012. *Standard Methods For the Examination of Water and Wastewater*, American Public Health Assocation, American Water Works Association, Water Environment Federation,

SonTek YSI Incorporated, 2009. *FlowTracker Handheld ADV Technical Manual*, SonTek YSI Incorporated,

Strecker, E., M. Quigley, B. Urbonas, J. Jones and J. Clary, 2001. Determining Urban Storm Water BMP Effectiveness. *Journal of Water Resources Planning and Management* **127**:144-149.

Teledyne ISCO, 2012a. *2105/2105Ci Interface Module: Installation and Operation Guide*, Teledyne ISCO.

Teledyne ISCO, 2012b. *Glacier Transportable Sampler: Installation and Operation Guide*, Teledyne ISCO.

The R Core Team, 2012. R: A Language and Environment for Statistical Computing. R Foundation for Statistical Computing.

Vacca, K. and B. Wadzuk, 2012. An Analysis of Soluble Reactive Phosphorus Removal Mechanisms in Surface-Flow Constructed Stormwater Wetlands. *In*: *World Environmental and Water Resources Congress 2012.* pp. 3475-3483.

Virginia Polytechnic Institute and State University Department of Civil Engineering, 1983. Final Report - MWCOG NURP.

Water Environment Federation and American Society of Civil Engineers, 1998. *Urban Runoff Quality Management*. 601 Wythe Street, Alexandria, VA 223144-1994.

Wetzel, R. G., 1983. *Limnology*, Saunders College Publishing, ISBN 0-03-057913-9.

4 SUMMARY AND CONCLUSIONS

4.1 Summary

The purpose of this study was to analyze the pollutant removal performance of an urban stormwater best management practice (BMP) retrofit. The Cinnamon Oaks BMP, which was originally a peak shaving pond, was retrofitted in 2009 by the Fairfax County Department of Public Works and Environmental Services (DPWES) to improve runoff quality to meet local requirements of the Chesapeake Bay Total Maximum Daily Load (TMDL). The retrofitted facility combined characteristics of traditional BMP design with aspects of low impact development (LID) practices. The design included a series of four micropools separated by rip-rap weirs and a series of four sand seeps. Following alteration of the flow path and creation of the micropools, the remainder of the original pond was planted with selected vegetation. In 2012, DPWES commissioned the Virginia Tech Occoquan Watershed Monitoring Laboratory (OWML) to conduct a field study with a view to determining the performance of the retrofit, and to provide observations and recommendations that might inform future BMP retrofit projects.

The Cinnamon Oaks BMP is located at the intersection of Ashburton Avenue and Saffron Drive in Herndon, Fairfax County, Virginia. Before the 2009 retrofit, the facility served as a peak shaving dry pond which was designed to reduce peak flows downstream; it had no water quality performance goals. The total drainage area for the pond is 11.2 acres that includes roads, sidewalks, residential plots, wooded-grass areas, and a stormwater pipe drainage system.

The BMP consists of two primary inlets to the retrofitted pond. The west inlet, which had a study designation of CO20, is a 24-inch reinforced concrete pipe (RCP). The west inlet, which had a study designation of CO30, is a 27-inch RCP. Both inlets were part of the original dry pond. CO20 serves a total area of 3.0 acres that includes drainage from Ashburton Avenue, a small part of West Ox Road, part of Saffron Drive, and residential lots along Ashburton Avenue. CO30 serves a drainage area of 5.5 acres that includes Tarragon Court, parts of Saffron Drive, and the majority of the associated residential lots. The remaining catchment area is the grass and wooded area around the pond and the pond area itself which total to 2.7 acres. The pond outlet had a study designation of CO10, and is a 24-inch RCP serving the pond outlet structure. The outlet structure is a concrete box with a full pool elevation of 7 ft. msl, and designed to pass the 50 year

storm. At flows below the design storm, water leave the pond via a 24-inch pipe set in the bottom of the outlet structure. The outlet is located on the southwest side adjacent to Ashburton Avenue. Stormwater leaving the pond at the outlet structure flows under Ashburton Avenue and to a nearby stream.

There are four micropools within the original pond footprint, which had study designations of CO40, CO50, CO60, and CO70. CO70 is located on the west side and receives drainage from the CO20 inlet. CO60 is located on the east side and receives drainage from the CO30 inlet and from CO70. CO60 drains into CO50. CO60 is located on the west side and receives drainage from CO50. When the water level in CO40 reaches the elevation of the outlet structure weir at CO10, stormwater begins to flow from the facility. The micropools are separated by natural material weirs composed of rip-rap and sand. Stormwater can move between ponds either by slowly seeping through the weirs or overtopping them during larger storm events. Due to the serpentine nature of the flow path through the pond, there is increased retention time to promote settling of particulate matter, and infiltration into the sub-soils. The micropools maintained a free water surface for the length of the study.

A series of four sand seeps separated with rock weirs are located between CO30 and CO60. The sand seeps reduce the flow velocity and create mini pools to promote infiltration. A concrete channel carries the flows from CO20 to CO70.

Monitoring of the retrofit began in October, 2012. Automated flow-monitoring and sampling equipment were installed at the two primary inlets and the outlet. The equipment provided for collection of continuous flow data and the retrieval of flow-weighted composite samples during storm events. The storm composite samples were analyzed at OWML to determine the event mean concentration (EMC) of constituents of interest for individual storm events. Measurements of micropool temperature, specific conductance, alkalinity, and pH were made on a weekly basis. Micropool grab samples were originally collected and analyzed monthly, but the frequency was changed to weekly in late November, 2013.

Between October 1, 2012 and March 1, 2014, hydrologic and constituent concentration data from 39 storm events were collected and analyzed for this study. Monitored storm event precipitation ranged from 0.18 inches to 5.76 inches with a median of 0.91 inches. Water quality constituents

monitored included total suspended solids (TSS), suspended sediment concentration (SSC), total dissolved solids (TDS), total phosphorus (TP), orthophosphate phosphorus (OP), total nitrogen (TN), oxidized nitrogen (OxN), ammonia nitrogen (NH_3N), total organic carbon (TOC), dissolved organic carbon (DOC), and trace metals: iron (Fe), manganese (Mn), copper (Cu), nickel (Ni), chromium (Cr), lead (Pb), and Zinc (Zn). Influent and effluent constituent loads for each event were calculated as the product of the EMCs and the total flow volumes.

Water quality datasets tend to be left-censored because of the difficulty in attaining laboratory analytical detection limits that result in no non-detect values. Censored datasets were analyzed using robust regression on ordered statistics (ROS) and the Kaplan-Meier (KM) method. In plotting a mixed dataset of censored and uncensored data on a cumulative probability scale, Robust ROS calculates the plotting positions separately. The uncensored values are plotted in the normal fashion, and a regression equation is calculated to best-fit the data. The regression equation is then used to estimate the censored values. The Kaplan-Meier Method is a nonparametric approach that was developed for right-censored data but has been adapted for use with left censored data. This method used ranks of the data to estimate the probability a point will be at or below the next lower concentration. By using the two methods, it was possible to include the effects of the censored data on the cumulative distribution without introducing the biases caused by using simple substitution methods (Helsel and Hirch 2002; Geosyntec Consultants and Wright Water Engineers 2009).

Three methods were used in the performance assessment: 1) comparison of summary statistics of constituent concentrations, 2) Summations of Loads method, and 3) Effluent Probability Method.

Boxplots of the influent and effluent EMCs as well as the micropool grab sample concentrations were used to facilitate a graphical comparison of the summary statics. The method utilized the full water quality dataset at both inflows and the outflow from all 39 monitored storm events, even if synoptic data were not available for all events. Observation of EMC changes at the median (the measure of central tendency) gave some indication of concentration reductions between the inflow points and the pond outflow. Observation of changes in distributions at the quartiles (25^{th} and 75^{th} percentiles) gave an indication of the changes in concentration ranges through the BMP. As with the inflows and outflow, the box plots for constituents of interest in the micropools gave some insights into internal pond processes. This approach to performance

assessment is common in the literature, but it should be noted that it is only applicable if inflow and outflow flows are well-balanced. If the facility flow balance is significantly affected by infiltration, evaporation, transpiration, or unaccounted-for flows, then concentration comparisons as a measure of performance are not recommended. A performance assessment that includes the effects of catchment and BMP hydrology by computing loads is especially import for BMPs that utilize storage and infiltration practices that reduce runoff volume (Strecker, Quigley et al. 2001; Chen, Lin et al. 2009; Geosyntec Consultants and Wright Water Engineers 2009). Despite its limitations, however, the graphical method of inspecting the distribution of EMC's provided a means of comparing influent and effluent storm event mean concentrations with the micropool grab samples. In this way, it was possible to observe how pollutant concentrations increased or decreased within the BMP system.

The Summation of Loads (SOL) method is based on the computation of the ratio of the sum of total effluent loads to the sum of total influent loads for all synoptically monitored storms. When the ratio is subtracted from unity, it provides a single percent reduction value that was representative of the entire study period. This method assumes that constituent removal over the entire monitoring period is the best measure of performance, that significant storm events that were not monitored had influent and effluent ratios similar to the monitored storm events, and that no materials were exported during dry periods (Minton 2005; Chen, Lin et al. 2009; Geosyntec Consultants and Wright Water Engineers 2009; Kayhanian, Roseen et al. 2009). For this study, a storm event was required to have constituent data from both the primary inlets and outlet to qualify for use in the Summation of Loads method.

The Effluent Probability Method (EPM) is a graphical comparison of the rank-ordered influent and effluent pollutant loads. Influent and effluent loads are appropriately transformed (usually log-transformed) and plotted on a parallel normal probability scale. Of the three methods used, the Effluent Probability Method is the most robust as it allows for comparisons of influent and effluent loads to be made for a range of storm event sizes (Strecker, Quigley et al. 2001; Quigley, Urbonas et al. 2002; Geosyntec Consultants and Wright Water Engineers 2009; Kayhanian, Roseen et al. 2009). Since the influent and effluent loads were rank-ordered, the Effluent Probability Method did not require strictly paired data sets. Thus, effluent data were available for use in this method even if the corresponding influent data were not available and vice versa. The

EPM did require an appropriate statistical test to determine if the influent and effluent loads were significantly different. For this study, the generalized Wilcoxon signed-rank test was used at the 95 percent confidence level of $p < 0.05$ (Helsel and Hirch 2002; Geosyntec Consultants and Wright Water Engineers 2009). In addition, robust regression on ordered statistics (ROS) methods were used to facilitate the inclusion of left-censored concentration data in the analysis.

The results from all three methods showed significant removal of TSS, SSC and copper. The SOL method results for TN and iron showed small positive performance but the results of the generalized Wilcoxon signed-rank test indicate that there was no statistical significant difference between the influent and effluent loads for these constituents. Negative performance was observed for TDS, TP, OP, TOC, DOC, soluble iron, and manganese. The Hurricane Sandy event was excluded in the SOL analysis for TP and TN because its inclusion would heavily skew the results for these constituents. However, the Hurricane Sandy event was included in the EPM plots and boxplots for all monitored constituents .Analysis of the remaining metal constituents could not be performed due to heavily censored datasets.

SOL analysis for TSS and SSC were 73% and 80%, respectively. The EPM plots showed that suspended sediment removal was achieved throughout the entire range of monitored storm events. Reductions decreased above the 50^{th} percentile. This was the expected result since larger storm events typically produce larger flow rates and runoff volumes. Influent and effluent TSS and SCC loads were computed to be statistically significantly different by the generalized Wilcoxon test. The series of micropools and rip-rap weirs provided sufficient residence time for the settling of sediments. The comparative boxplots of TSS and SCC concentrations indicate that there was an increase in concentration between CO40 and CO10. This was likely due to the shallow depths at CO10 where sediment and organic matter build up near the water surface.

SOL results for TP and OP were -36% and -83%, respectively. The EPM plots showed exports of TP and OP throughout the entire range of monitored storm event sizes. These results were unexpected since phosphorus removal typically coincides well with sediment removal. The comparative boxplots showed that TP and OP micropool grab sample concentrations of CO60 were significantly greater than the event mean concentrations of the two primary inlets. Phosphorus concentrations decreased in the proceeding micropools. This suggests that micropool CO60 was serving as a source of phosphorus.

SOL results for TN, OxN, and NH_3N were 12%, 19%, and 55%, respectively. The influent and effluent datasets for TN were found to not be statistically significantly different. Due to nitrogen transformations, analysis of TN should be the parameter used to determine nitrogen removal. Therefore, it cannot be concluded that the BMP retrofit is significantly removing nitrogen from stormwater runoff.

The SOL method results for TOC and DOC were -8% and -41%, respectively. In the EPM, the probability plots and generalized Wilcoxon test showed little difference between the influent and effluent organic carbon datasets. Export of organic carbon is not uncommon in BMPs that utilize vegetation growth (Li and Davis 2009). There was a thriving mixture of vegetation both within and around the micropools that include trees, shrubs, cattails, arrowheads, and duckweed during the spring and summer months. Much of this vegetation died off during the fall and winter. Chlorophyll-a measurements made in the micropools suggested that Cinnamon Oaks experienced high-levels of algal growth during the monitoring period, which doubtless resulted in an enhancement of the organic matter burden.

The SOL method gave removal of 15% for total iron. The SOL results for soluble iron were -109% which may suggest the transformation of insoluble iron to soluble iron within the BMP system. The comparative boxplots showed increases in concentration of both total and soluble iron within CO60 compared to the EMC concentrations at the inlets.

For manganese, the SOL method showed export from the BMP with a result of -193%. The EPM plots showed exports of manganese increasing with storm event size. Datasets for influent soluble manganese were greater than 80% censored so the ROS methods could not be used to calculate summary statistics. The effluent dataset had less than 30% censored data points and had a median value of 24.2 μg/L. Although the magnitude of the difference between the influent and effluent datasets could not be computed, the datasets still suggested that there was an increase of soluble manganese within the BMP system.

The BMP achieved a removal efficiency of 79% for copper based on the SOL method. The other trace metals monitored in this study had datasets that were greater than 80% censored. ROS methods could not be used to calculate summary statistics and therefore, no removal analysis could be done on these constituents.

The increases in TP, OP, soluble iron, and soluble manganese are consistent with the presence of anoxic zones within BMP, specifically in the CO60 micropool. The redox potential of the system dictates the transport and capture of these constituents. Under aerobic conditions with a high redox potential, insoluble iron will precipitate with phosphorus to form ferric hydroxide/phosphate complexes, which will settle along with insoluble manganese and other sediment material. As long as aerobic conditions are maintained, iron, manganese, and phosphorus will remain bound to the bottom sediment layer of the BMP. Redox potential decreases as dissolved oxygen concentrations decrease. Under anoxic conditions, insoluble iron and manganese are reduced to their soluble forms. This facilitates the release of sediment-bound manganese, iron and phosphorus back into the stormwater (Wetzel 1983; Minton 2005).

The majority of the storage volume within CO60 had been taken up with deposited sediment and decaying vegetation. The rate of organic loading and the oxygen demand of the sediment determine the rate of dissolved oxygen depletion in the water (Wetzel 1983; Minton 2005). It is possible that the sediment deposits and the microbial degradation of vegetation consumed dissolved oxygen within the BMP which facilitated that release of sediment-bound nutrients and metals. The decaying vegetation may have also been responsible for the poor removal performance of TN and TP. As the vegetation degraded, it is possible that nutrients were released back into the water column. During storm events, wind and hydrodynamic mixing due to flowing water could have been responsible for re-suspension of the sediment and organic matter beds and mobilization of soluble constituents in the pore water.

Another possibility for the poor observed performance is the existence of an unknown inflow source; possibly sewage from groundwater flow. An investigation of the BMP watershed area did not reveal possible sources of sewage and total coliform measurements made in the micropools were within typical ranges for stormwater, not domestic wastewater. It was concluded that sewage was an unlikely reason for poor BMP performance.

4.2 Conclusions and Recommendations

The primary goals of the Cinnamon Oaks BMP retrofit were to improve the removal of suspended solids, nitrogen, and phosphorus from stormwater runoff. It is clear that only suspended solids loads were being significantly reduced by the BMP. The BMP retrofit design

removed pollutants between the individual series of micropools as intended. However, possibly due to its increased organic loading, it appears that micropool CO60 is now leaching nutrients and reducing the overall effectiveness of the BMP retrofit. Stormwater management facilities, especially those that utilize permanent pools and vegetation, must receive regular inspections and maintenance to prevent significant impairment on pollutant removal performance. Recommendations include:

1. Because sediment deposits at the outlet are a common problem in BMP maintenance (Lord and Hunt 2010), it is recommended that an increase in the water depth near the outlet be used to reduce sediment buildup near the water surface.
2. An annual program of harvesting vegetation both within and around the BMP should be considered (Water Environment Federation and American Society of Civil Engineers 1998; Davis, Hunt et al. 2009; Geosyntec Consultants and Wright Water Engineers 2009). Harvesting should be done before the die-back season to prevent decaying vegetation from releasing nutrients back into the BMP. The removal of organic matter by harvesting vegetation should help reduce episodes of micropool anoxia, and the associated release of nutrients from sediments and degrading organic matter. Such a program will also permanently remove nutrients from within the BMP system.
3. A regular program of dredging of the sediment and organic matter bed within the micropools should be considered. While the data from this study do not suggest a frequency for this activity, it should be done on a regular basis, especially within CO60, to prevent pollutant saturated sediment from leaching pollutants back into the water(Baker, Treese et al. 2010).

Lastly, because of the difficulty in conducting a performance assessment not biased by the internal cycling observed, it is also recommended that monitoring and analysis of the BMP resume only after maintenance has been performed. This will promote further understanding of the retrofit design and provide valuable information on the effect of maintenance practices on long-term performance.

References

Bahr, R., T. Brown, L. Hansen, J. Kelly, J. Papacosma, V. Snead, B. Stack, R. Stack and S. Stewart, 2012. Recommendations of the Expert Panel to Define Removal Rates for Urban Stormwater Retrofit Projects.

Baker, K. H., D. P. Treese and S. E. Clark, 2010. Nutrient Leaching from Disturbed Soil Horizons. *In*: *World Environmental and Water Resources Congress 2010.* pp. 2927-2938.

CH2M Hill, 2000. Technical Memorandum 1, Urban Stormwater Assessment, prepared for North Carolina Department of Environment and Natural Resources.

Chang, E., P. Chiang, Y. Lin and H. Tsai, 2005. Evaluation of Source Water Quality Standards for Total Coliforms, TOC, and COD in Taiwan. *Practice Periodical of Hazardous, Toxic, and Radioactive Waste Management* **9**:193-203.

Chen, C.-F., J.-Y. Lin, C.-H. Huang, W.-L. Chen and N.-L. Chueh, 2009. Performance evaluation of a full-scale natural treatment system for nonpoint source and point source pollution removal. *Environ Monit Assess* **157**:391-406.

Clark, S. E. and C. Y. S. Sui, 2008. Measuring Solids Concentration in Stormwater Runoff: Comparison of Analytical Methods. *Environmental Science Technology* **42**:511-516.

Conko, K. M., K. C. Rice and M. M. Kennedy, 2004. Atmospheric wet deposition of trace elements to a suburban environment, Reston, Virginia, USA. *Atmospheric Environment* **38**:4025-4033.

D.R. Helsel and R.M. Hirch, 2002. Statistical Methods in Water Resources. United States Geological Survey.

Davis, A., 2008. Field Performance of Bioretention: Hydrology Impacts. *Journal of Hydrologic Engineering* **13**:90-95.

Davis, A., W. Hunt, R. Traver and M. Clar, 2009. Bioretention Technology: Overview of Current Practice and Future Needs. *Journal of Environmental Engineering* **135**:109-117.

Davis, A. P., 2007. Field Performance of Bioretention: Water Quality. *Environmental Engineering Science* **24**:1048-1064.

Davis, A. P. and C.-h. Hsieh, 2004. Evaluation of Bioretention for Treatment of Urban Storm Water Runoff. *In*: *World Water & Environmental Resources Congress 2003.* pp. 1-8.

Environmental Protection Agency, 1992. Environmental Impacts of Stormwater Discharges.

Environmental Protection Agency, 2010a. Chesapeake Bay Total Maximum Daily Load for Nitrogen, Phosphorus and Sediment, E. P. Environmental Protection Agency.

Environmental Protection Agency, 2010b. Sources of Nitrogen, Phosphorus, and Sediment to the Chesapeake Bay, Environmental Protection Agency.

Environmental Protection Agency, 2012. Three Keys to BMP Performance - Concentration, Volume and Total Load.

Erickson, A., J. Gulliver and P. Weiss, 2007. Enhanced Sand Filtration for Storm Water Phosphorus Removal. *Journal of Environmental Engineering* **133**:485-497.

Fairfax County Department of Information Technology, 2011. Soils Map 35-2. The County of Fairfax, Fairfax, Virginia.

Fairfax County Department of Public Works and Environmental Services, 2012. Fairfax County Cinnamon Oaks projections using the CBP Expert Panel Method.

Geosyntec Consultants and Wright Water Engineers, 2009. Urban stormwater BMP performance monitoring.

Grady, C. P. L., G. T. Daigger, N. G. Love and C. D. M. Filipe, 2011. *Biological Wastewater Treatment*, IWA Publishing.

Hawkins, R. H., T. J. Ward, D. E. Woodward and J. A. V. Mulluem, 2009. *Curve Number Hydrology: State of the Practice*. Reston, VA, American Society of Civil Engineers,

Helsel, D. R., 2012. *Statistis for Censored Environmental Data Using Minitab and R*.

Hunt, W., A. Davis and R. Traver, 2012. Meeting Hydrologic and Water Quality Goals through Targeted Bioretention Design. *Journal of Environmental Engineering* **138**:698-707.

Hunt, W., A. Jarrett, J. Smith and L. Sharkey, 2006. Evaluating Bioretention Hydrology and Nutrient Removal at Three Field Sites in North Carolina. *Journal of Irrigation and Drainage Engineering* **132**:600-608.

Kayhanian, M., R. Roseen, J. Lenhart and G. Williams, 2009. Potential Data Analysis Methodology to Evaluate the Performance of Manufactured BMPs. *In*: *World Environmental and Water Resources Congress 2009.* pp. 1-10.

Leica Geosystems, 2012. *Leica FlexLine plus User Manual*. Heerbrugg, Switzerland, Leica Geosystems.

Li, H. and A. Davis, 2009. Water Quality Improvement through Reductions of Pollutant Loads Using Bioretention. *Journal of Environmental Engineering* **135**:567-576.

Lord, W. G. and W. F. Hunt, 2010. Stormwater BMP Inspection and Maintenance Program in North Carolina—A 3 Year Update. *In*: *Low Impact Development 2010.* pp. 612-618.

Lucas, W. and M. Greenway, 2011. Phosphorus Retention by Bioretention Mesocosms Using Media Formulated for Phosphorus Sorption: Response to Accelerated Loads. *Journal of Irrigation and Drainage Engineering* **137**:144-153.

McCuen, R. H., 2005. *Hydrologic Analysis and Design*, Pearson Education, Inc.

Minton, G., 2005. *Stormwater Treatment-Biological, Chemical, and Engineering Principles*, Sheridan Books, Inc.

National Weather Service, 2012-2014. WFO Monthly/Daily Climate Data - Washington Dulles DC.

Ng, T. L., J. W. Eheart and X. Hu, 2007. Discharge Trading Programs Based on Constructed Wetlands for Nutrient Trading. *In*: *World Environmental and Water Resources Congress 2007.* pp. 1-8.

NRCS, 1986. Urban Hydrology for Small Watersheds TR-55.

Pickering, R. J., 1978. Equipment & Supplies -- Church Splitteres. United States Geological Survey.

Pomeroy, C., E. Strecker, C. Rowney, M. Leisenring, A. Poresky, L. Roesner and M. Barrett, 2012. BMP Performance Algorithms for the BMP Selection/Receiving Water Protection Toolbox. *In*: *World Environmental and Water Resources Congress 2012.* pp. 3523-3532.

Program, N. A. D., 2009. National Trends Network Data-Mason Neck Station (VA10) [online data]. NADP Program Office, Illinois State Water Survey, 2204 Griffith Dr., Champaign, IL 61820.

Qizhong Guo, P. E., Ph.D., 2005. Development of Adjustment and Scaling Factors for Measured Suspended Solids Removal Performance of Stormwater Hydrodynamic Treatment Devices. *In*: *Impacts of Global Climate Change.* pp. 1-10.

Rice, E. W., R. B. Baird, A. D. Eaton and L. S. Clesceri, 2012. *Standard Methods For the Examination of Water and Wastewater*, American Public Health Assocation, American Water Works Association, Water Environment Federation.

SonTek YSI Incorporated, 2009. *FlowTracker Handheld ADV Technical Manual*, SonTek YSI Incorporated.

Strecker, E., M. Quigley, B. Urbonas, J. Jones and J. Clary, 2001. Determining Urban Storm Water BMP Effectiveness. *Journal of Water Resources Planning and Management* **127**:144-149.

Teledyne ISCO, 2012a. *2105/2105Ci Interface Module: Installation and Operation Guide*, Teledyne ISCO.

Teledyne ISCO, 2012b. *Glacier Transportable Sampler: Installation and Operation Guide*, Teledyne ISCO.

Vacca, K. and B. Wadzuk, 2012. An Analysis of Soluble Reactive Phosphorus Removal Mechanisms in Surface-Flow Constructed Stormwater Wetlands. *In*: *World Environmental and Water Resources Congress 2012.* pp. 3475-3483.

Virginia Polytechnic Institute and State University Department of Civil Engineering, 1983. Final Report - MWCOG NURP.

Water Environment Federation and American Society of Civil Engineers, 1998. *Urban Runoff Quality Management*. 601 Wythe Street, Alexandria, VA 223144-1994,

Wetzel, R. G., 1983. *Limnology*, Saunders College Publishing, ISBN 0-03-057913-9

APPENDIX A Hydrographs and cumulative flow volume plots

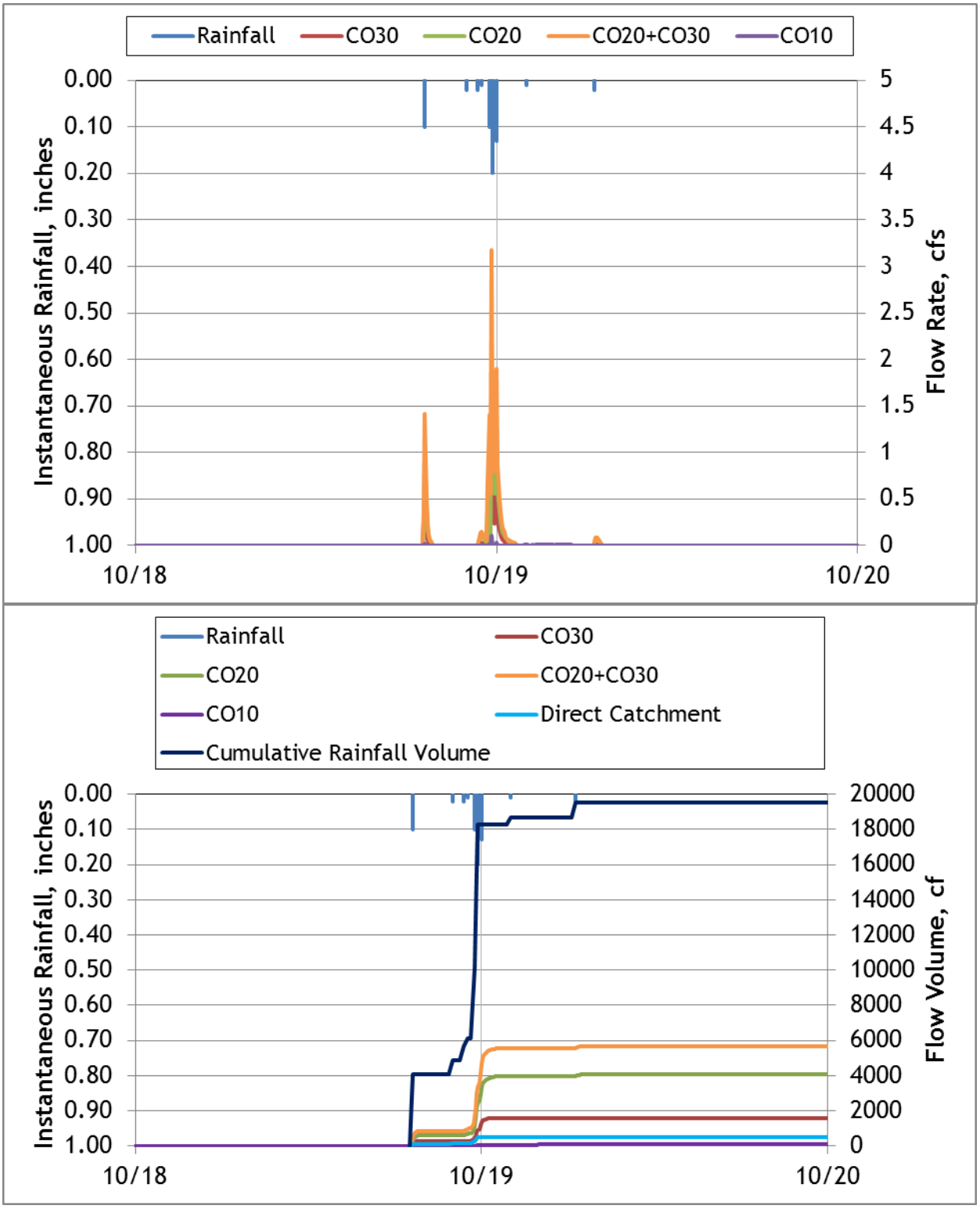

Figure A-1. Hydrograph and cumulative flow volumes for October 18-20, 2012

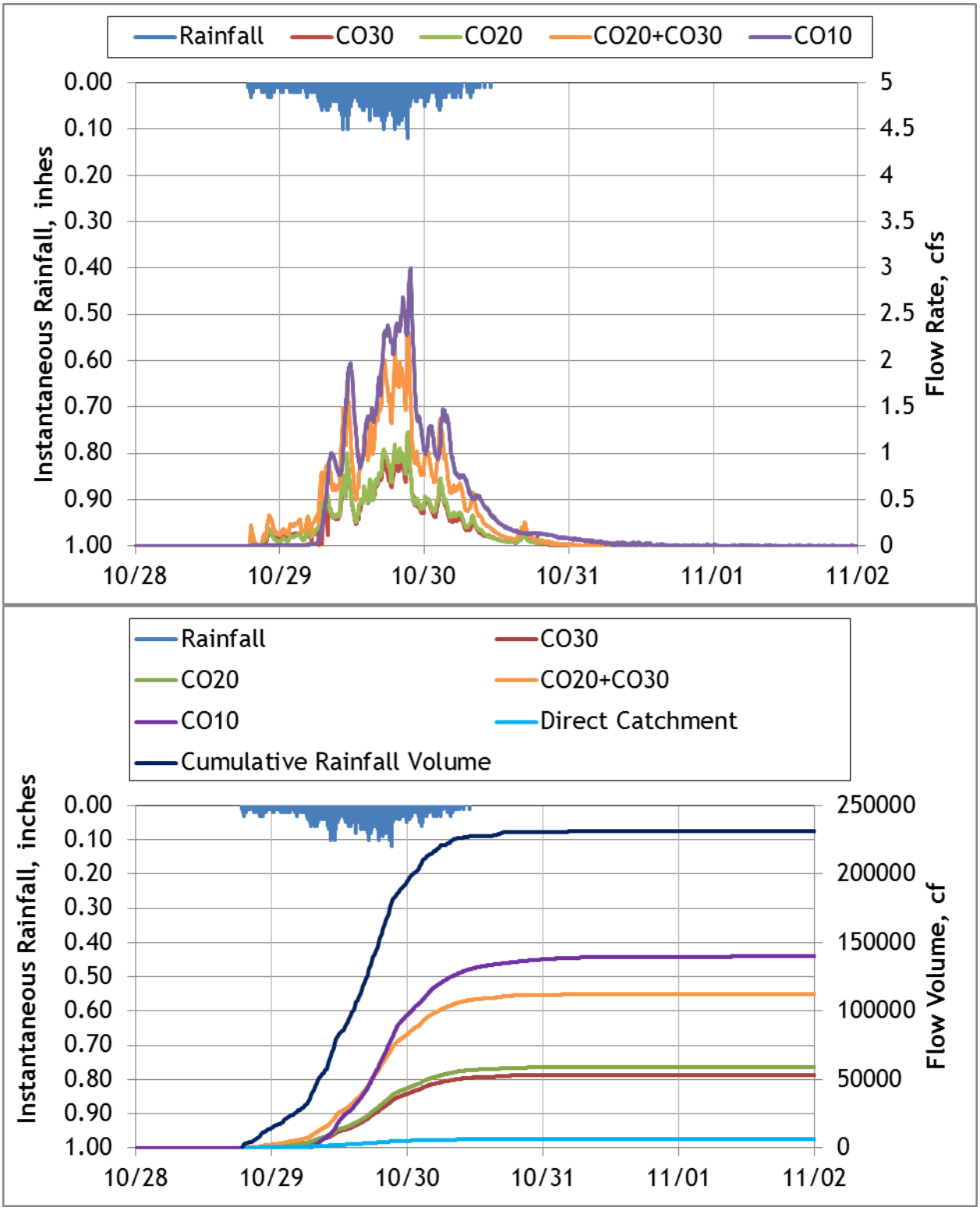

Figure A-2. Hydrograph and cumulative flow volumes for October 28- November 02, 2012

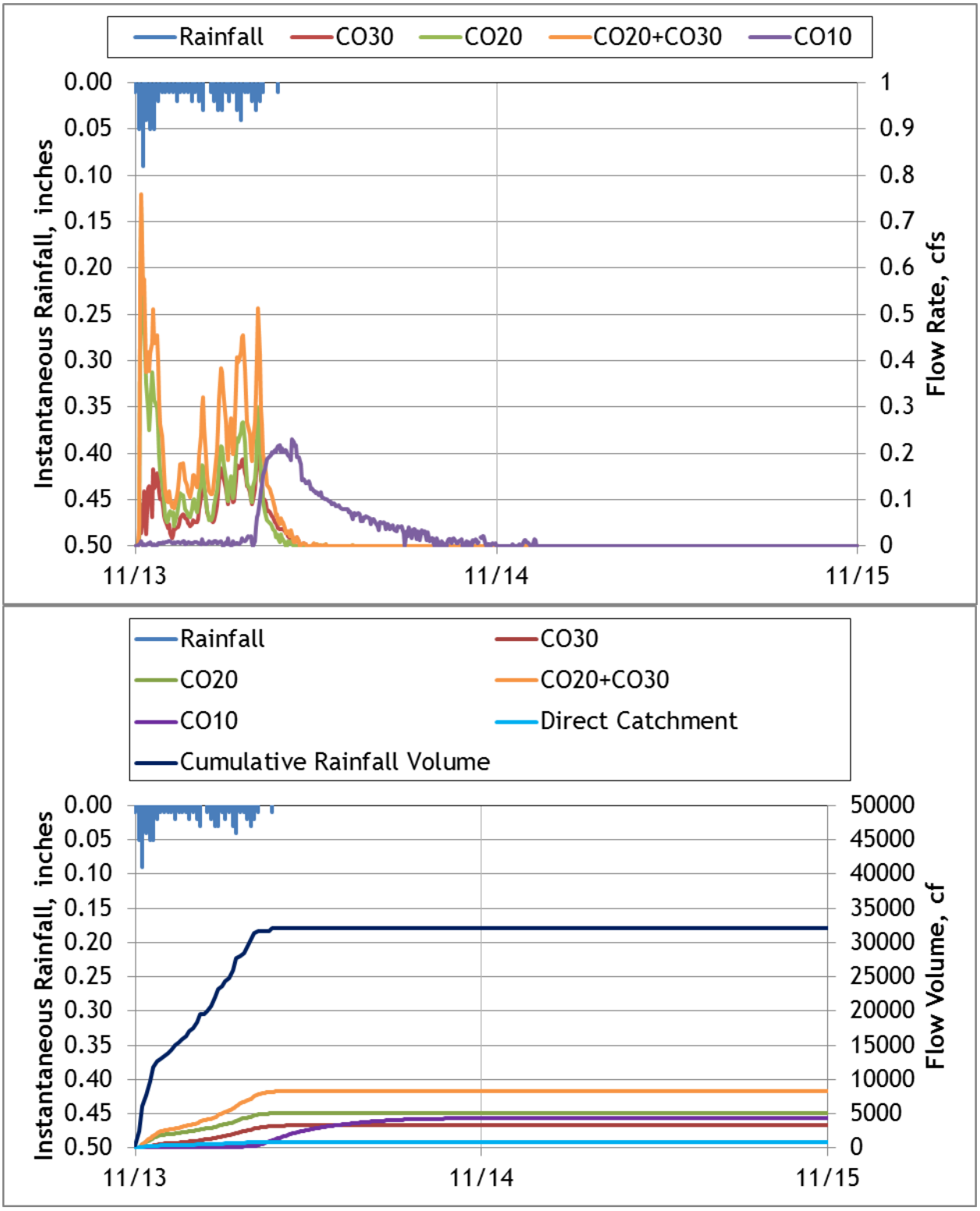

Figure A-3. Hydrograph and cumulative flow volumes for November 13-15, 2012

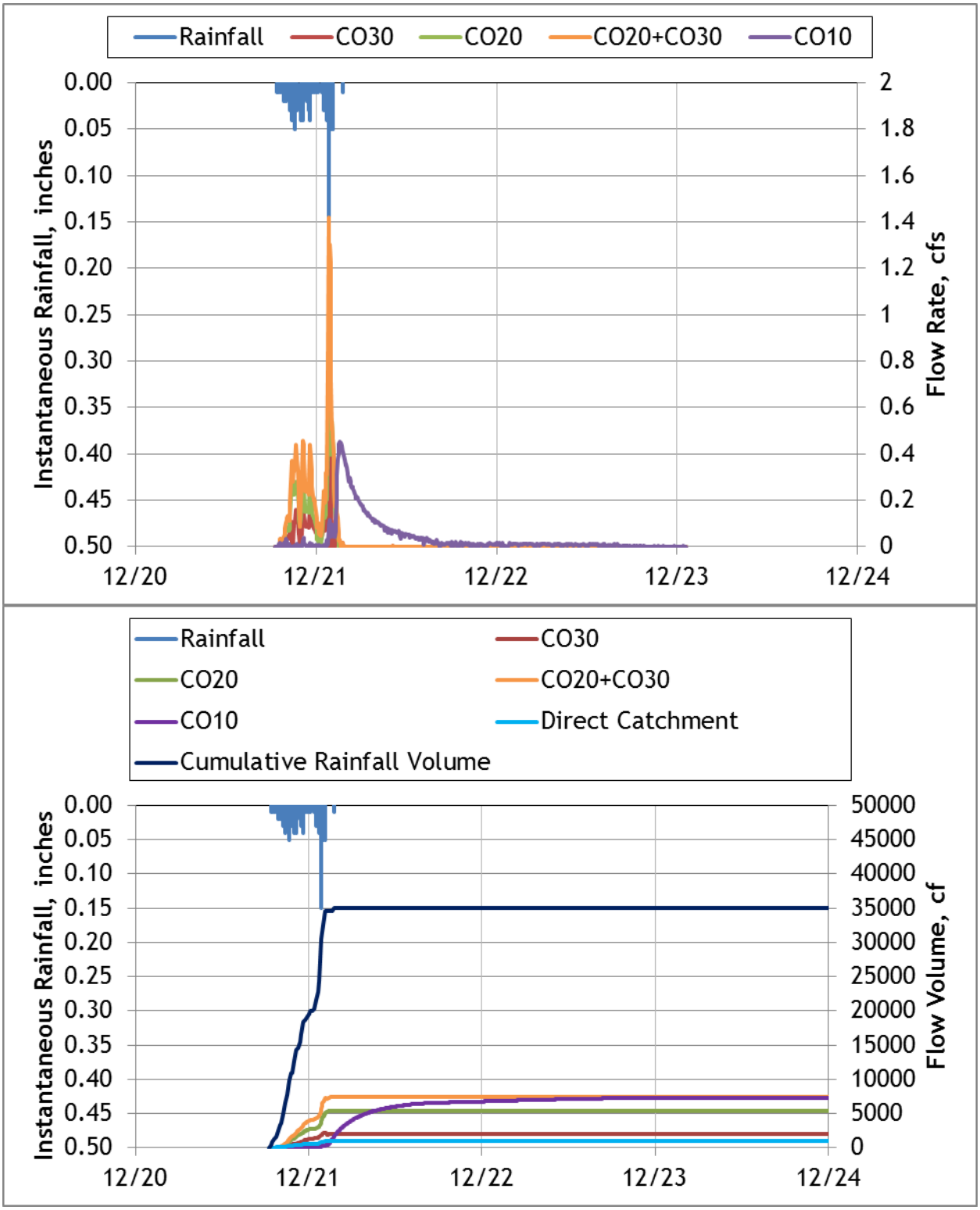

Figure A-4. Hydrograph and cumulative flow volumes for December 20-24, 2012

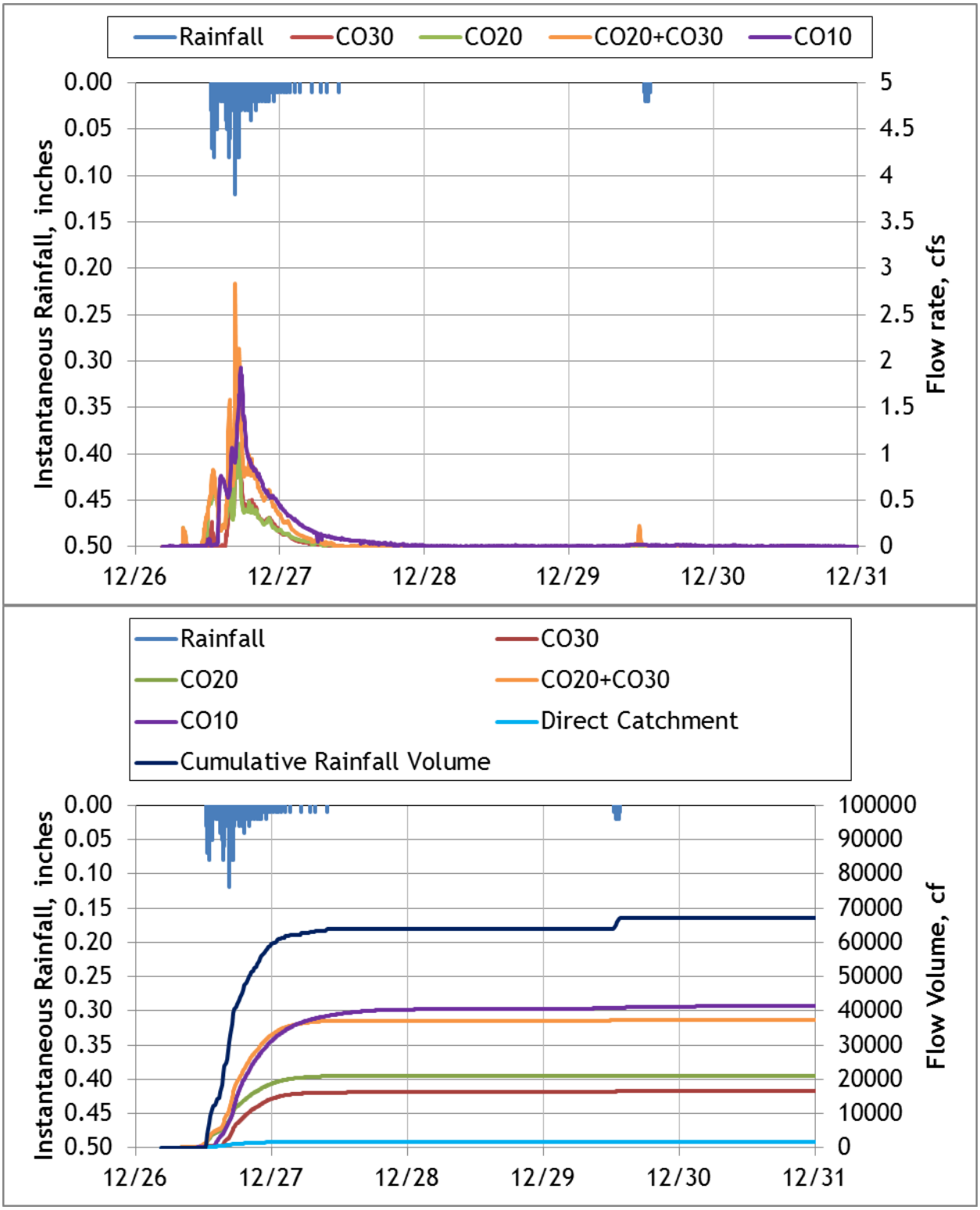

Figure A-5. Hydrograph and cumulative flow volumes for December 26-31, 2012

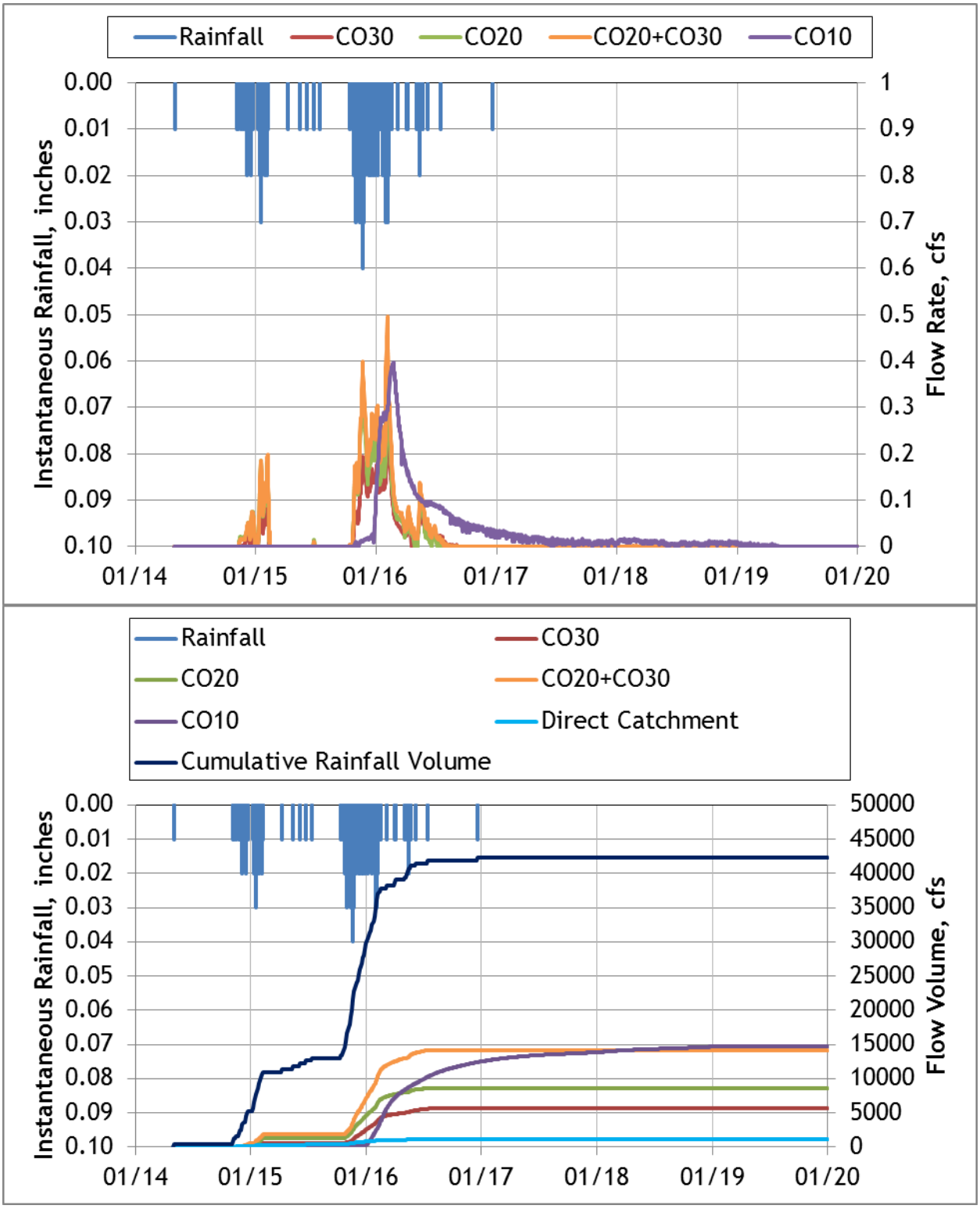

Figure A-6. Hydrograph and cumulative flow volumes for January 14-20, 2013

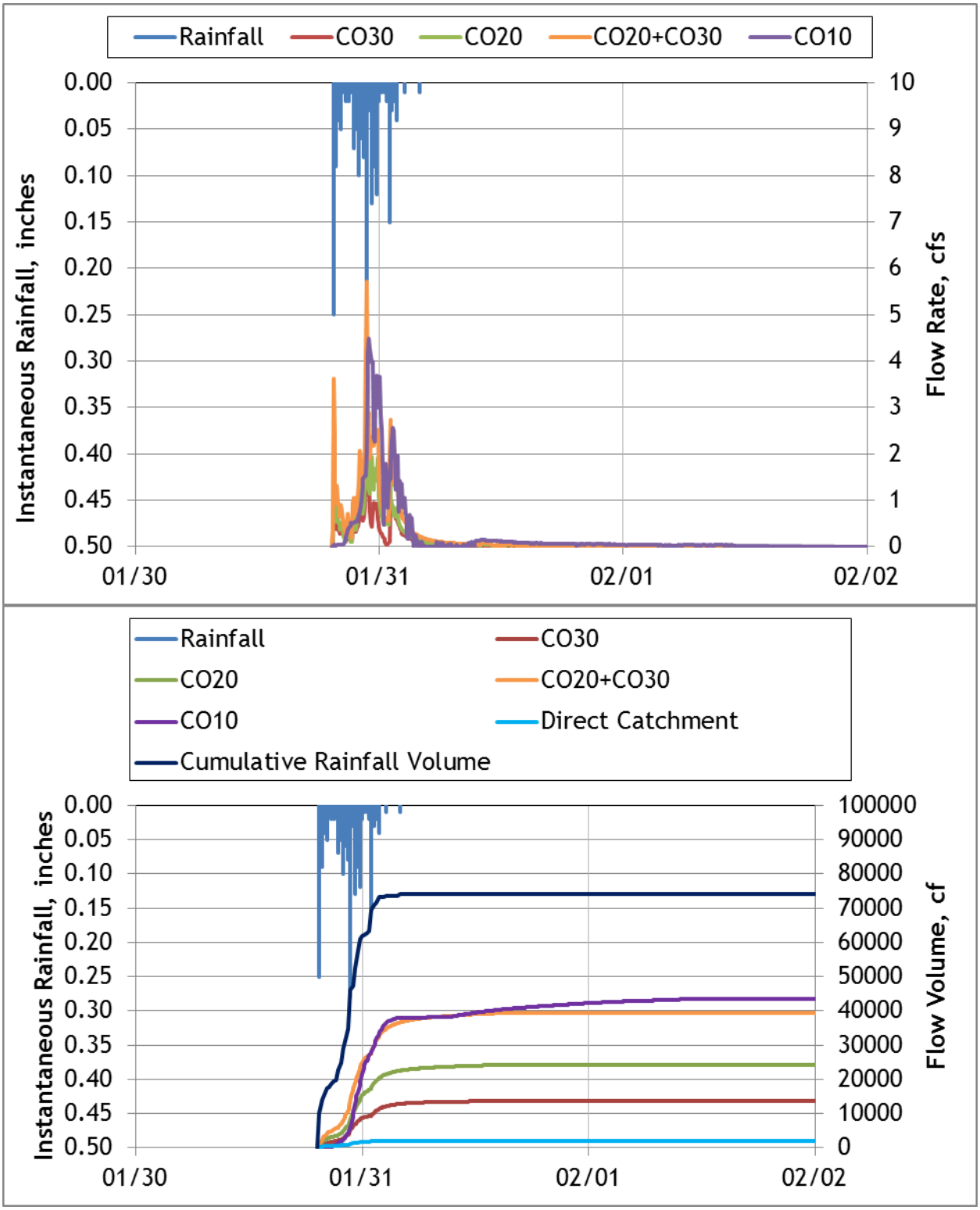

Figure A-7. Hydrograph and cumulative flow volumes for January 30-February 02, 2013

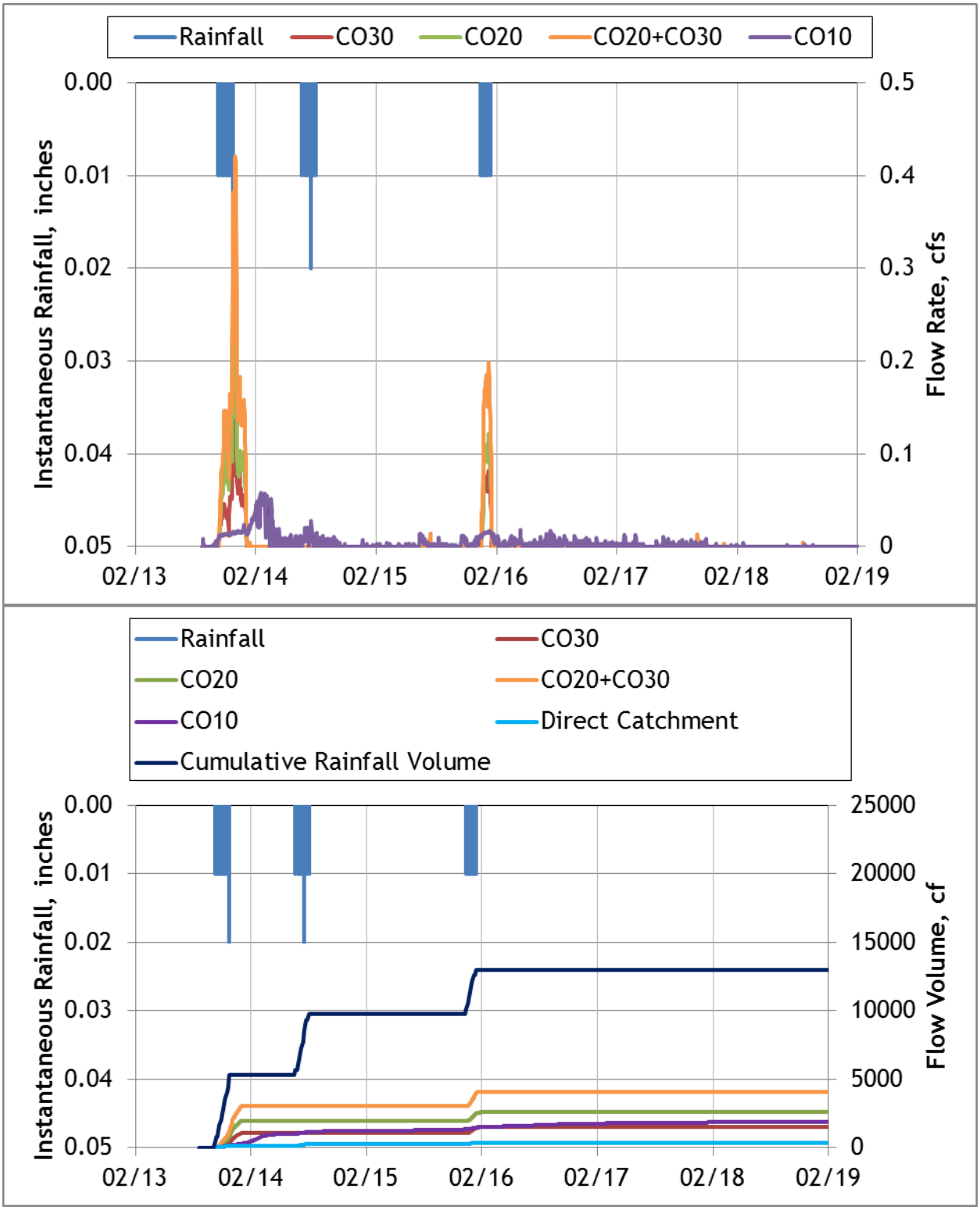

Figure A-8. Hydrograph and cumulative flow volumes for February 13-19, 2013

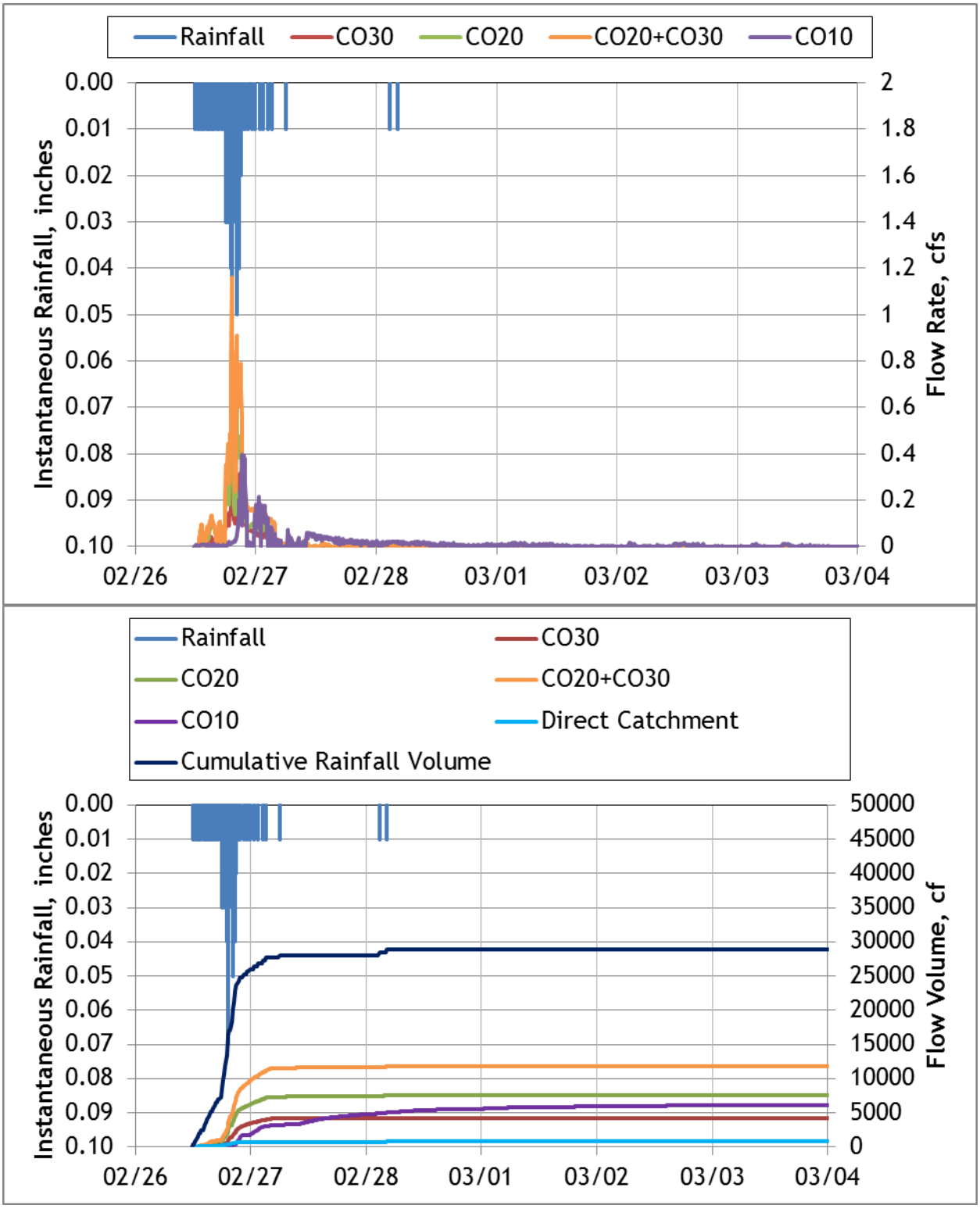

Figure A-9. Hydrograph and cumulative flow volumes for February 26-March 04, 2013

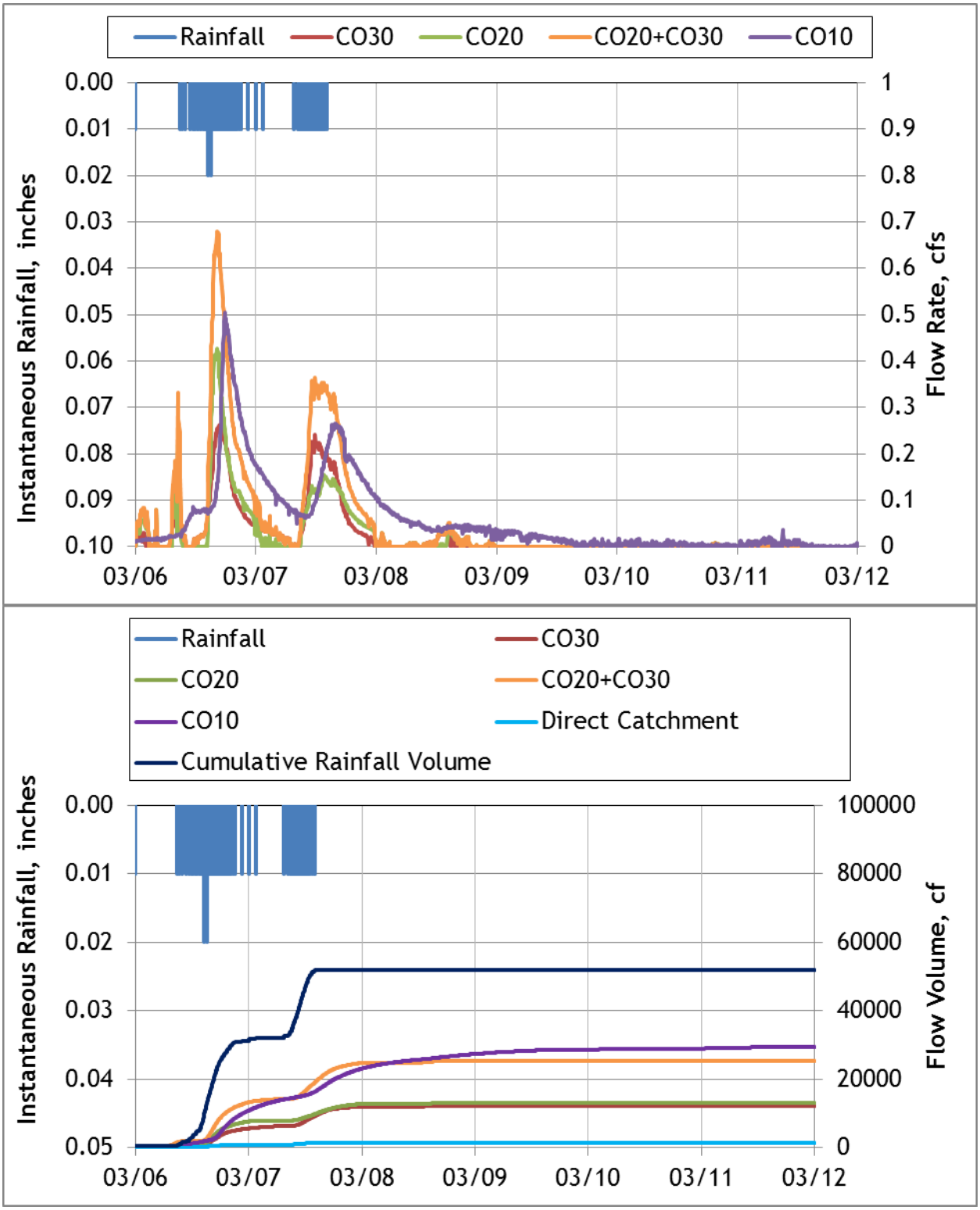

Figure A-10. Hydrograph and cumulative flow volumes for March 06-12, 2013
Correction factor of 1.1 applied to CO20.

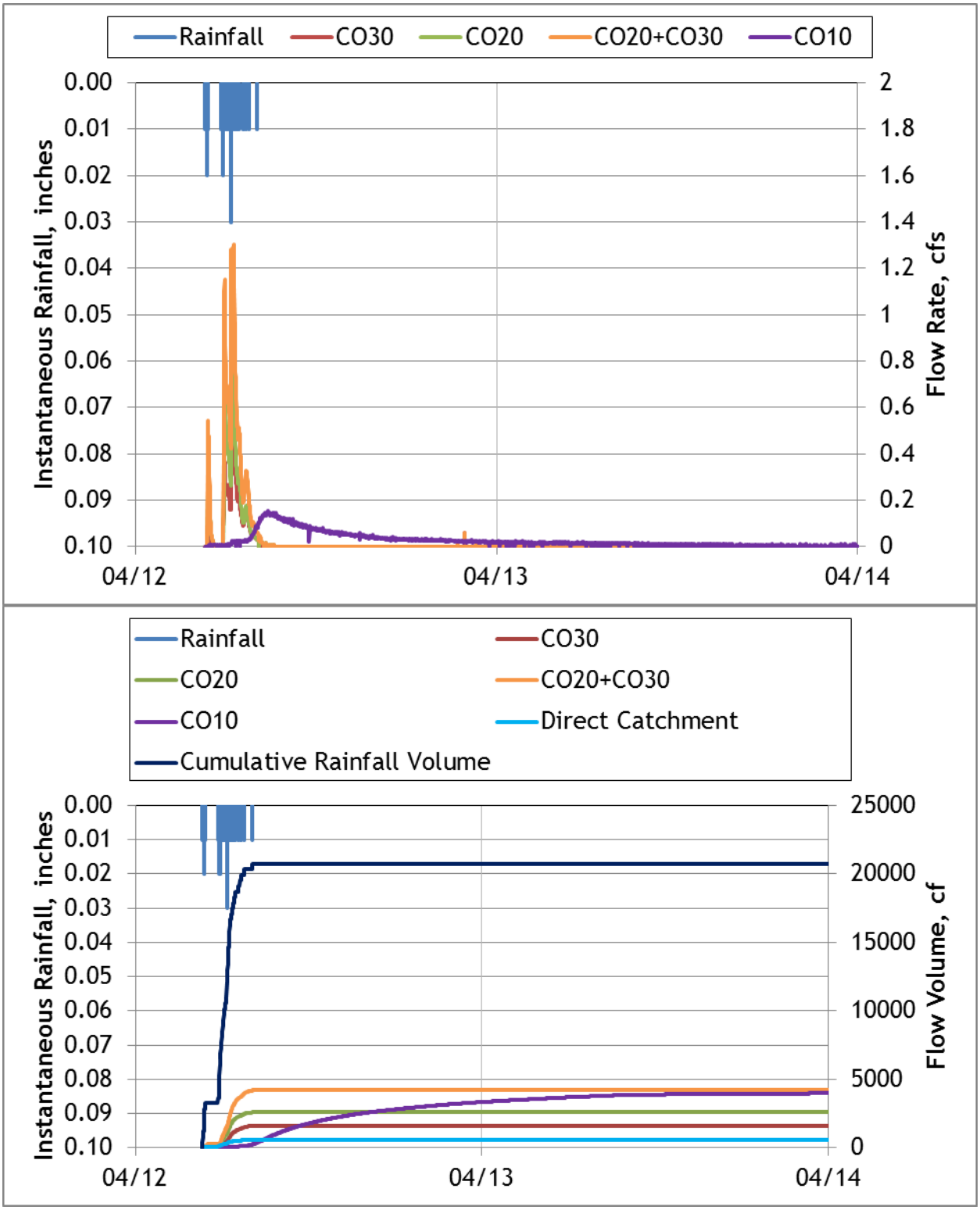

Figure A-11. Hydrograph and cumulative flow volumes for April 12-14, 2012

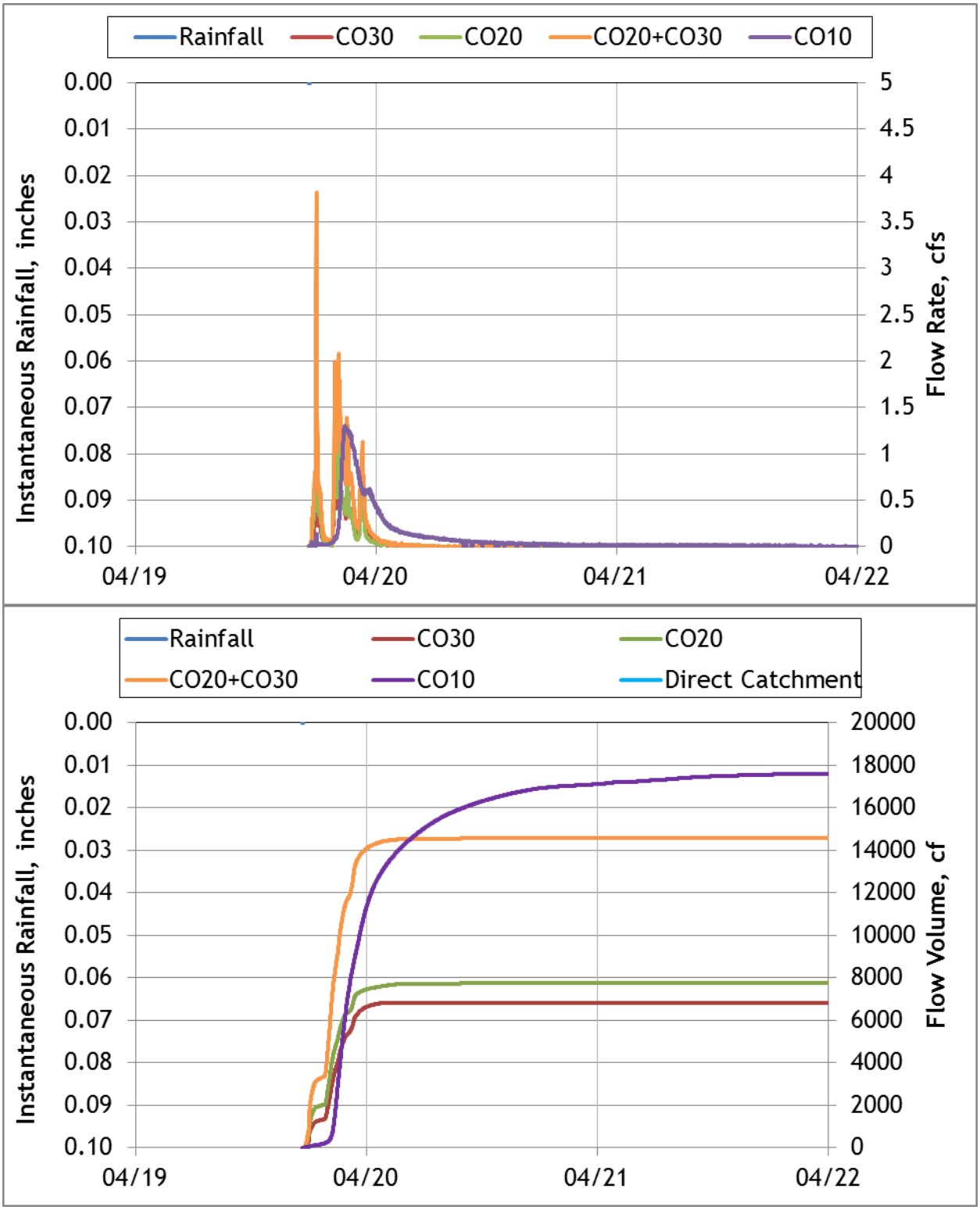

Figure A-12. Hydrograph and cumulative flow volumes for April 19-22, 2012
Malfunction at Cinnamon Oaks rain gage. The Dulles Airport rain data was used as a replacement. Total Rain = 1.20".

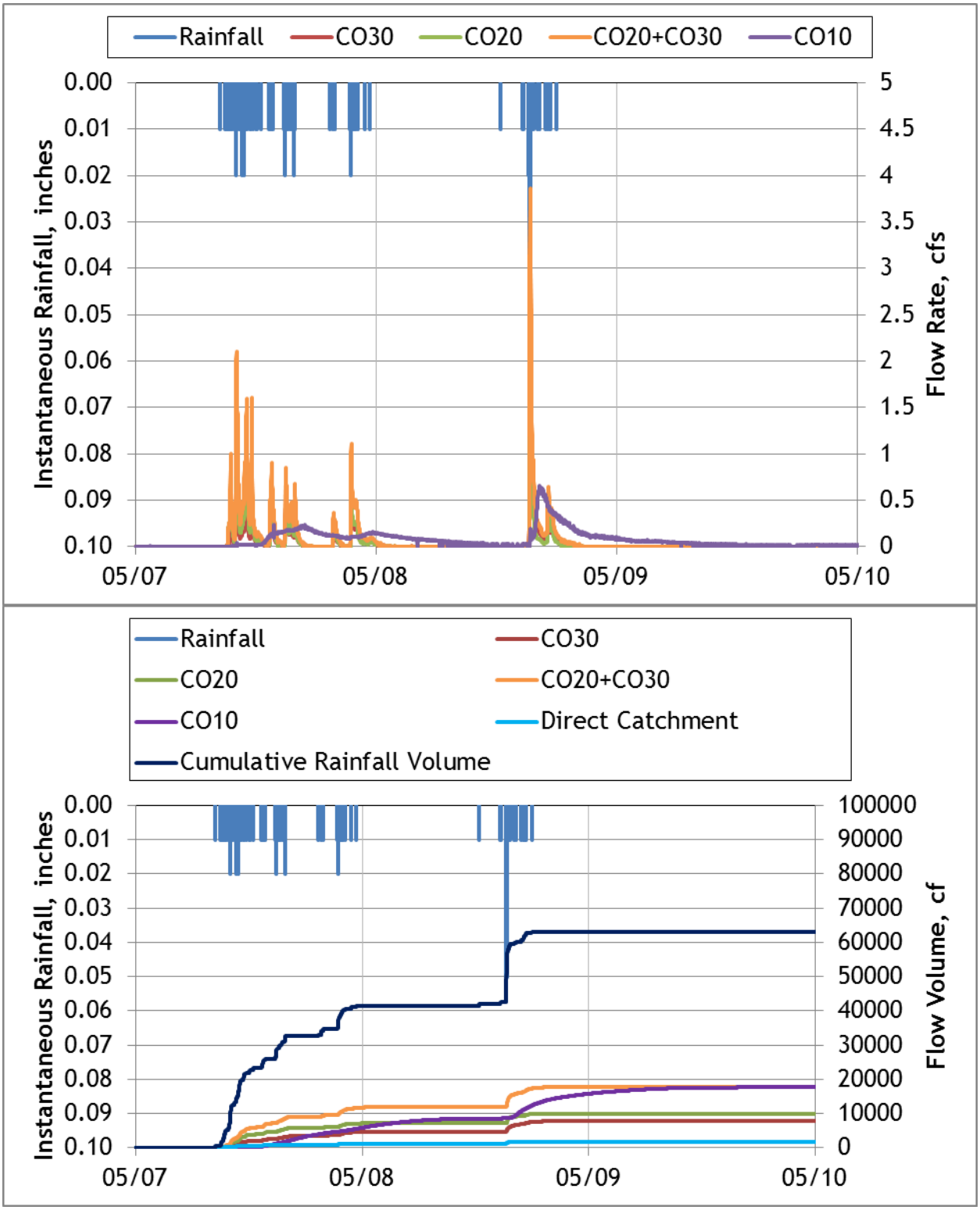

Figure A-13. Hydrograph and cumulative flow volumes for May 07-10, 2013

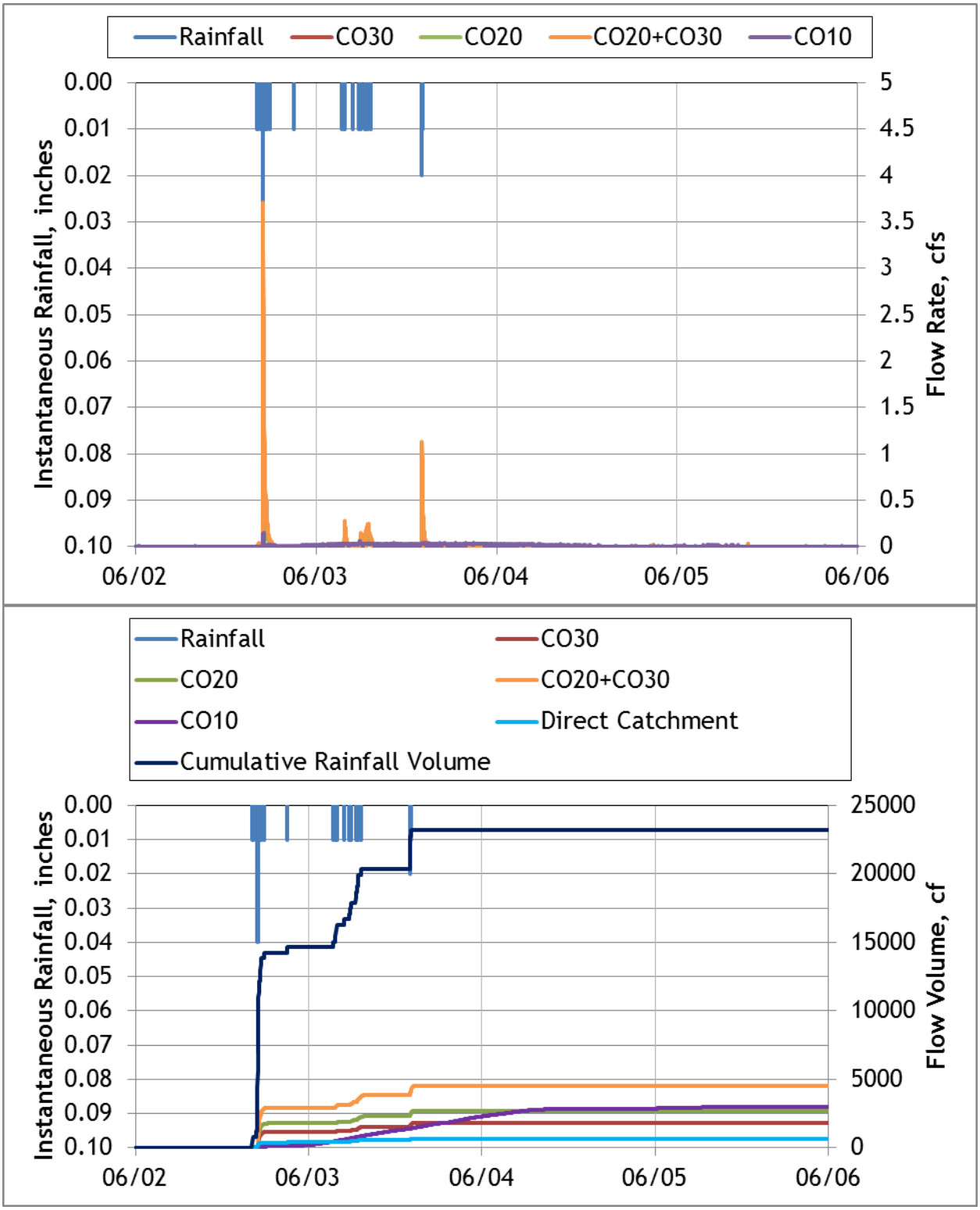

Figure A-14. Hydrograph and cumulative flow volumes for June 02-06, 2013

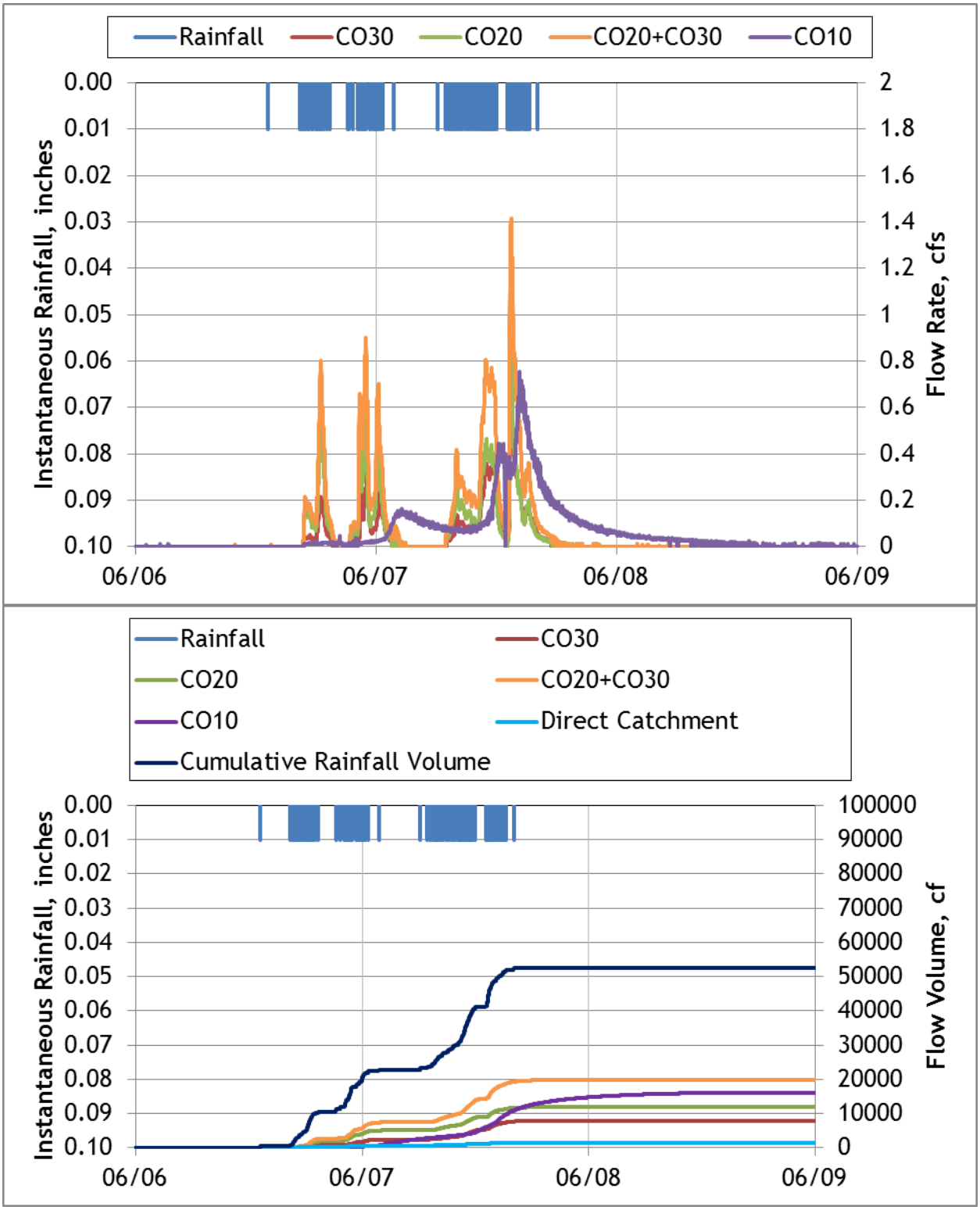

Figure A-15. Hydrograph and cumulative flow volumes for June 06-09, 2013
Correction factor of 1.1 applied to CO20.

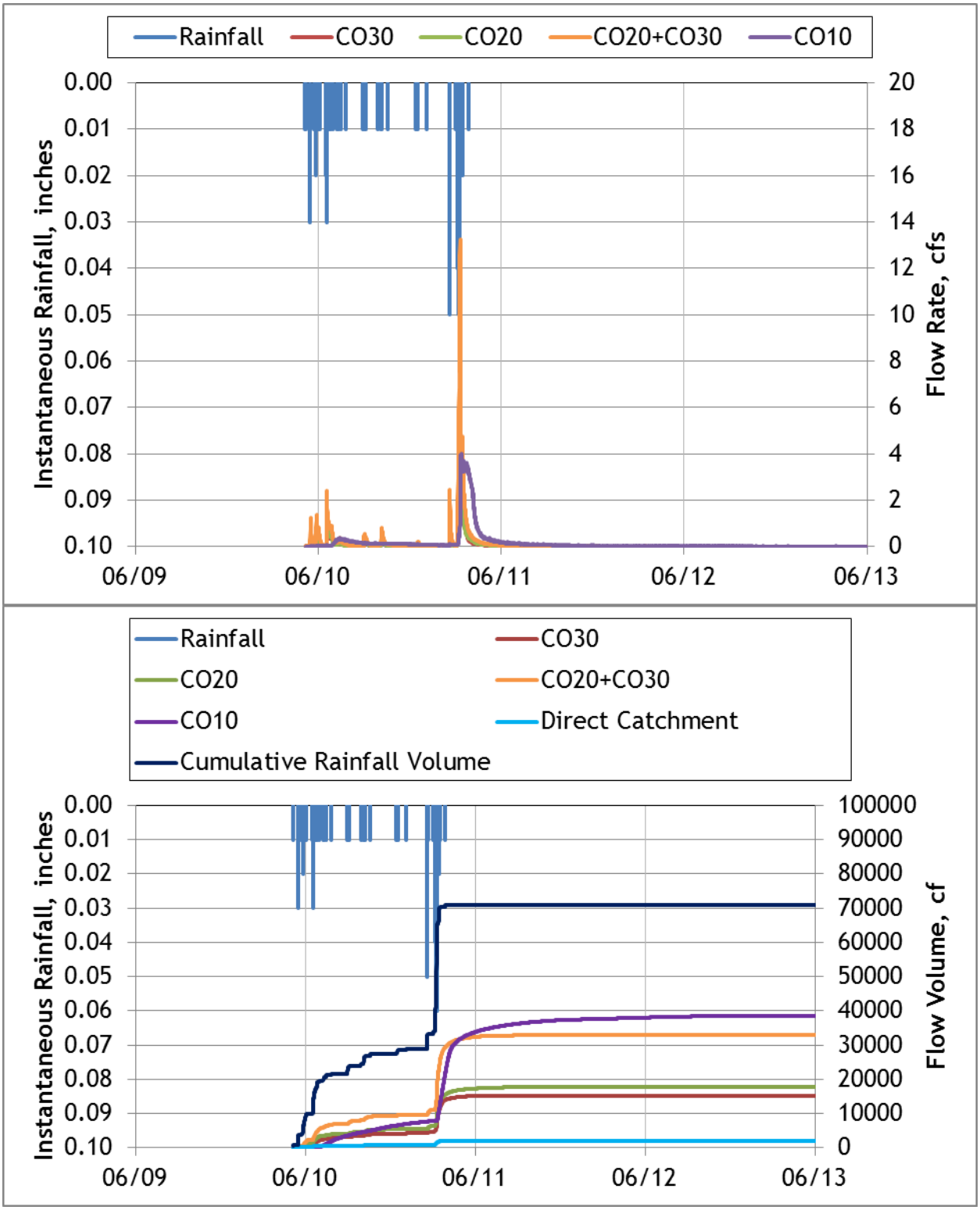

Figure A-16. Hydrograph and cumulative flow volumes for June 09-13, 2013

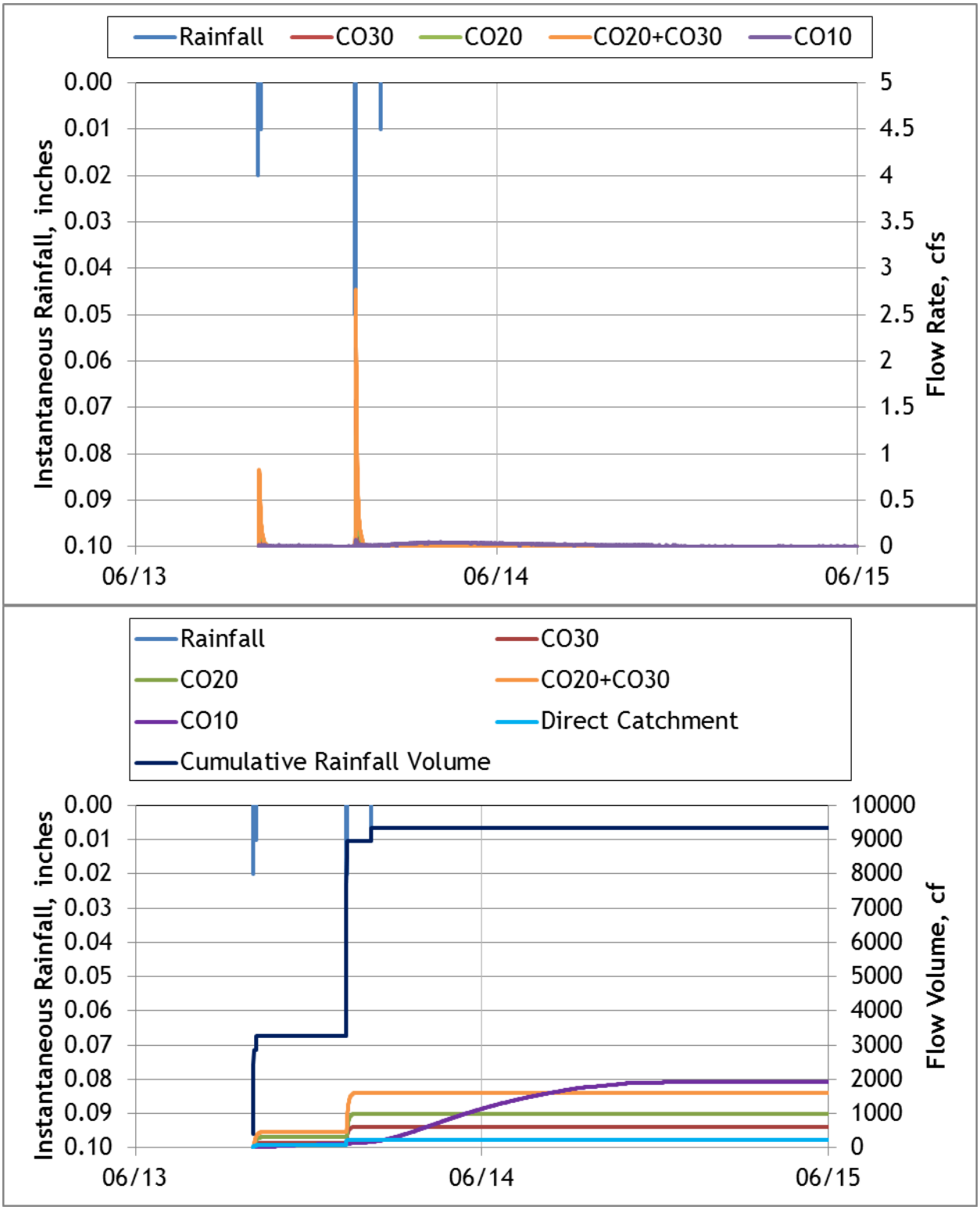

Figure A-17. Hydrograph and cumulative flow volumes for June 13-15, 2013

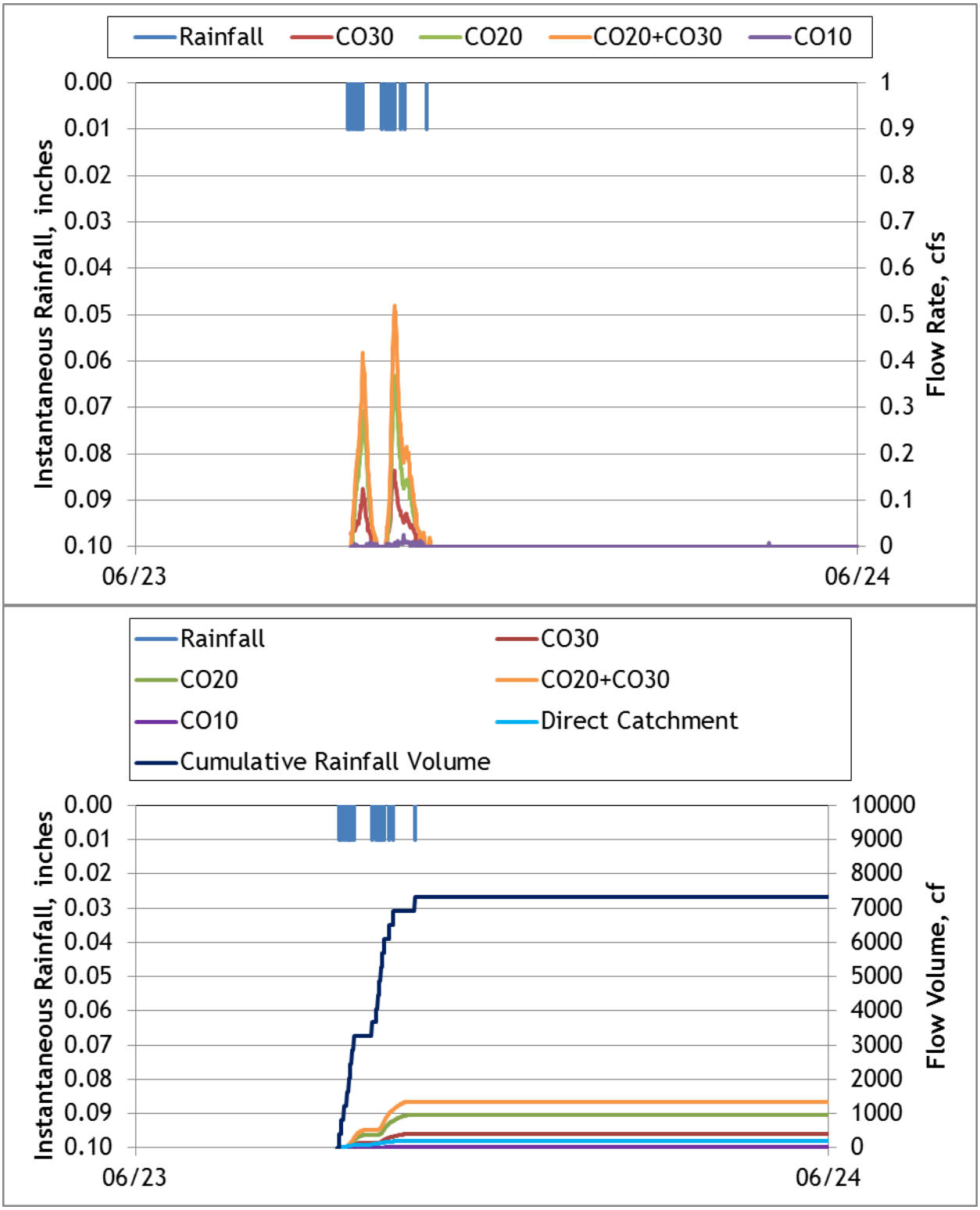

Figure A-18. Hydrograph and cumulative flow volumes for June 23-24, 2013

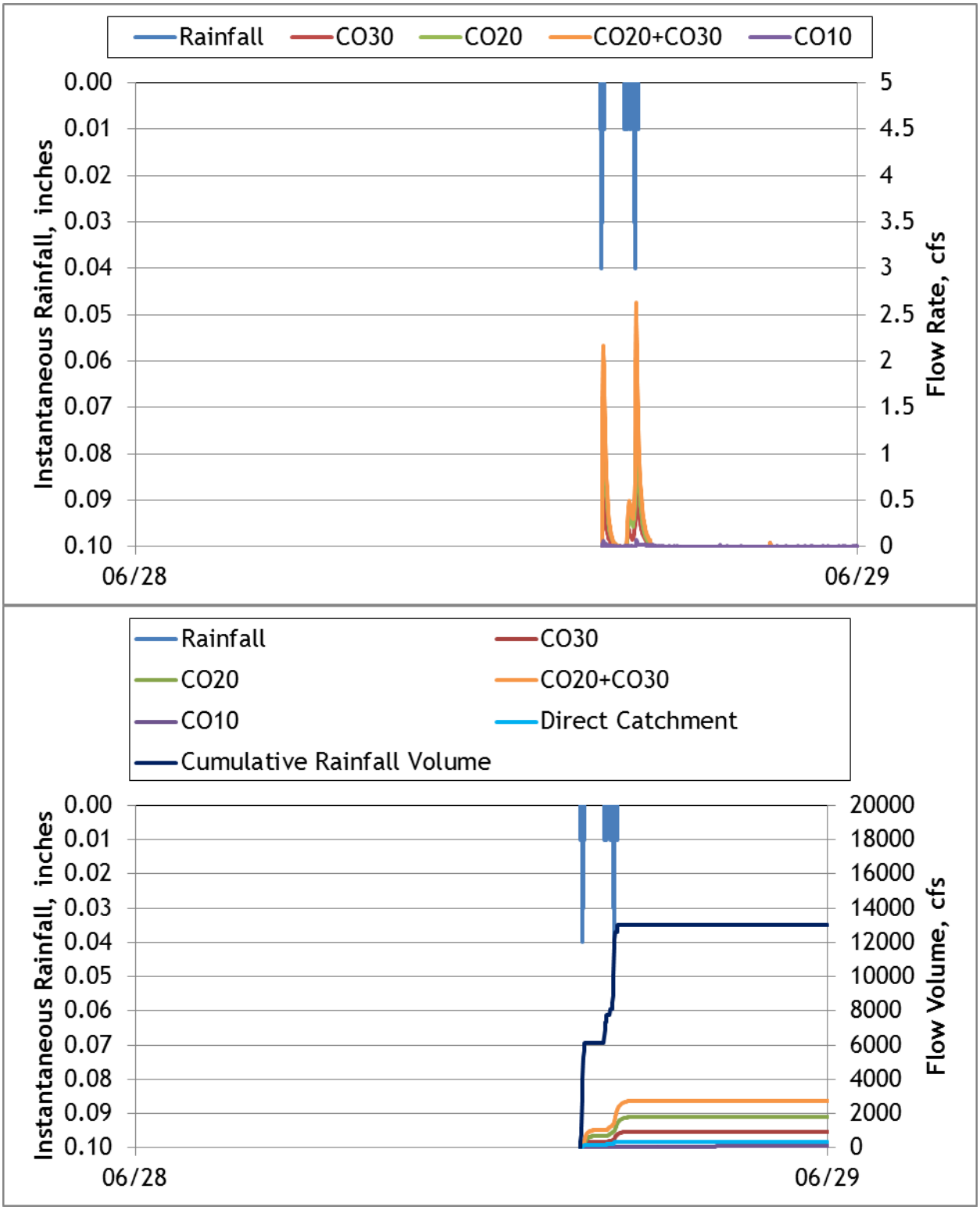

Figure A-19. Hydrograph and cumulative flow volumes for June 28-29, 2013

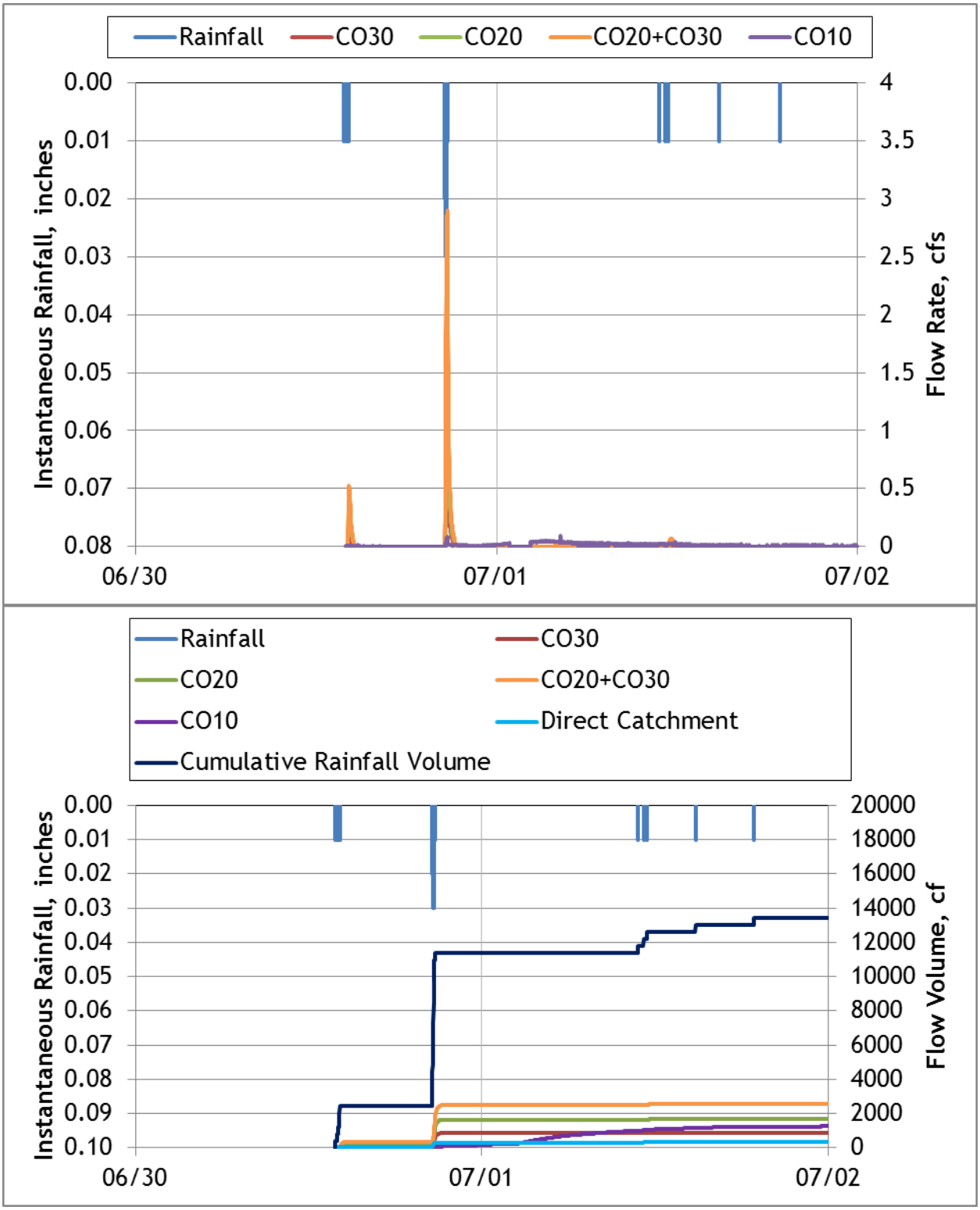

Figure A-20. Hydrograph and cumulative flow volumes for June 30-July 02, 2013

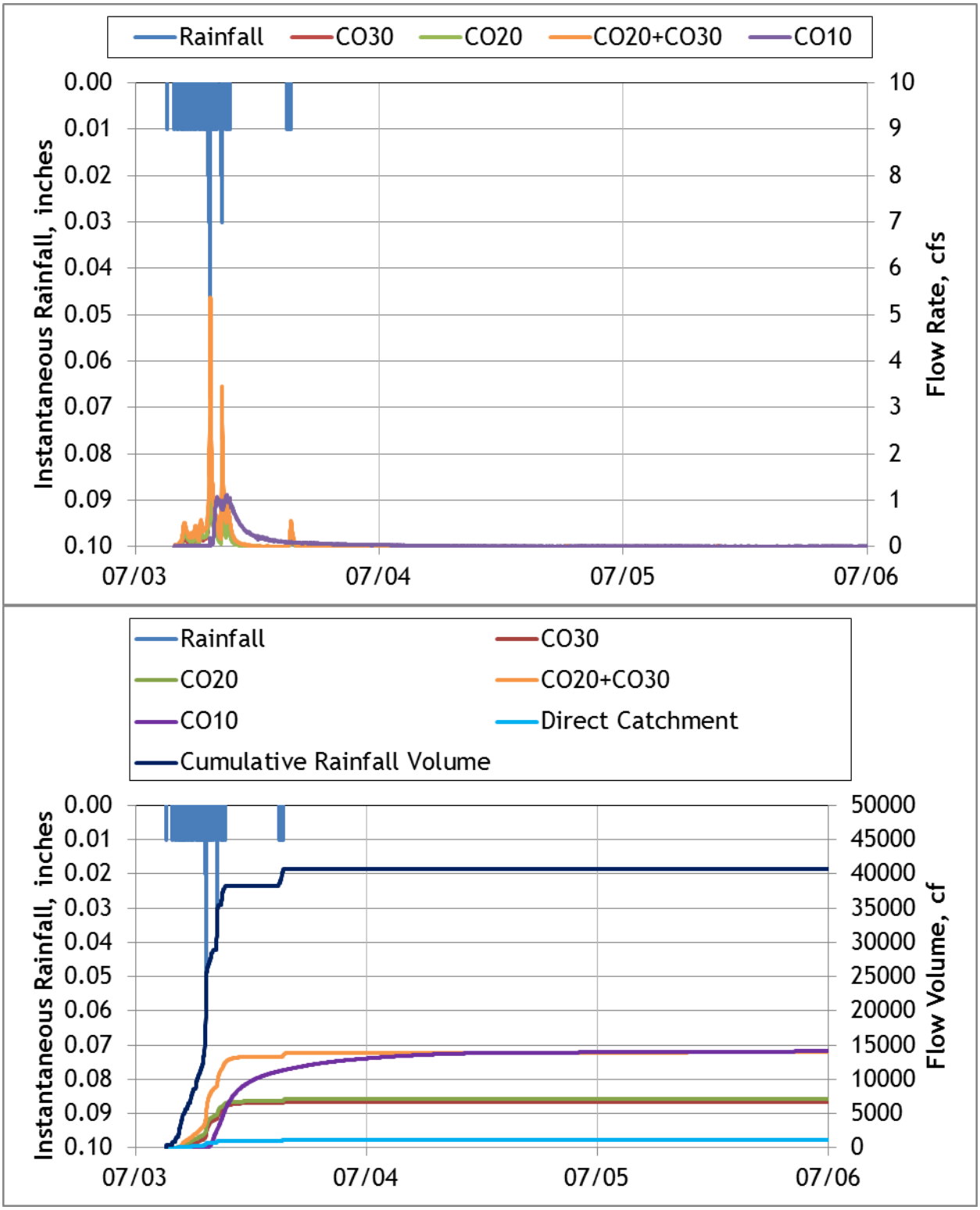

Figure A-21. Hydrograph and cumulative flow volumes for July 03-06, 2013

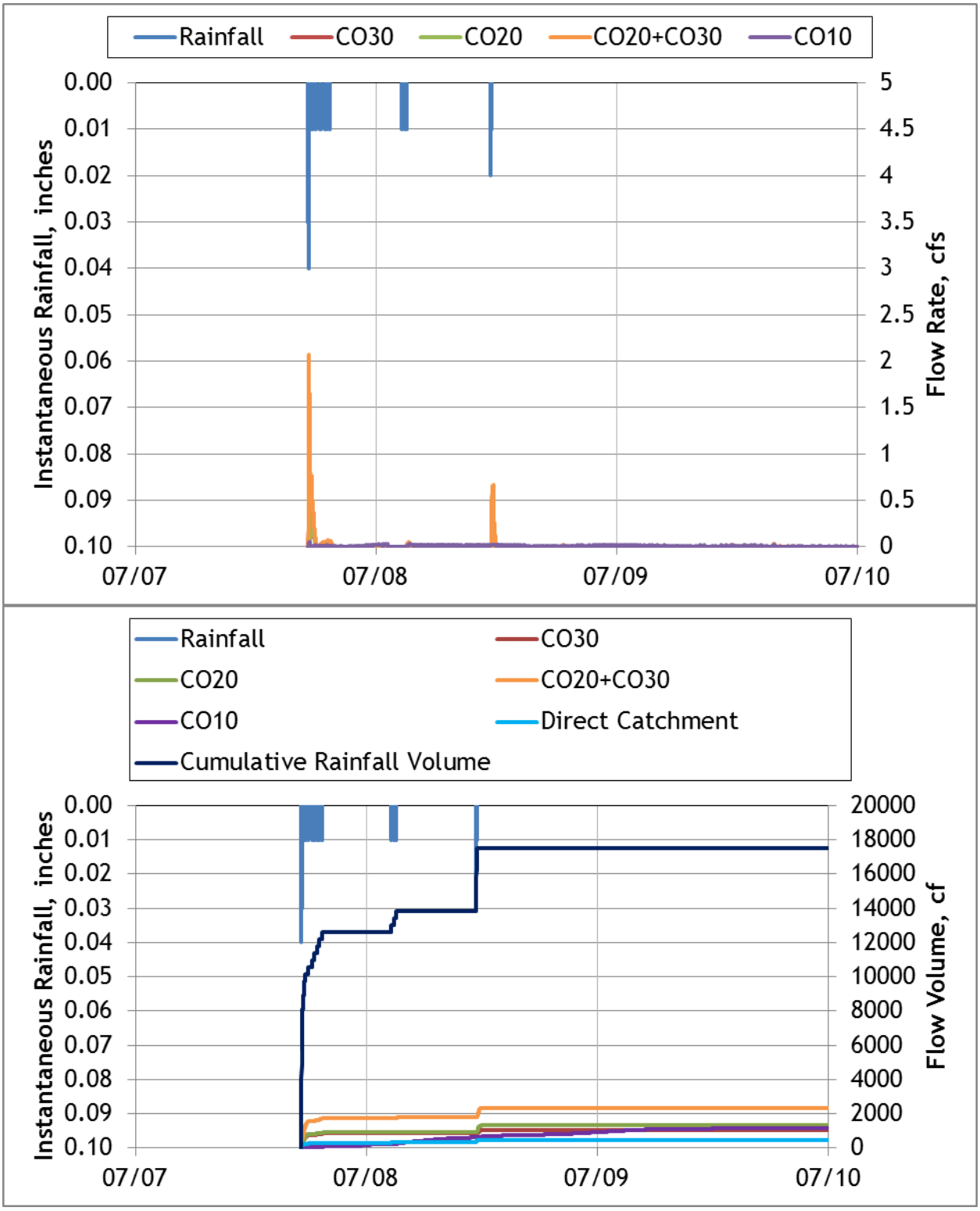

Figure A-22. Hydrograph and cumulative flow volumes for July 07-10, 2013

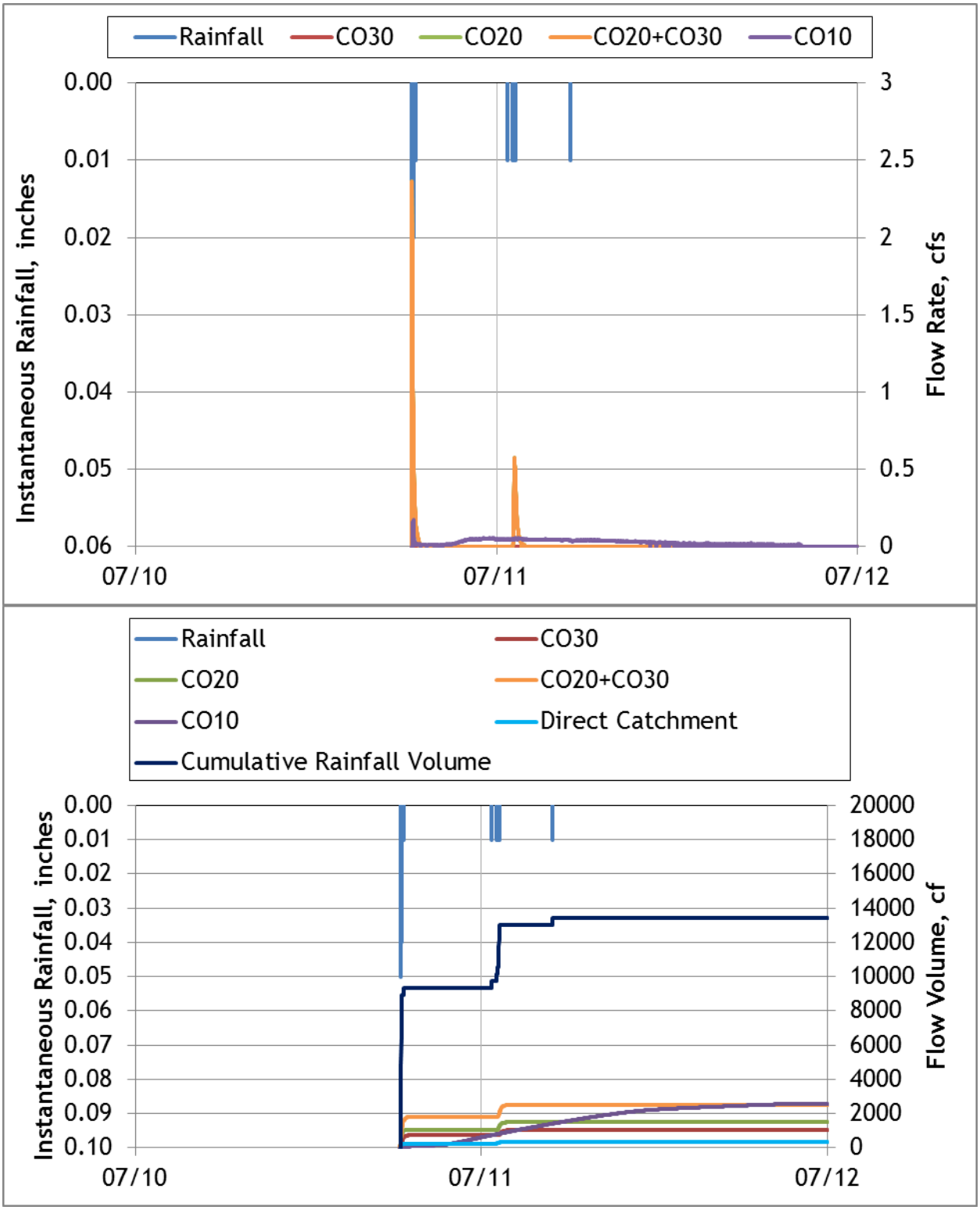

Figure A-23. Hydrograph and cumulative flow volumes for July 10-12, 2013

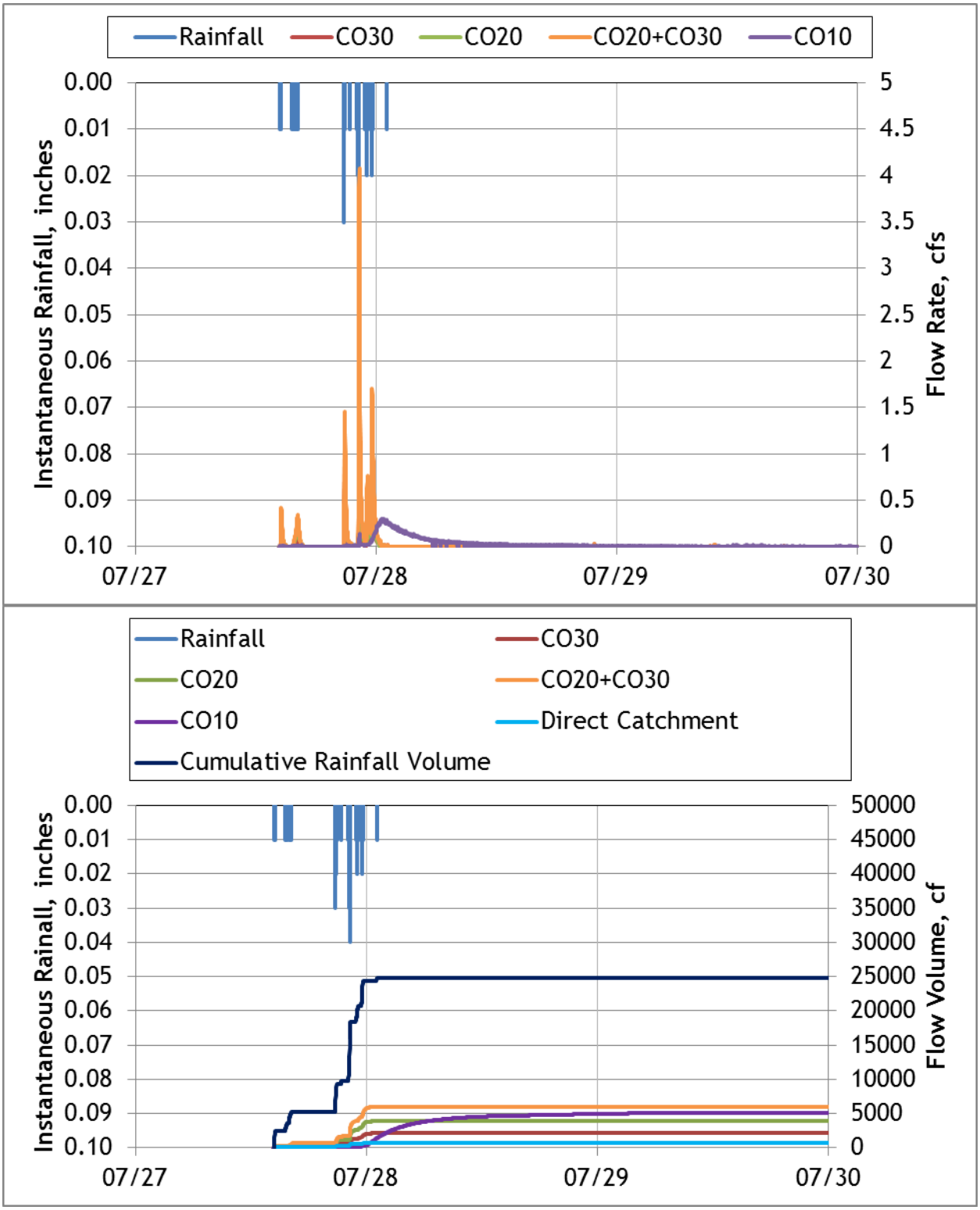

Figure A-24. Hydrograph and cumulative flow volumes for July 27-30, 2013

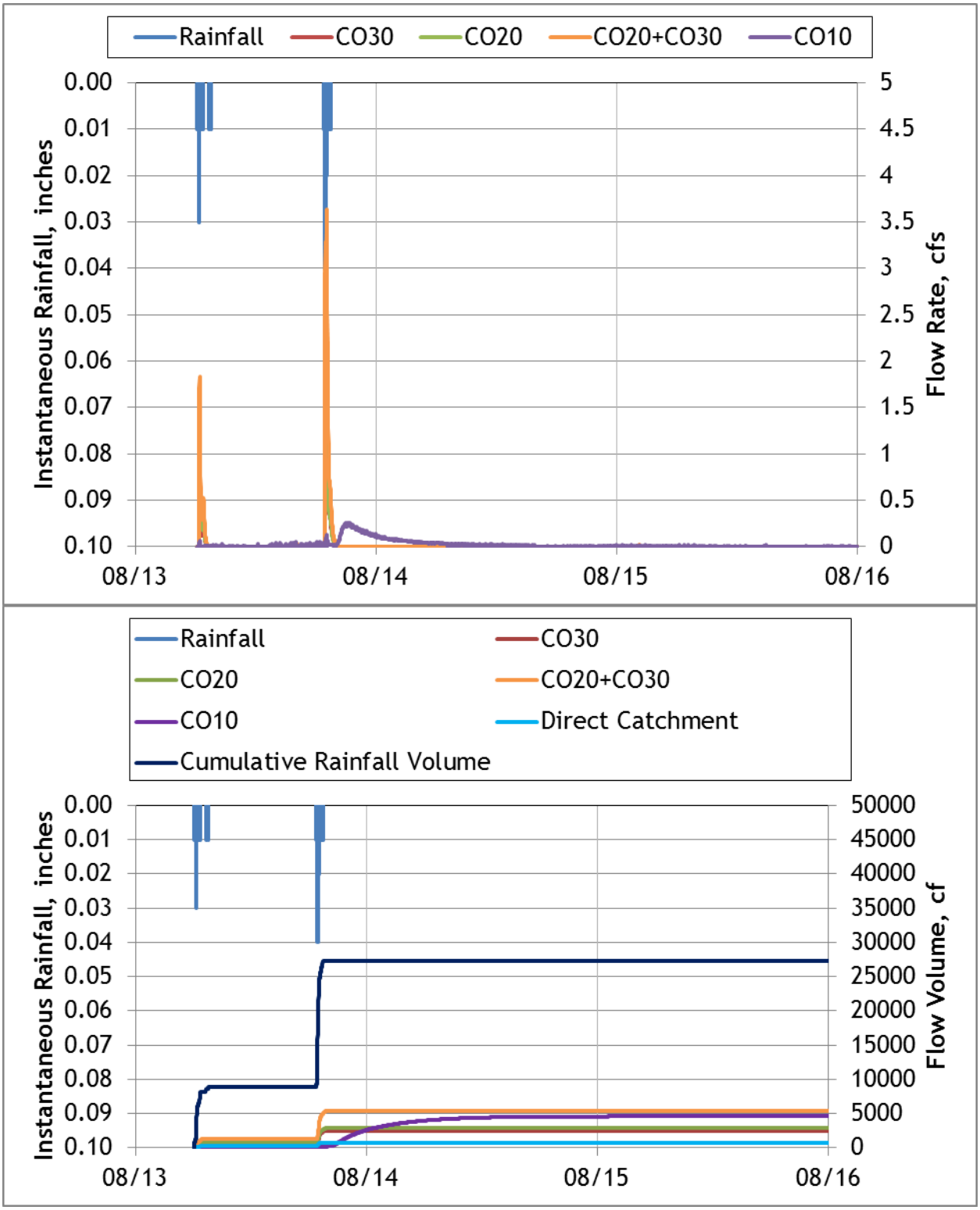

Figure A-25. Hydrograph and cumulative flow volumes for August 13-16, 2013

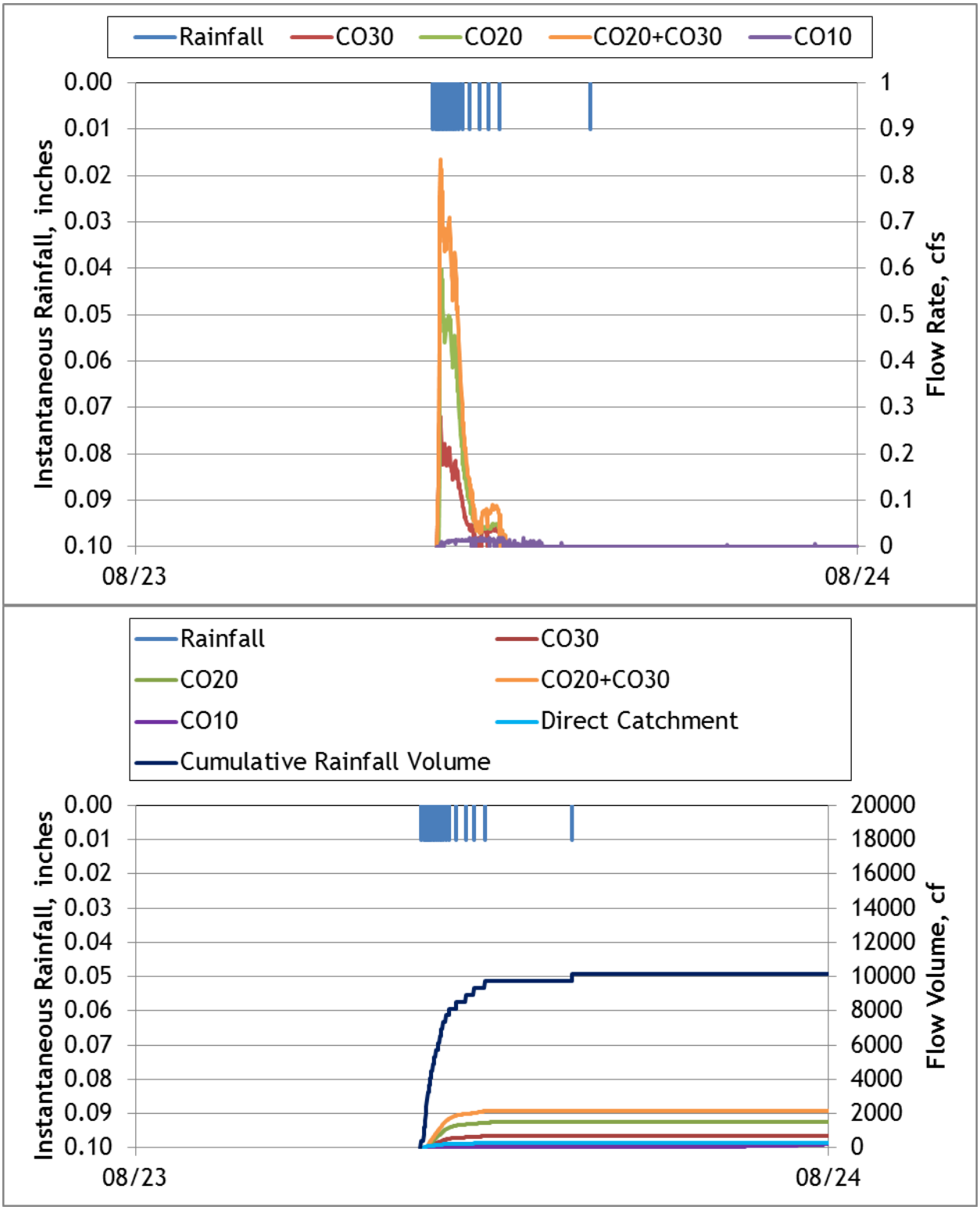

Figure A-26. Hydrograph and cumulative flow volumes for August 23-24, 2013

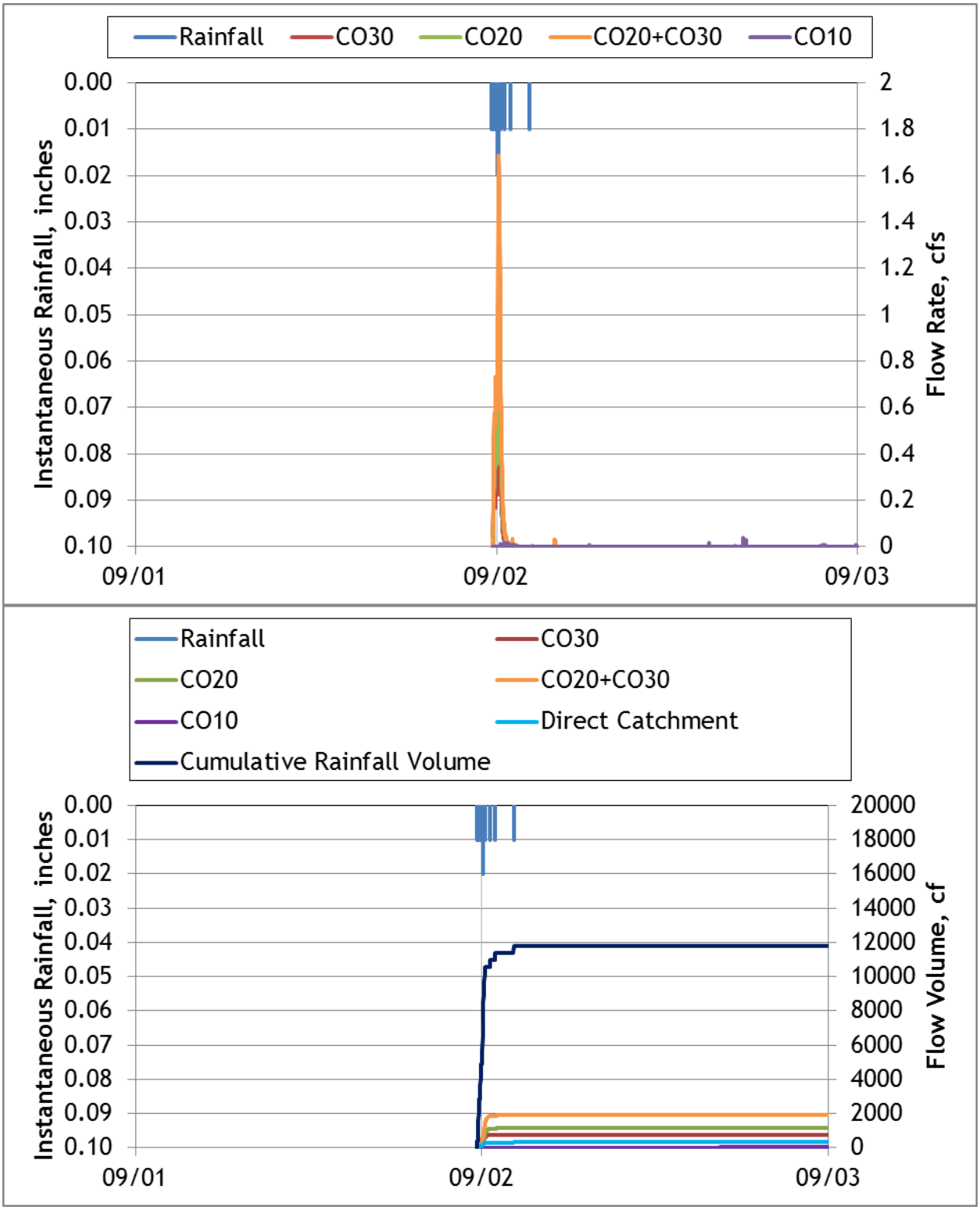

Figure A- 27. Hydrograph and cumulative flow volumes for September 01-03, 2013

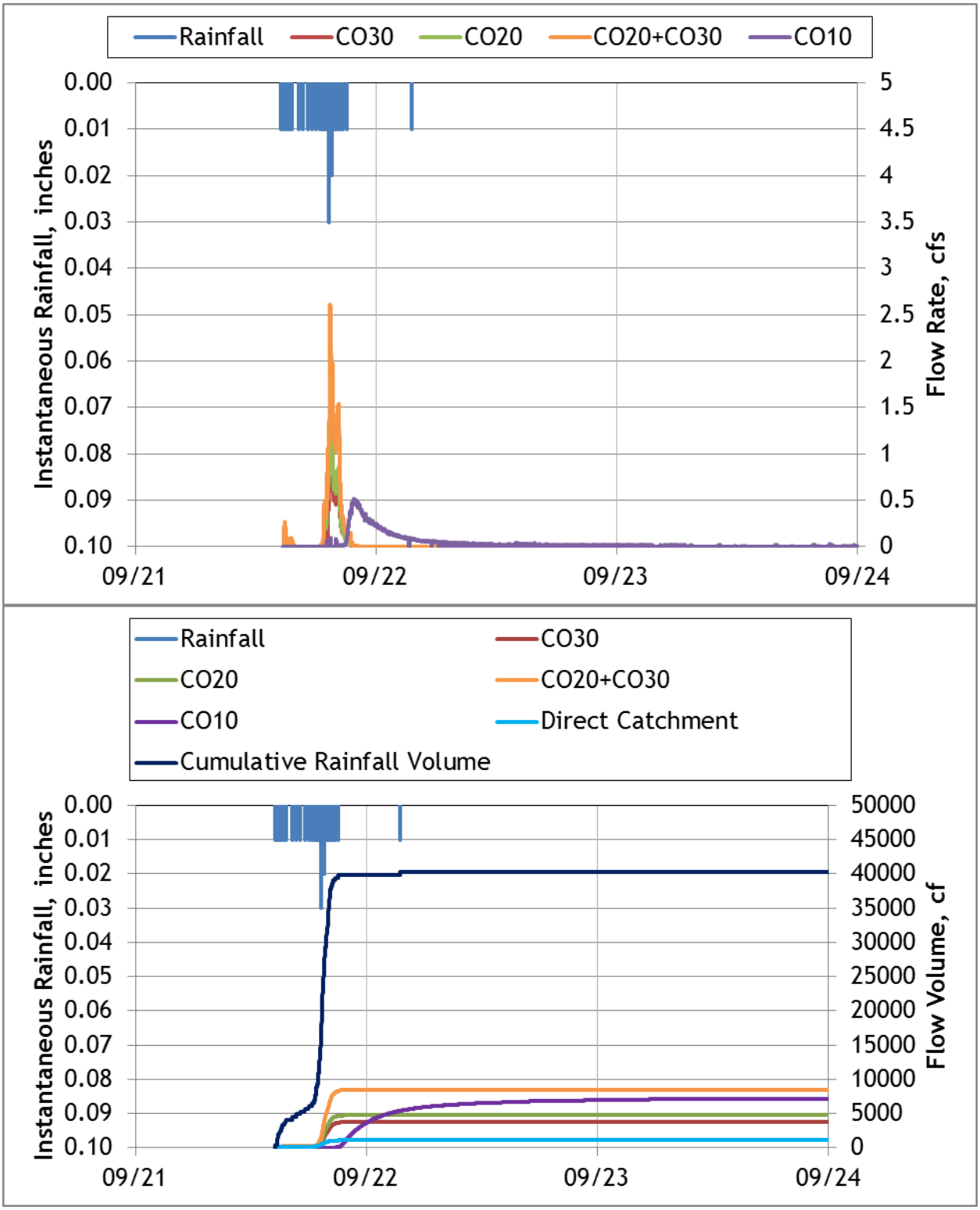

Figure A-28. Hydrograph and cumulative flow volumes for September 21-24, 2013

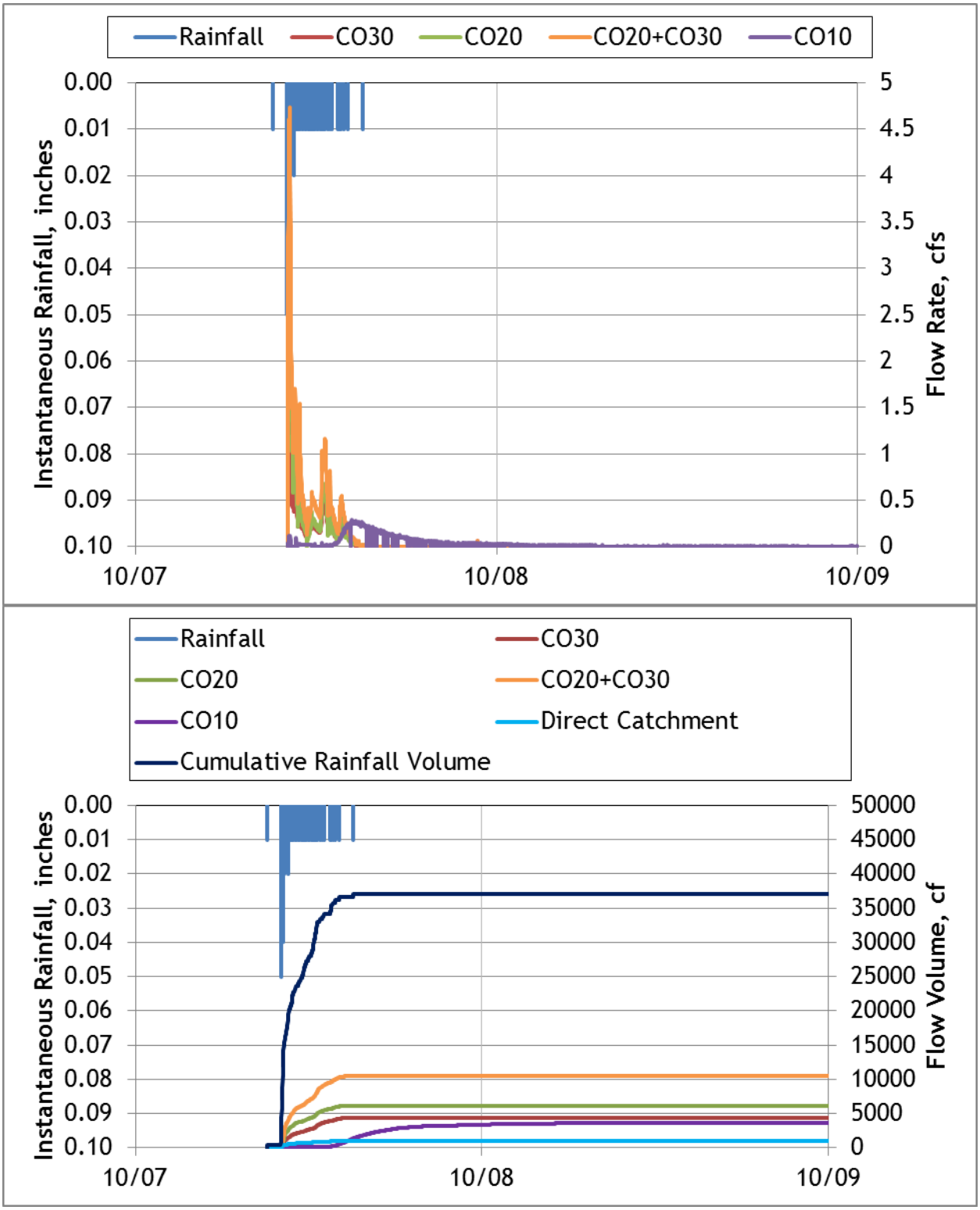

Figure A-29. Hydrograph and cumulative flow volumes for October 07-09, 2013

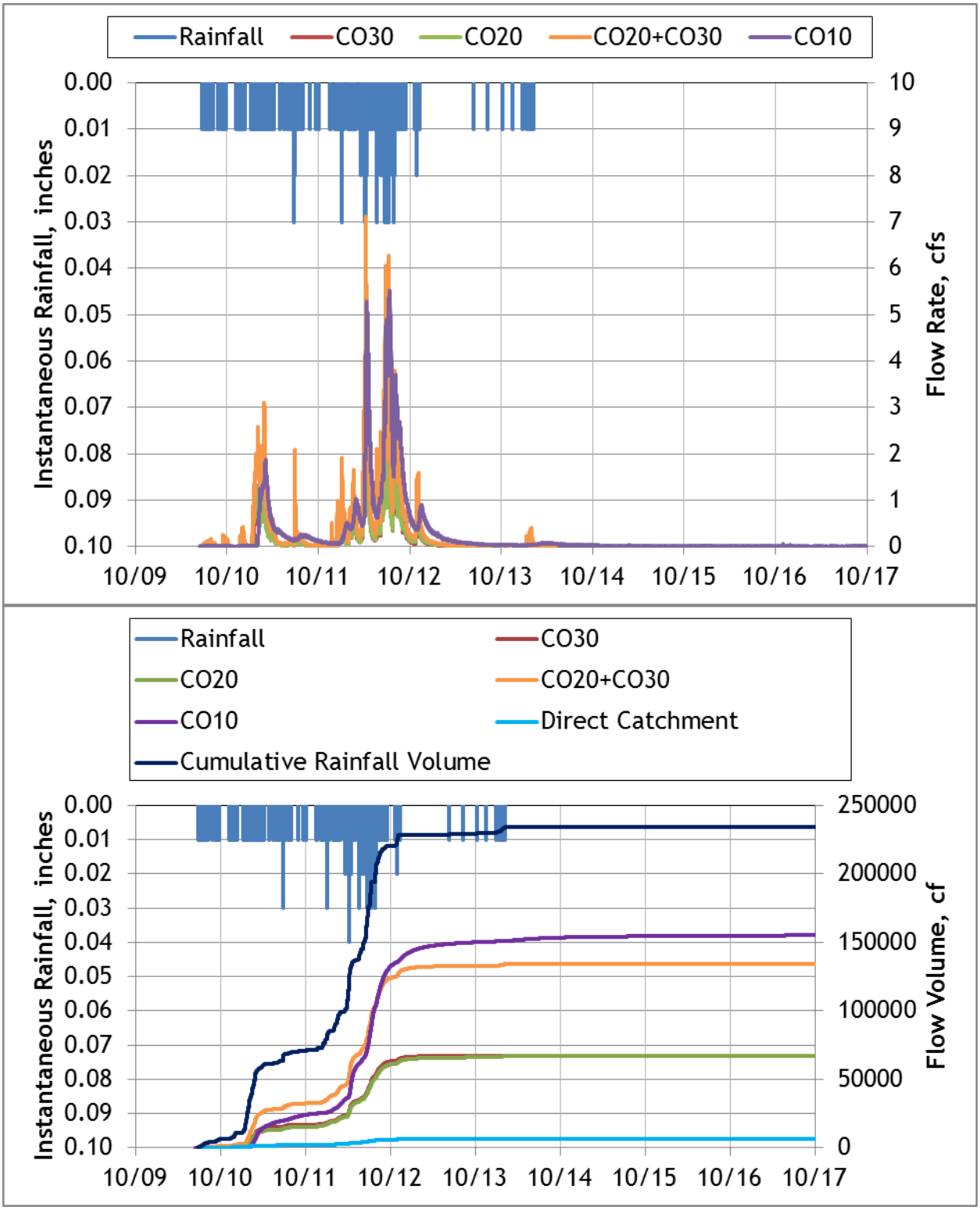

Figure A-30. Hydrograph and cumulative flow volumes for October 09-17, 2013

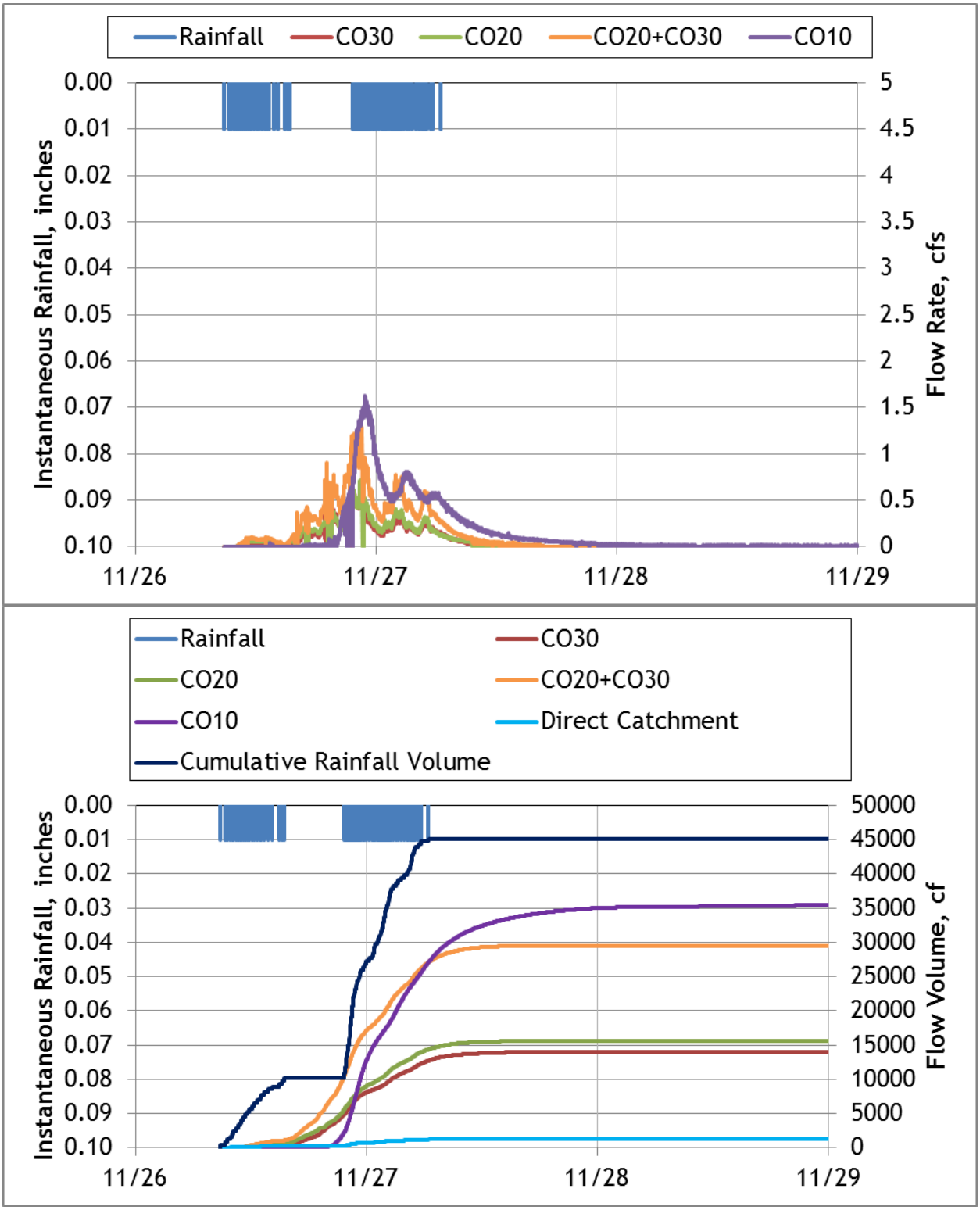

Figure A-31. Hydrograph and cumulative flow volumes for November 26-29, 2013

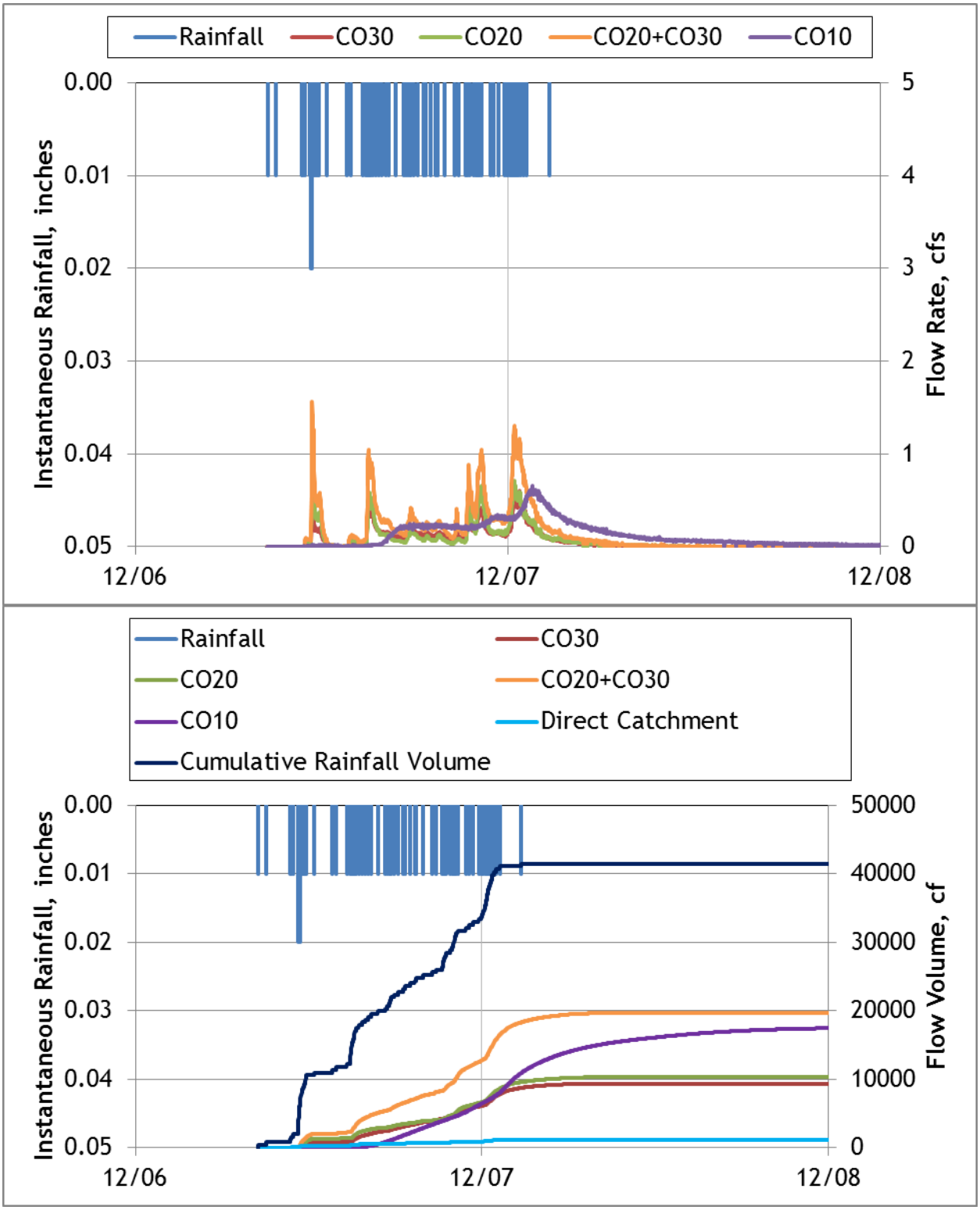

Figure A-32. Hydrograph and cumulative flow volumes for December 06-08, 2013
Snow prevented accurate measurements of rain data. The Dulles Airport rain data was used as a replacement. Total Rain = 1.02".

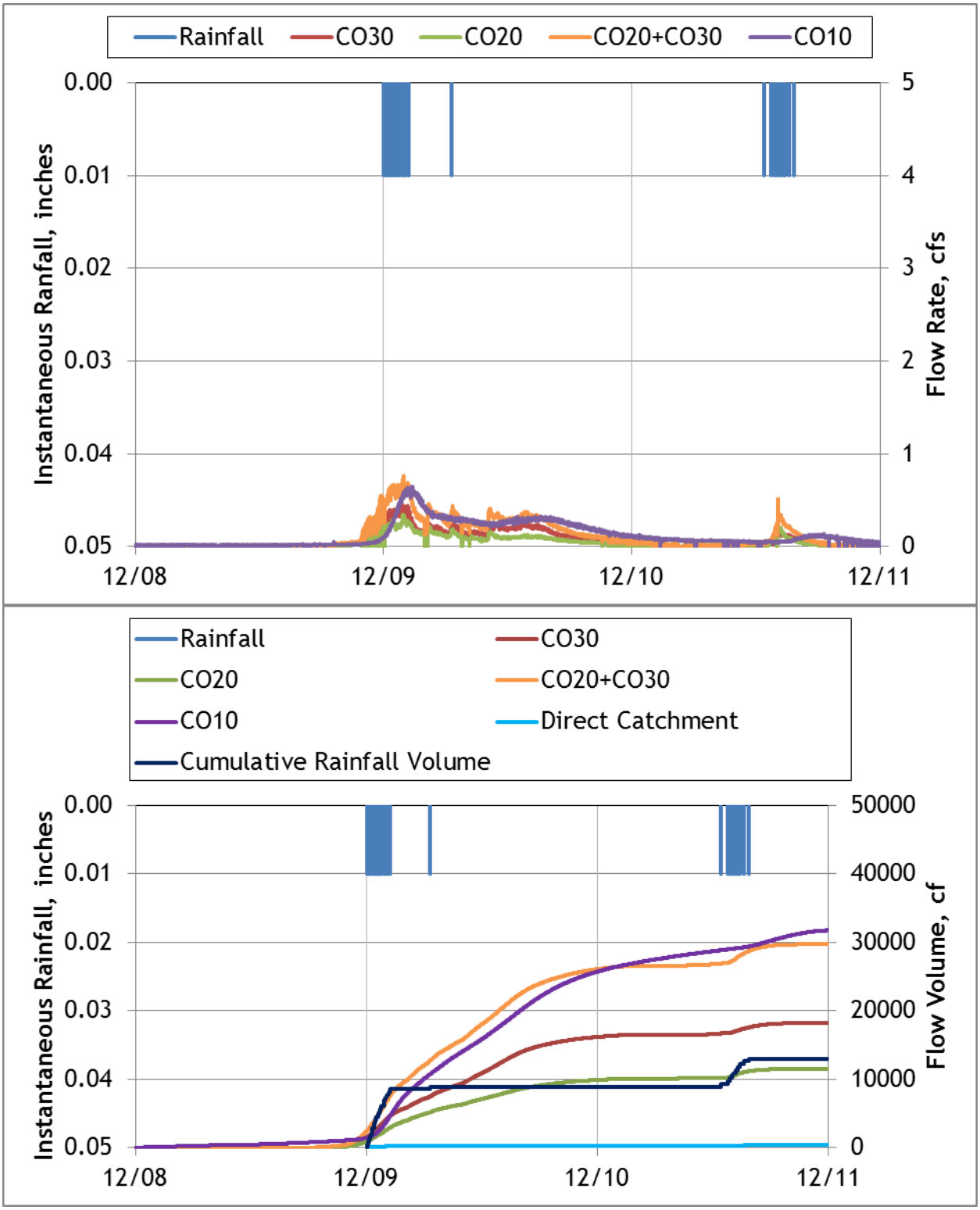

Figure A- 33. Hydrograph and cumulative flow volumes for December 08-011, 2013
Snow prevented accurate measurements of rain data. The Dulles Airport rain data was used as a replacement. Total Rain = 1.50".

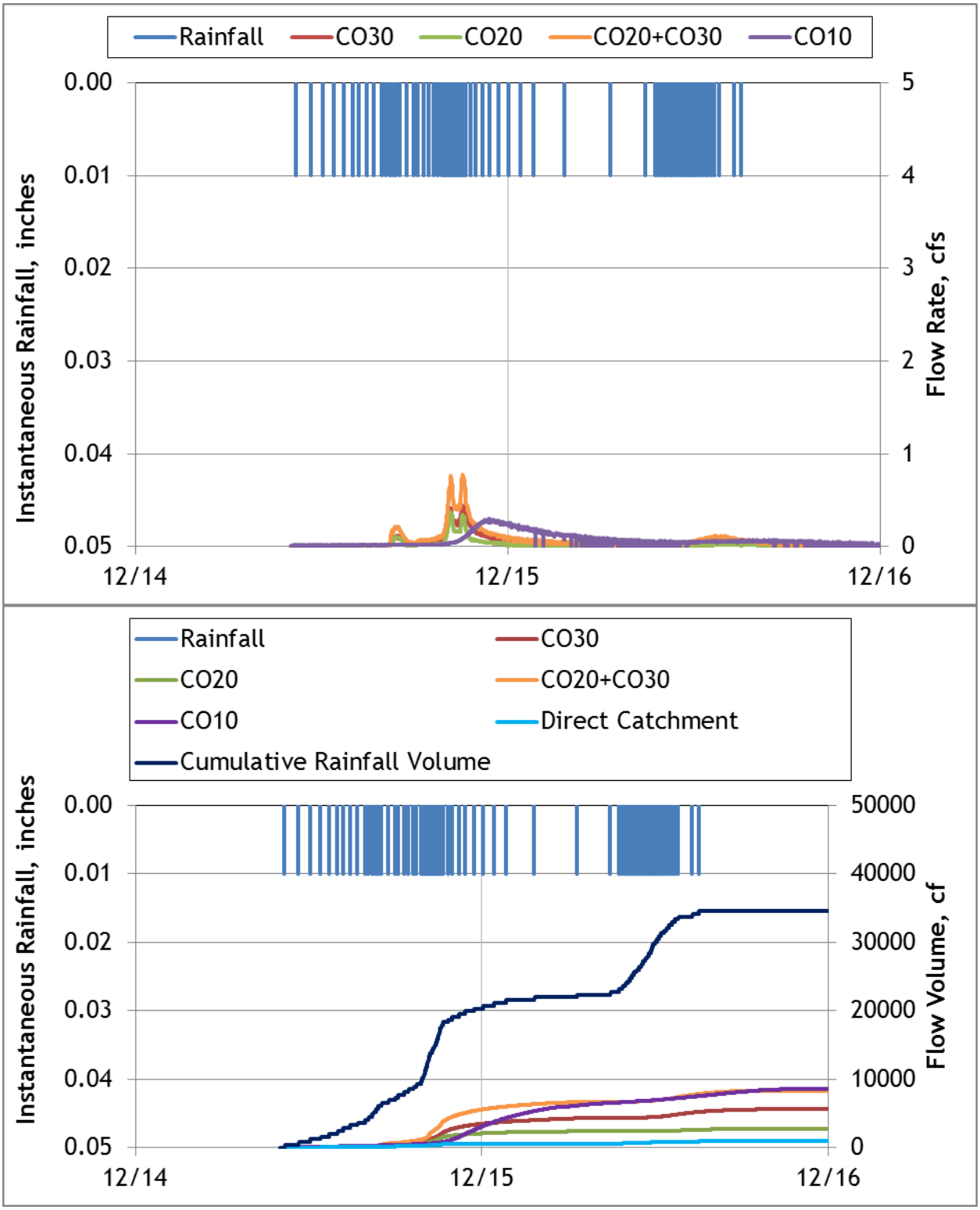

Figure A-34. Hydrograph and cumulative flow volumes for December 14-16, 2013

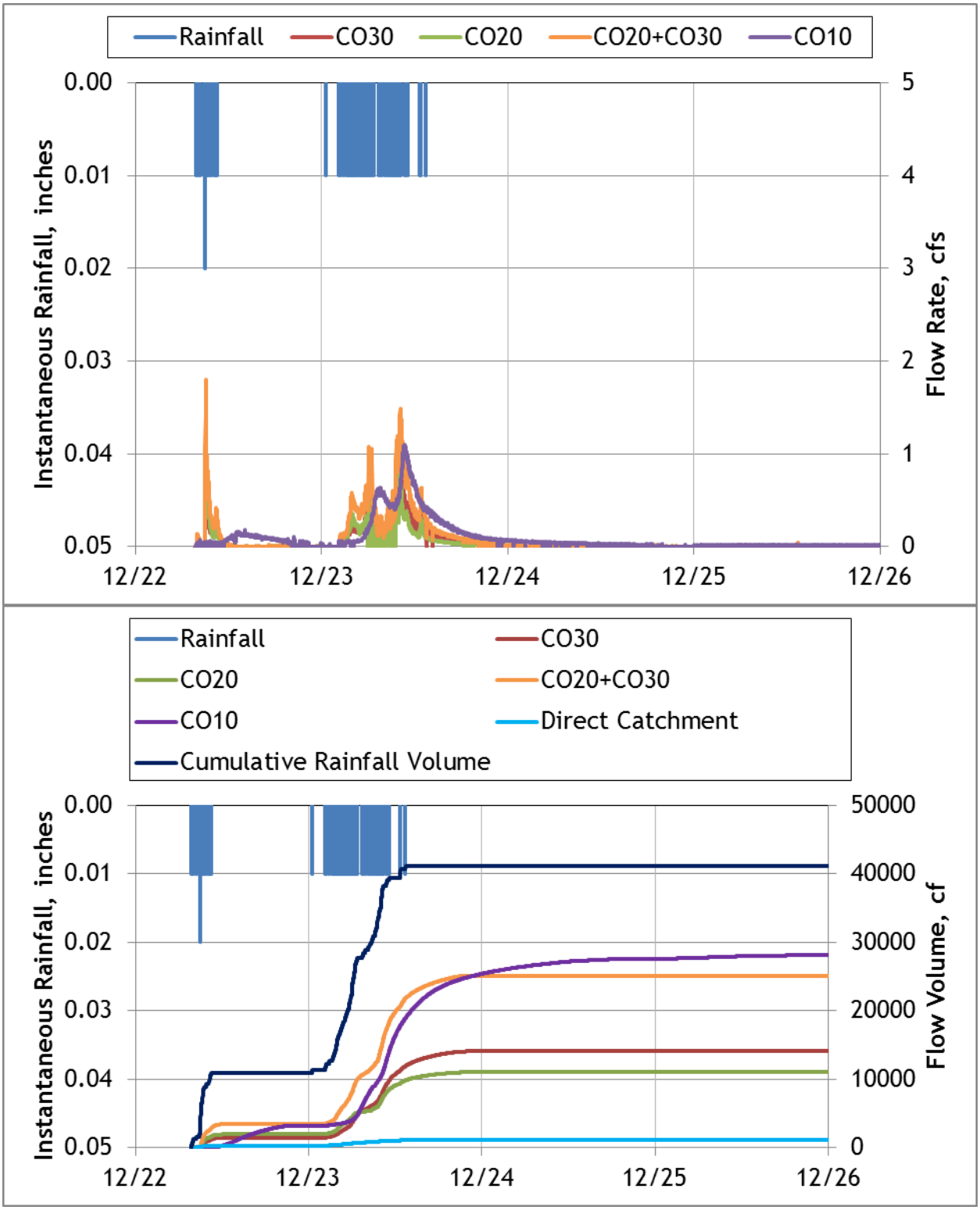

Figure A- 35. Hydrograph and cumulative flow volumes for December 22-26, 2013

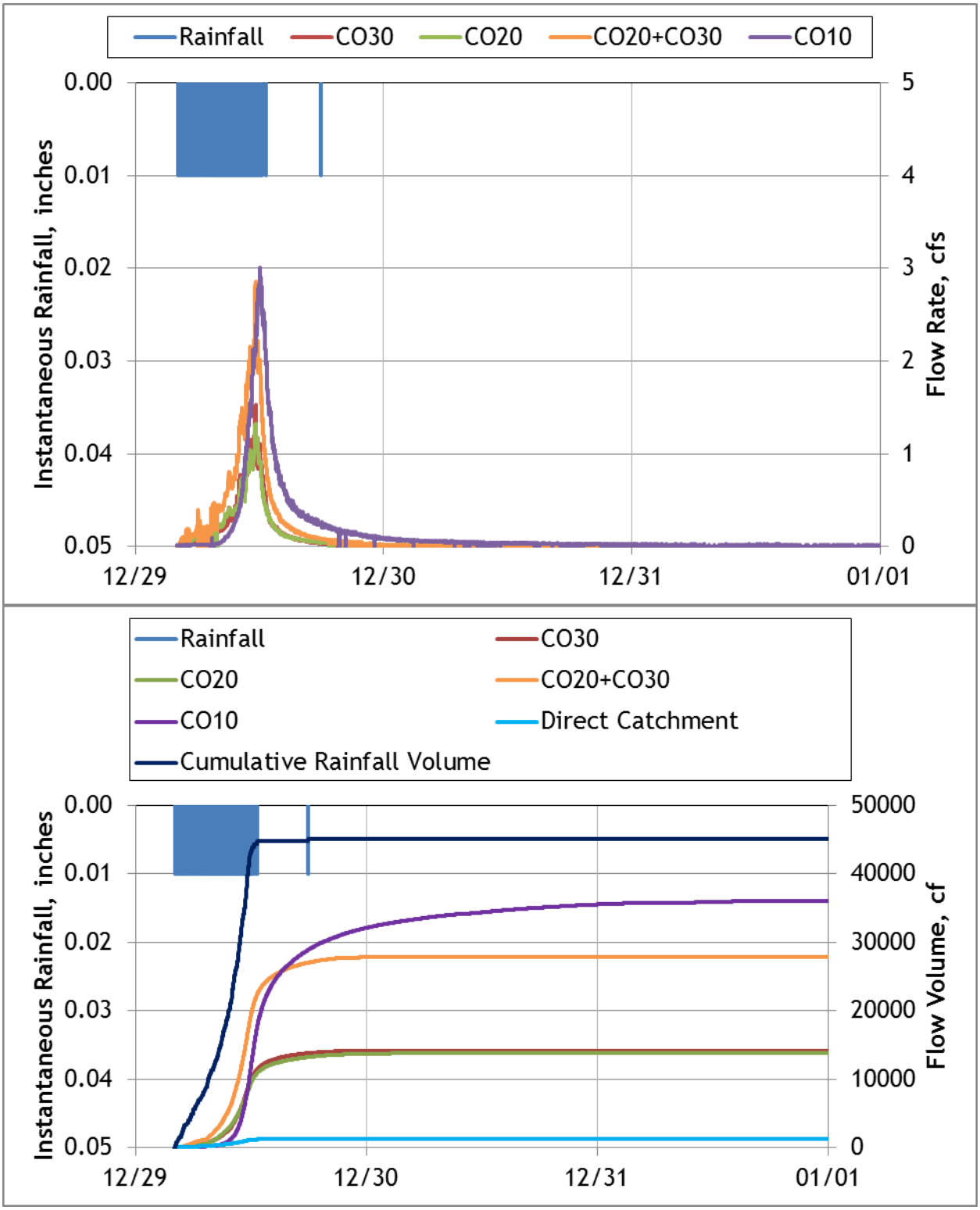

Figure A- 36. Hydrograph and cumulative flow volumes for December 29, 2013-January 01, 2014

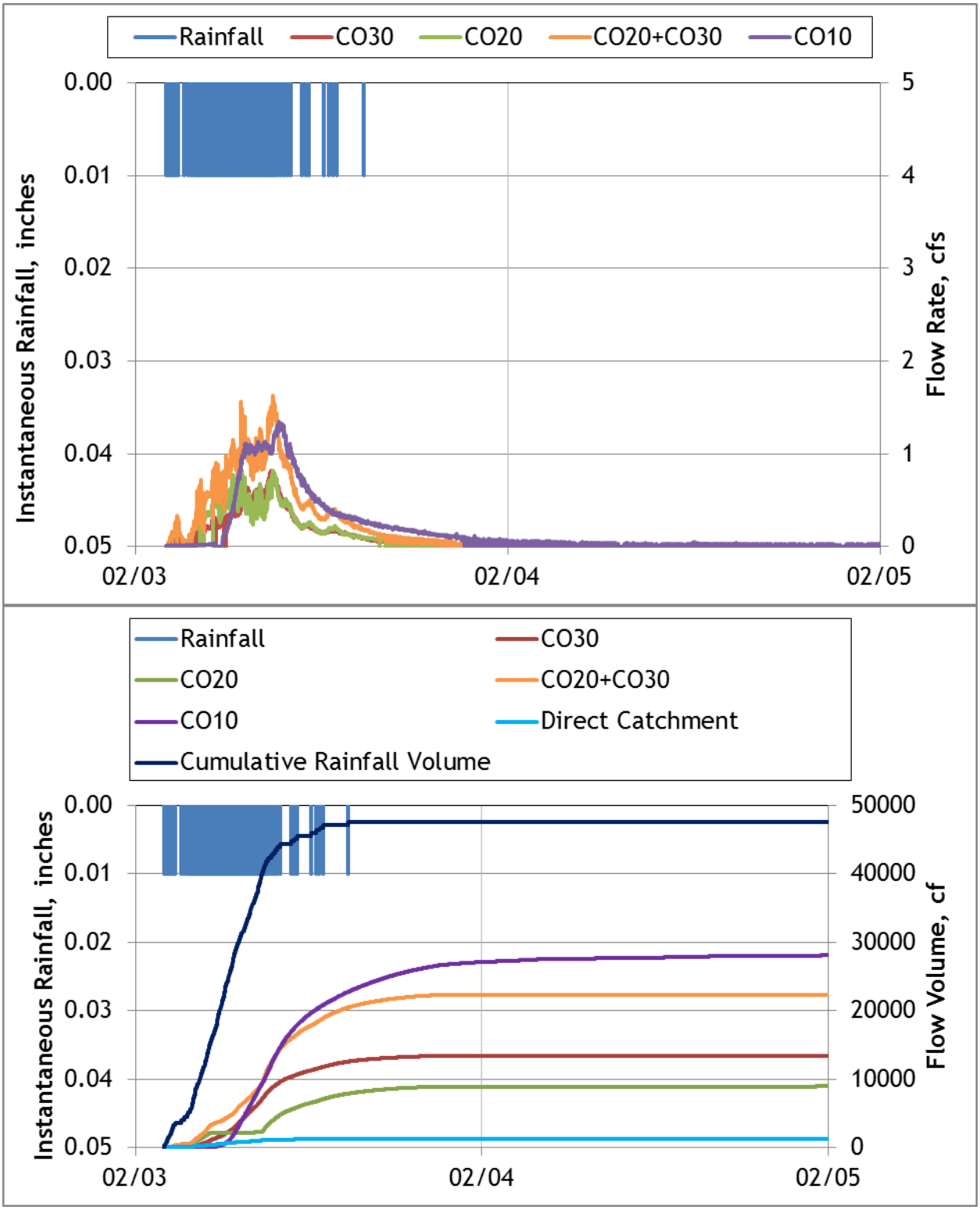

Figure A- 37. Hydrograph and cumulative flow volumes for February 03-05, 2014

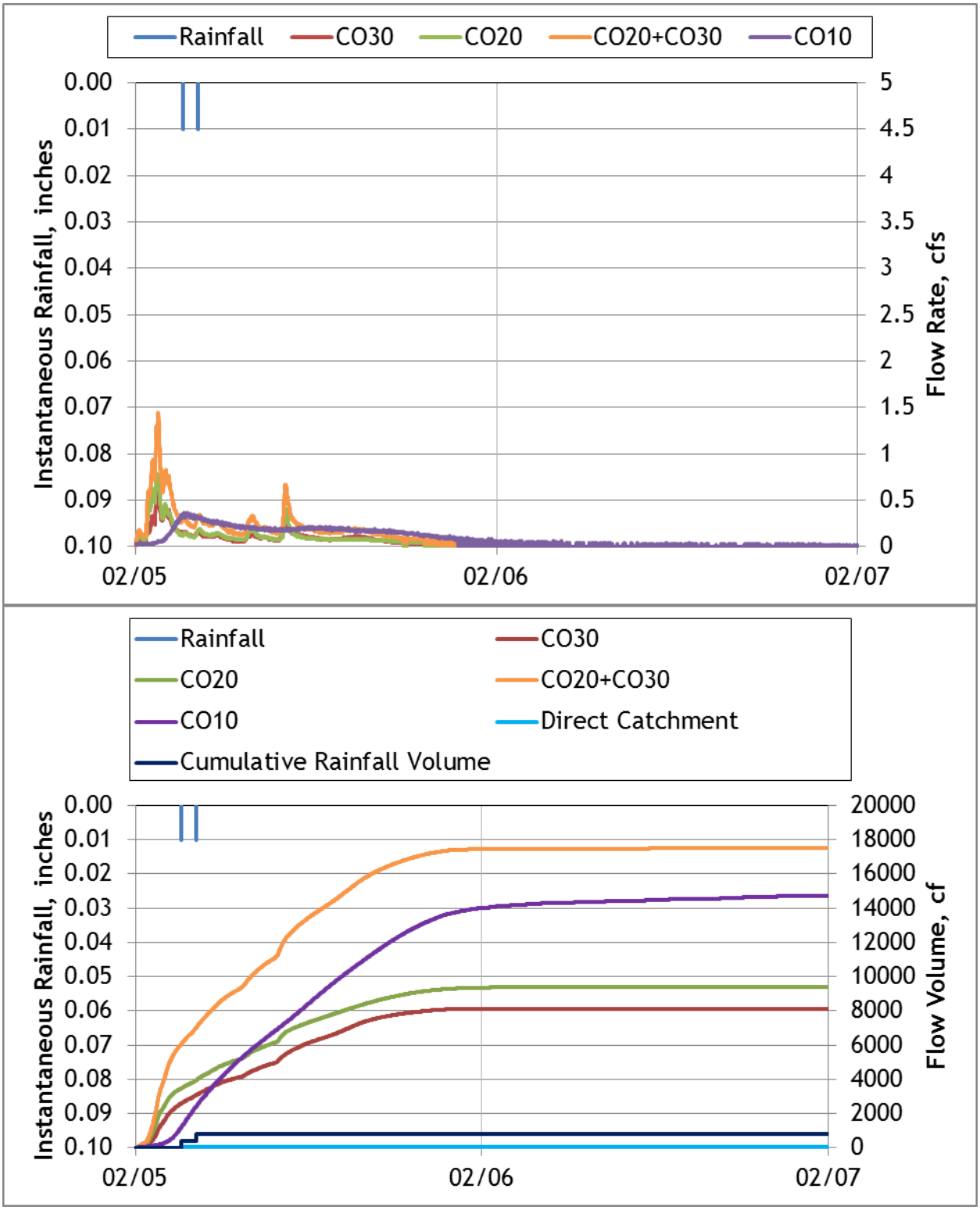

Figure A- 38. Hydrograph and cumulative flow volumes for February 05-07, 2014
Snow prevented accurate measurements of rain data. The Dulles Airport rain data was used as a replacement. Total Rain = 0.55".

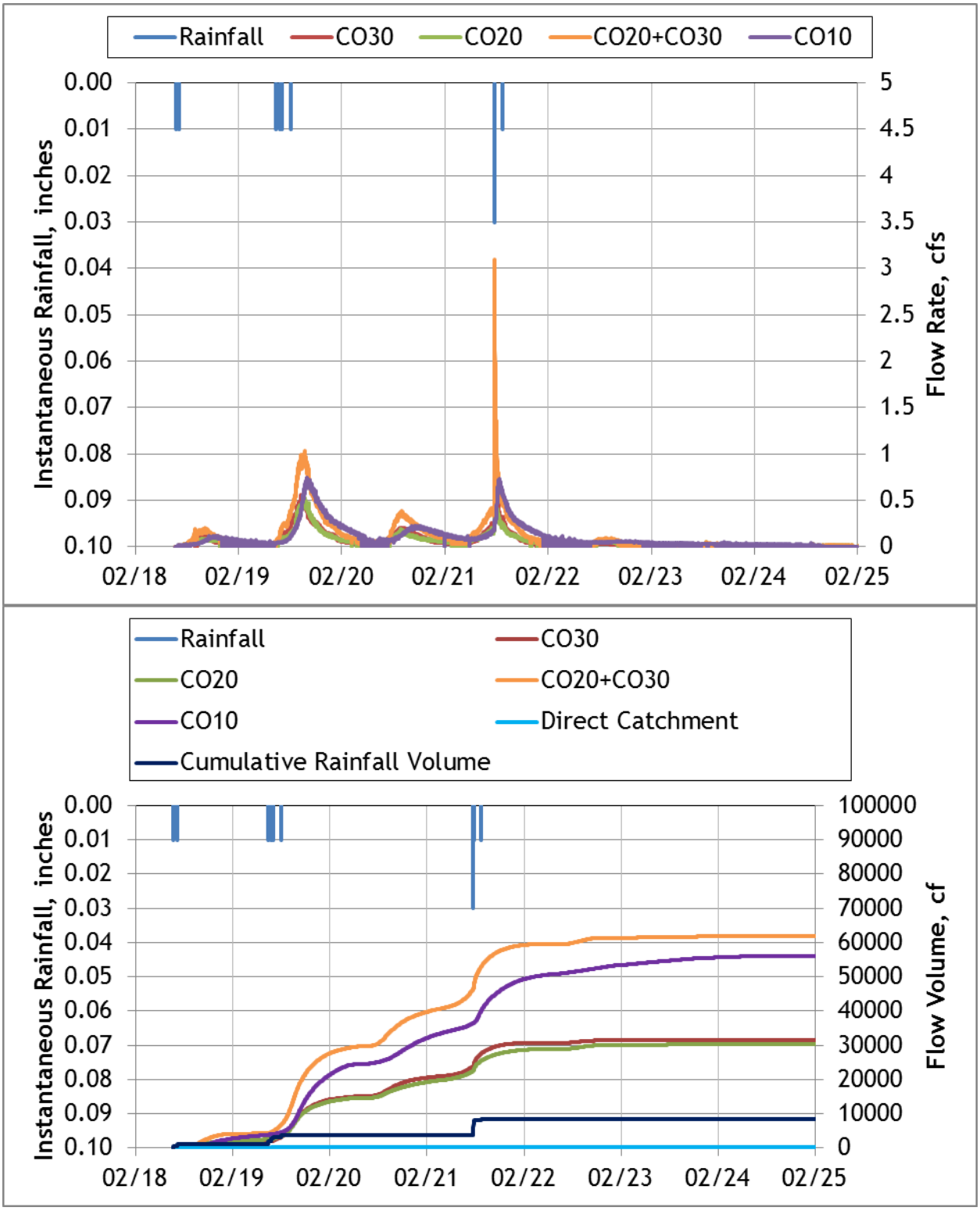

Figure A- 39. Hydrograph and cumulative flow volumes for February 18-25, 2014
Mix of snow and rain prevented accurate measurements of rain data. The Dulles Airport rain data was used as a replacement. Total Rain = 1.82".

APPENDIX B Water quality data boxplots

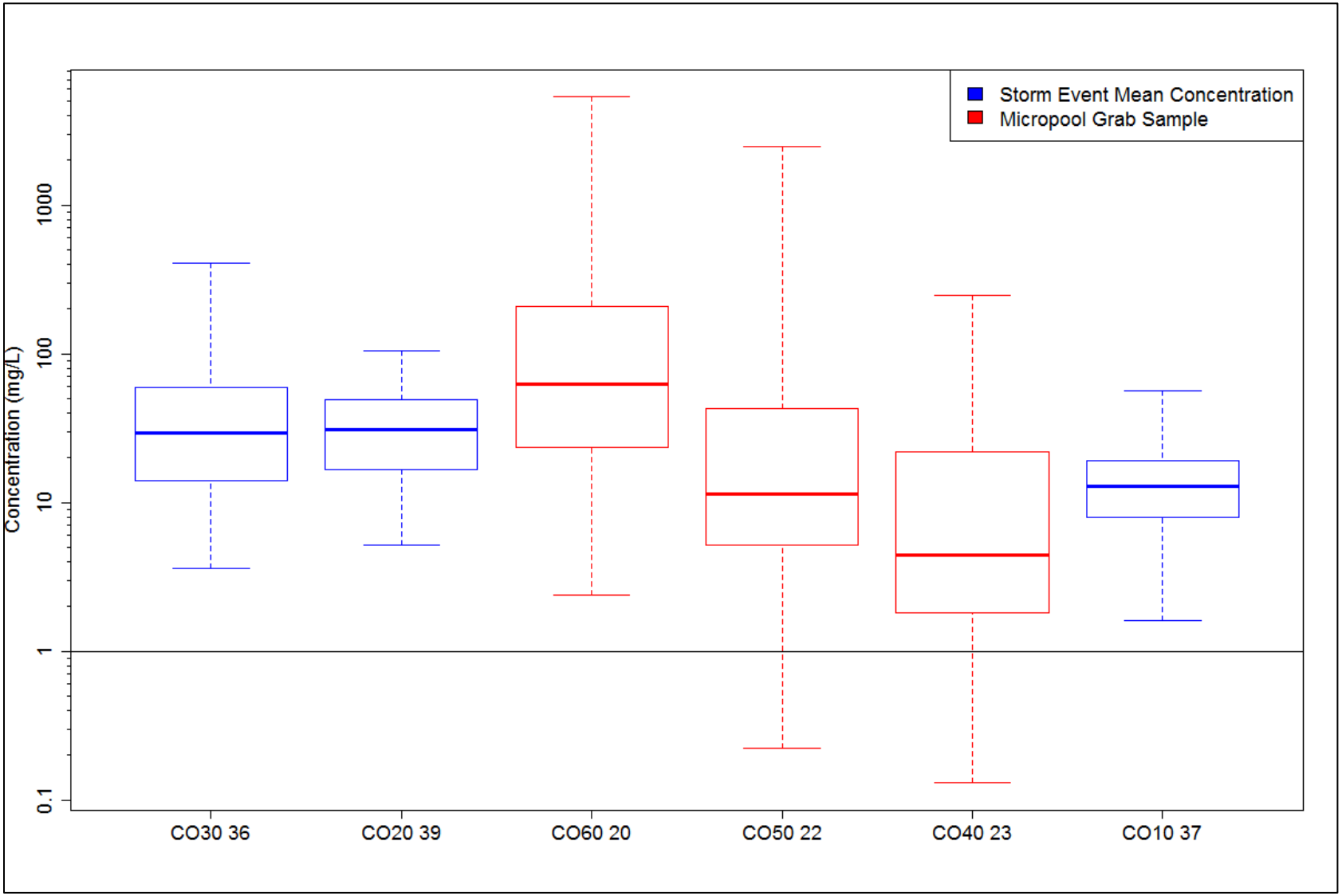

Figure B-1. Boxplots of influent and effluent event mean concentrations and micropool grab samples for total suspended solids.

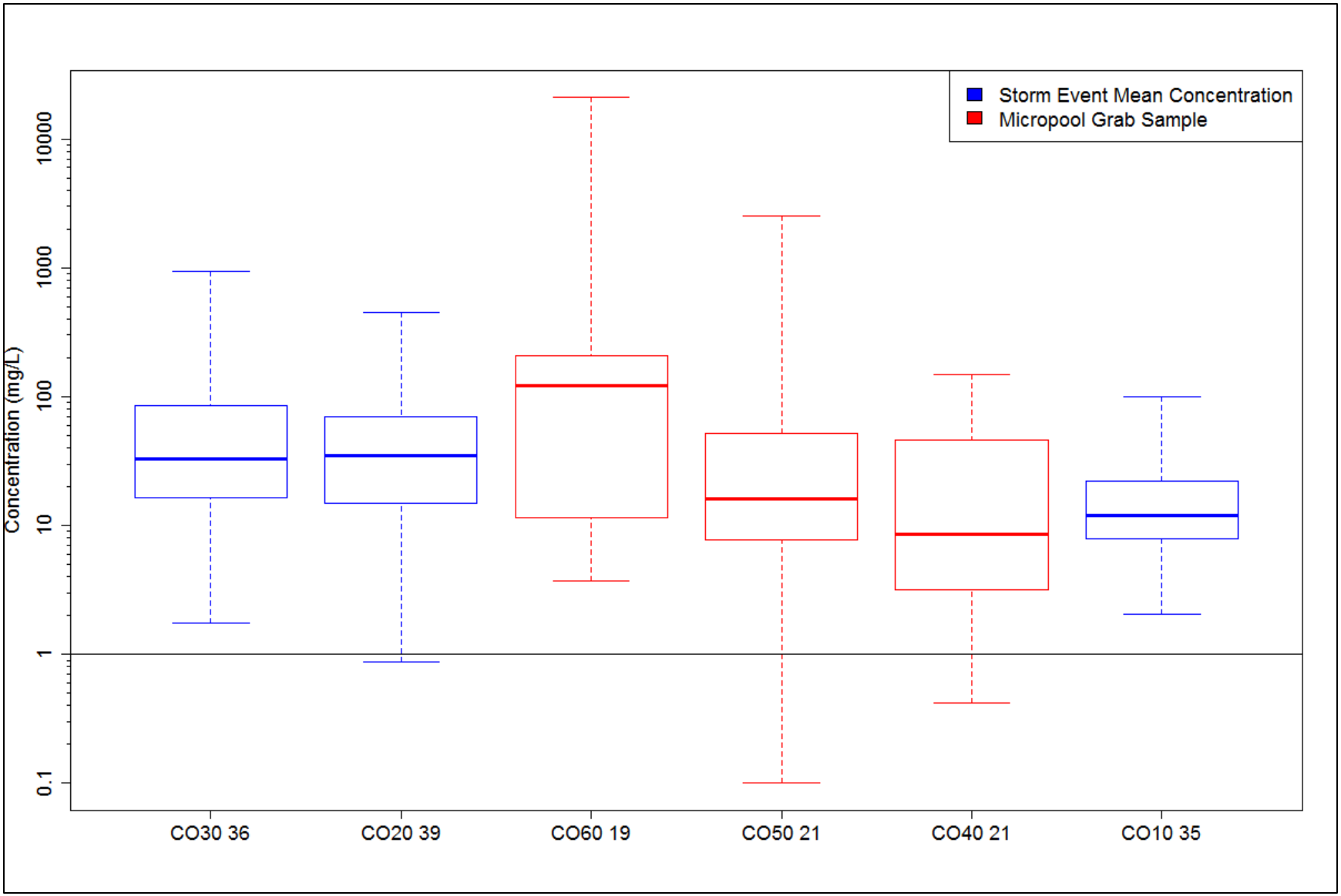

Figure B-2. Boxplots of influent and effluent event mean concentrations and micropool grab samples for suspended sediment concentration.

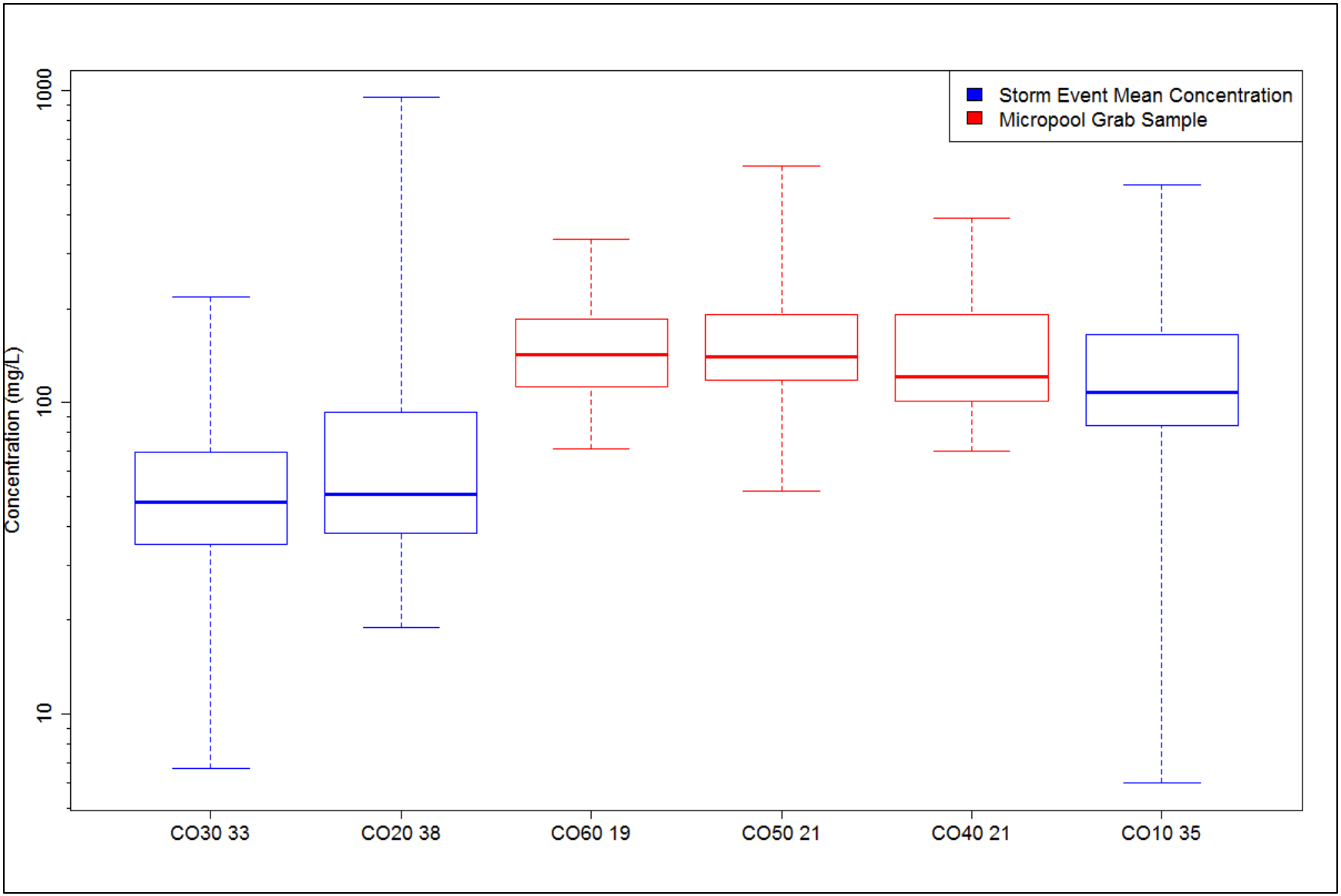

Figure B-3. Boxplots of influent and effluent event mean concentrations and micropool grab samples for total dissolved solids.

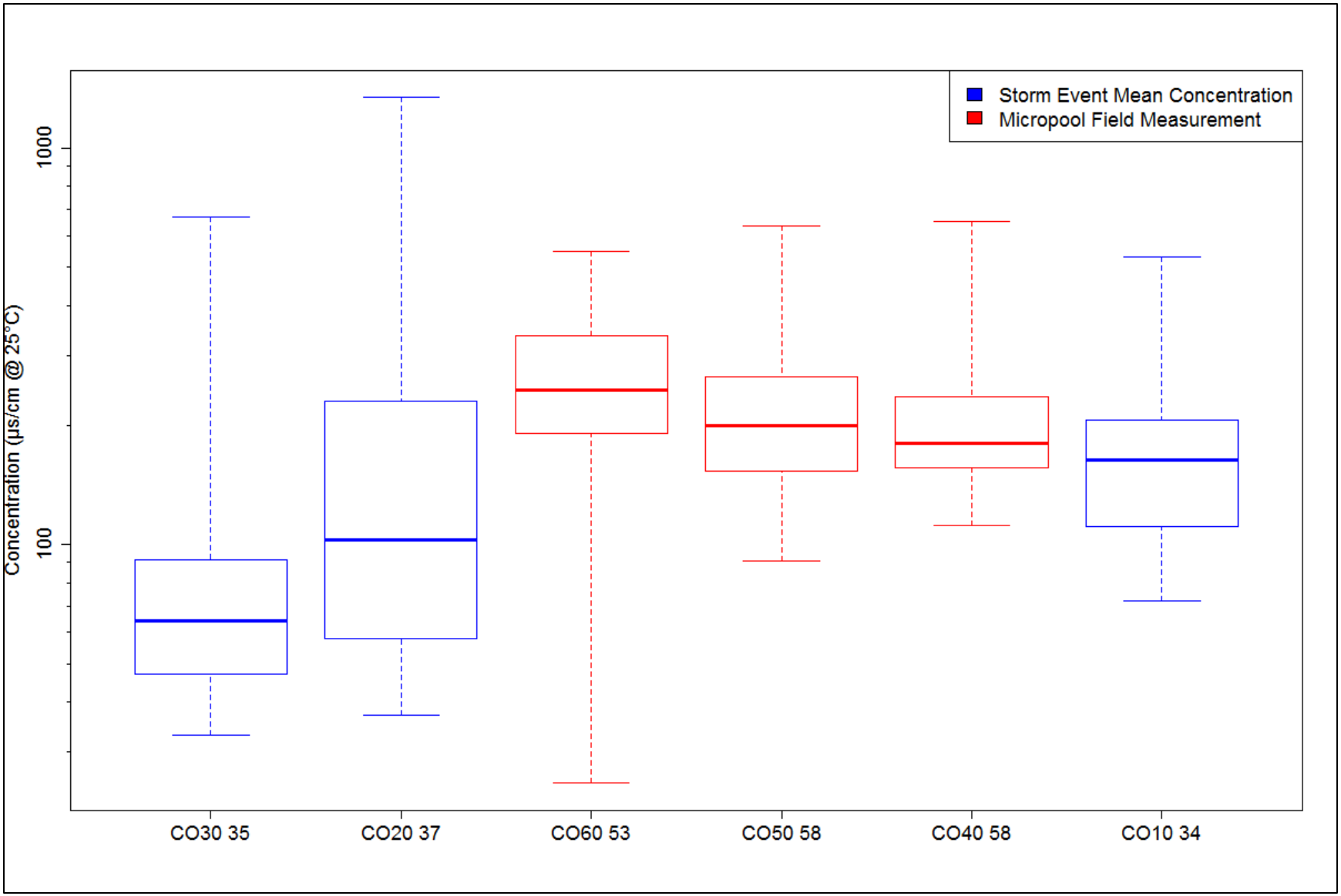

Figure B-4. Boxplots of influent and effluent event mean concentrations and micropool field measurements for specific conductance.

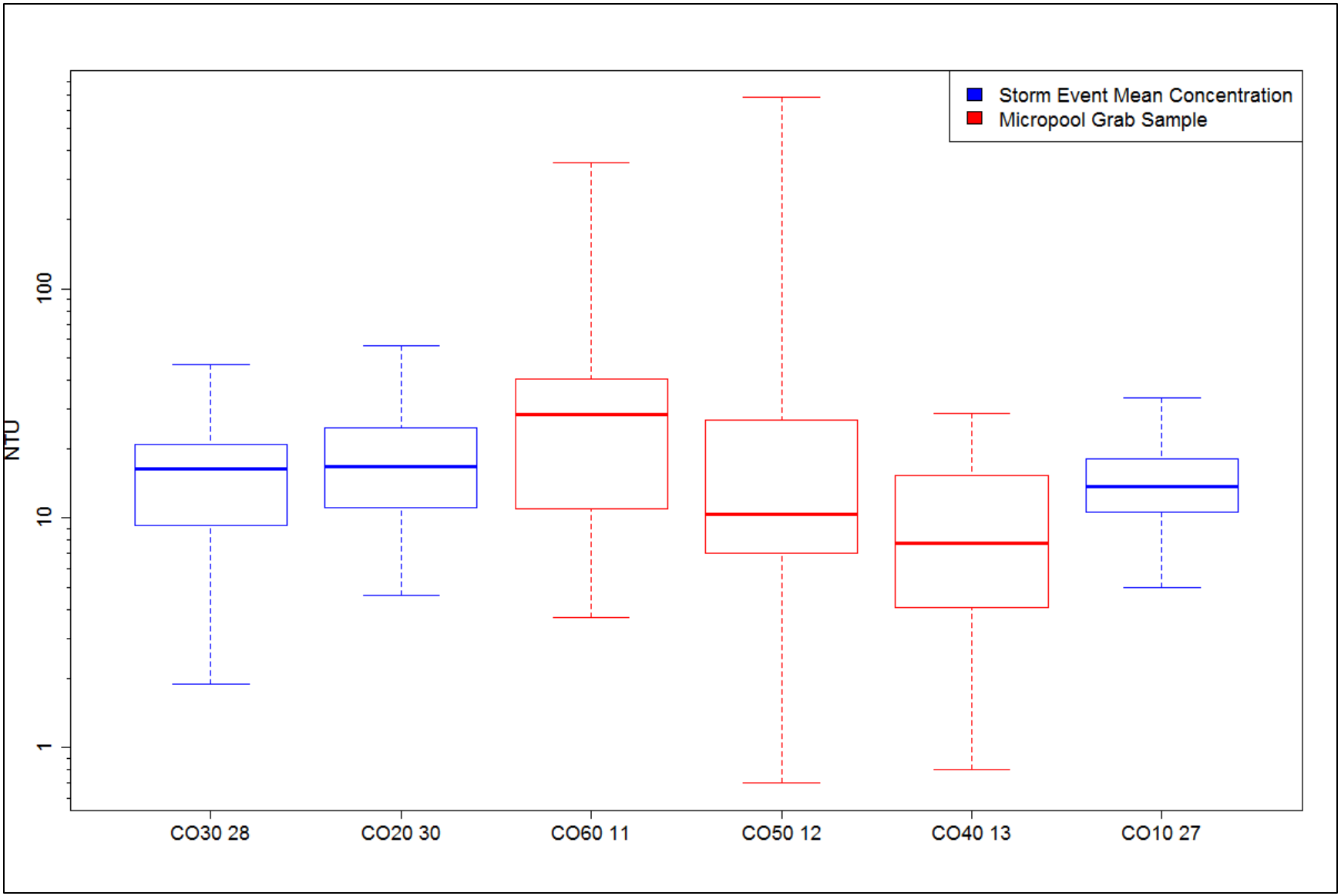

Figure B-5. Boxplots of influent and effluent event mean concentrations and micropool field measurements for turbidity.

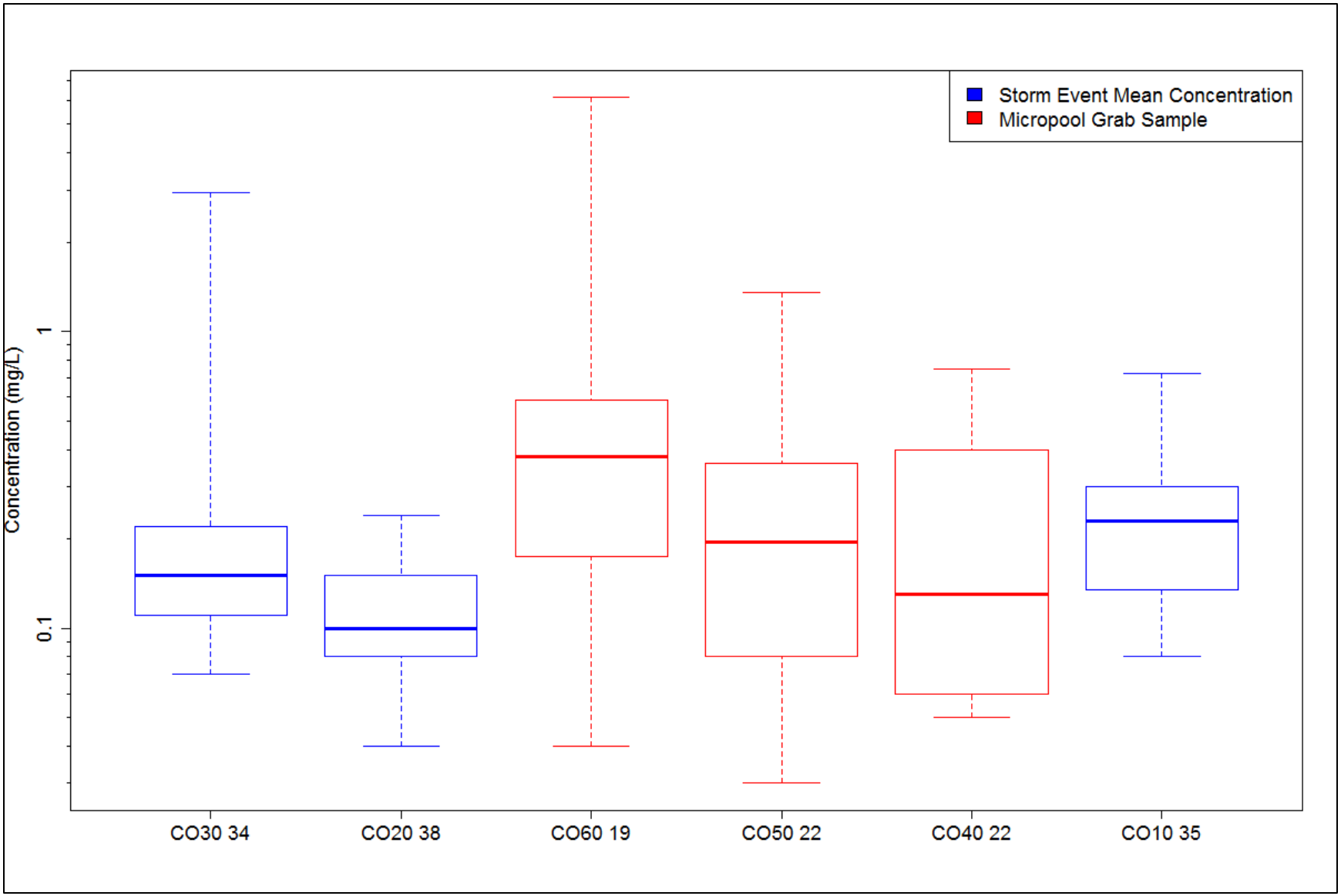

Figure B-6. Boxplots of influent and effluent event mean concentrations and micropool grab samples for total phosphorus.

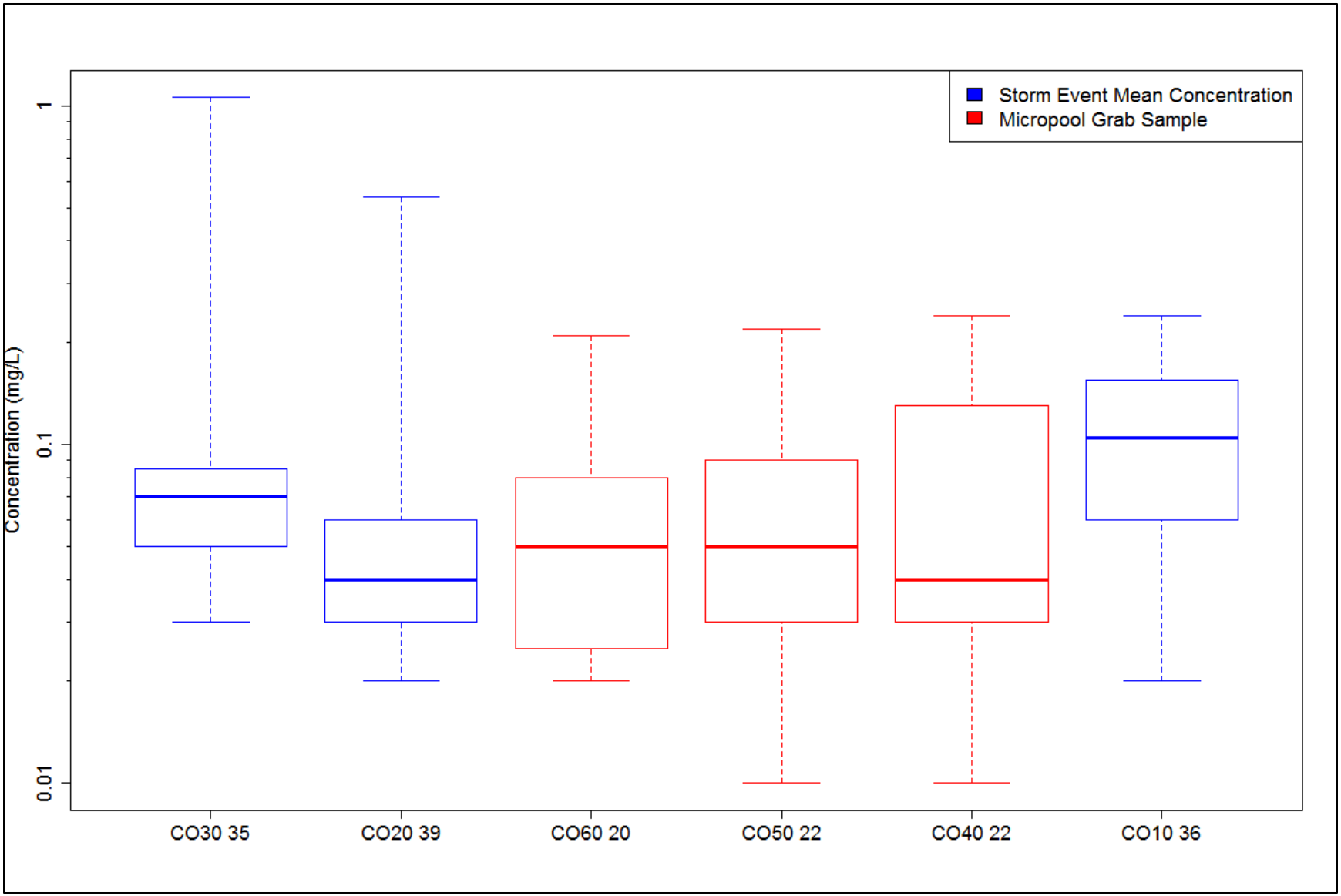

Figure B-7. Boxplots of influent and effluent event mean concentrations and micropool grab samples for orthophosphate phosphorus.

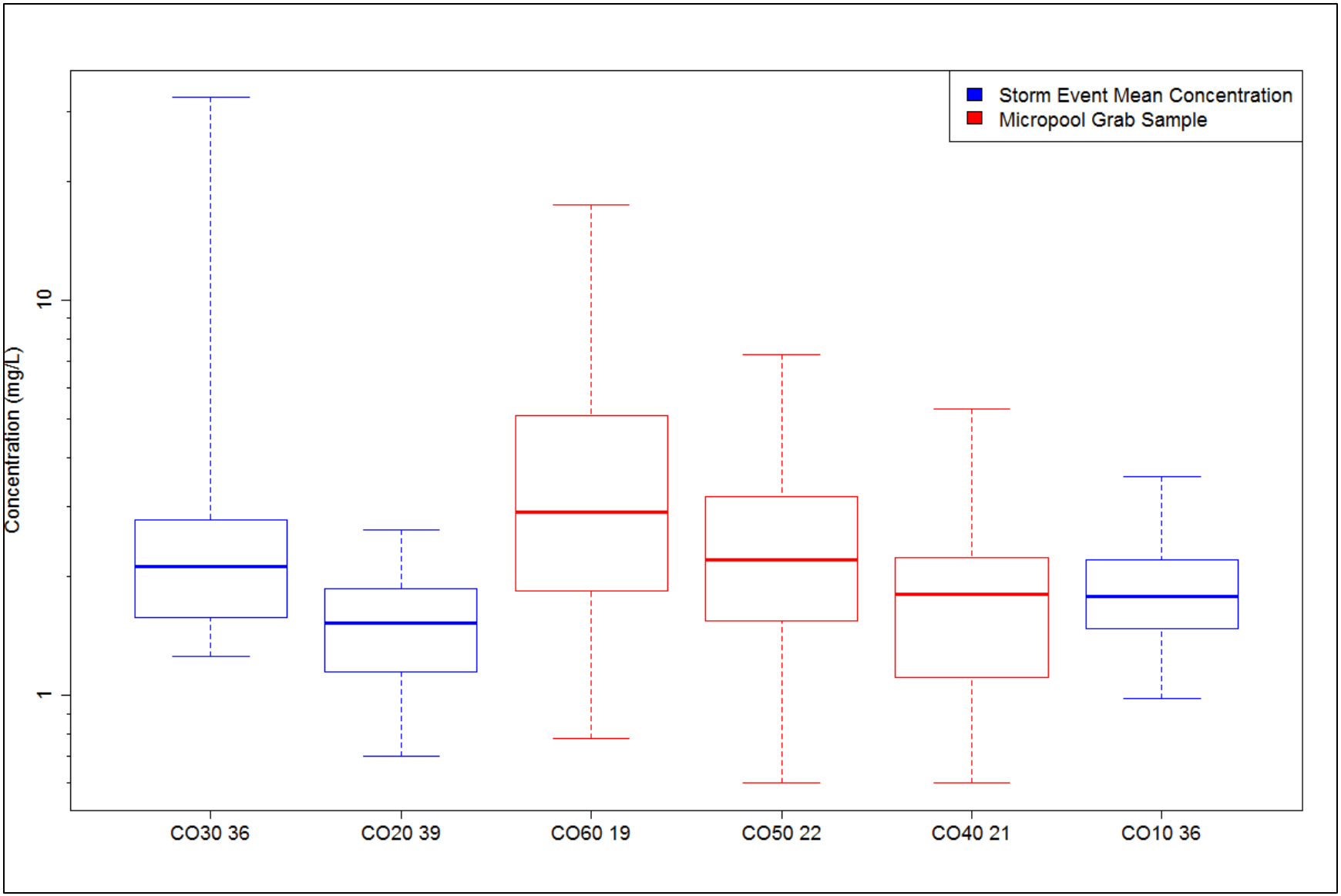

Figure B-8. Boxplots of influent and effluent event mean concentrations and micropool grab samples for total nitrogen.

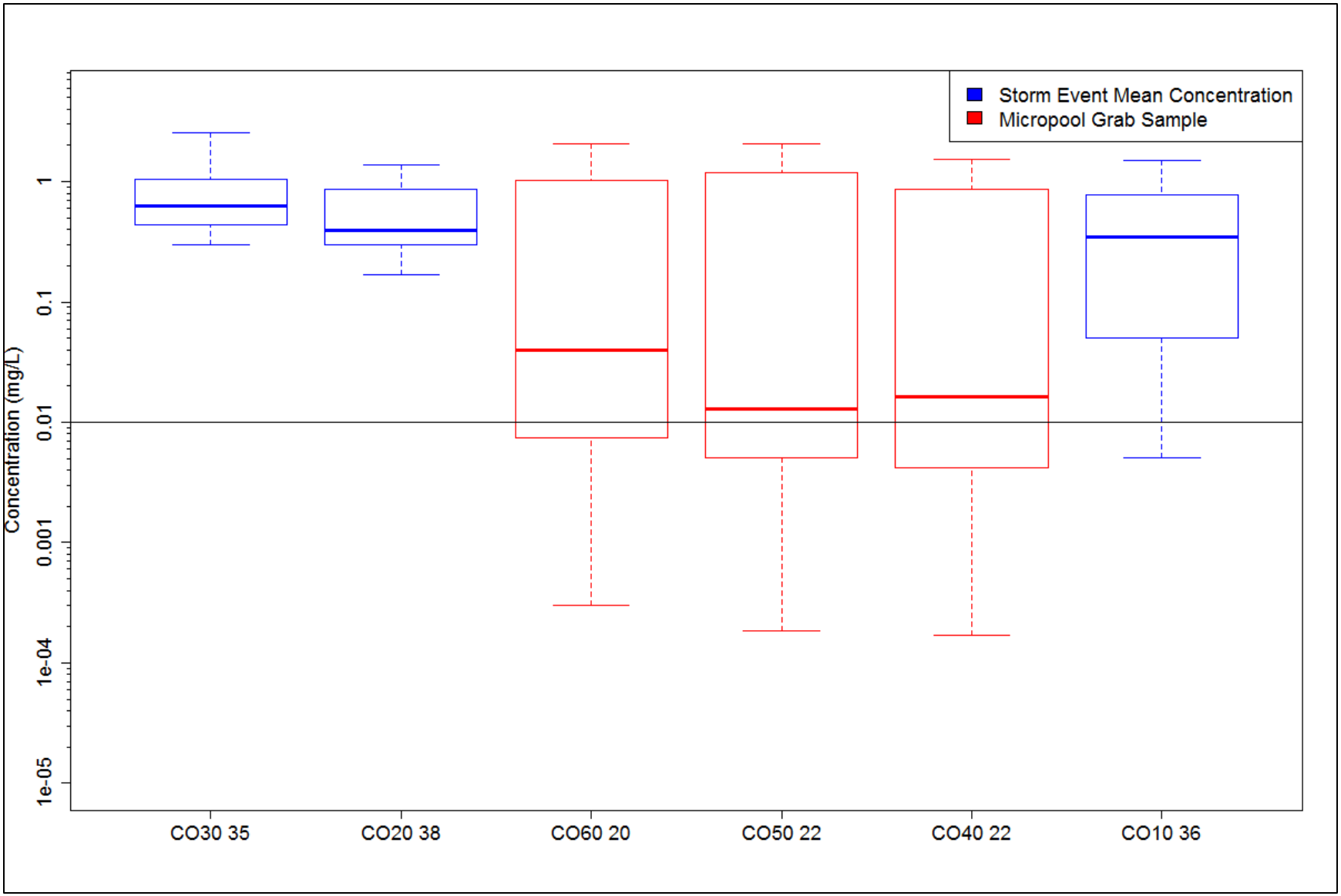

Figure B-9. Boxplots of influent and effluent event mean concentrations and micropool grab samples for oxidized nitrogen.

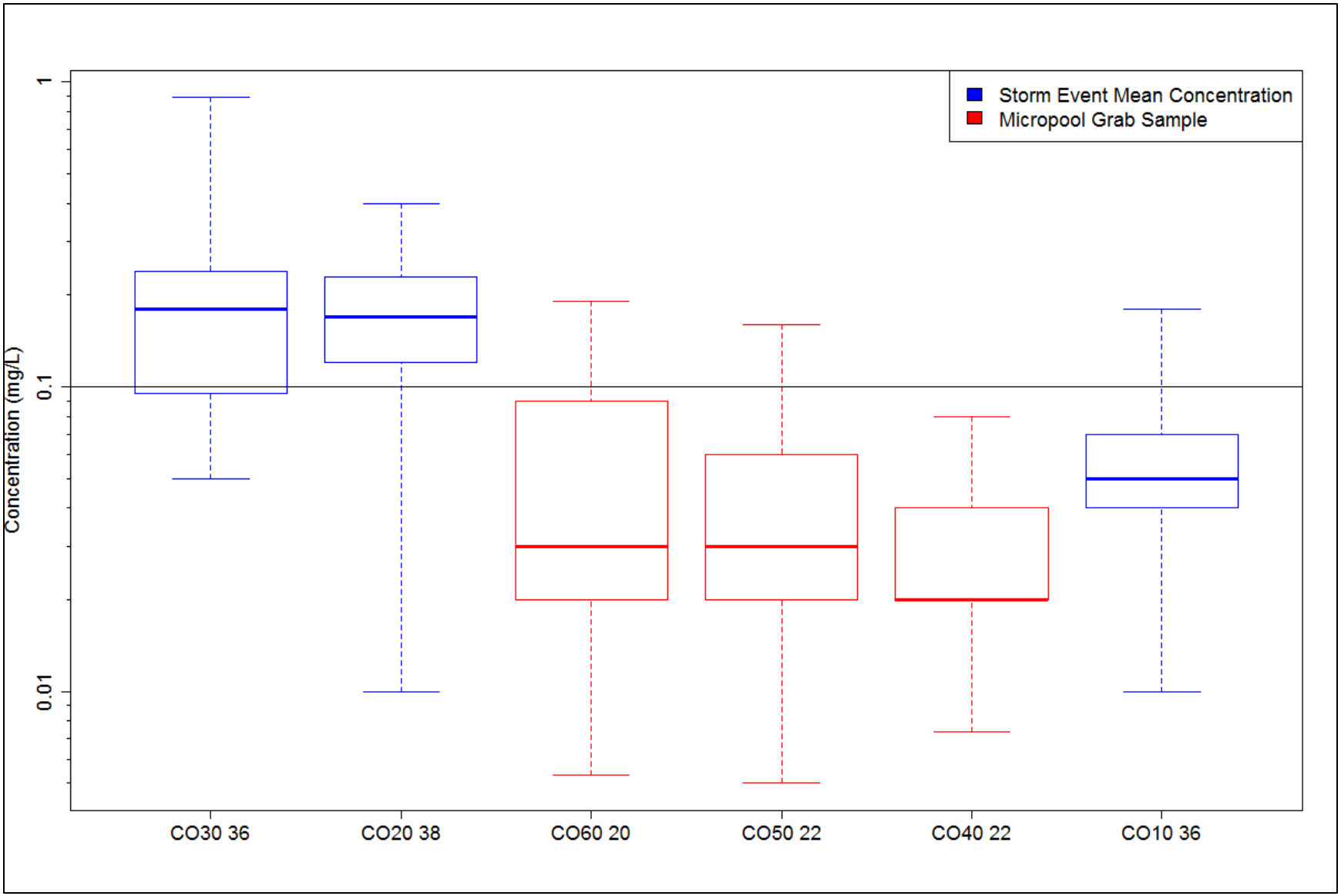

Figure B-10. Boxplots of influent and effluent event mean concentrations and micropool grab samples for ammonia nitrogen.

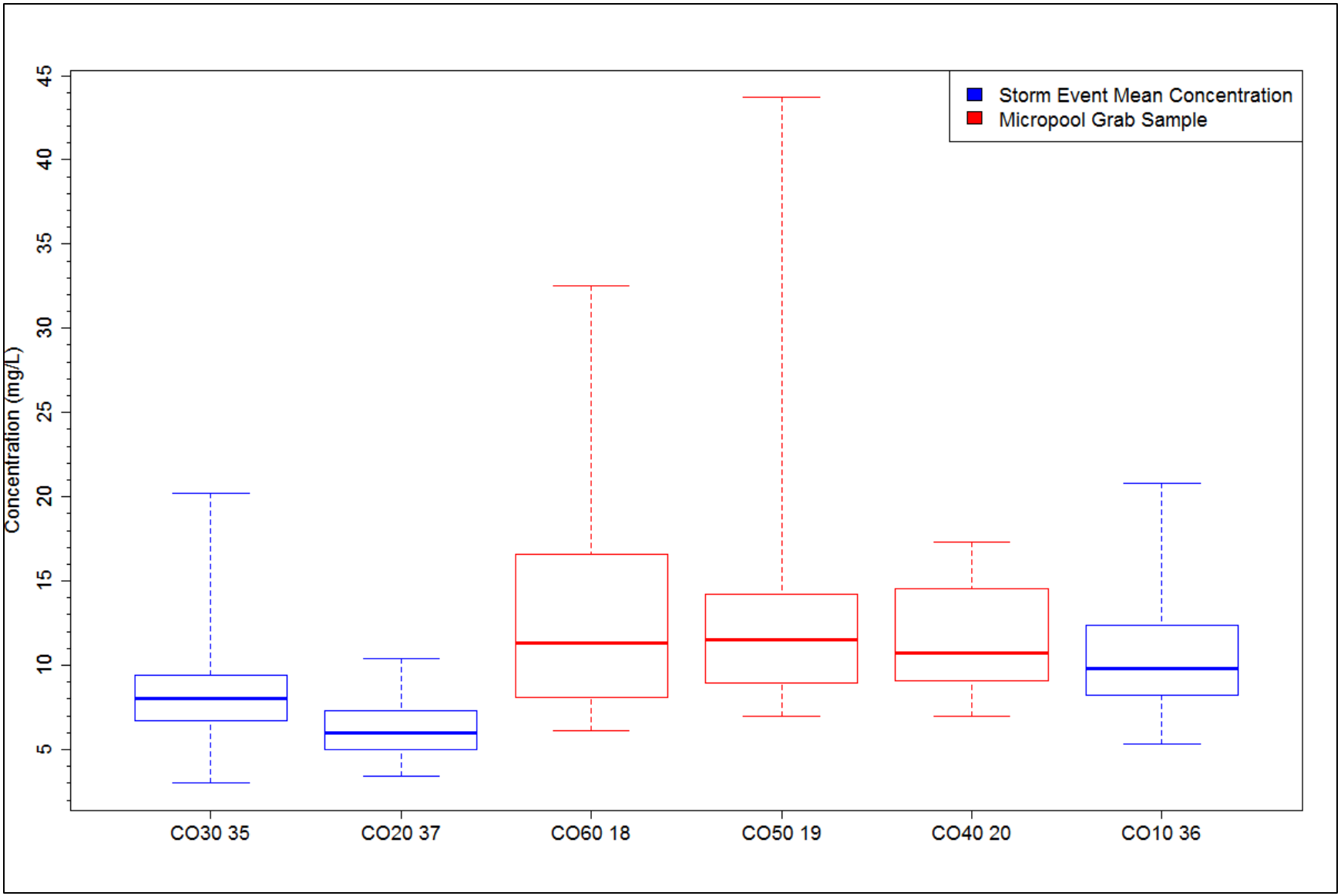

Figure B-11. Boxplots of influent and effluent event mean concentrations and micropool grab samples for total organic carbon.

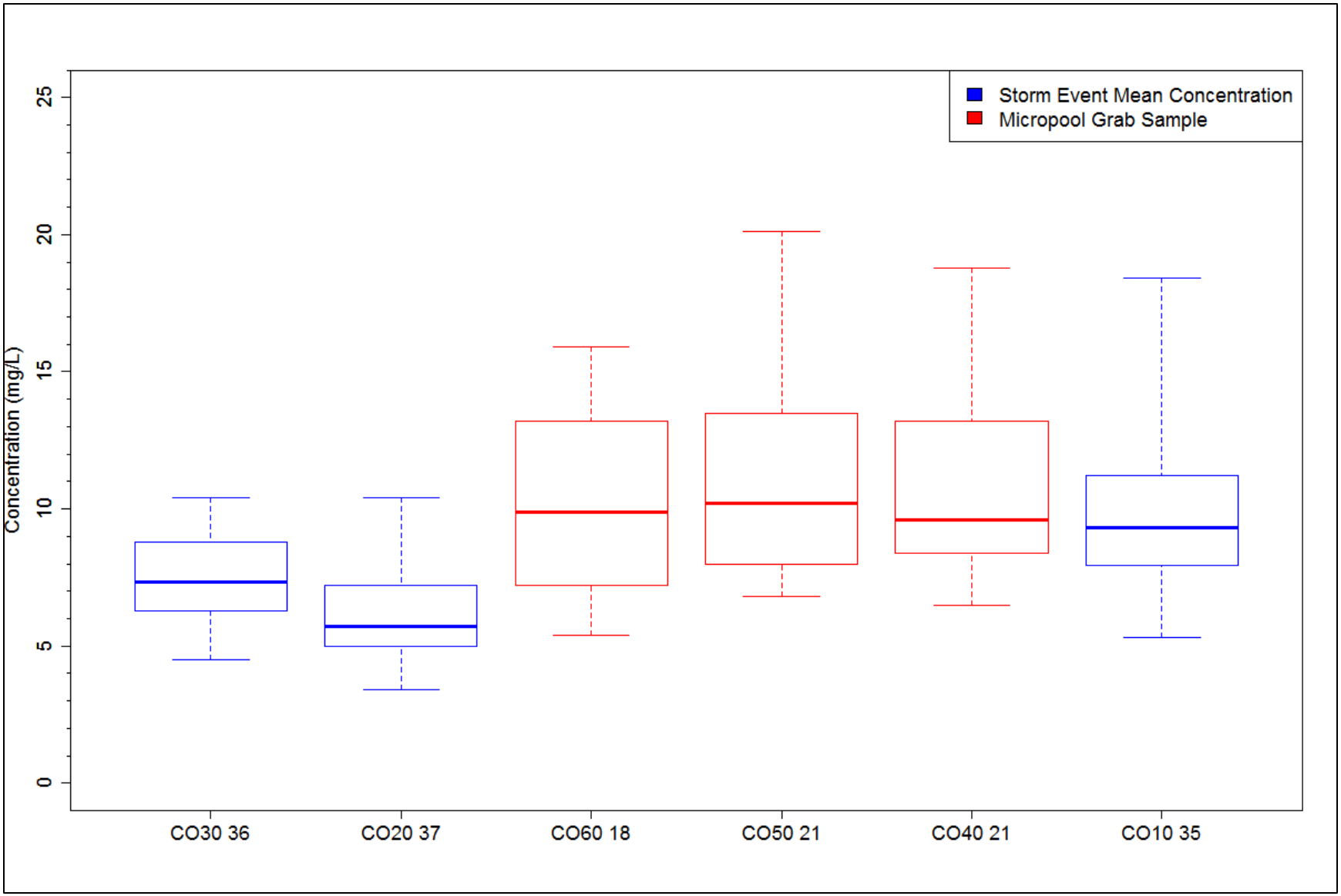

Figure B-12. Boxplots of influent and effluent event mean concentrations and micropool grab samples for dissolved organic carbon.

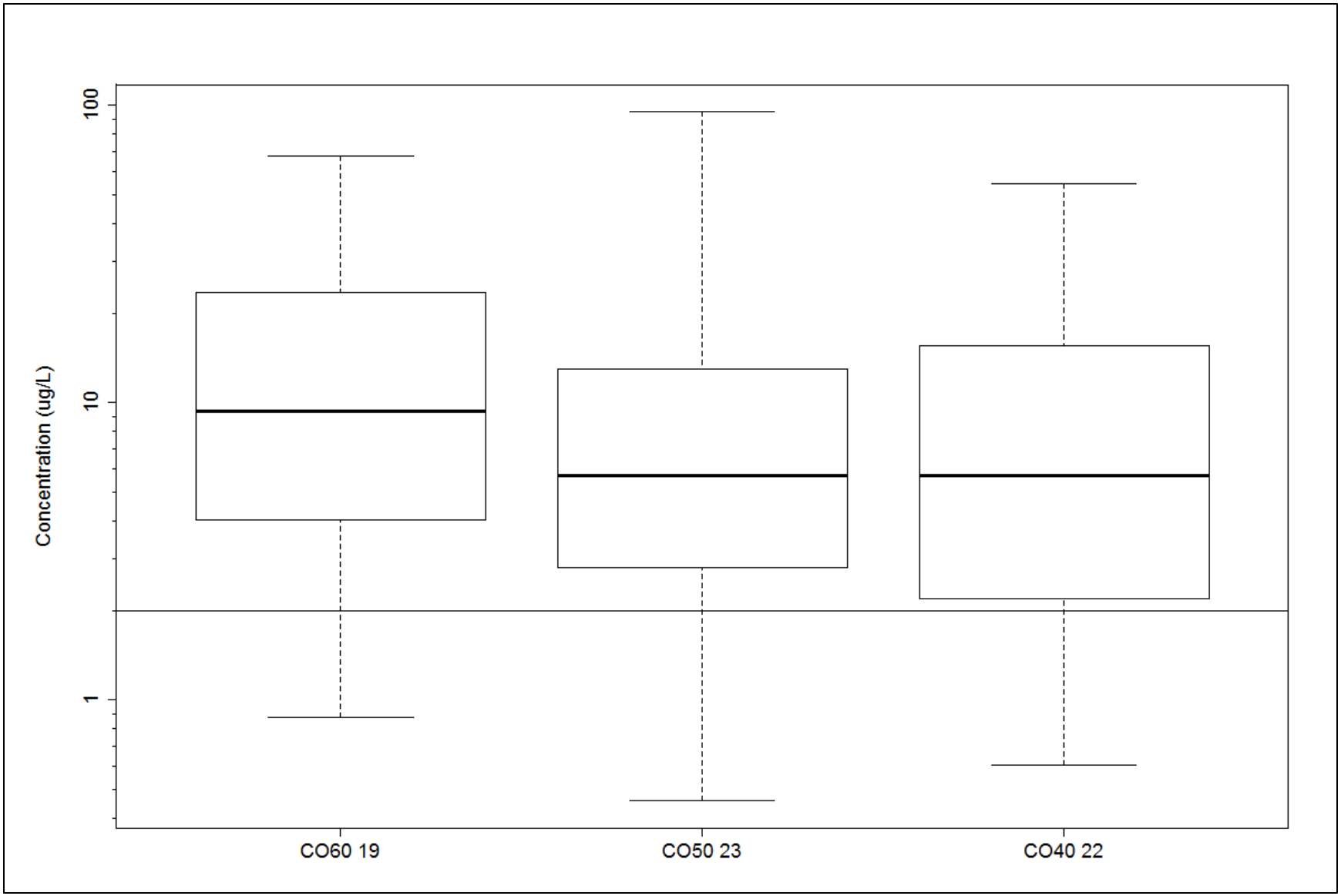

Figure B-13. Boxplots micropool for chlorophyll-a.

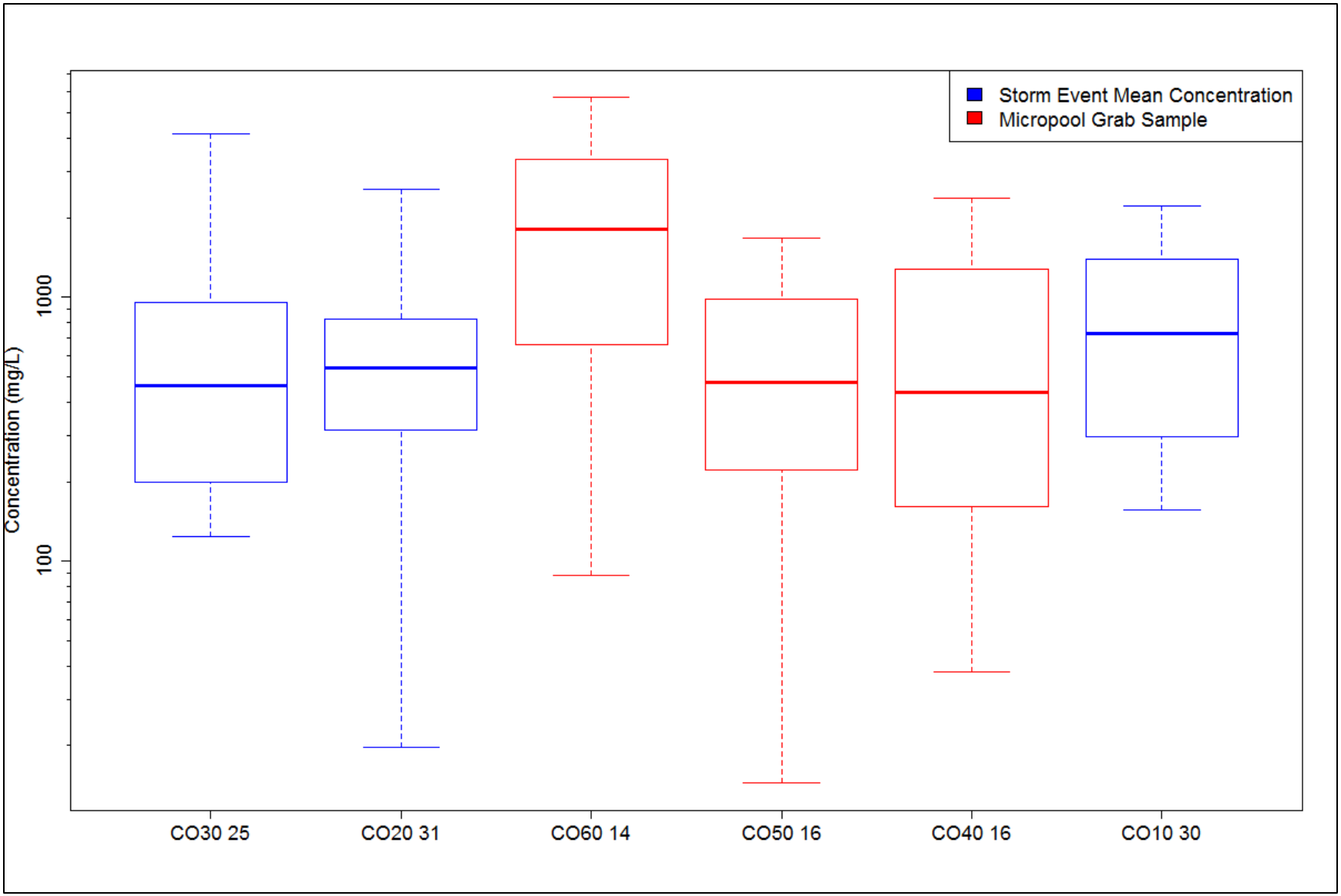

Figure B-14. Boxplots of influent and effluent event mean concentrations and micropool grab samples for total iron.

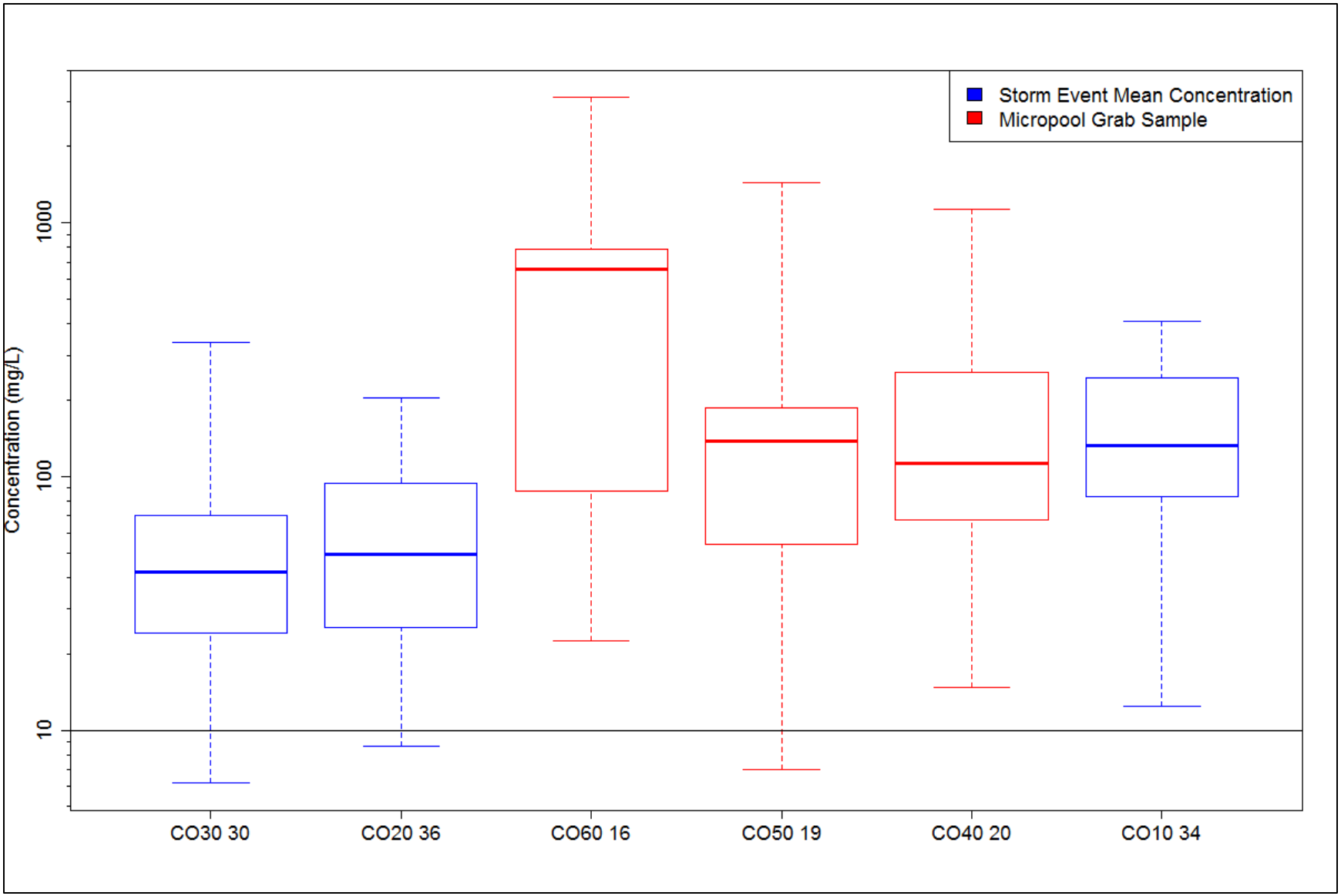

Figure B-15. Boxplots of influent and effluent event mean concentrations and micropool grab samples for soluble iron.

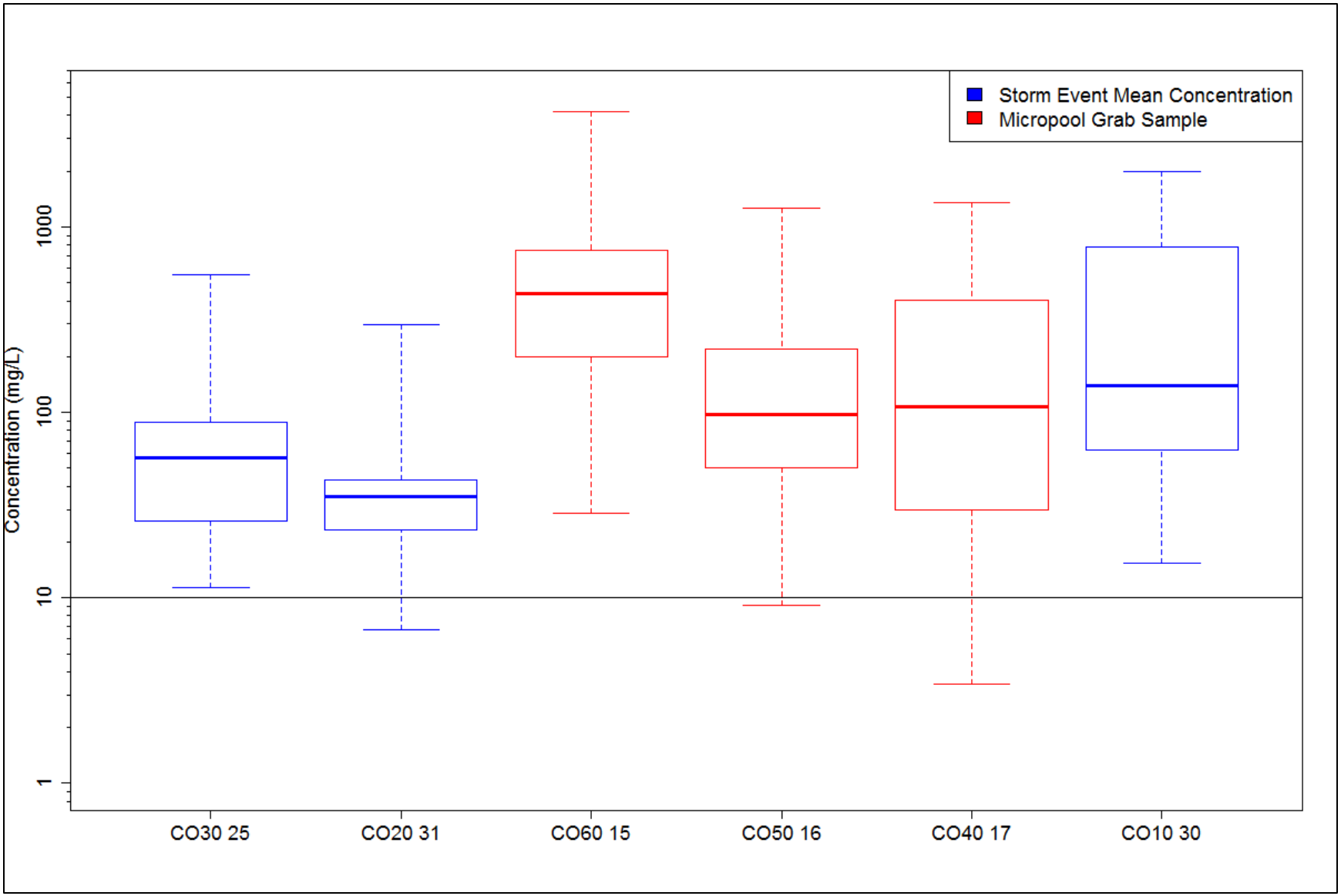

Figure B-16. Boxplots of influent and effluent event mean concentrations and micropool grab samples for total manganese.

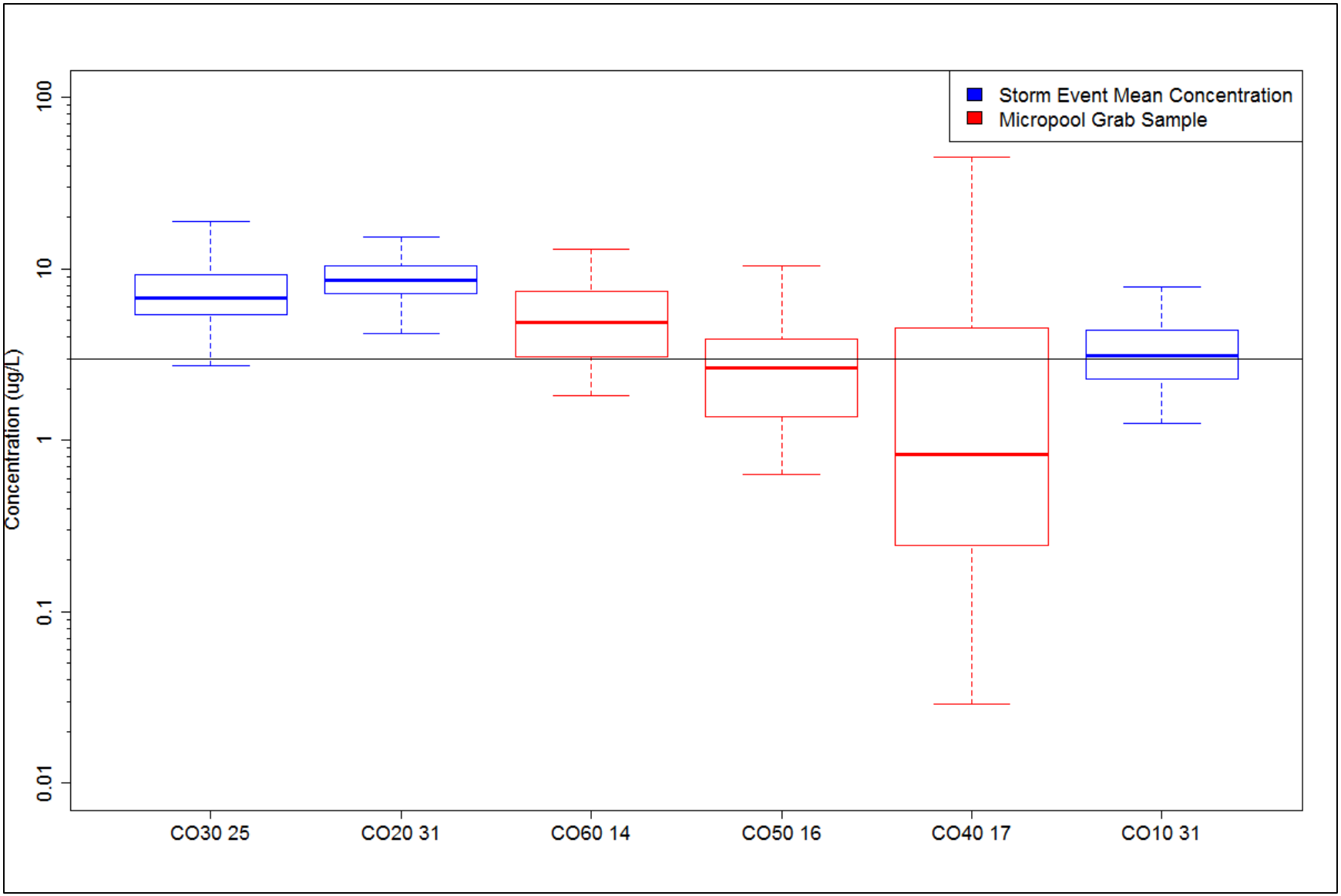

Figure B-17. Boxplots of influent and effluent event mean concentrations and micropool grab samples for total copper.

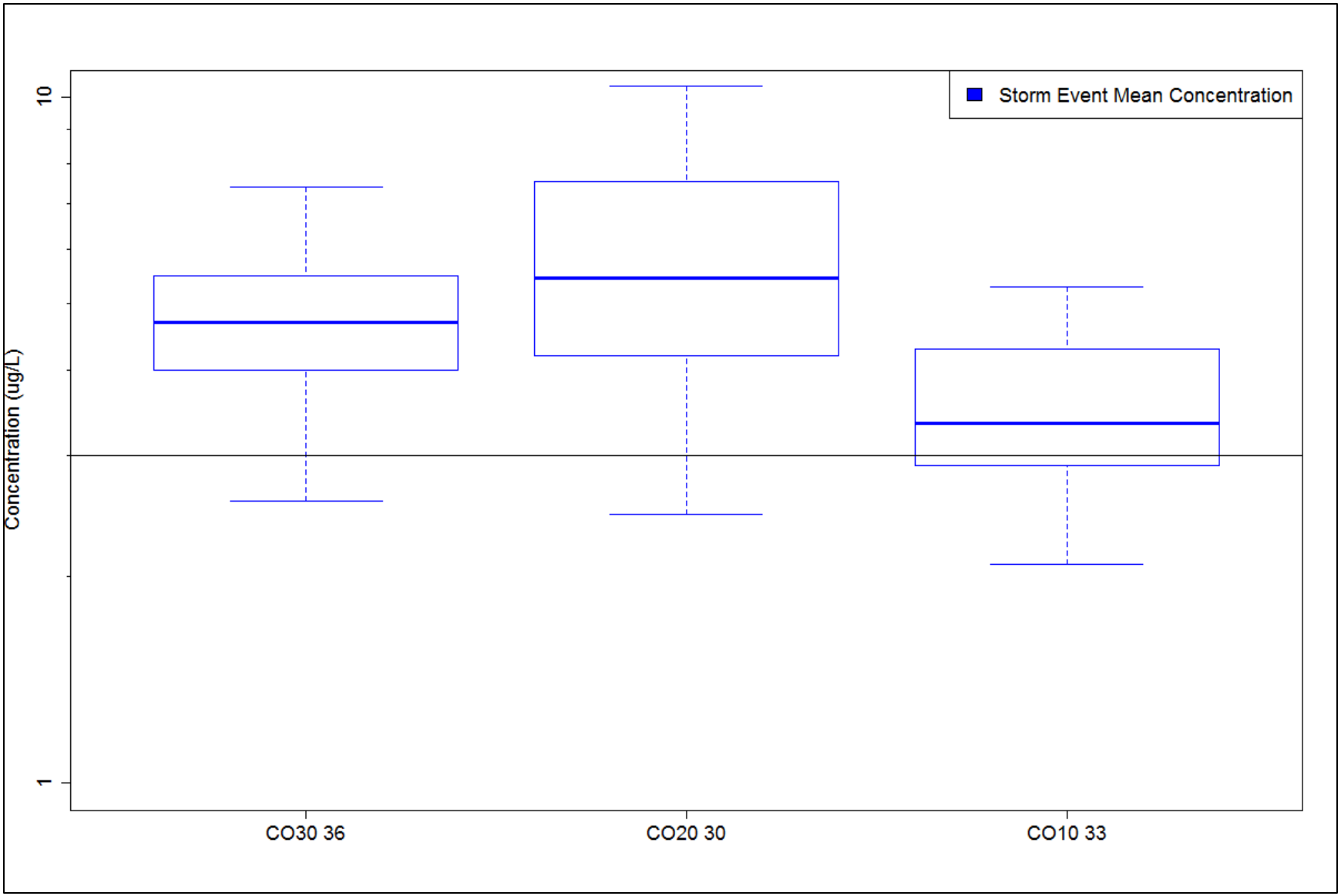

Figure B-18. Boxplots of influent and effluent event mean concentrations and micropool grab samples for soluble copper.

APPENDIX C Pollutant concentration time series plots

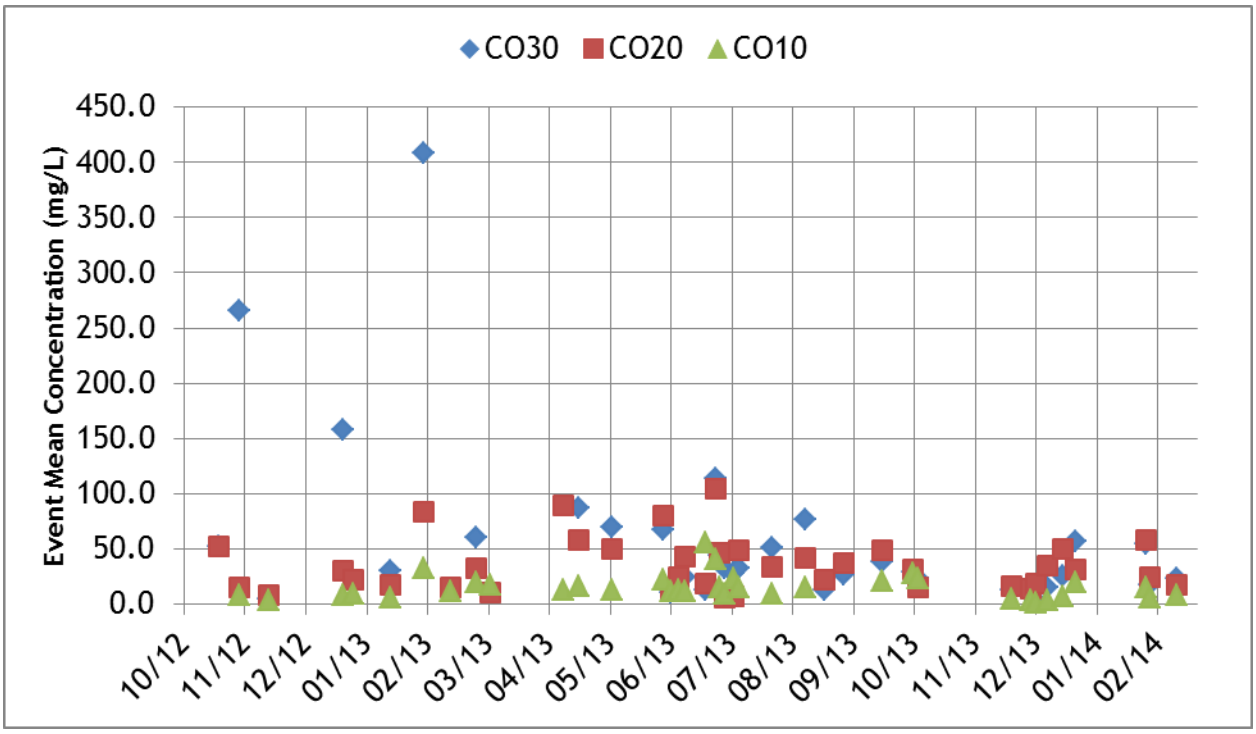

Figure C-1. Time series plot of station event mean concentrations for total suspended solids.

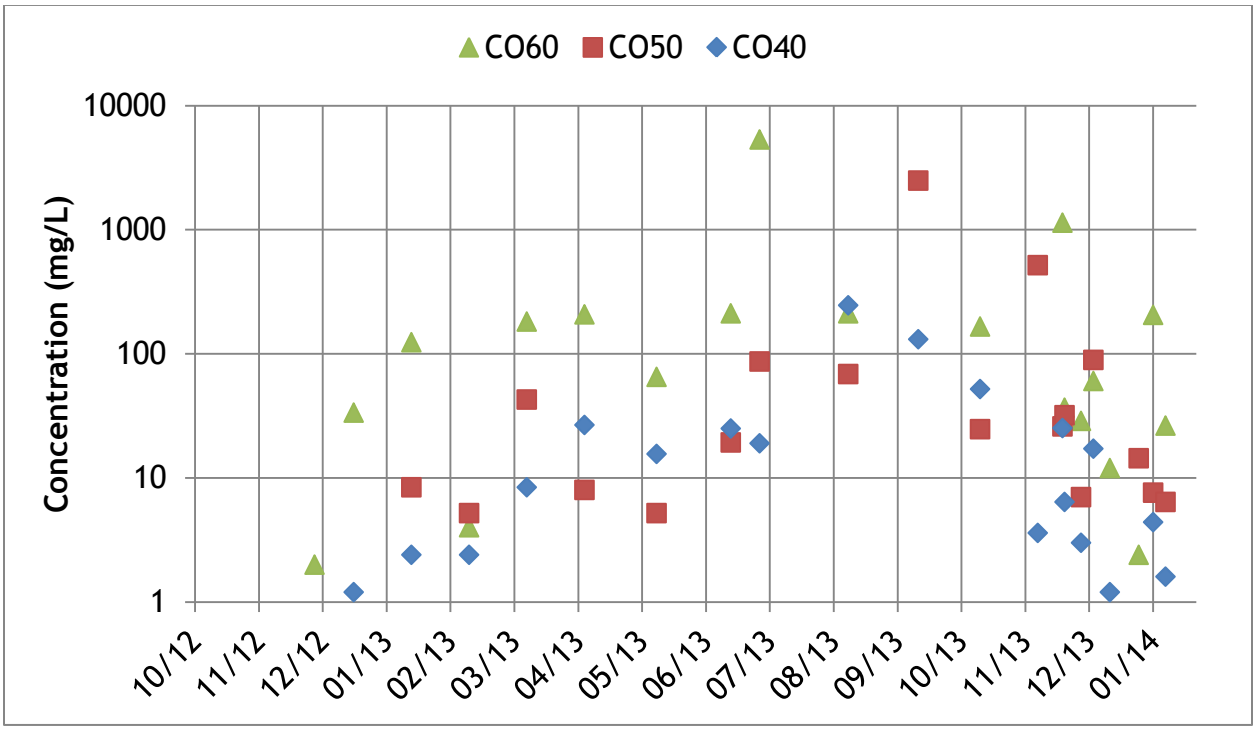

Figure C-2. Time series plot of micropool grab sample concentrations for total suspended solids.

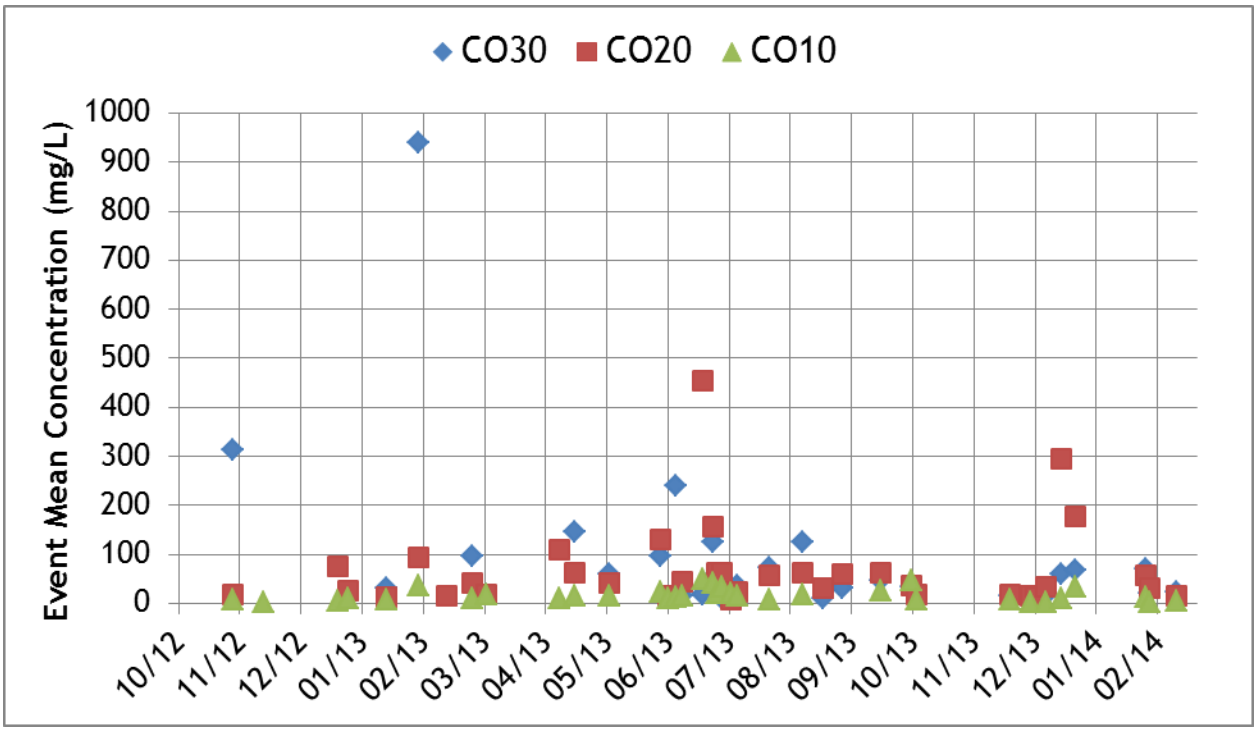

Figure C-3. Time series plot of station event mean concentrations for suspended sediment concentration.

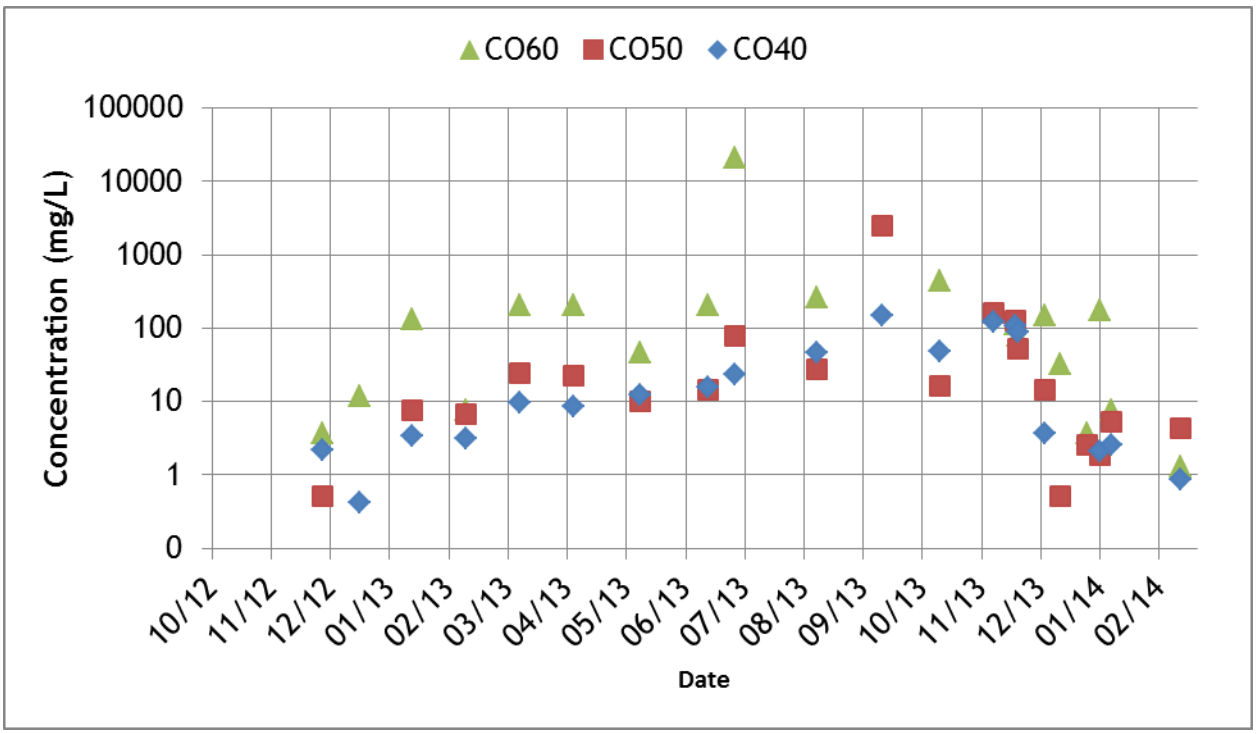

Figure C-4. Time series plot of micropool grab sample concentrations for suspended sediment concentration.

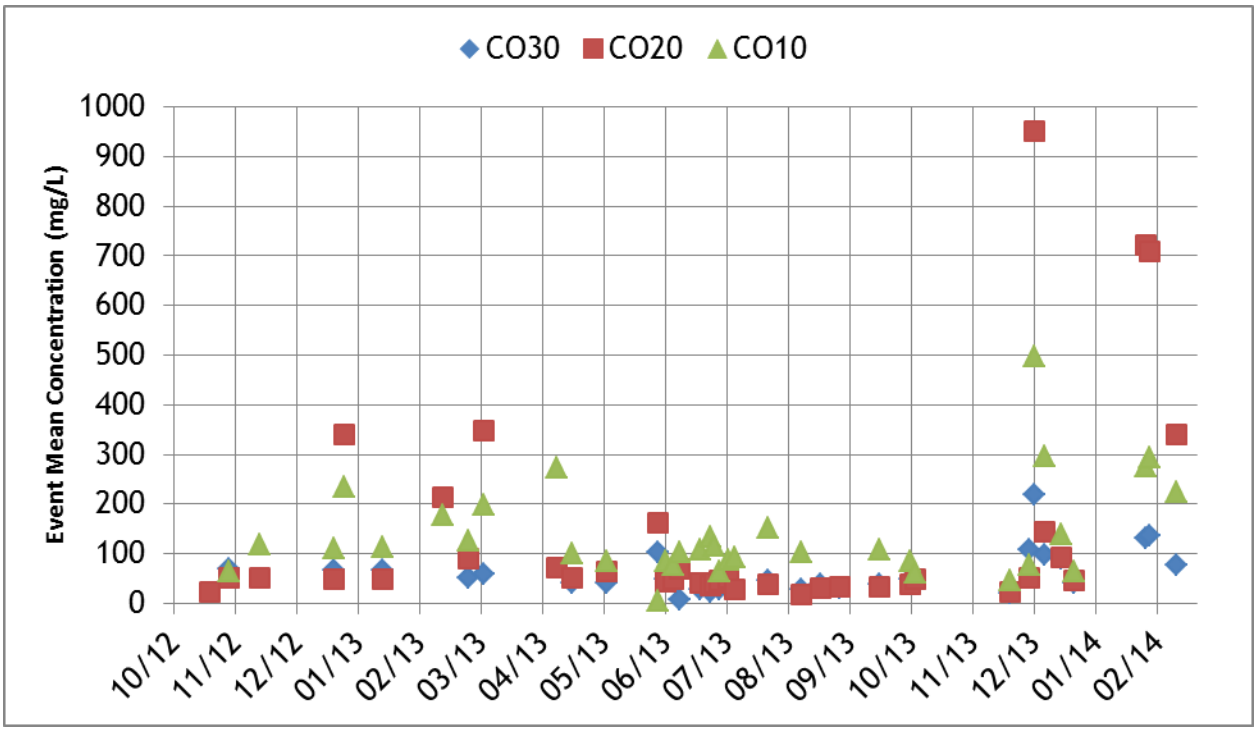

Figure C-5. Time series plot of station event mean concentrations for total dissolved solids.

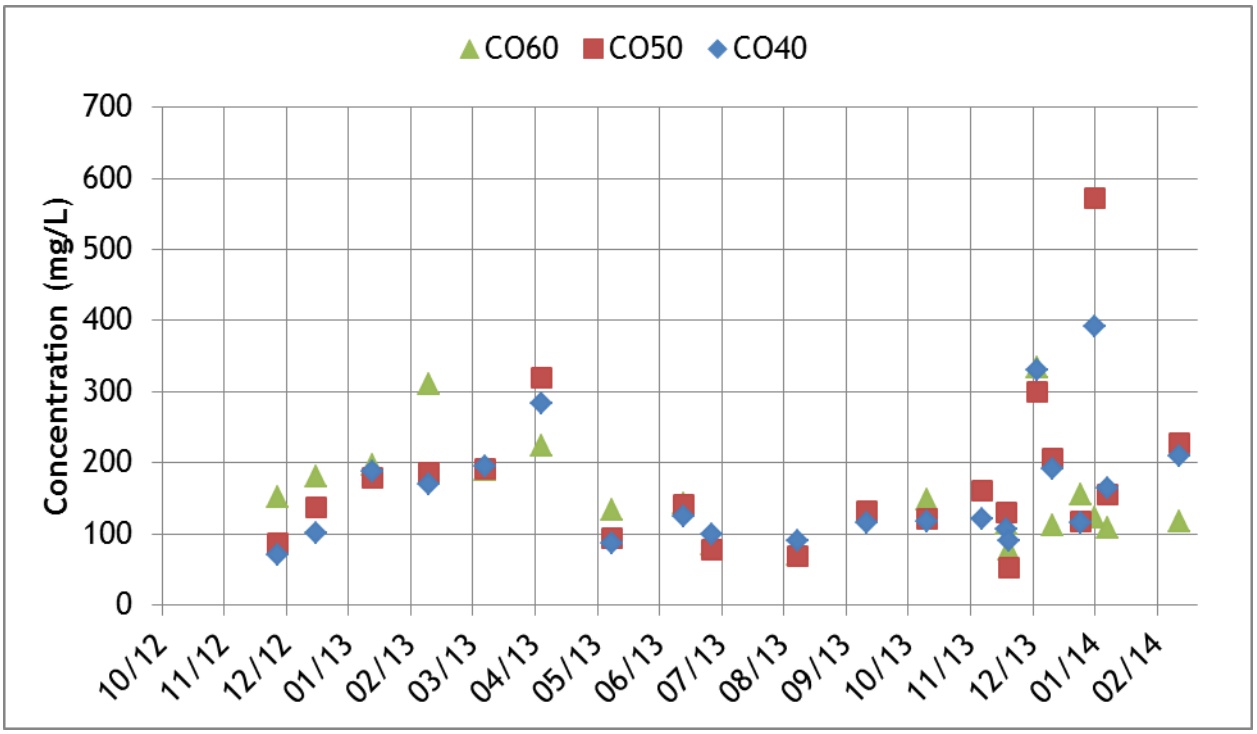

Figure C-6. Time series plot of micropool grab sample concentrations for total dissolved solids.

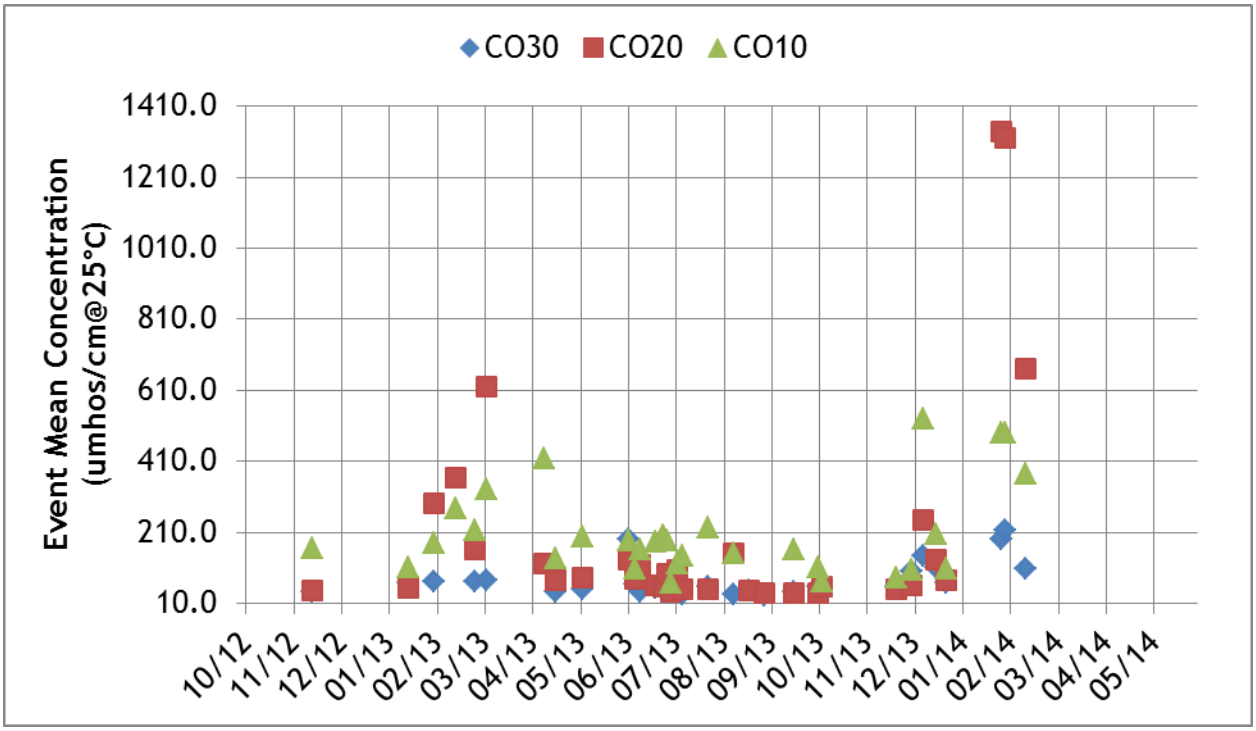

Figure C-7. Time series plot of station event mean concentrations for specific conductance.

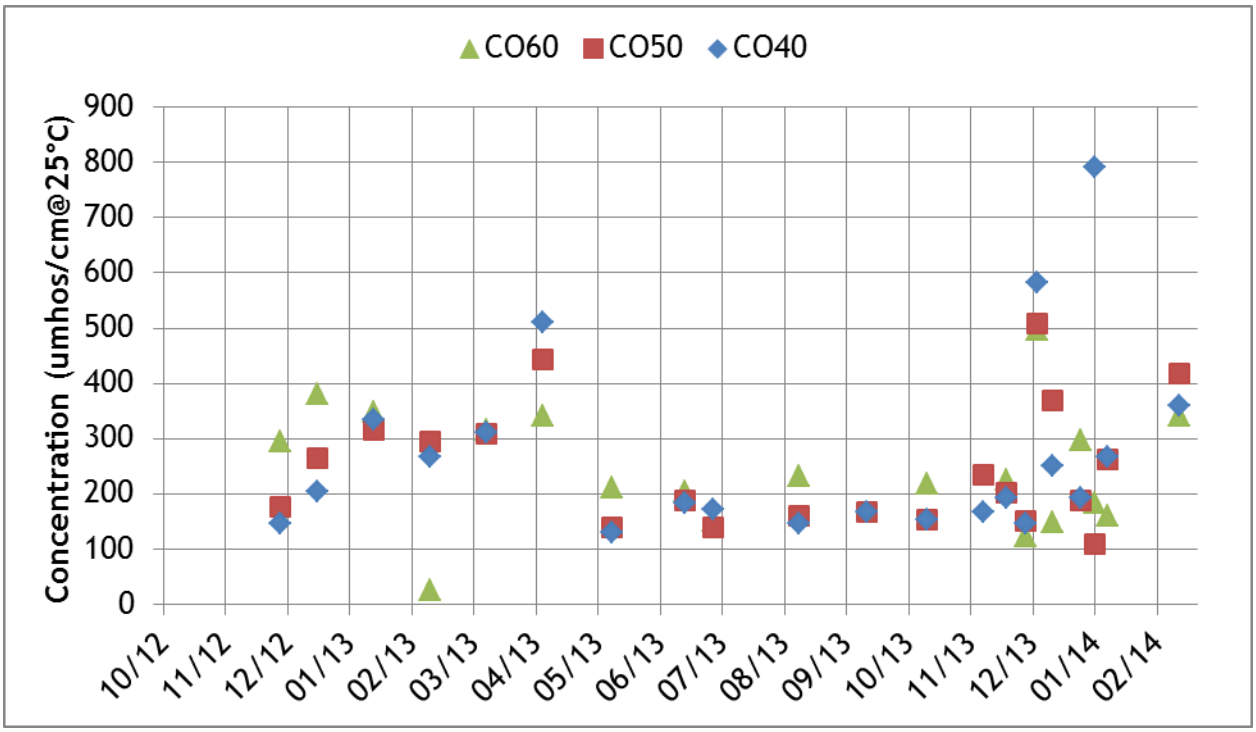

Figure C-8. Time series plot of micropool grab sample concentrations for specific conductance.

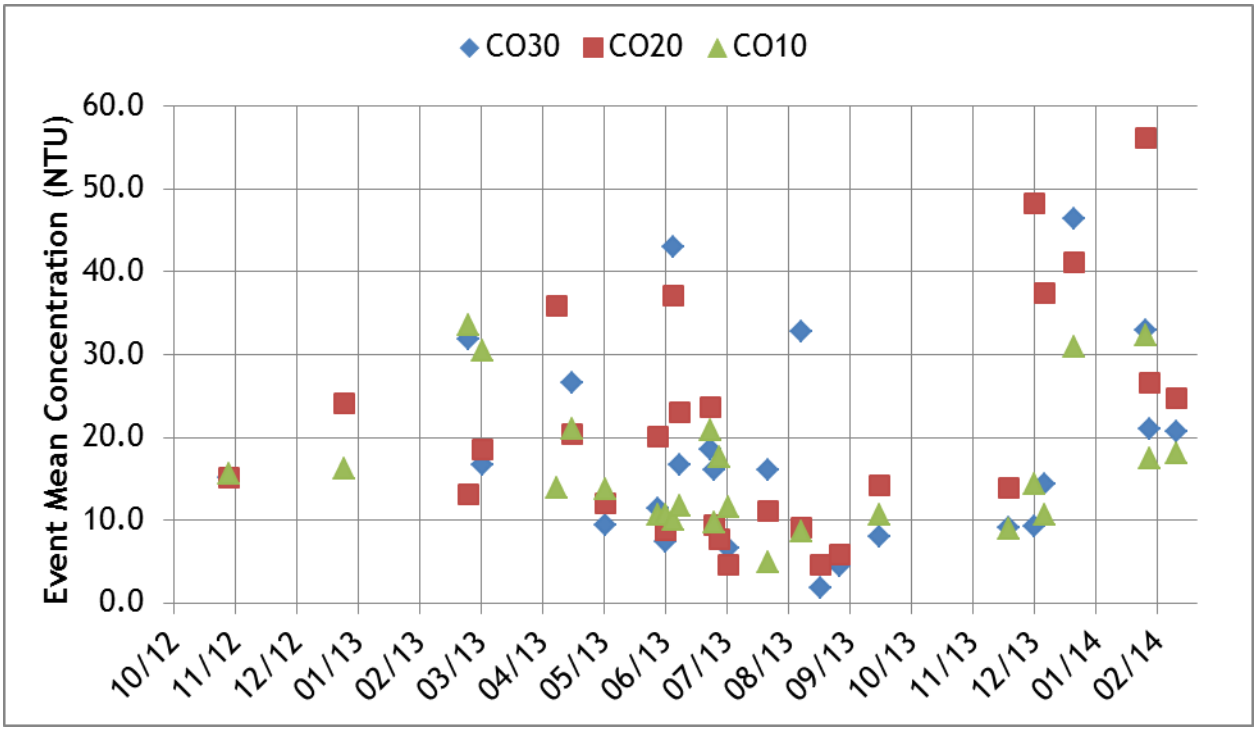

Figure C-9. Time series plot of station event mean concentrations for turbidity.

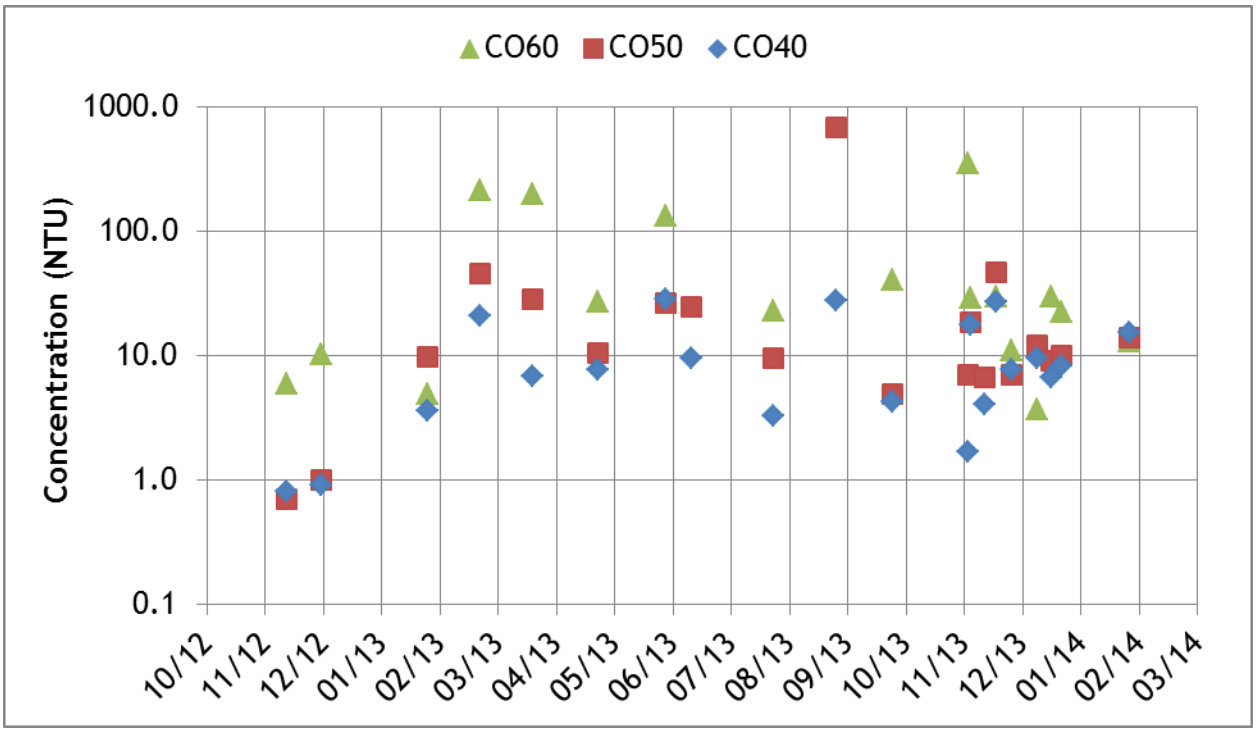

Figure C-10. Time series plot of micropool grab sample concentrations for turbidity.

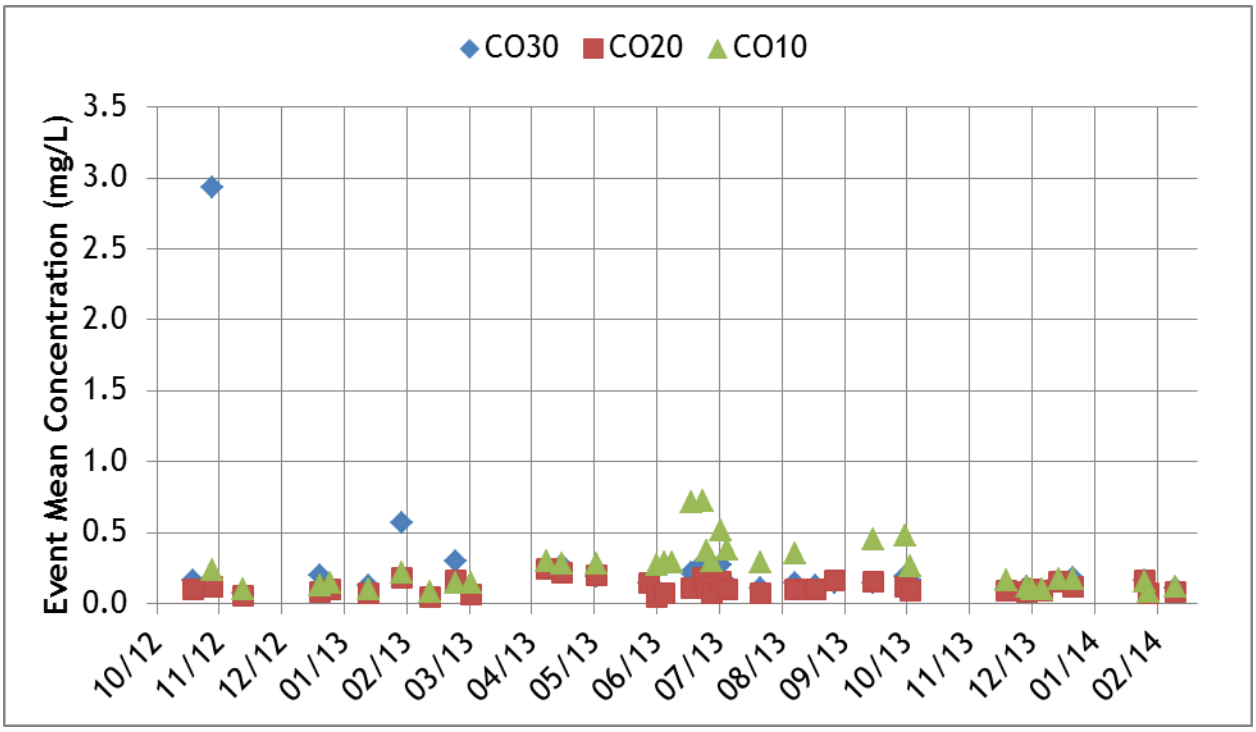

Figure C-11. Time series plot of station event mean concentrations for total phosphorus.

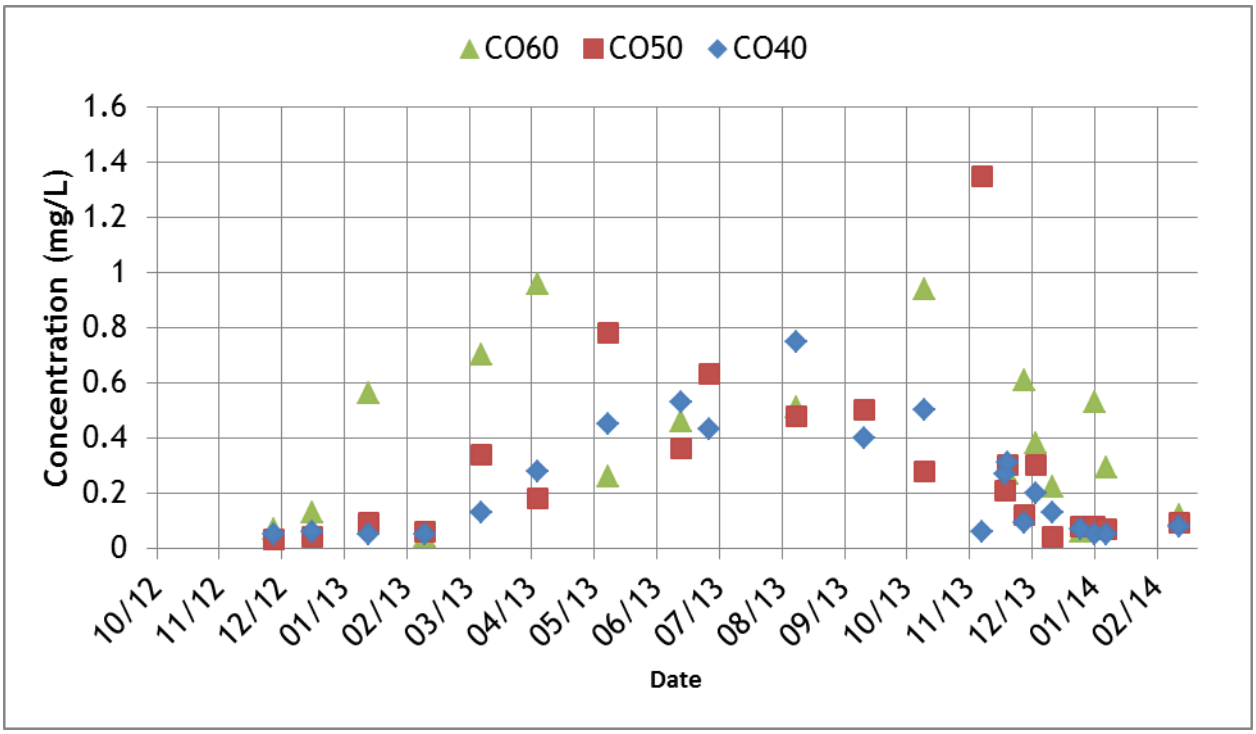

Figure C-12. Time series plot of micropool grab sample concentrations for total phosphorus.

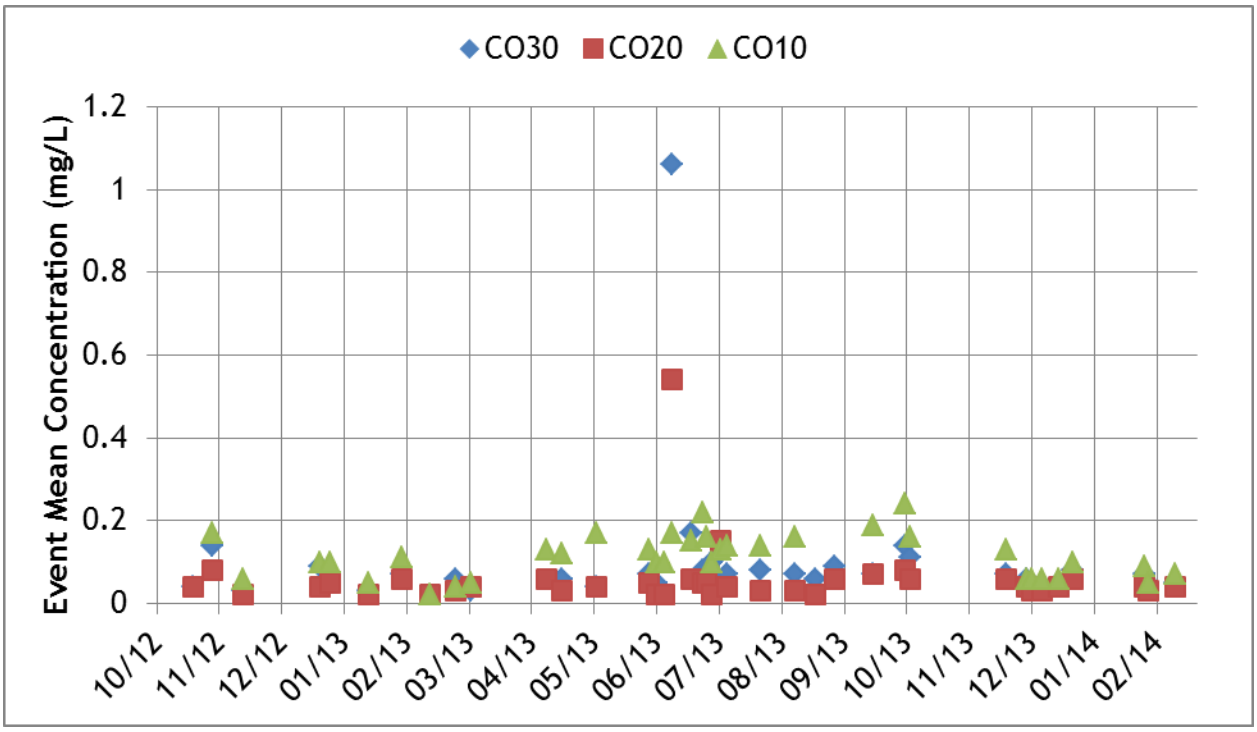

Figure C-13. Time series plot of station event mean concentrations for orthophosphate phosphorus.

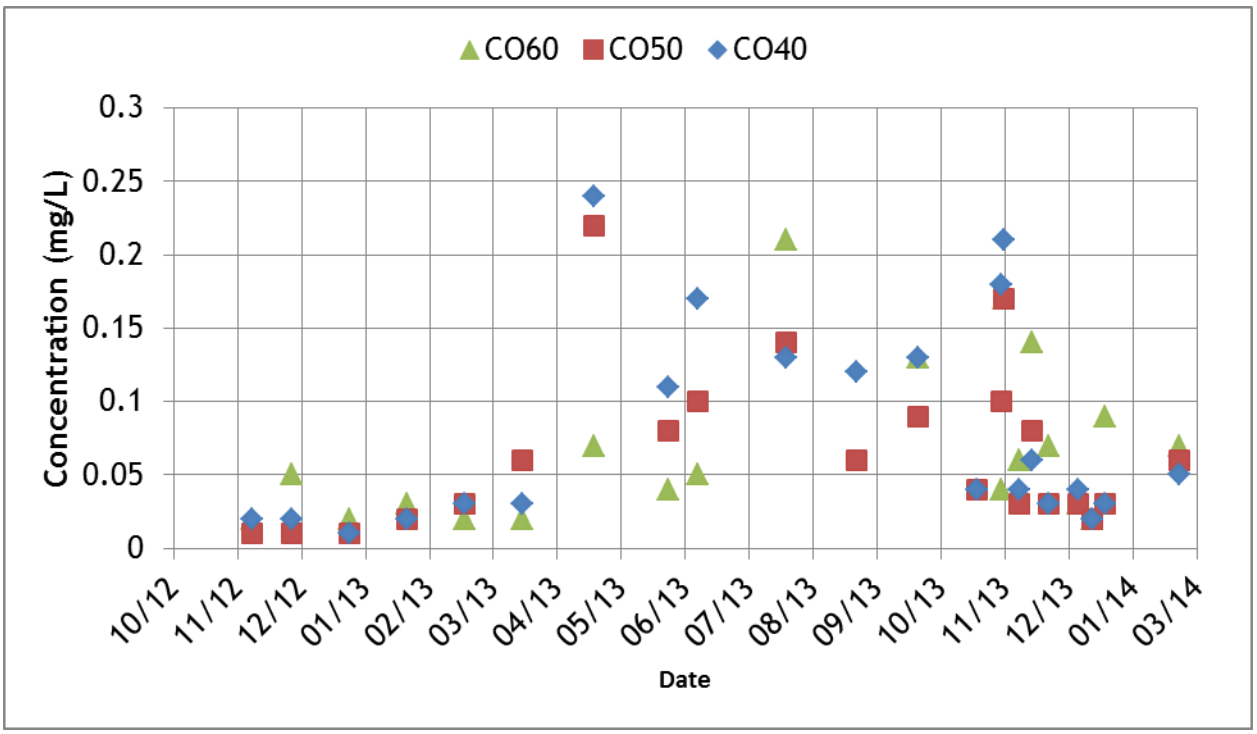

Figure C-14. Time series plot of micropool grab sample concentrations for orthophosphate phosphorus.

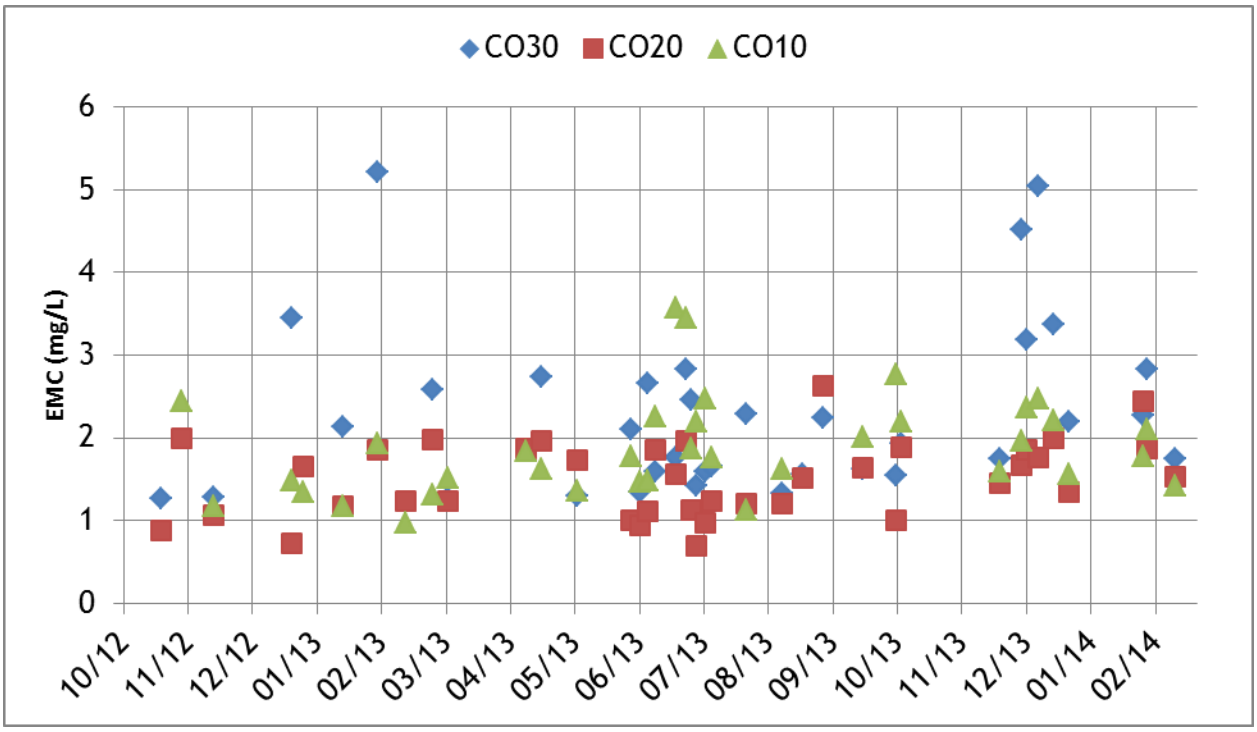

Figure C-15. Time series plot of station event mean concentrations for total nitrogen.

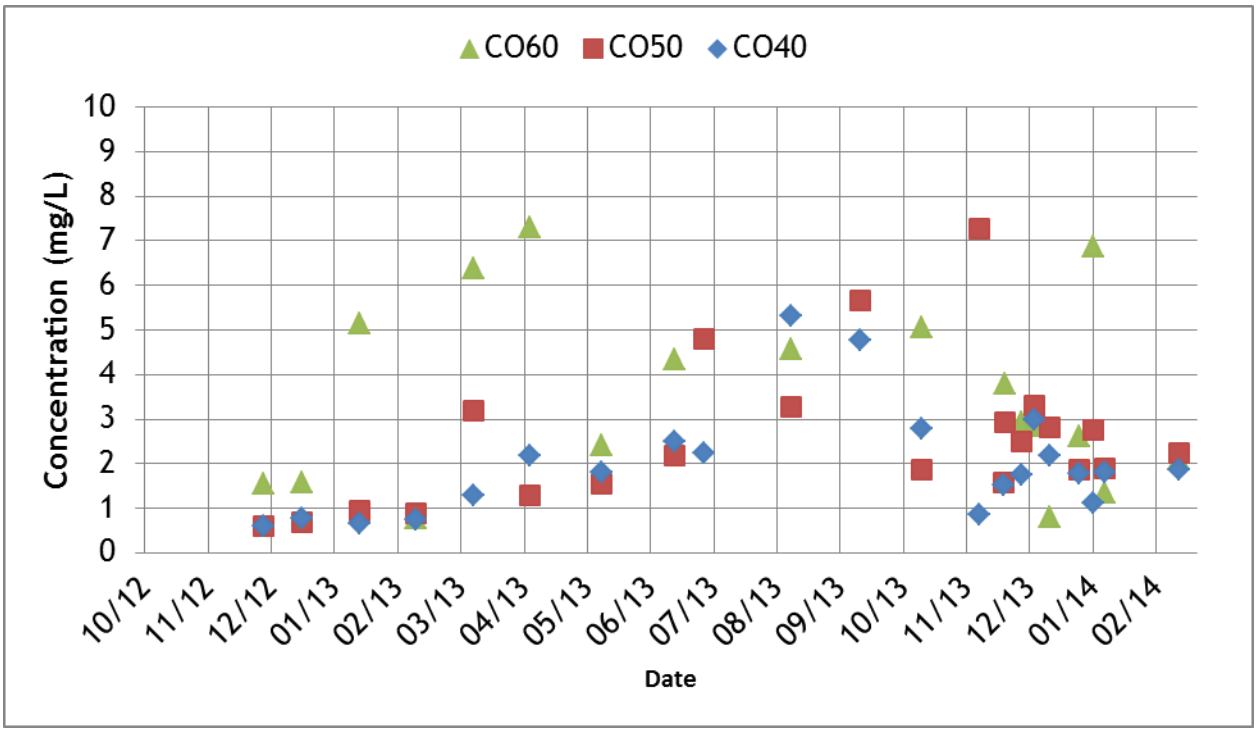

Figure C-16. Time series plot of micropool grab samples for total nitrogen.

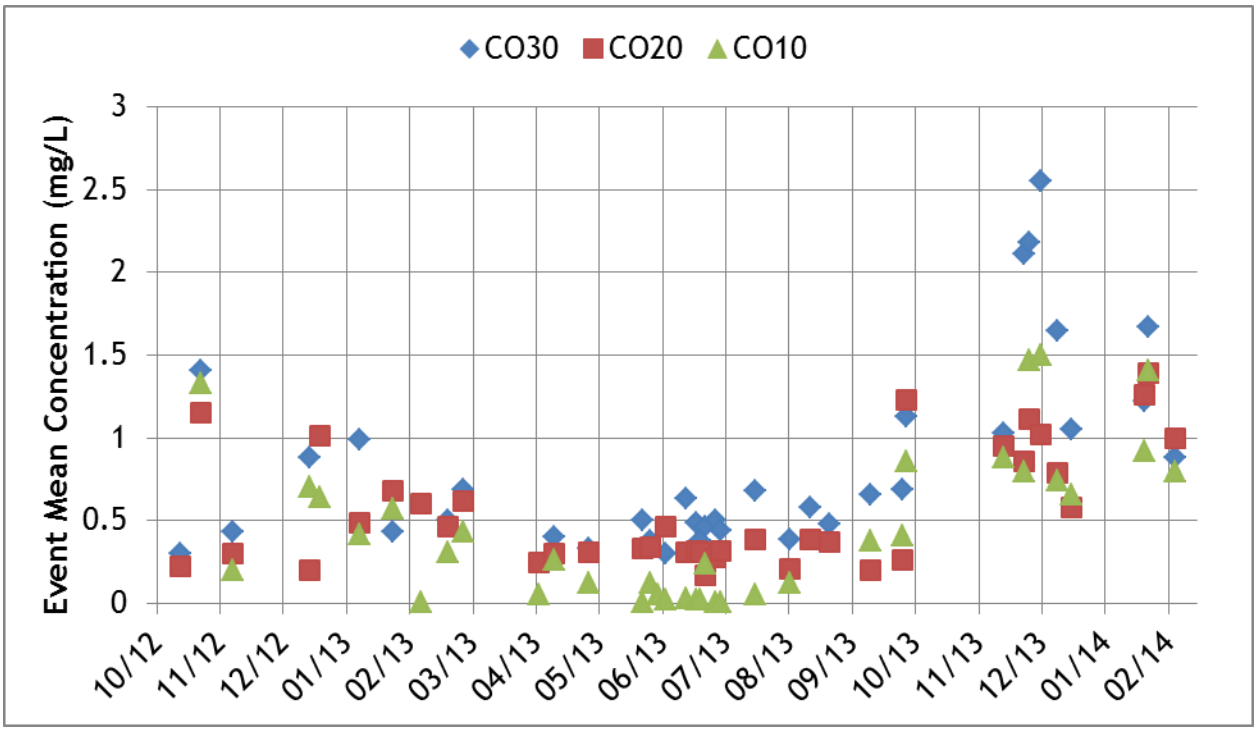

Figure C-17. Time series plot of station event mean concentrations for oxidized nitrogen.

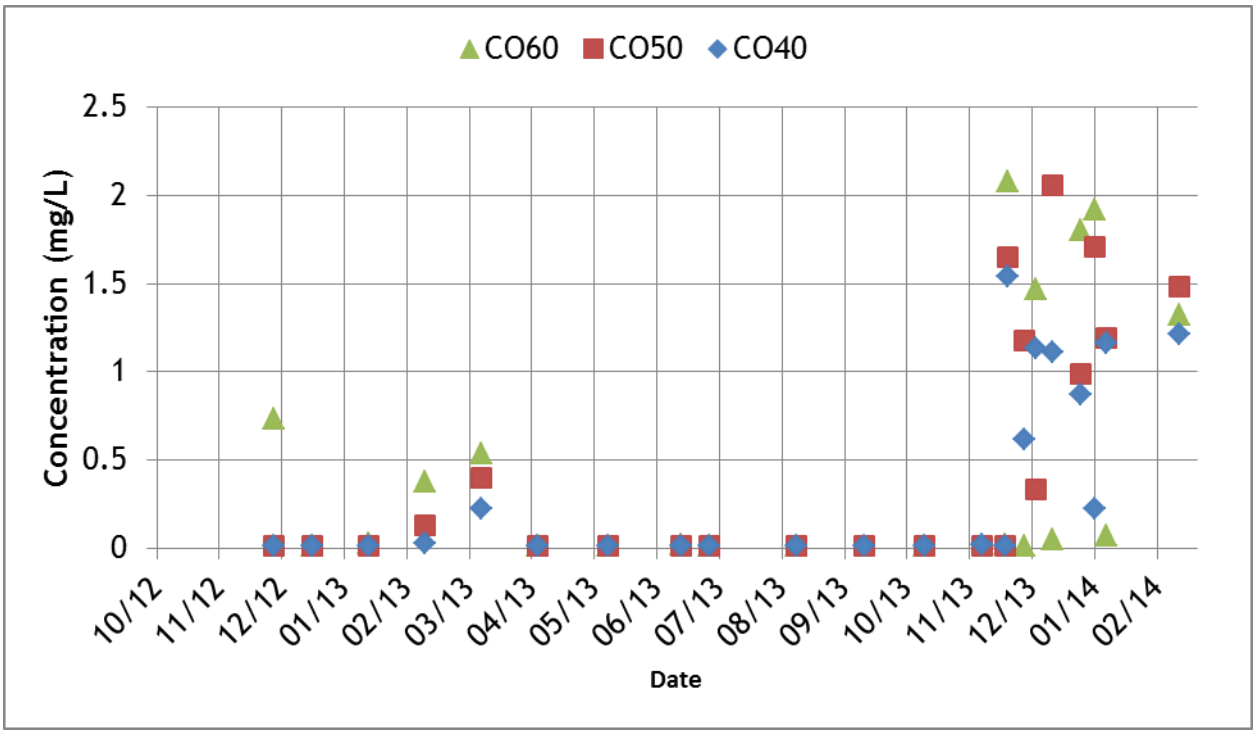

Figure C-18. Time series plot of micropool grab samples for oxidized nitrogen.

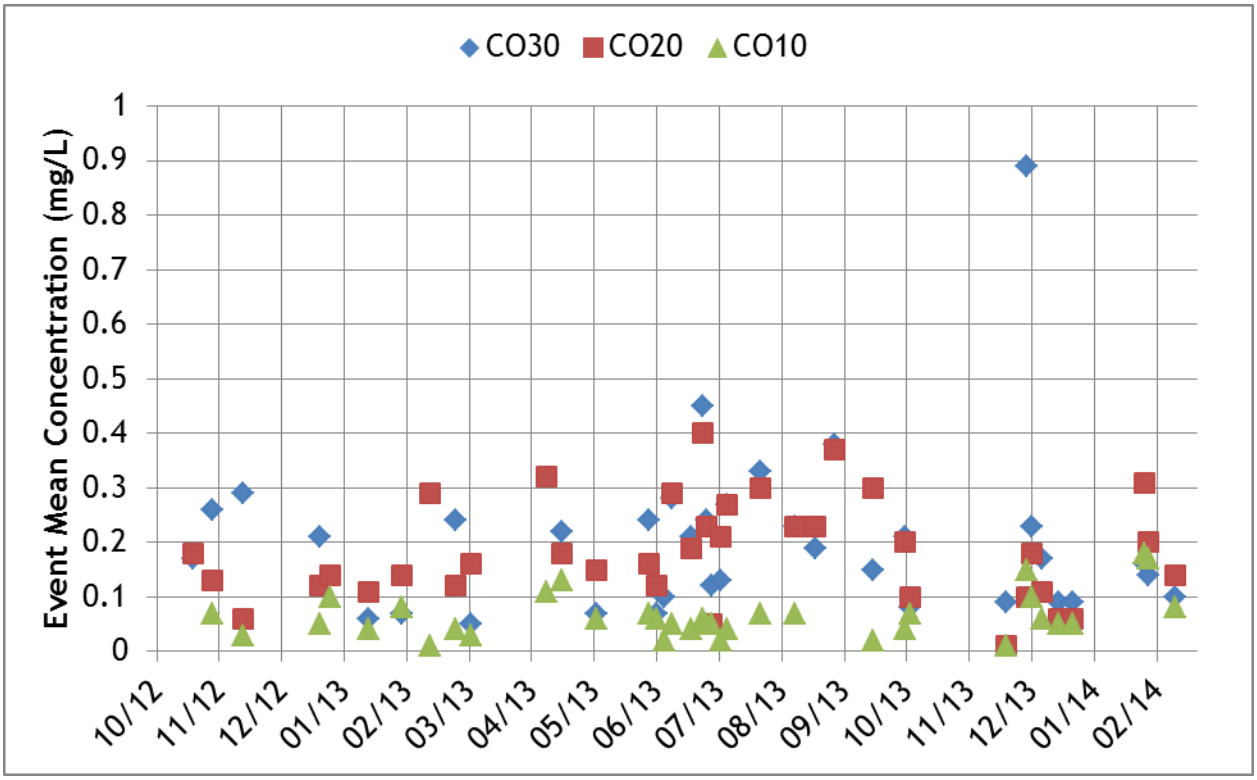

Figure C-19. Time series plot of station event mean concentrations for ammonia nitrogen.

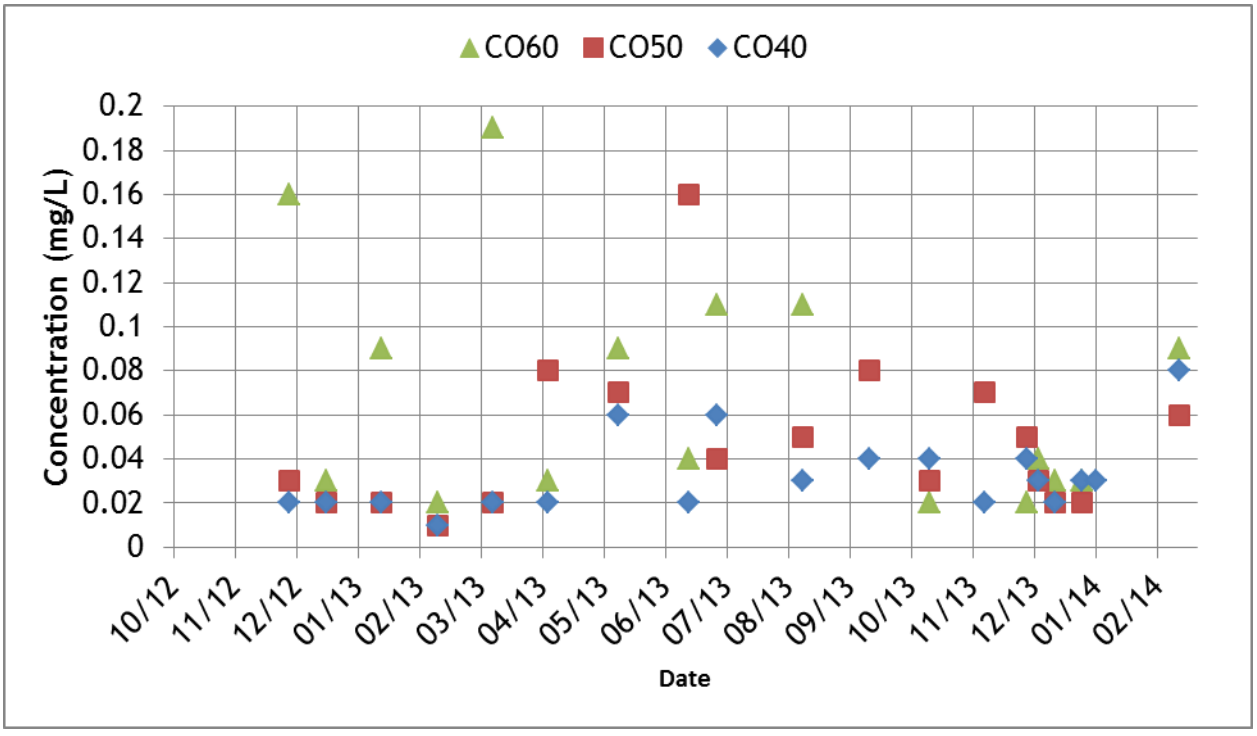

Figure C-20. Time series plot of micropool grab samples for ammonia nitrogen.

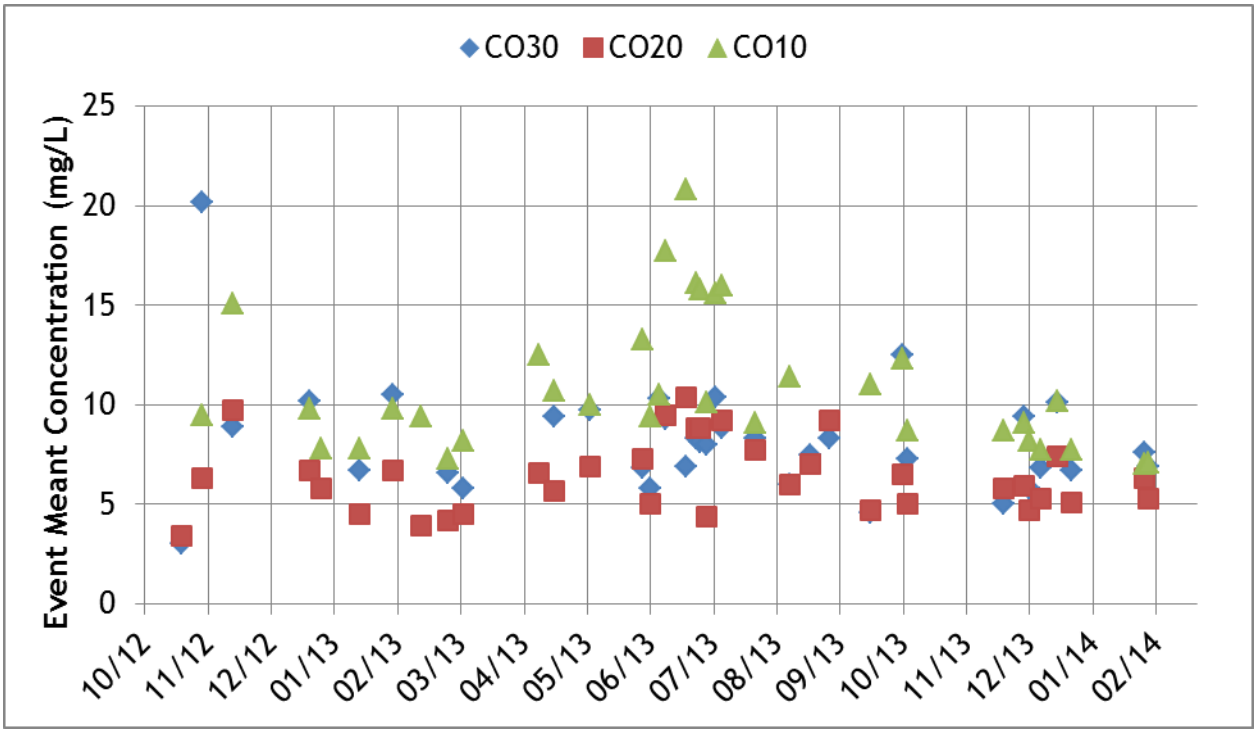

Figure C-21. Time series plot of station event mean concentrations for total organic carbon.

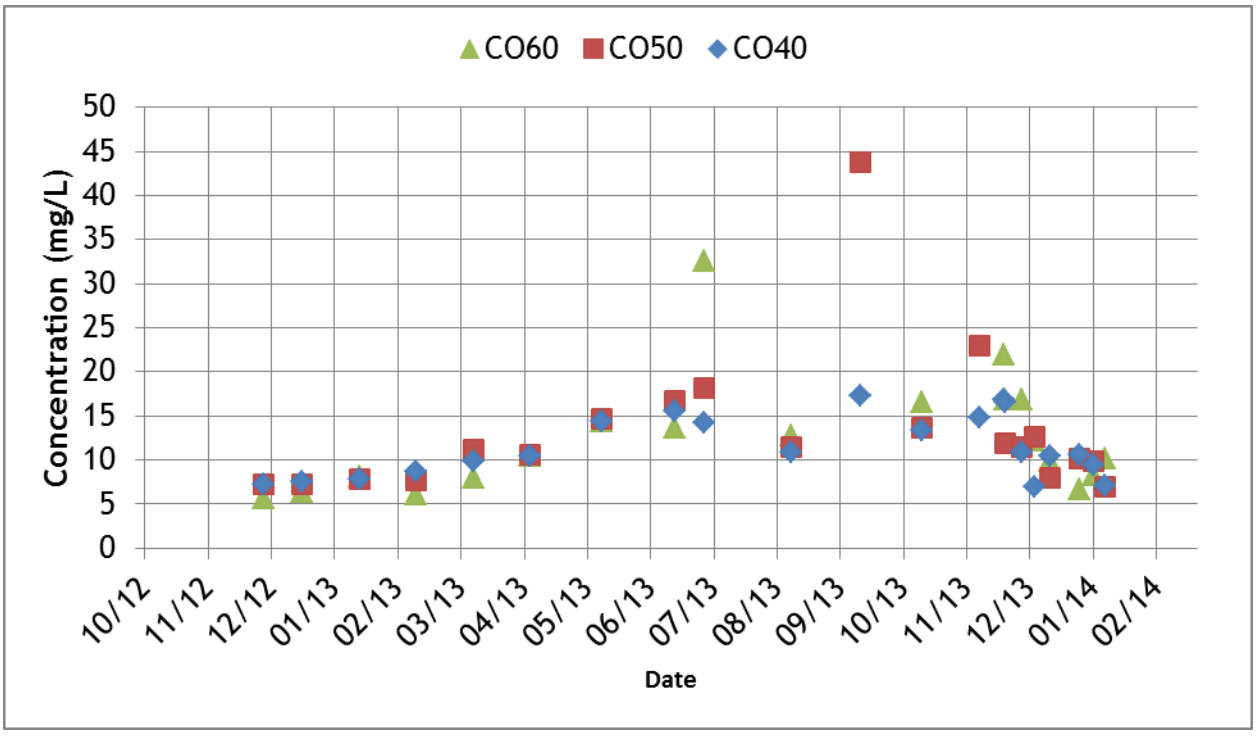

Figure C-22. Time series plot of micropool grab samples for total organic carbon.

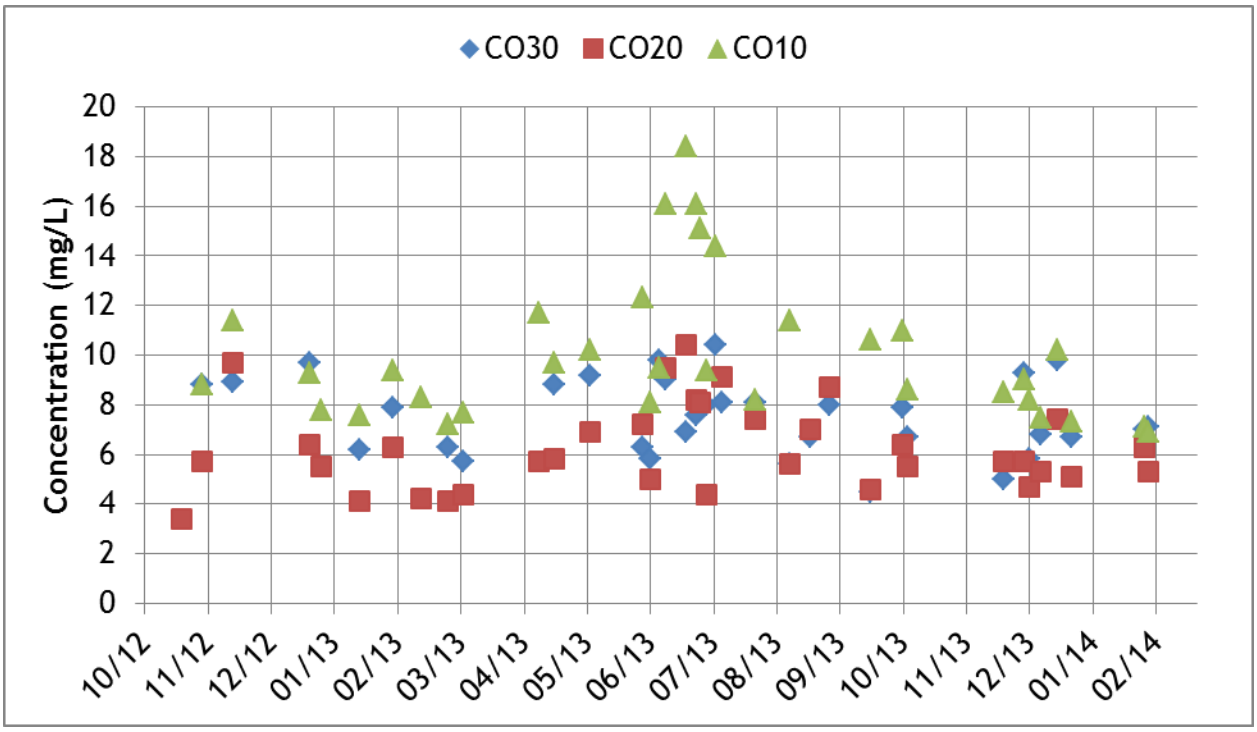

Figure C-23. Time series plot of station event mean concentrations for dissolved organic carbon.

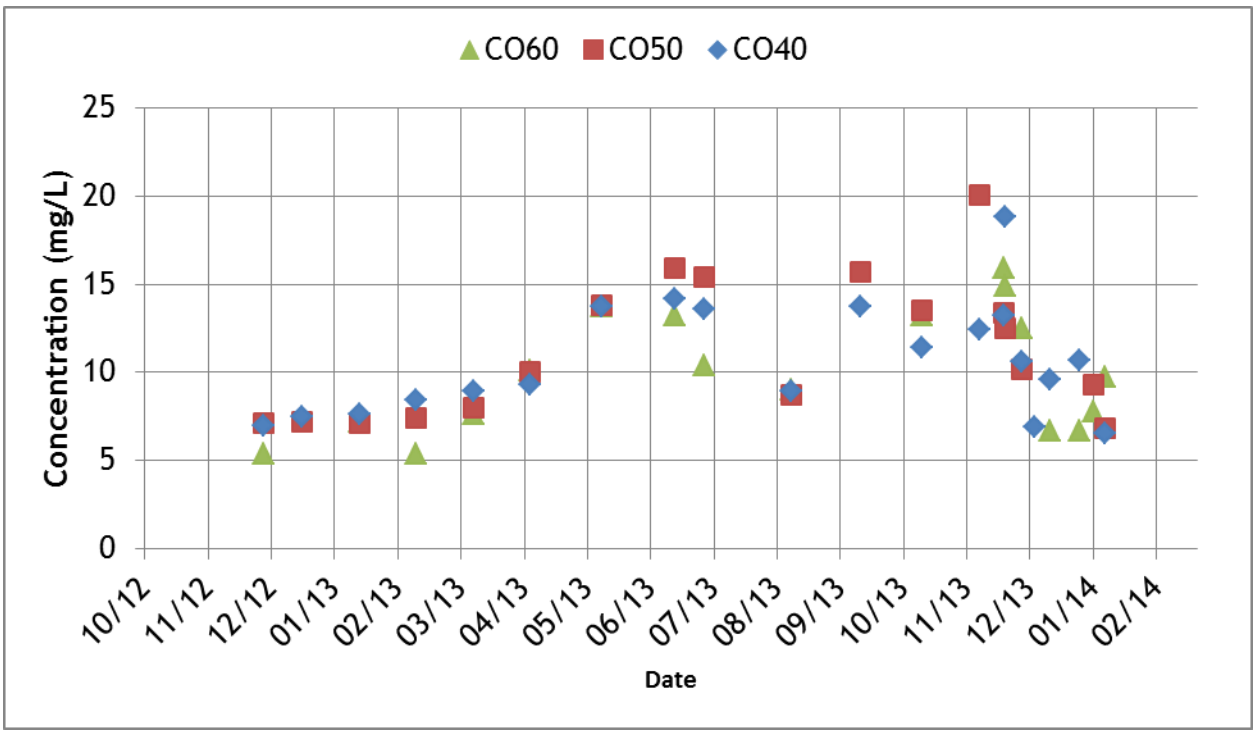

Figure C-24. Time series plot of micropool grab samples for dissolved organic carbon.

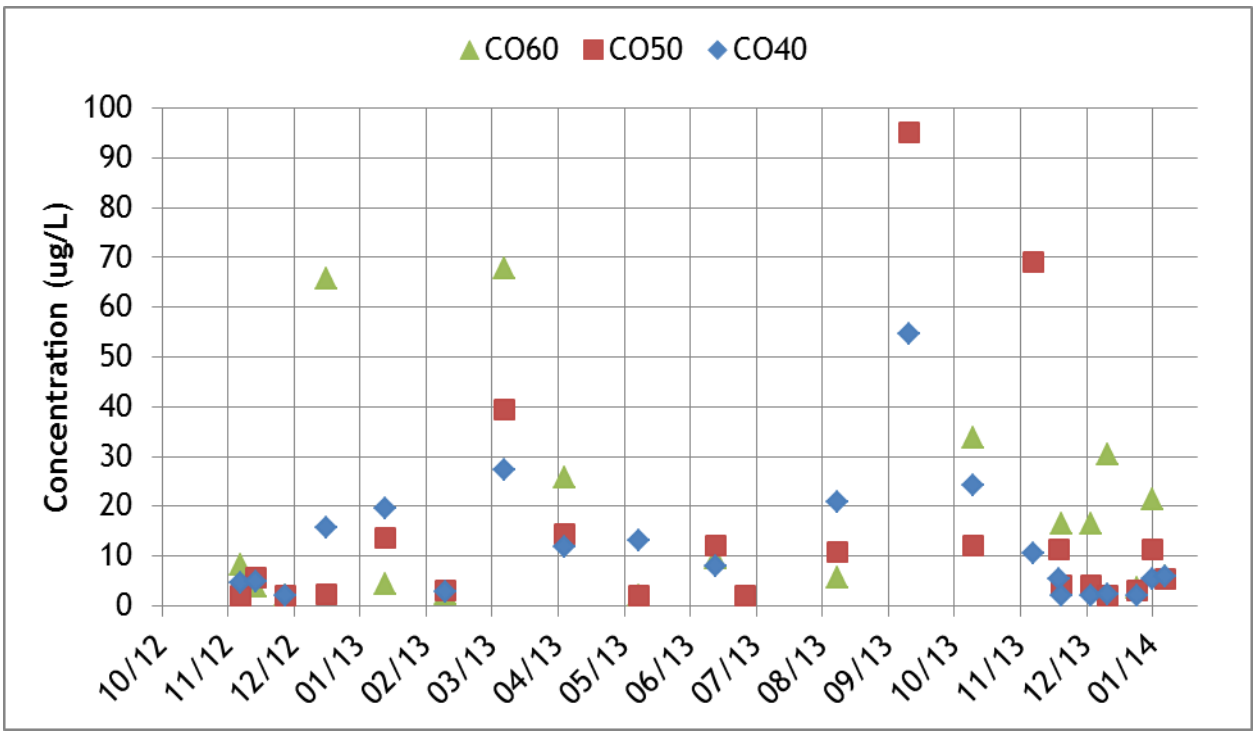

Figure C-25. Time series plot of micropool grab samples for chlorophyll-a.

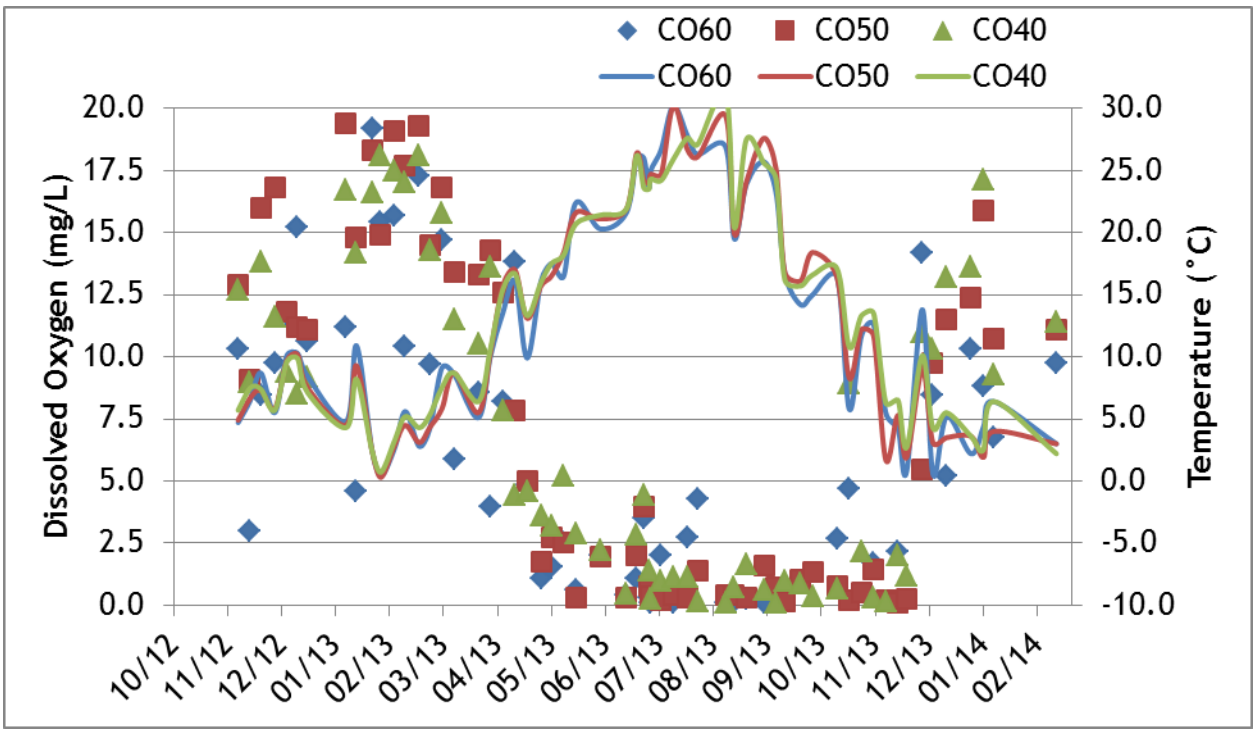

Figure C-26. Time series plot of micropool field temperature and dissolved oxygen measurements.

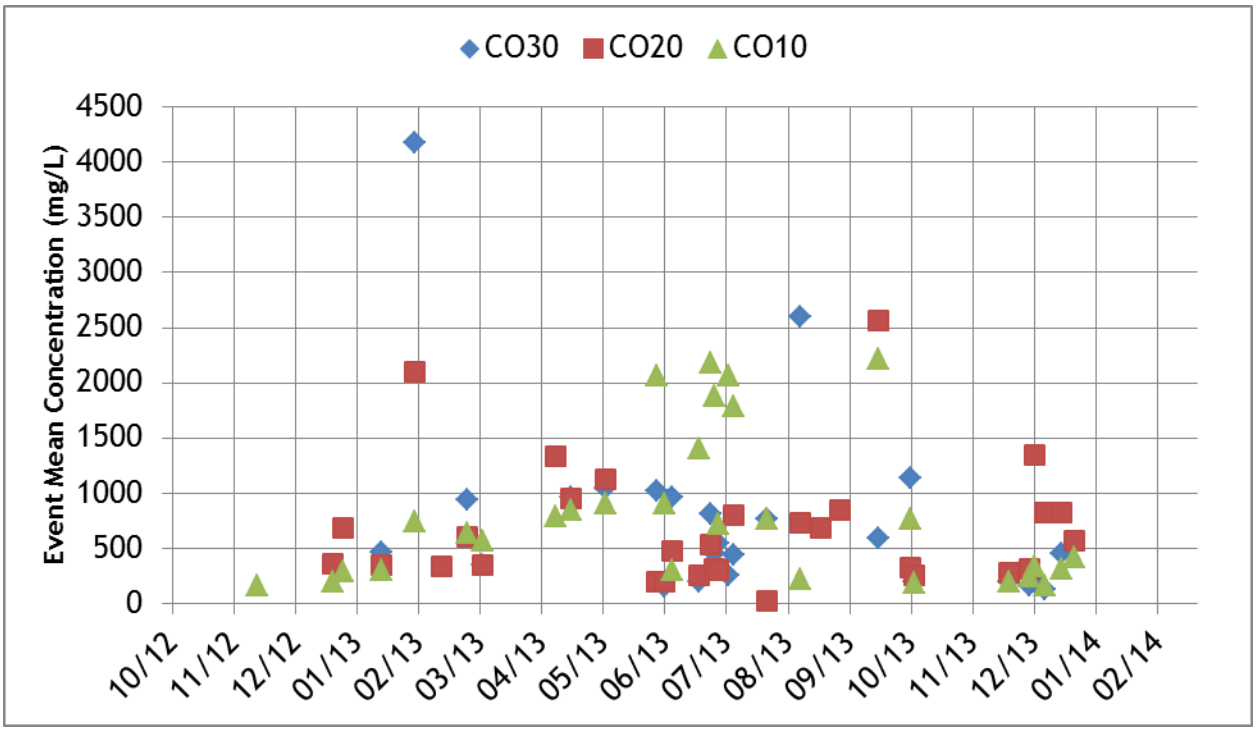

Figure C-27. Time series plot of station event mean concentrations for total iron.

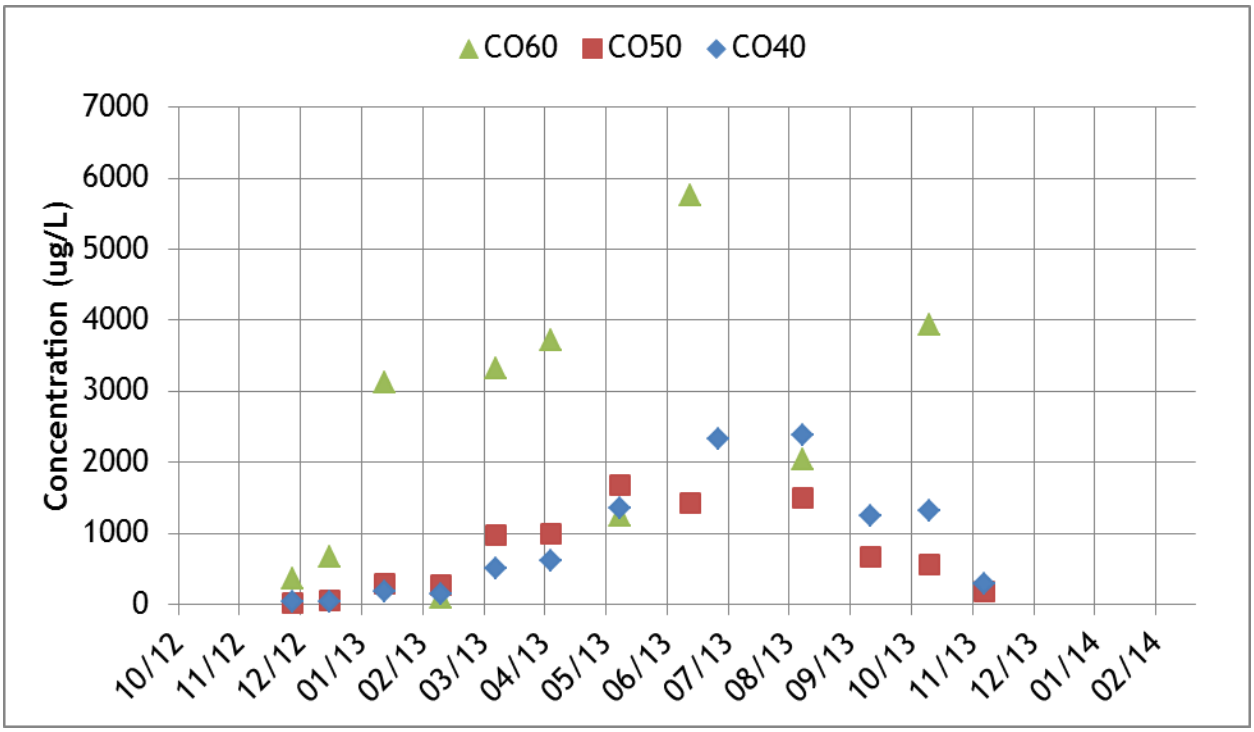

Figure C-28. Time series plot of micropool grab samples for total iron.

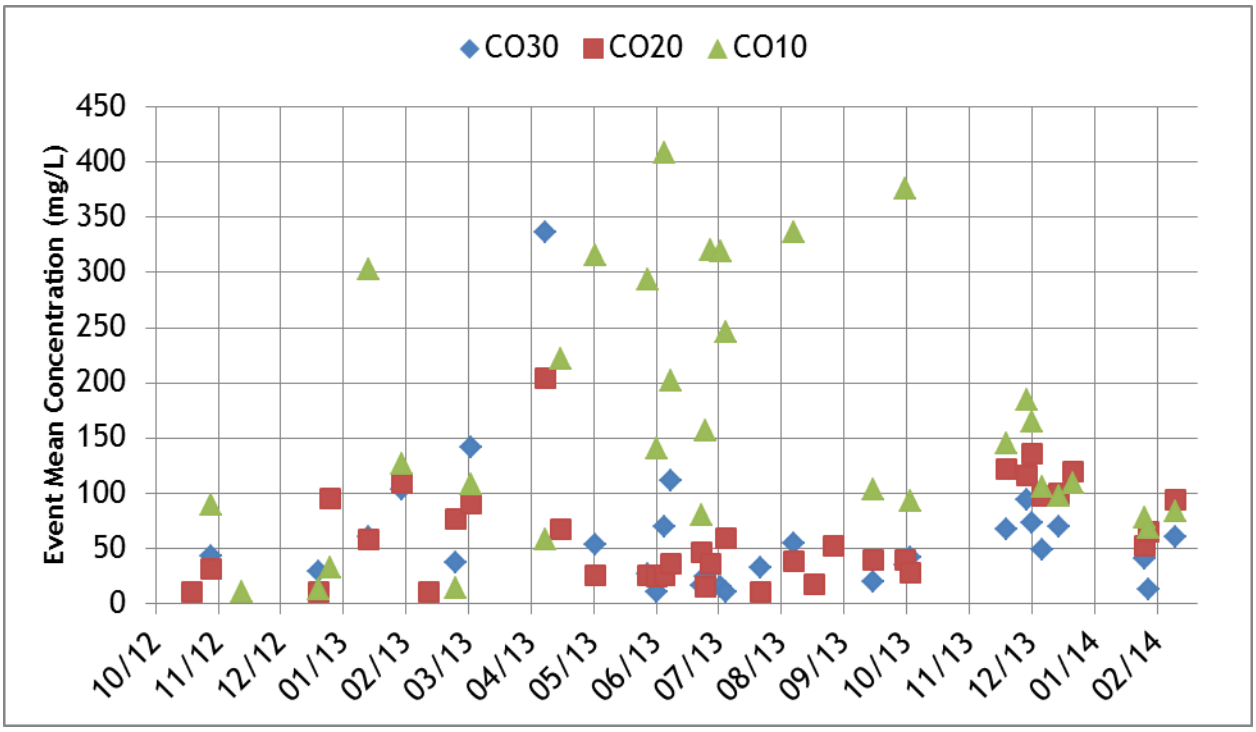

Figure C-29. Time series plot of station event mean concentrations for soluble iron.

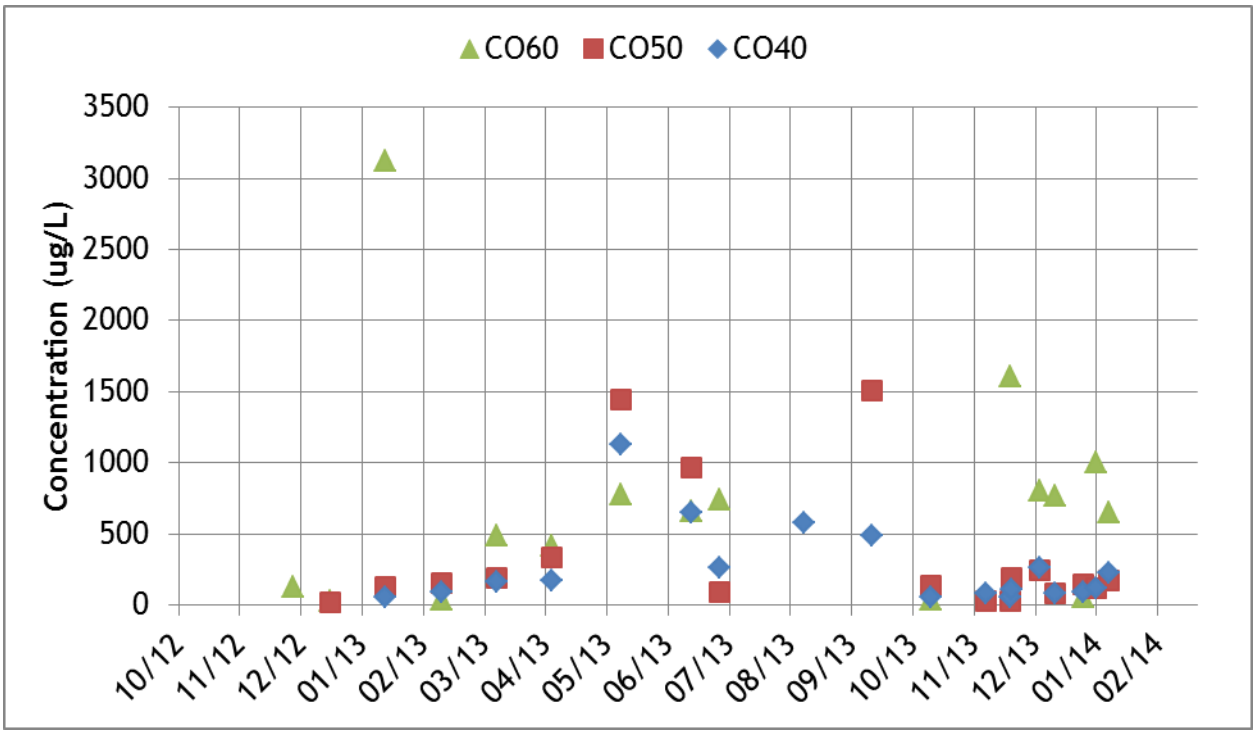

Figure C-30. Time series plot of micropool grab samples for soluble iron.

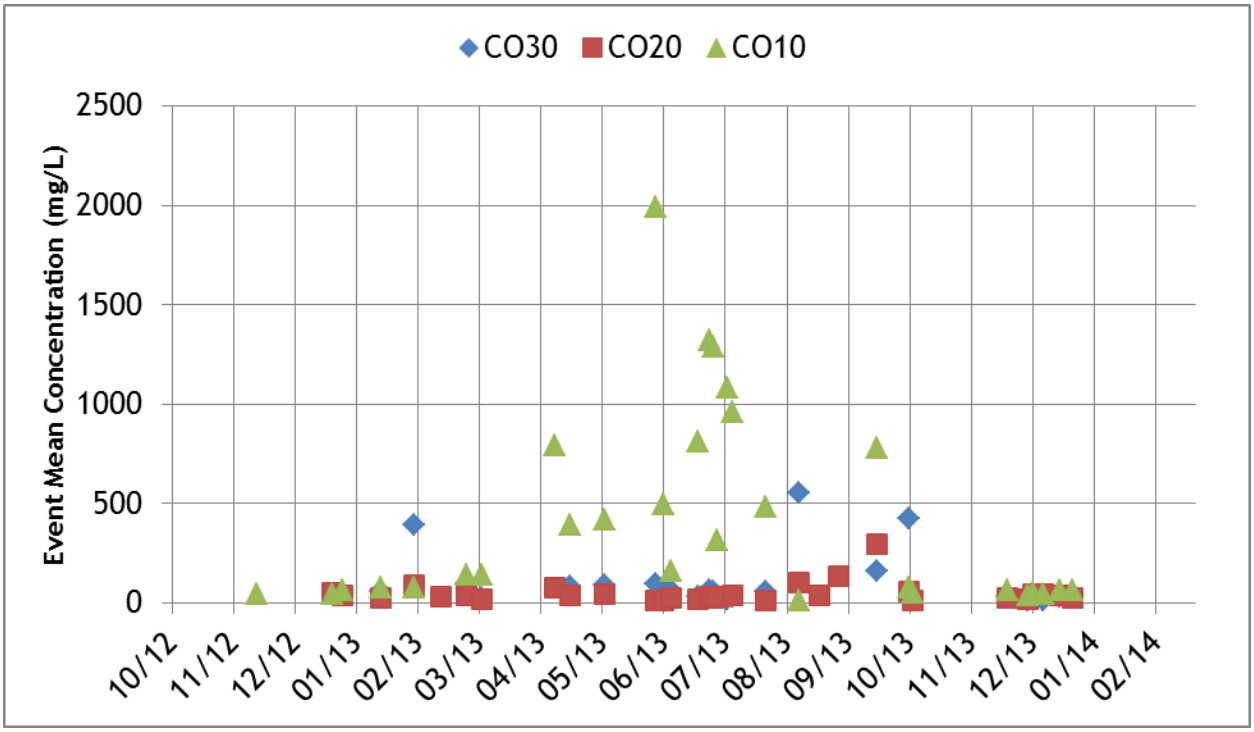

Figure C-31. Time series plot of station event mean concentrations for total manganese.

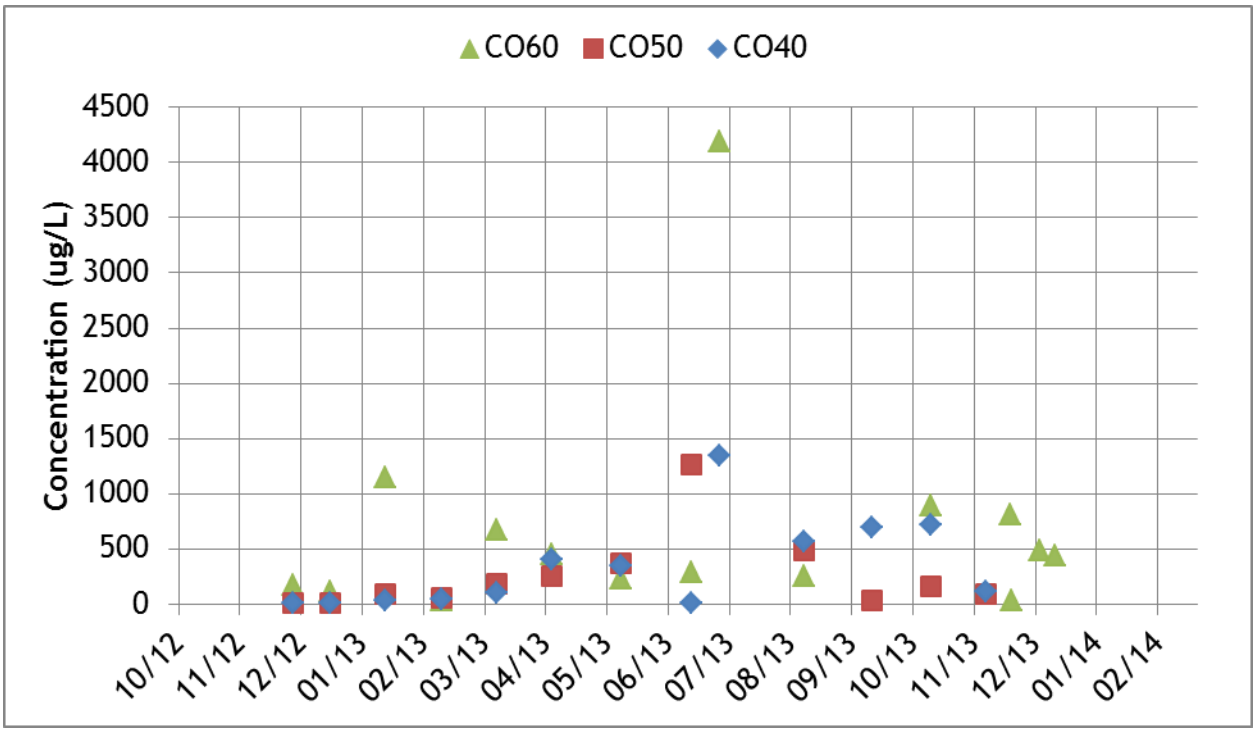

Figure C-32. Time series plot of micropool grab samples for total manganese.

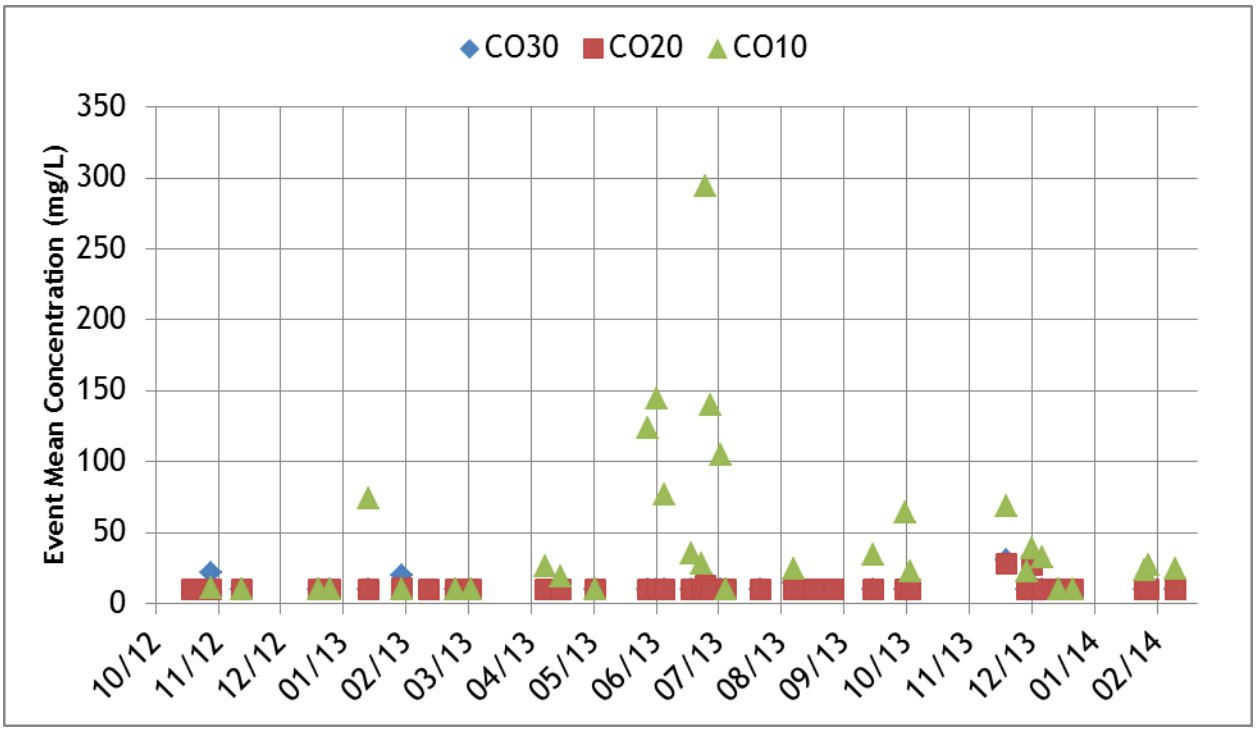

Figure C-33. Time series plot of station event mean concentrations for soluble manganese.

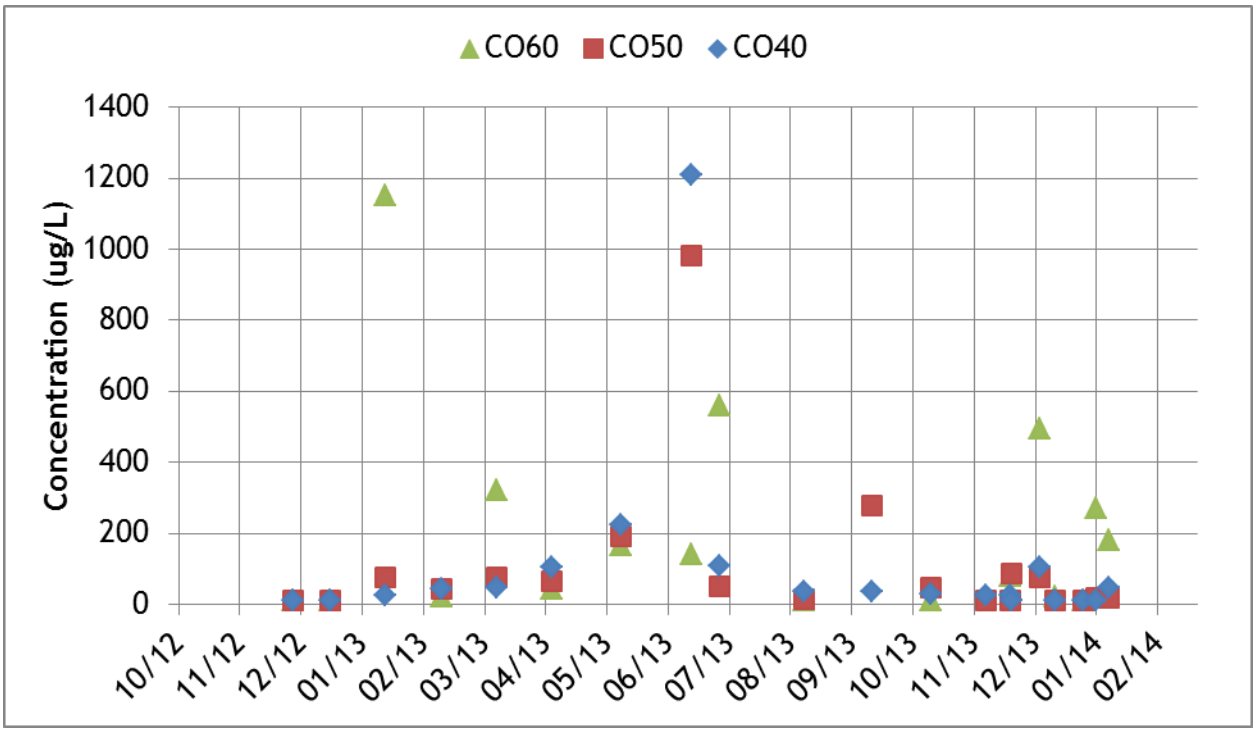

Figure C-34. Time series plot of micropool grab samples for soluble manganese.

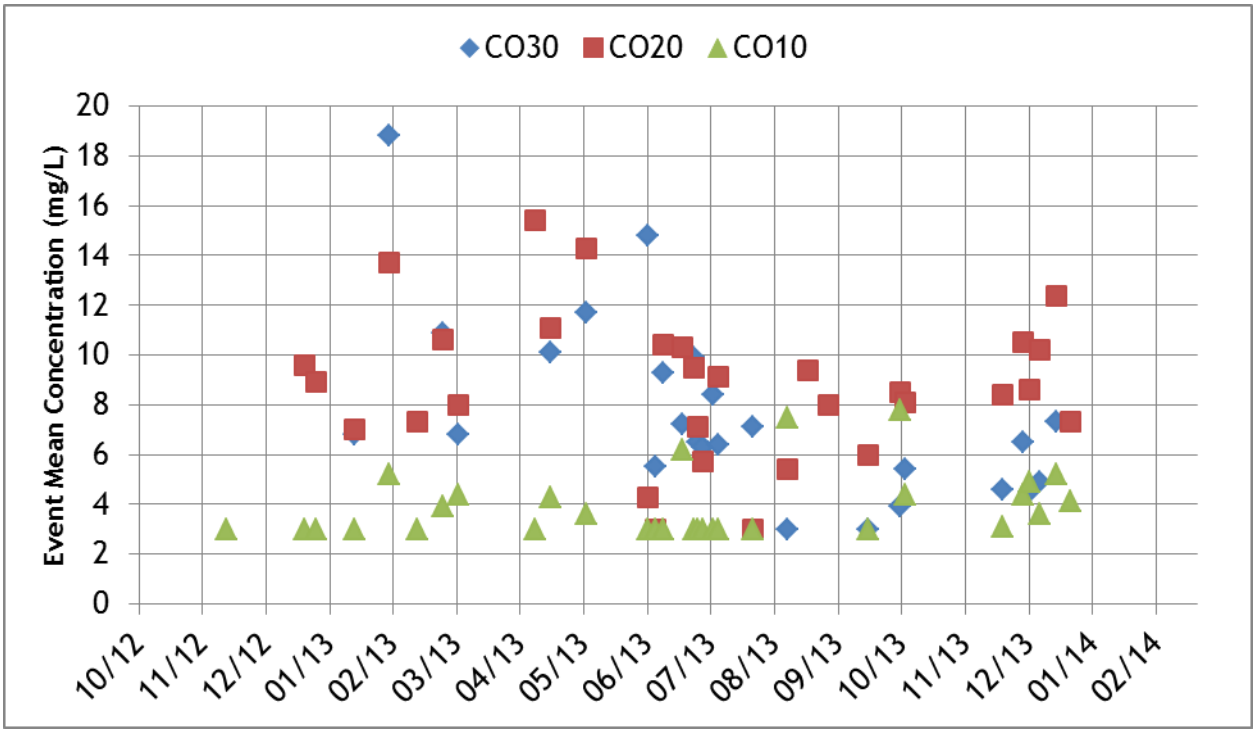

Figure C-35. Time series plot of station event mean concentrations for total copper.

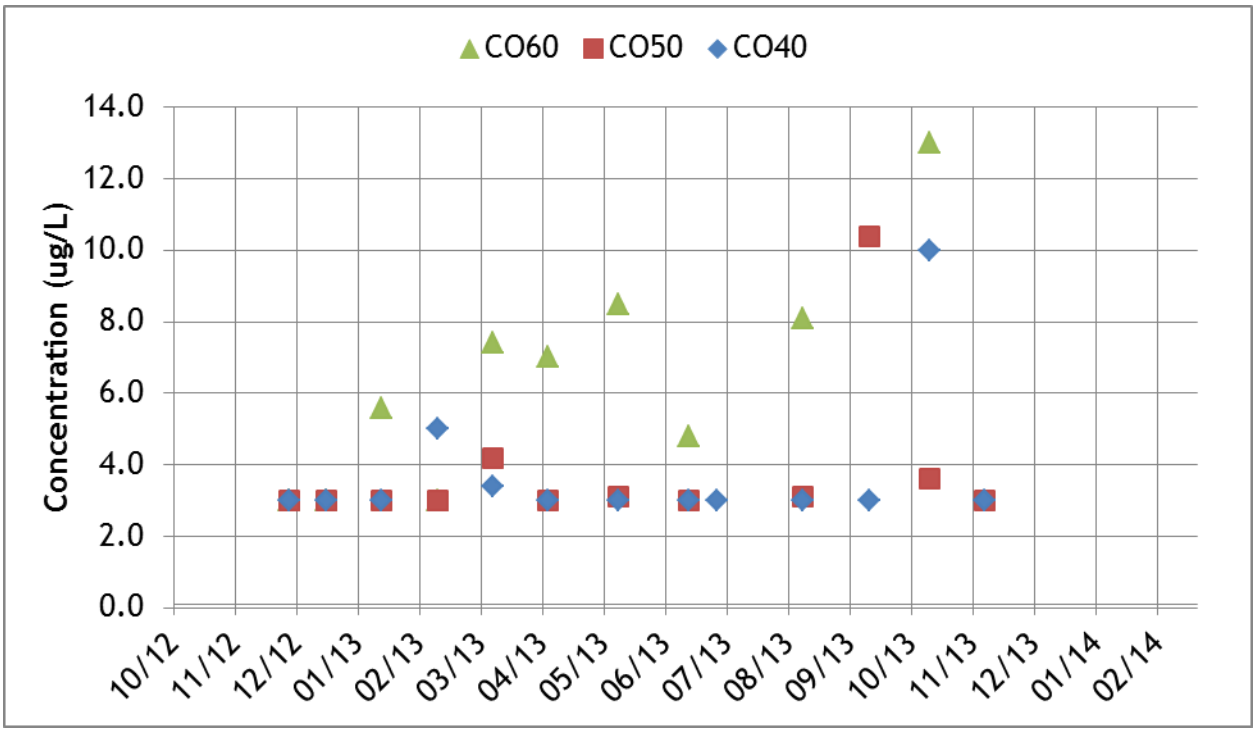

Figure C-36. Time series plot of micropool grab samples for total copper.

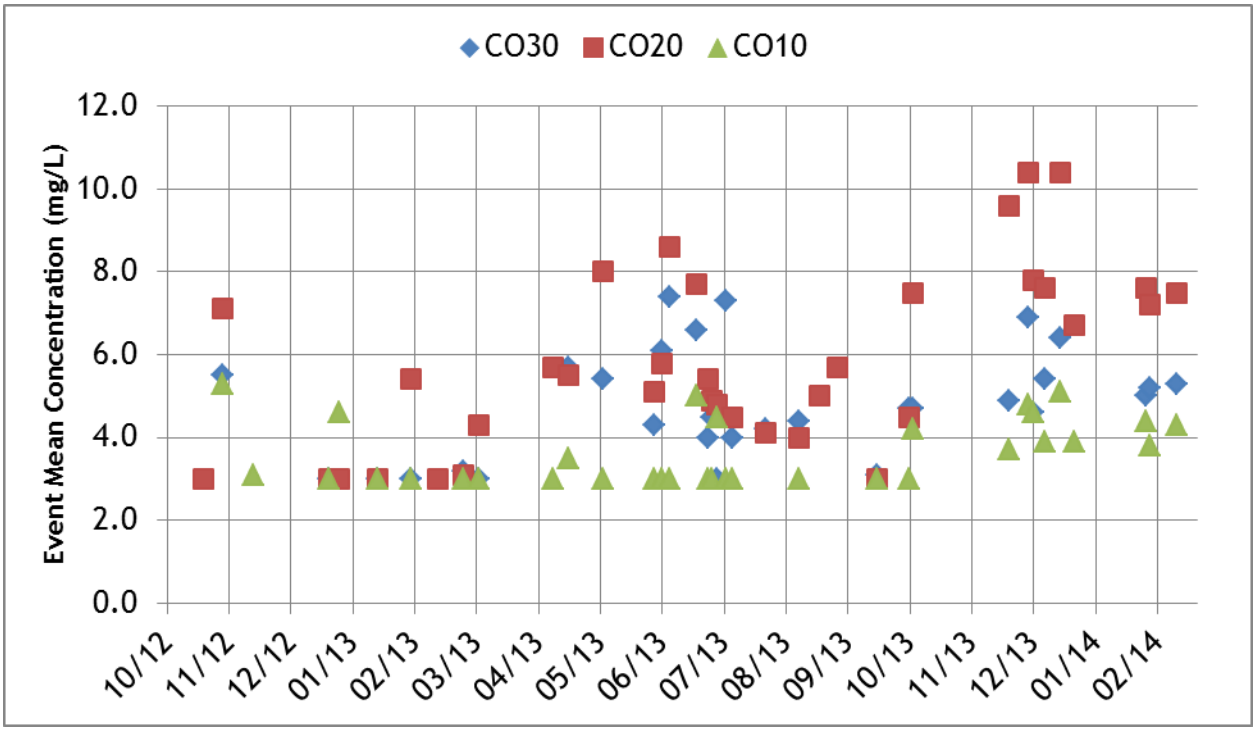

Figure C-37. Time series plot of station event mean concentrations for soluble copper.

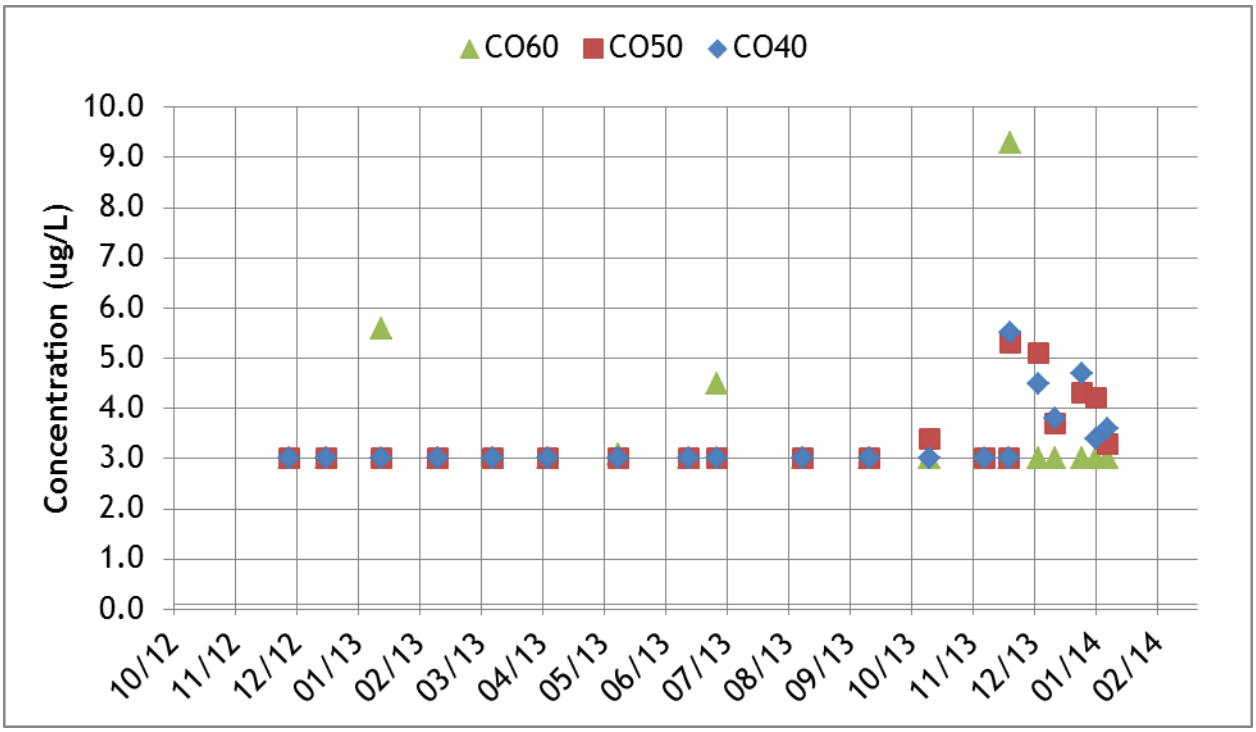

Figure C-38. Time series plot of micropool grab samples for soluble copper.

APPENDIX D Effluent Probability Plots

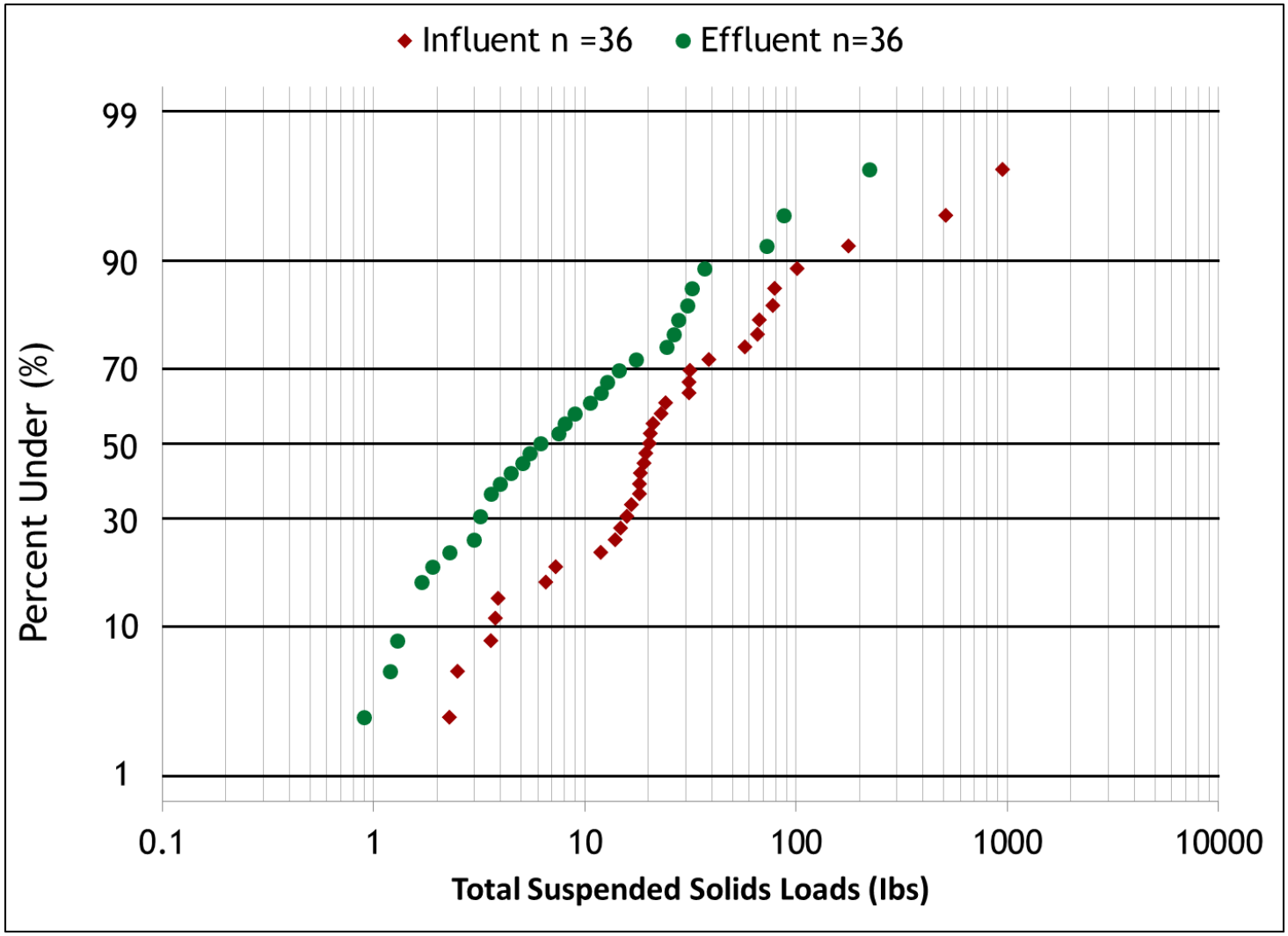

Figure D-1. Effluent Probability Method plot for influent and effluent loads for total suspended solids.

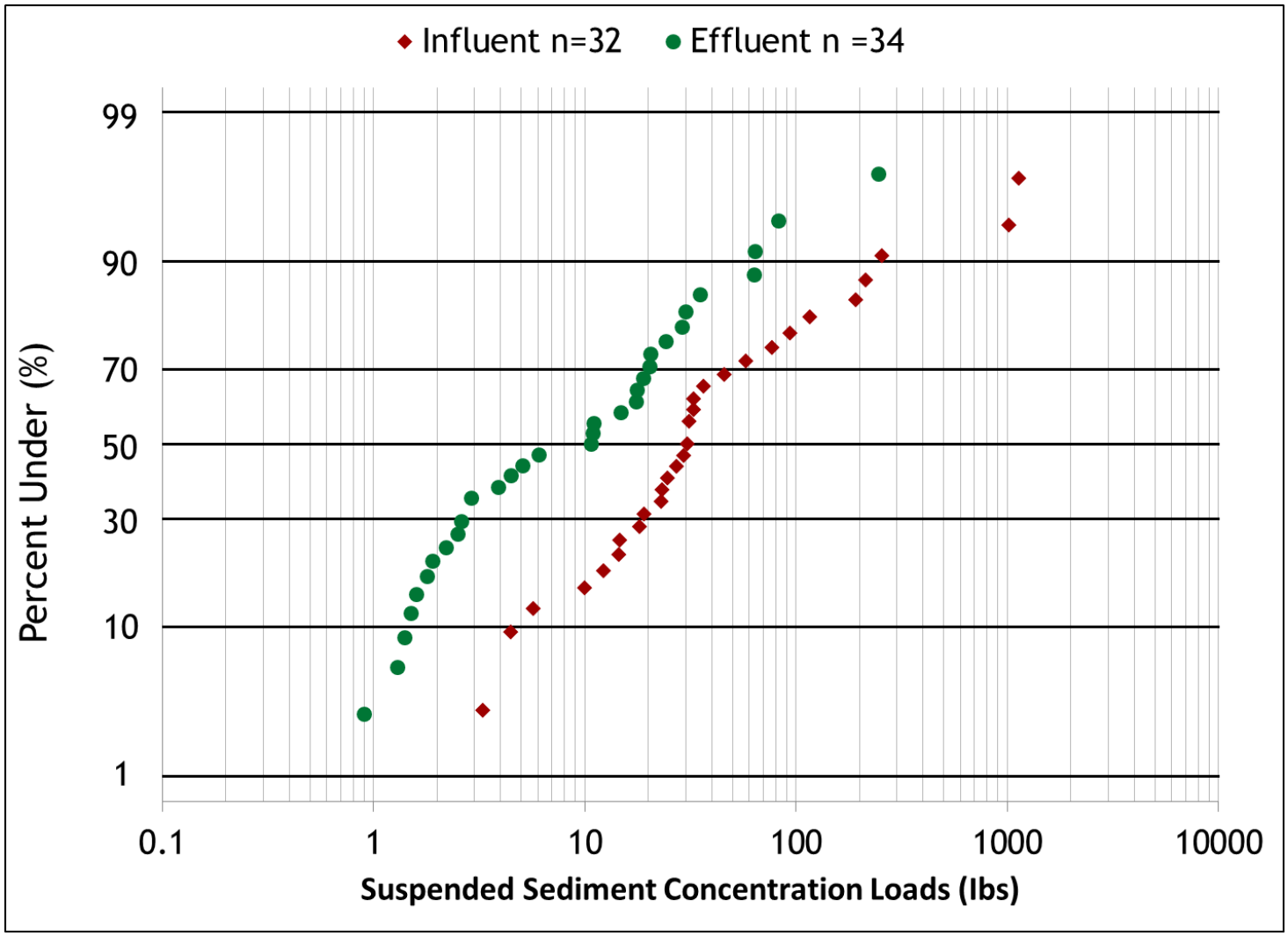

Figure D-2. Effluent Probability Method plot of influent and effluent loads for suspended sediment concentration.

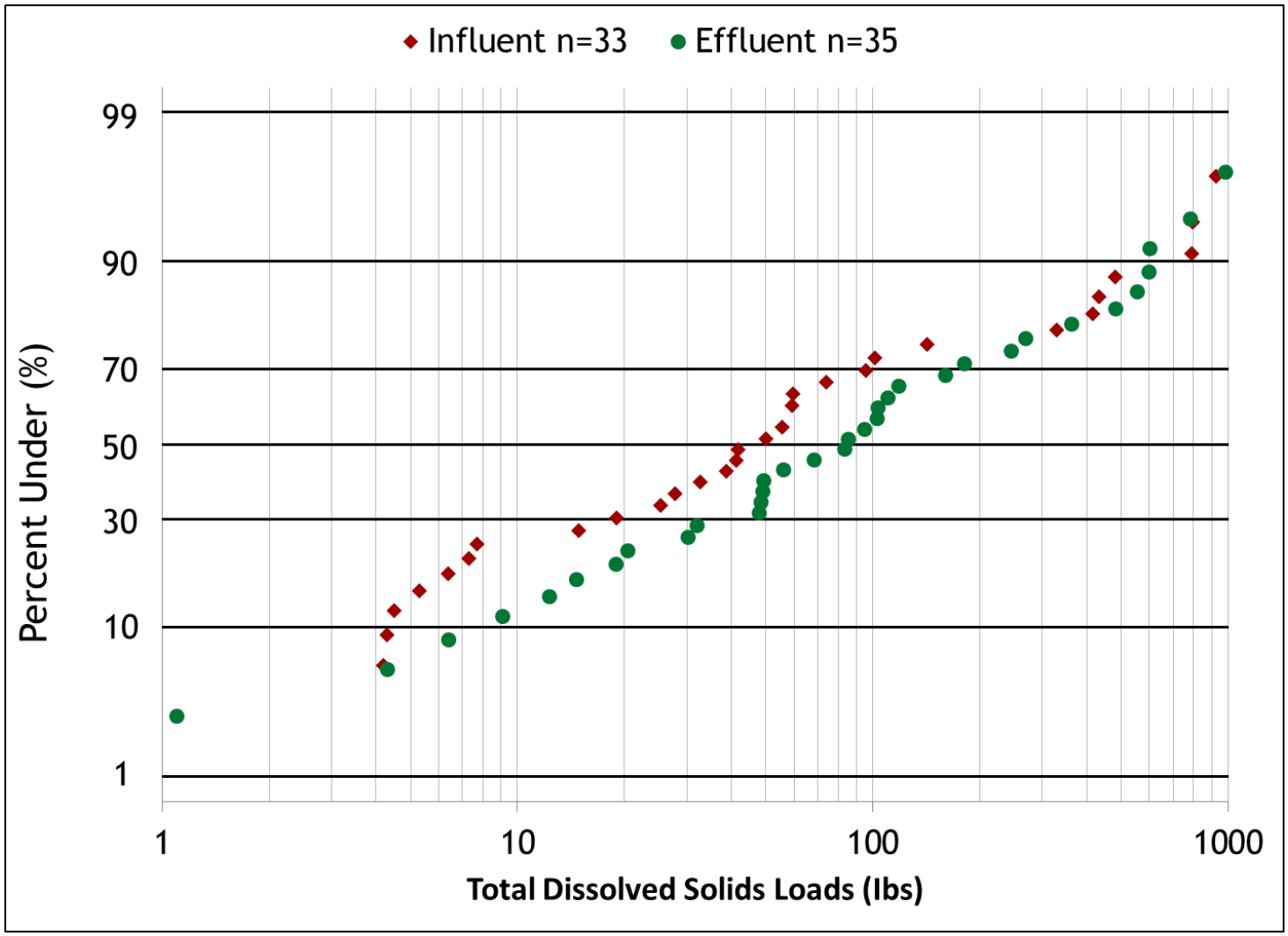

Figure D-3. Effluent Probability Method plot of influent and effluent loads for total dissolved solids.

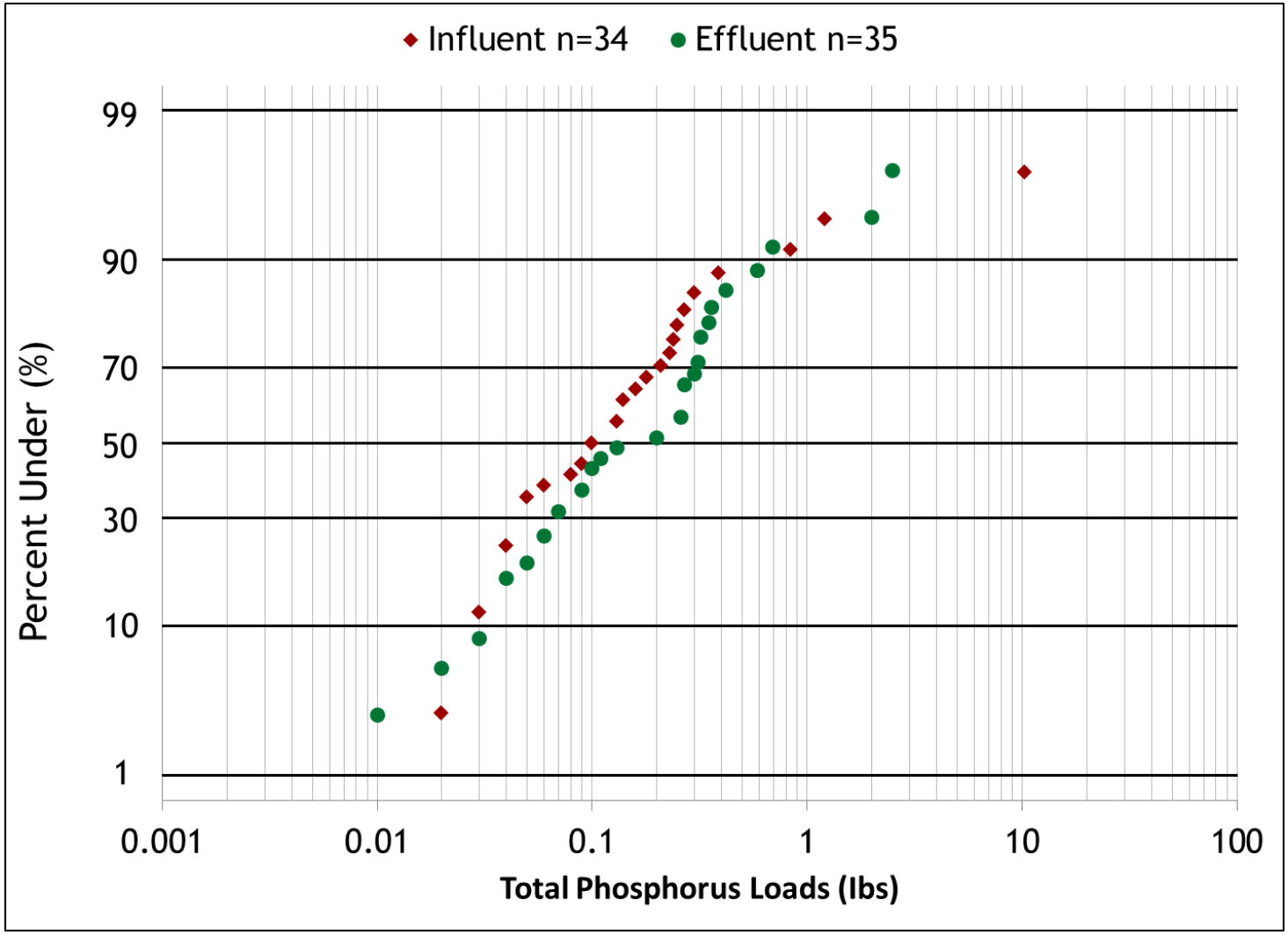

Figure D-4. Effluent Probability Method plot of influent and effluent loads for total phosphorus

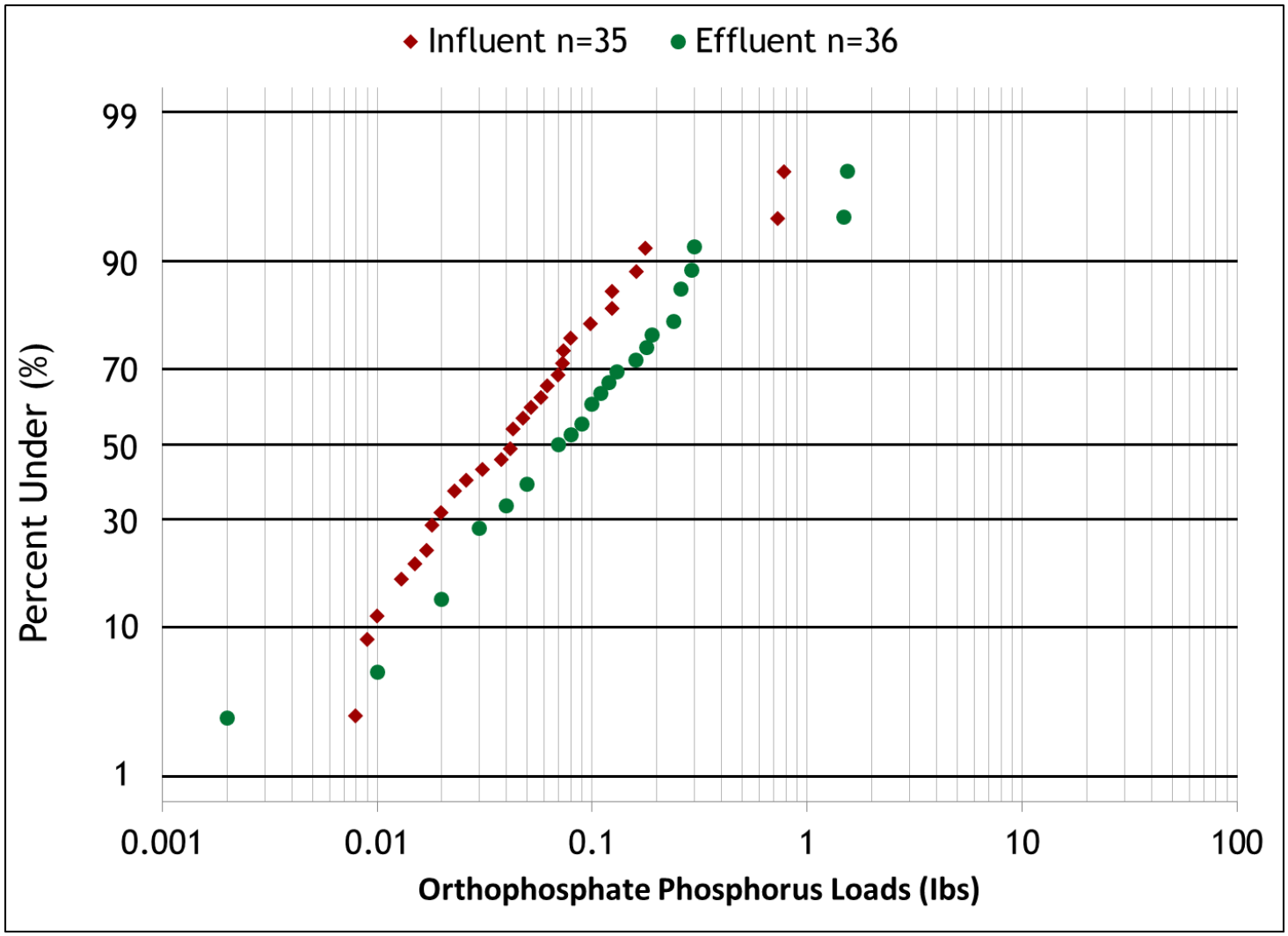

Figure D-5. Effluent Probability Method plot of influent and effluent loads for orthophosphate phosphorus.

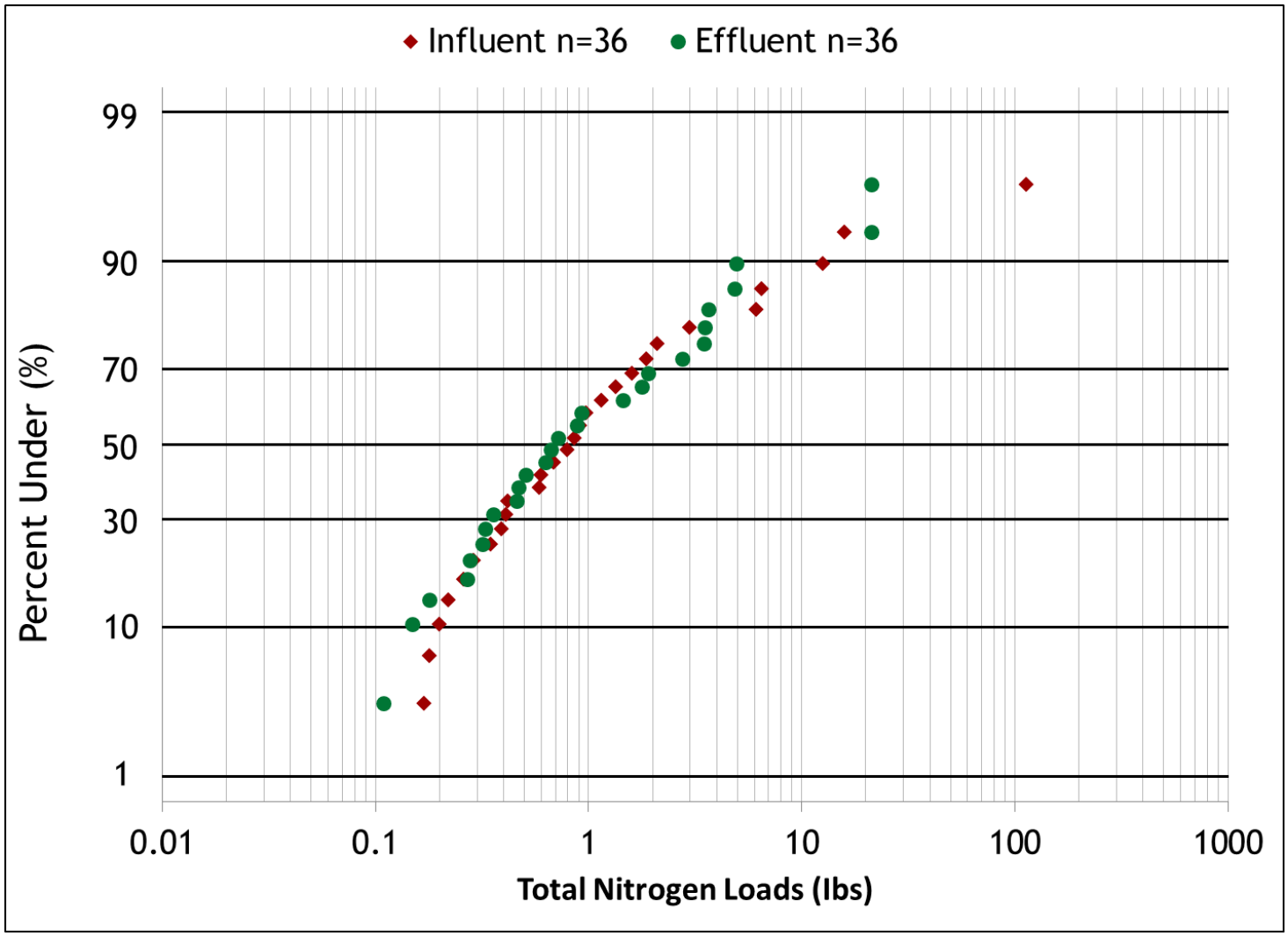

Figure D-6. Effluent Probability Method plot of influent and effluent loads for total nitrogen.

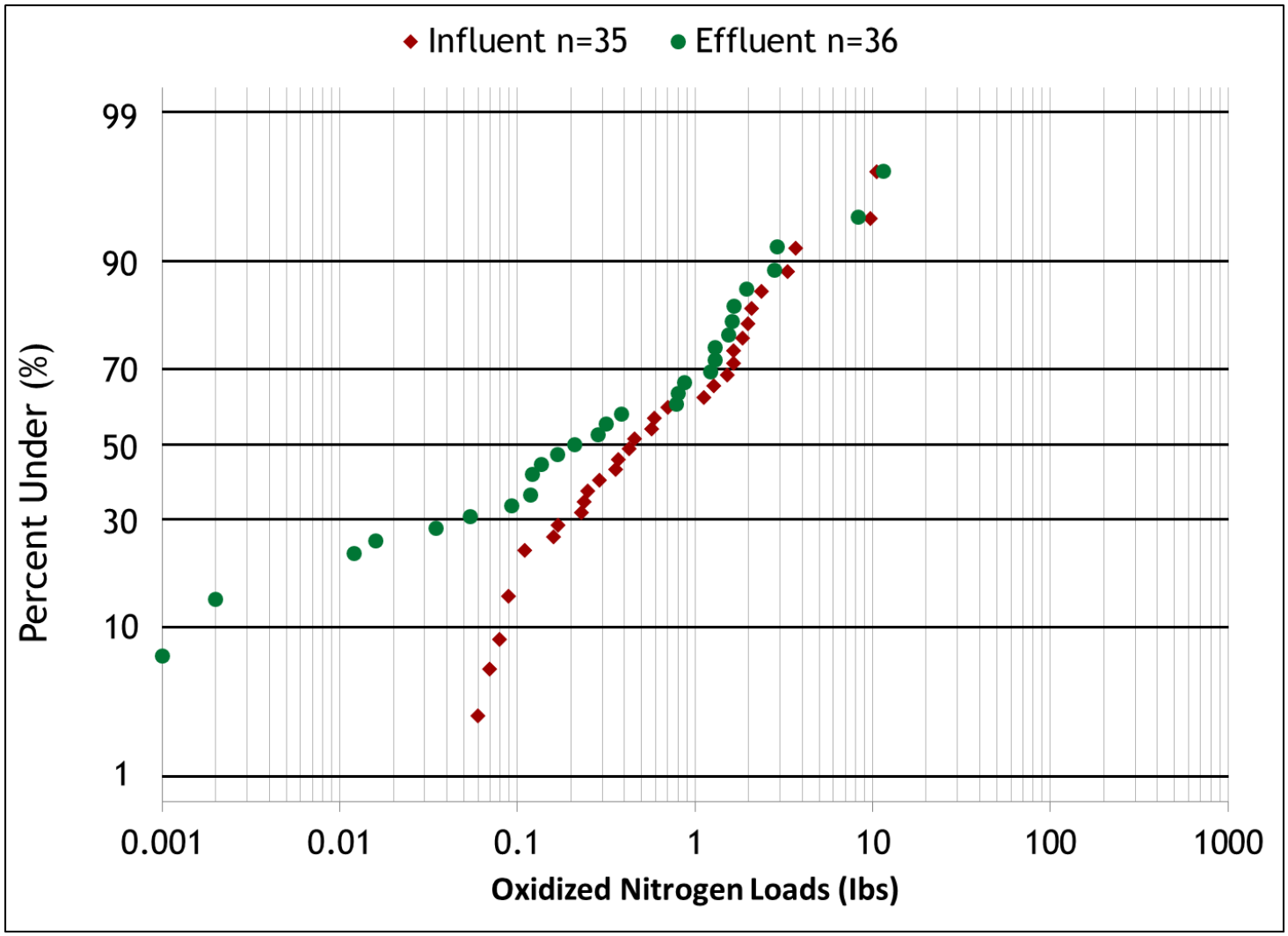

Figure D-7. Effluent Probability Method plot of influent and effluent loads for oxidized nitrogen.

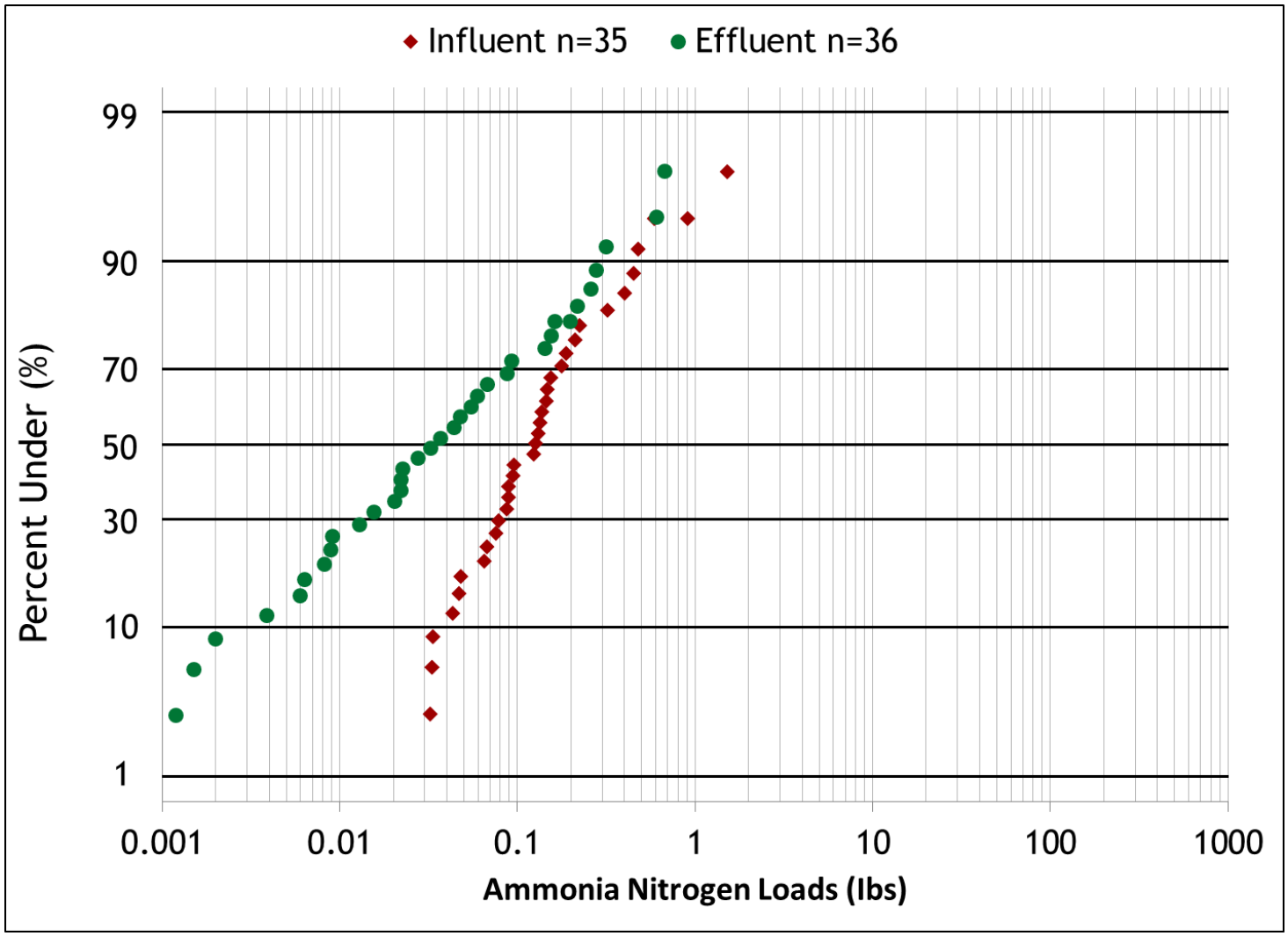

Figure D-8. Effluent Probability Method plot of influent and effluent loads for ammonia nitrogen.

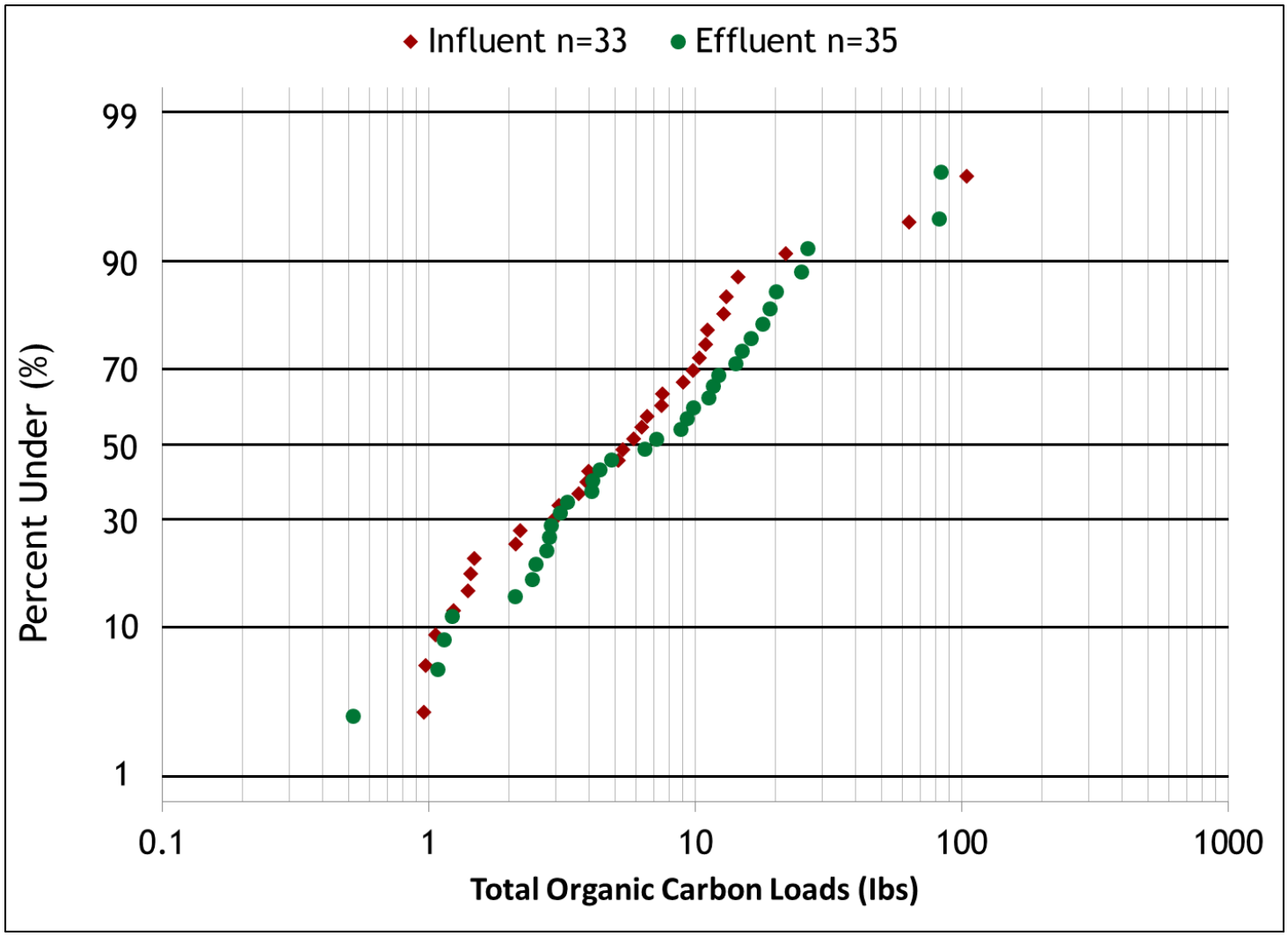

Figure D-9. Effluent Probability Method plot of influent and effluent loads for total organic carbon.

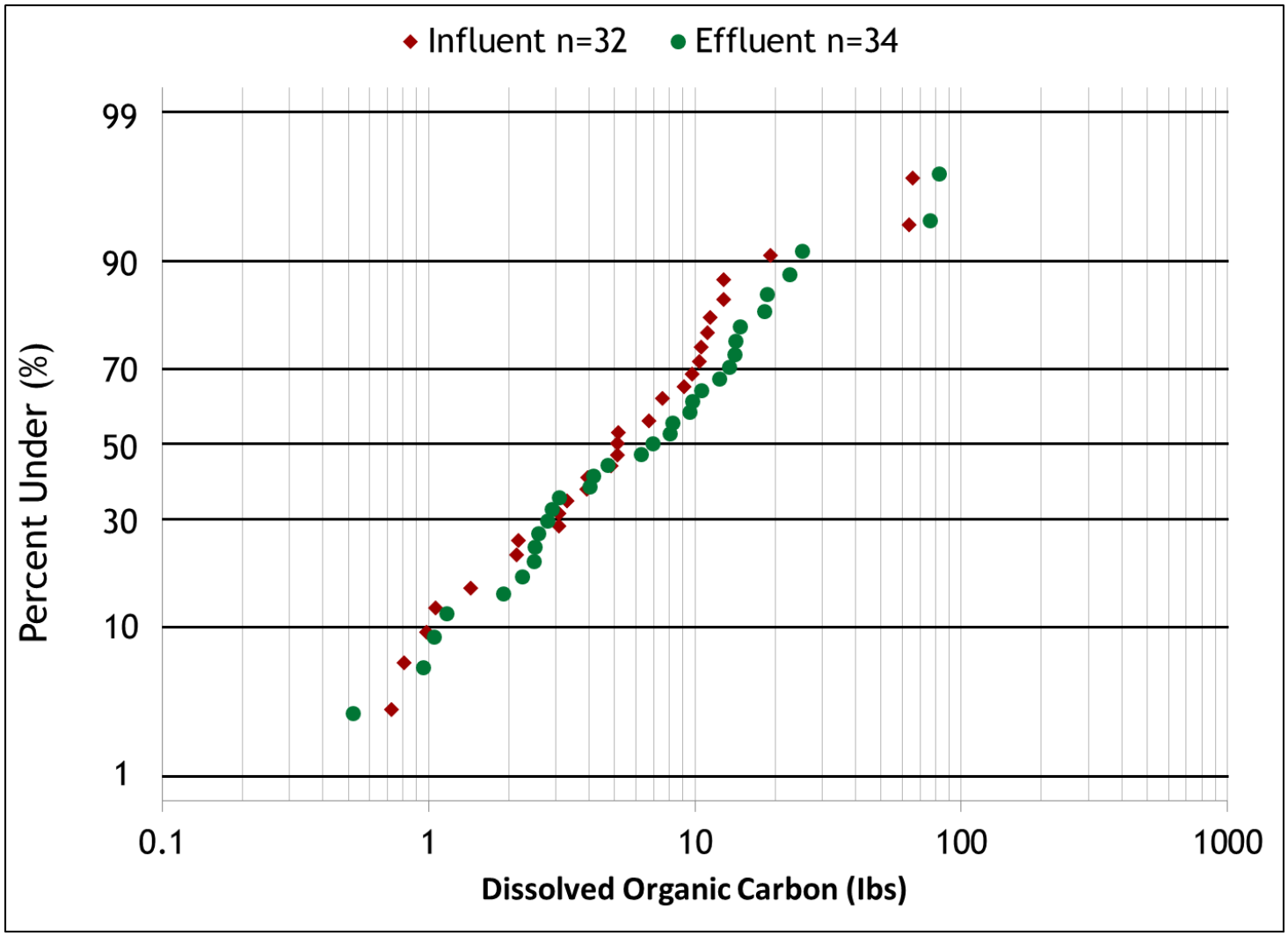

Figure D-10. Effluent Probability Method plot of influent and effluent loads for dissolved organic carbon.

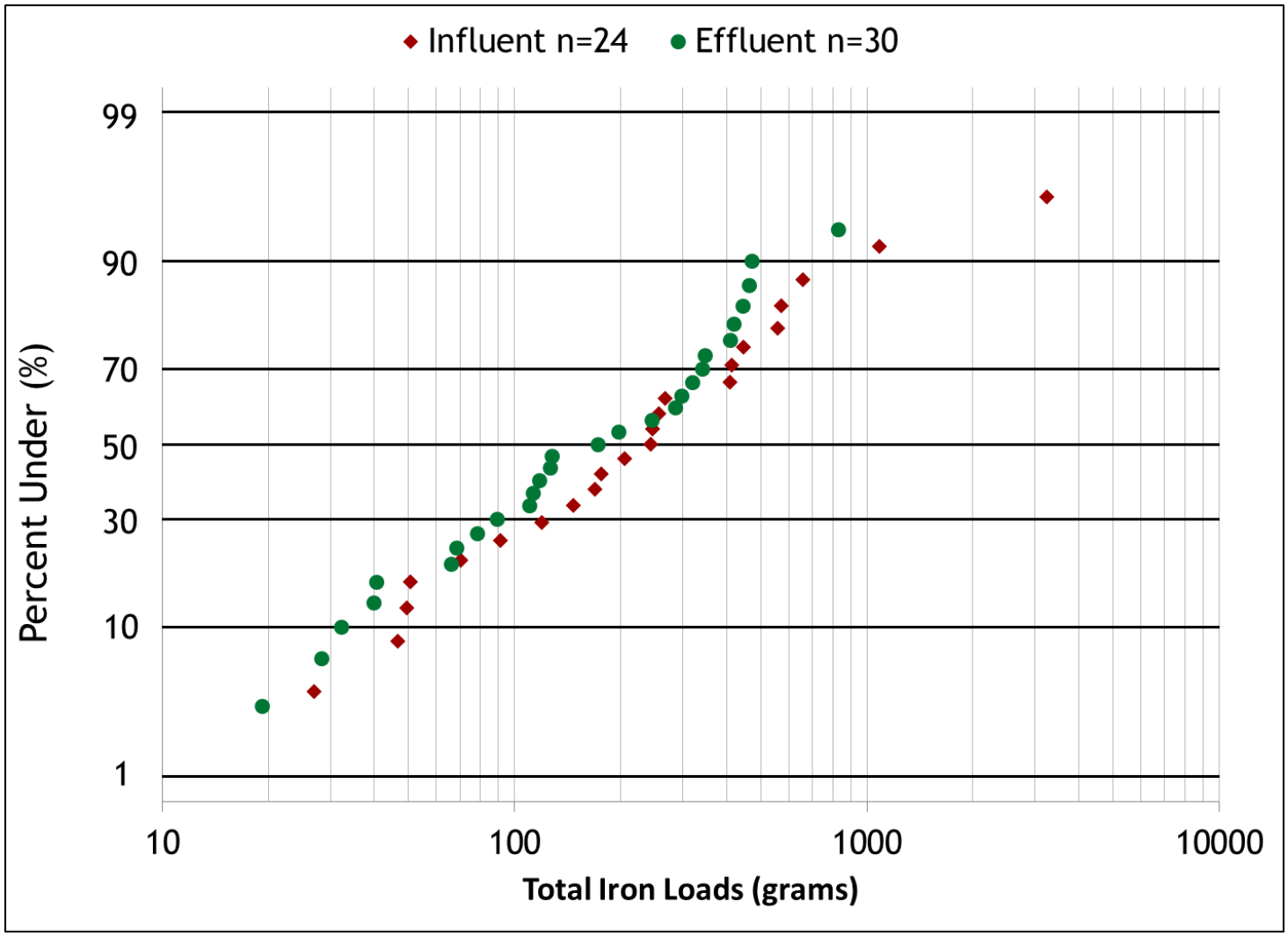

Figure D-11. Effluent Probability Method plot of influent and effluent loads for total iron.

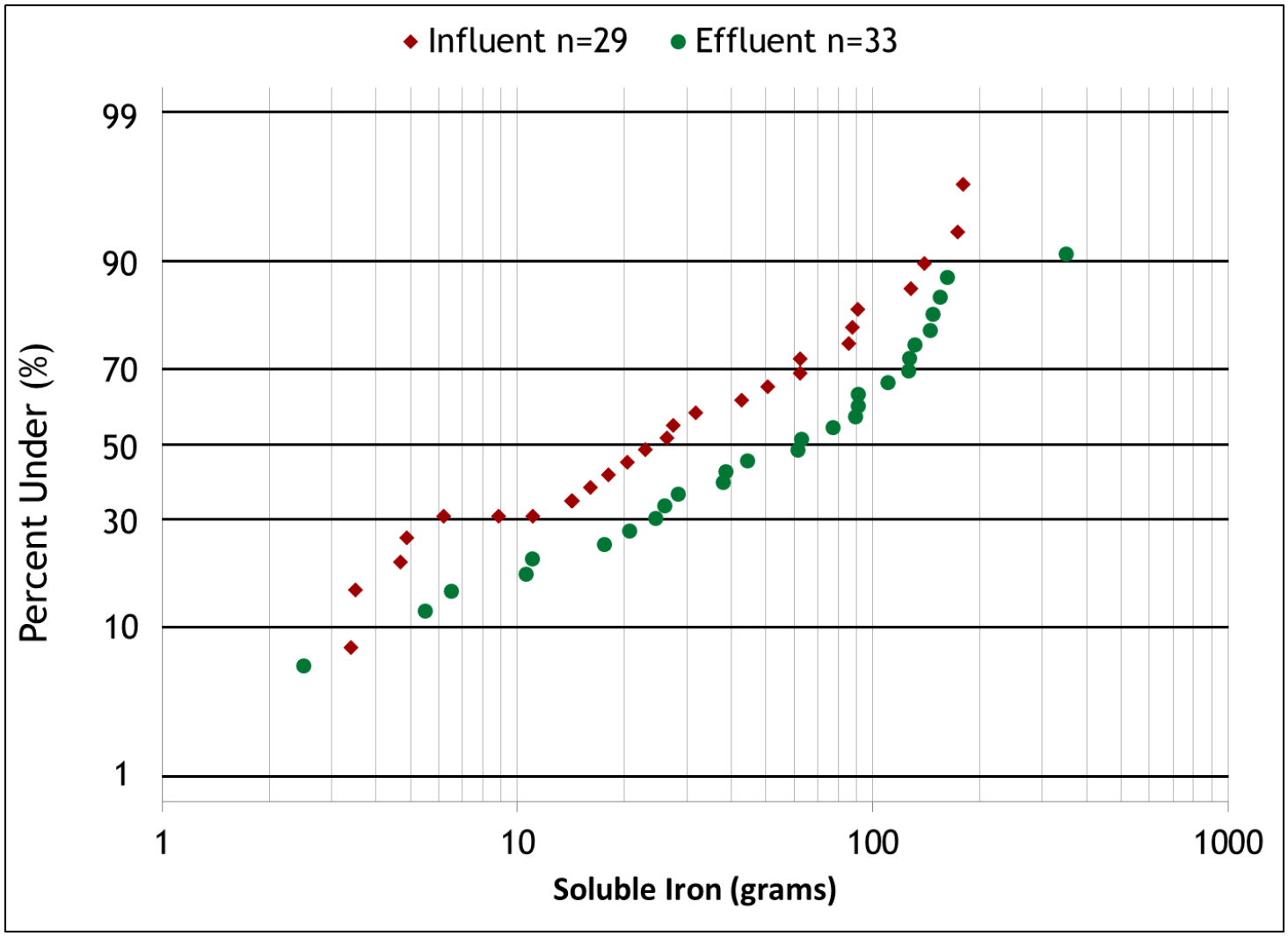

Figure D-12. Effluent Probability Method plot of influent and effluent loads for soluble iron.

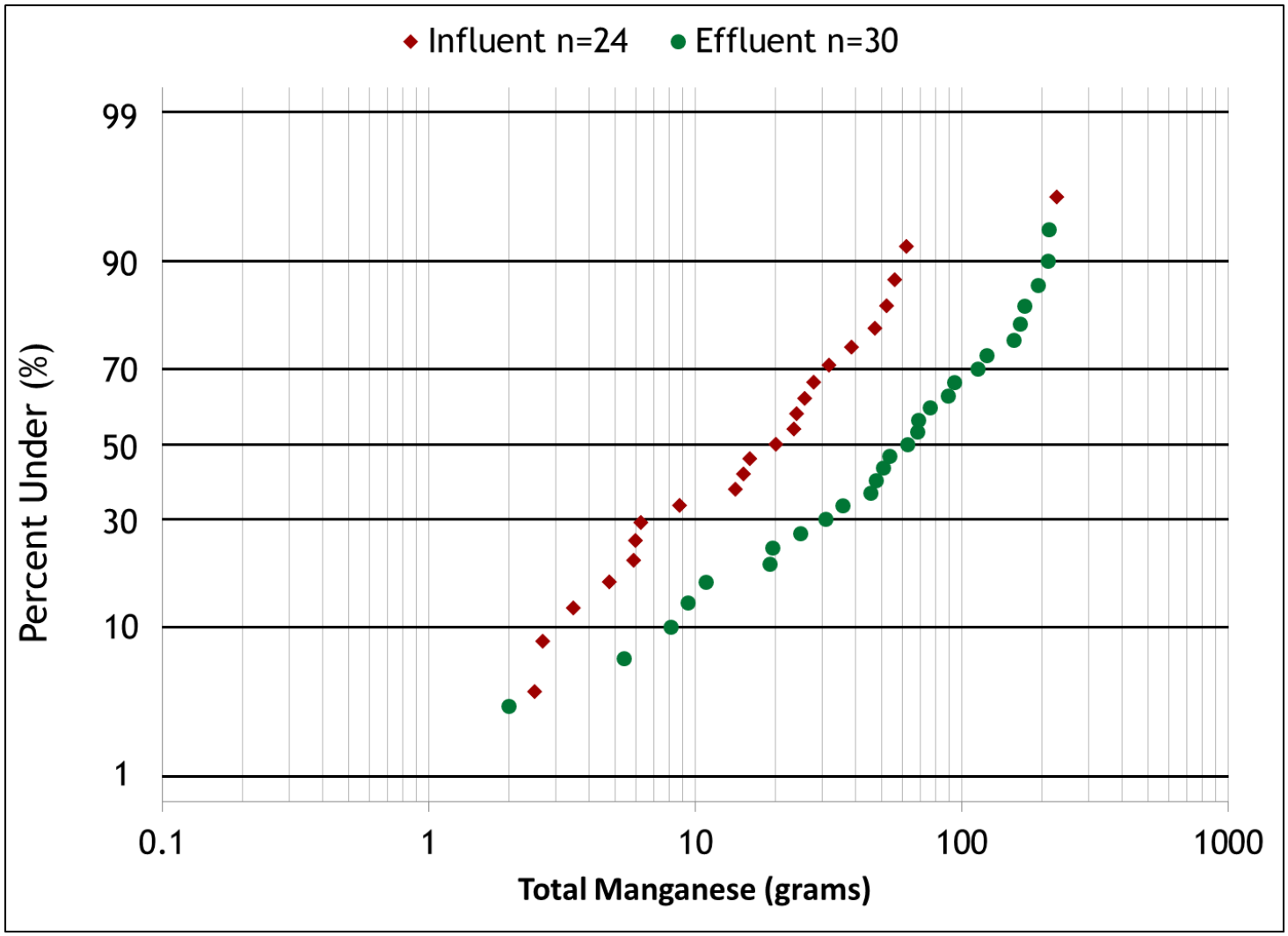

Figure D-13. Effluent Probability Method plot of influent and effluent loads for total manganese.

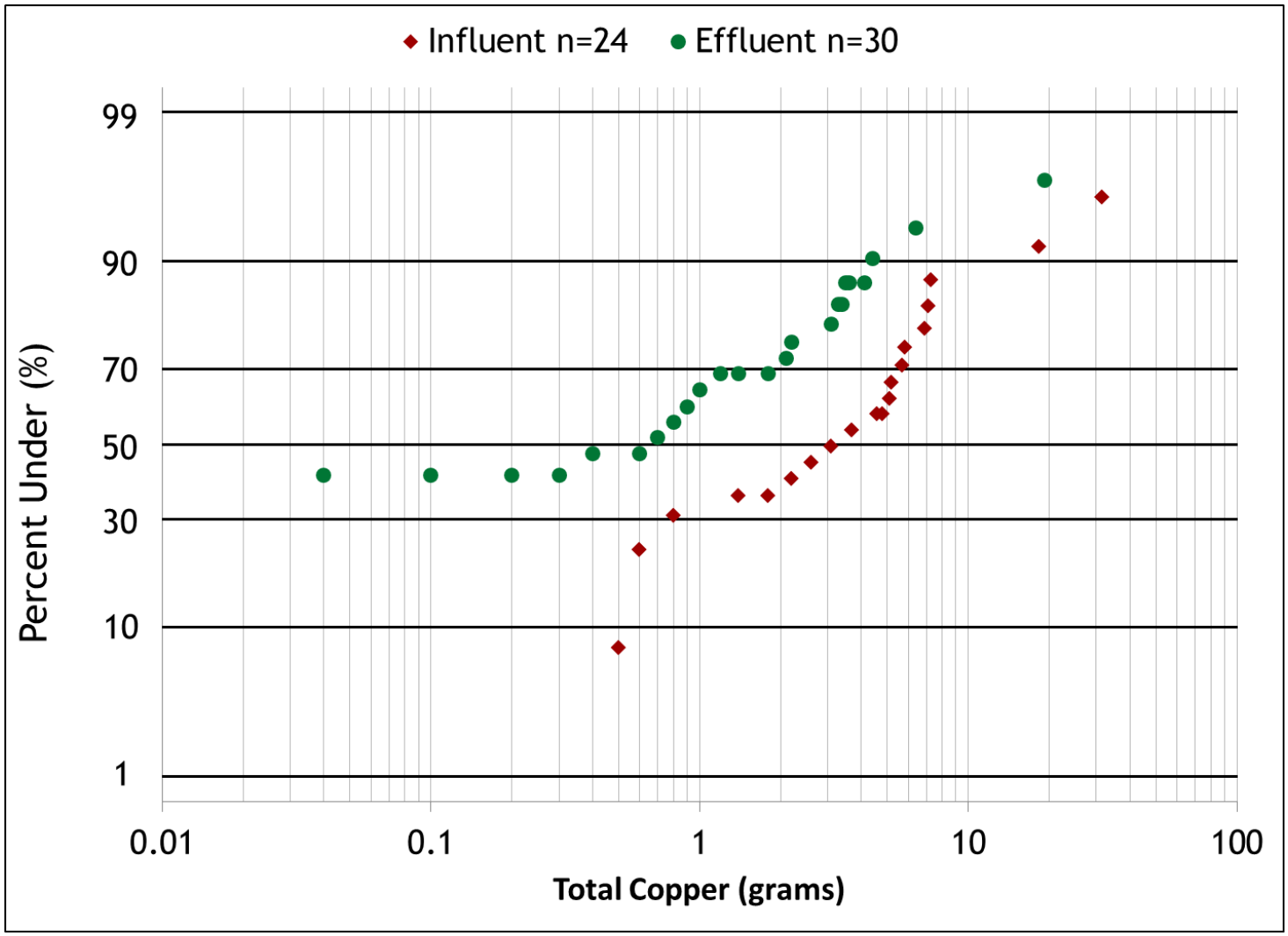

Figure D-14. Effluent Probability Method plot of influent and effluent loads for total copper.

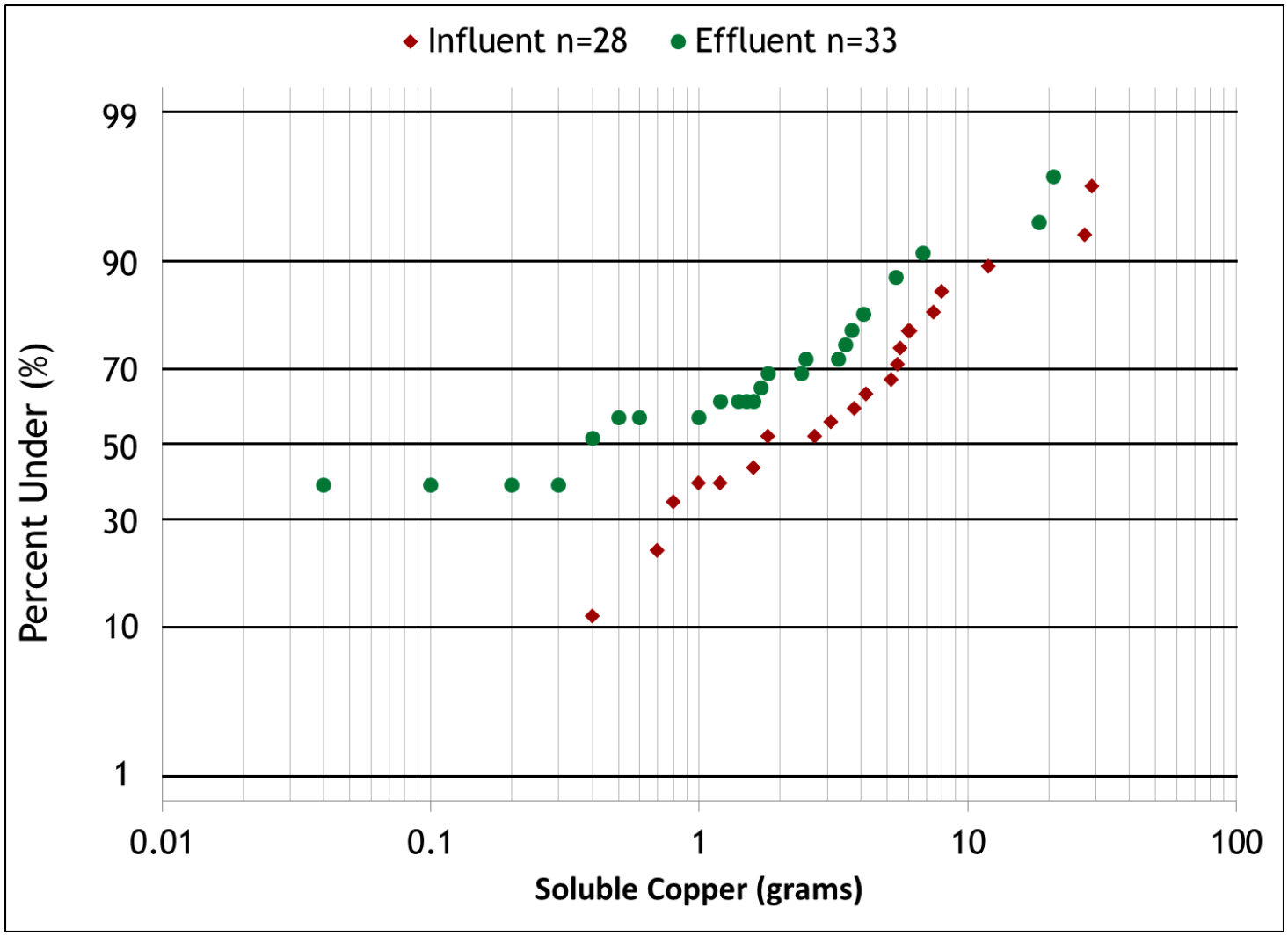

Figure D-15. Effluent Probability Method plot of influent and effluent loads for soluble copper.

APPENDIX E Q-Q Plots

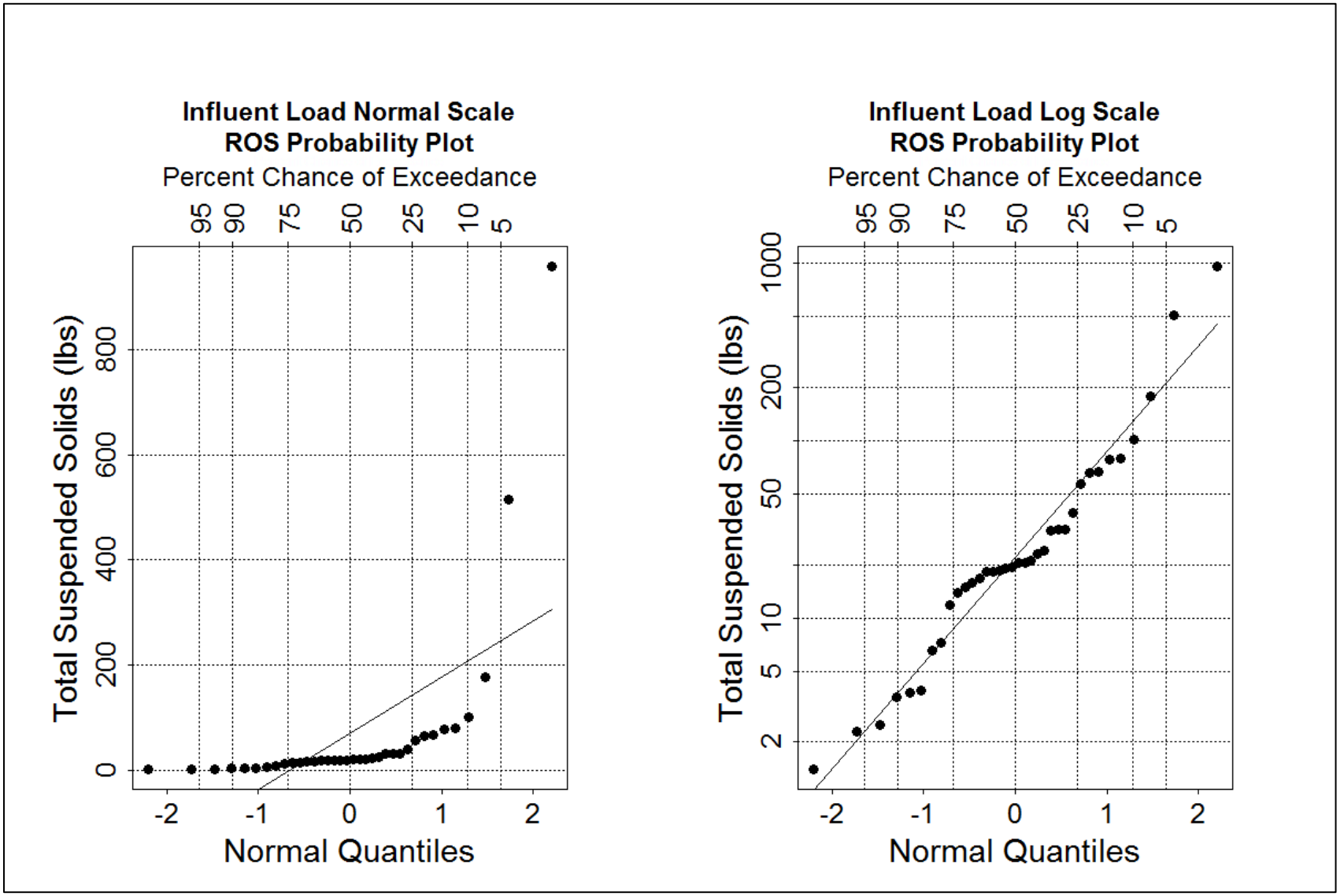

Figure E-1. Q-Q plots of influent loads for total suspended solids.

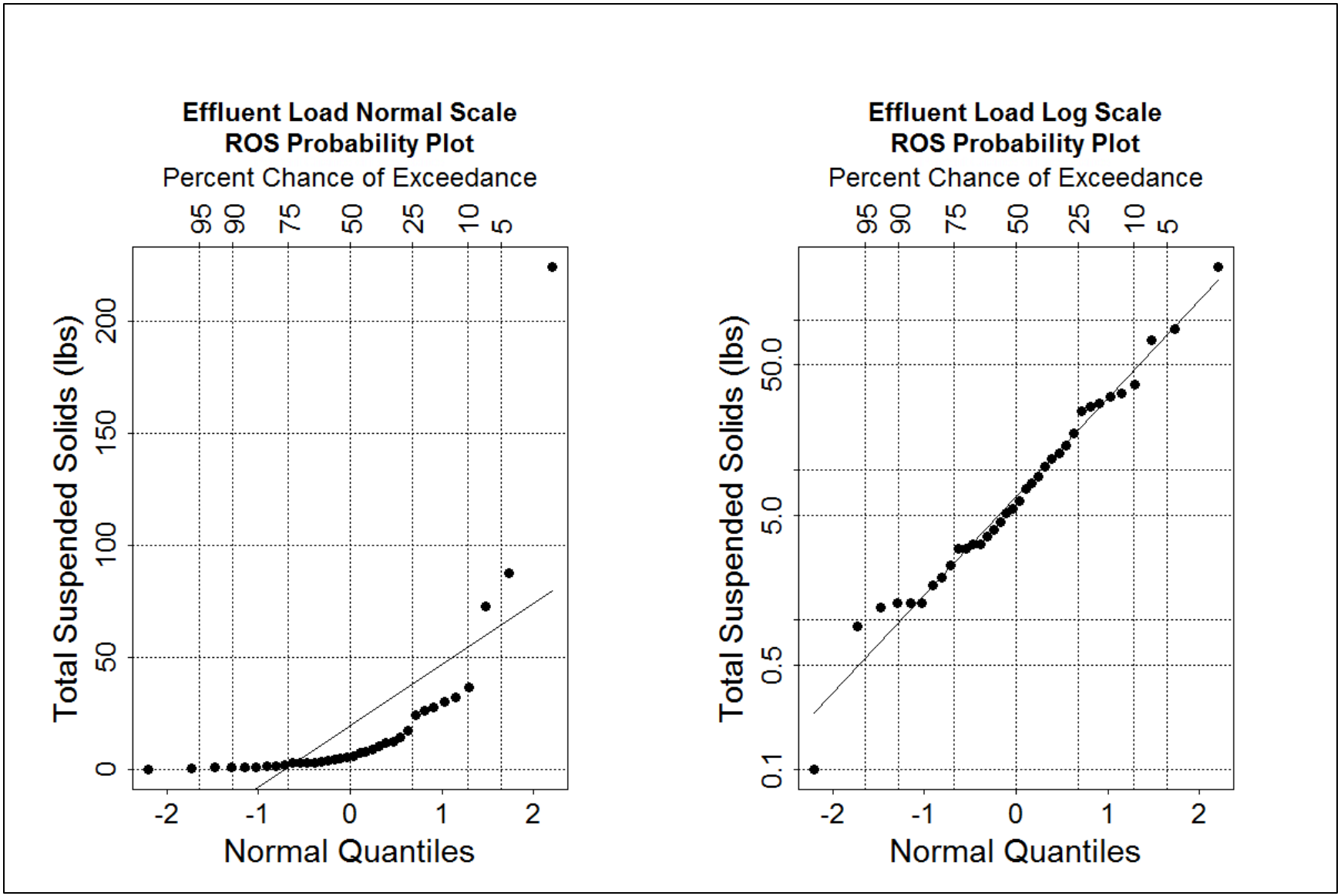

Figure E-2. Q-Q plots of effluent loads for total suspended solids.

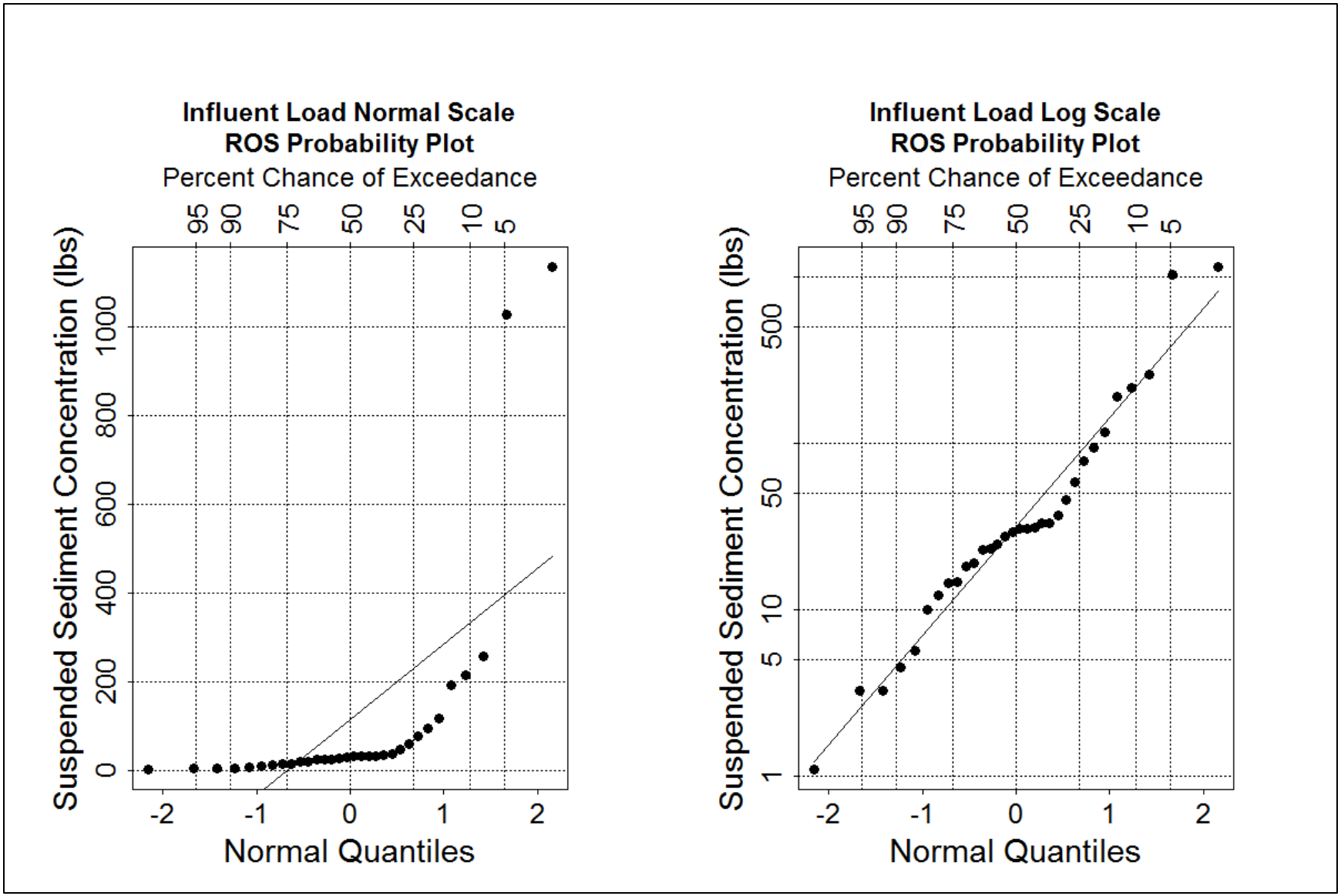

Figure E-3. Q-Q plots of influent loads for suspended sediment concentration.

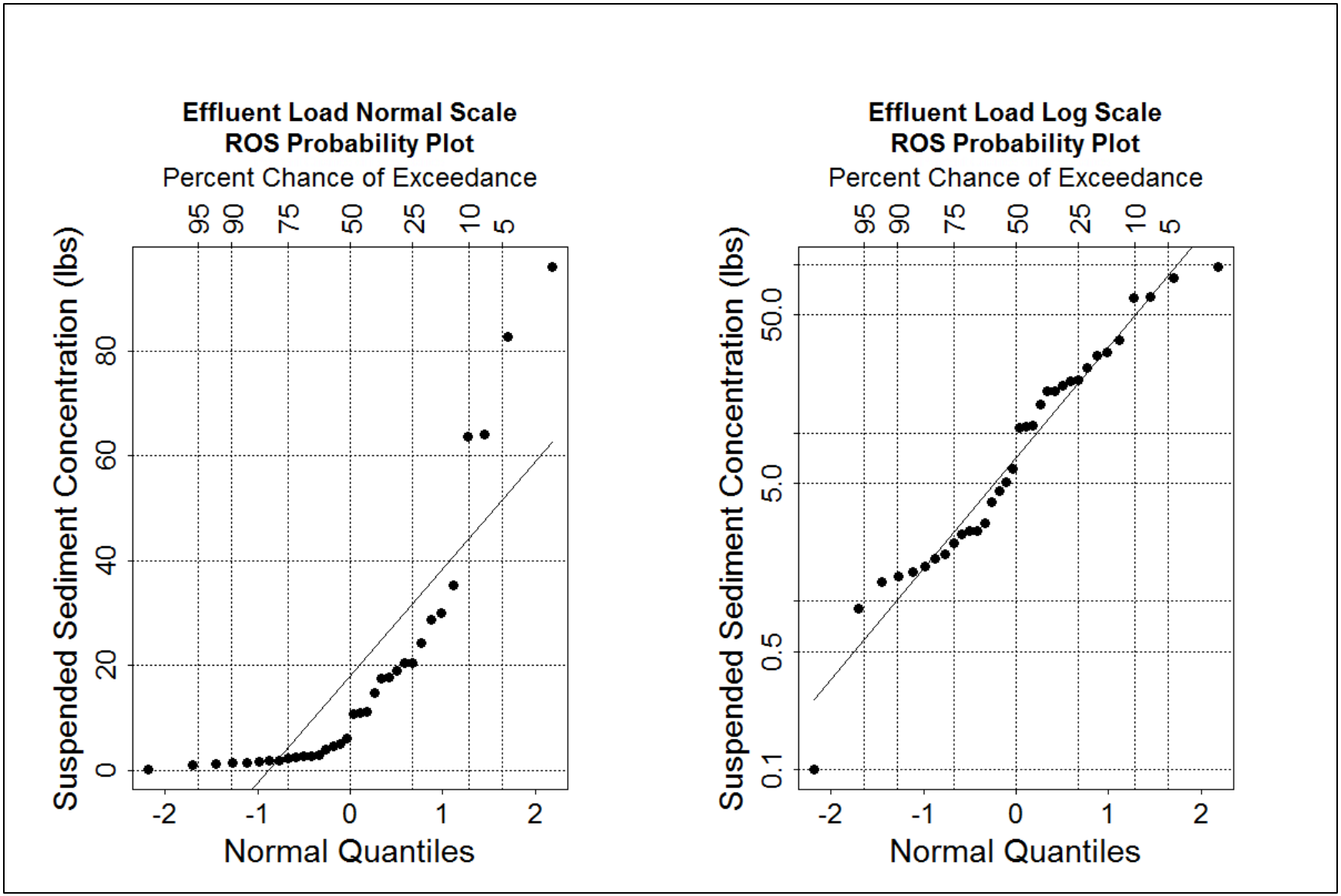

Figure E-4. Q-Q plots of effluent loads for suspended sediment concentration.

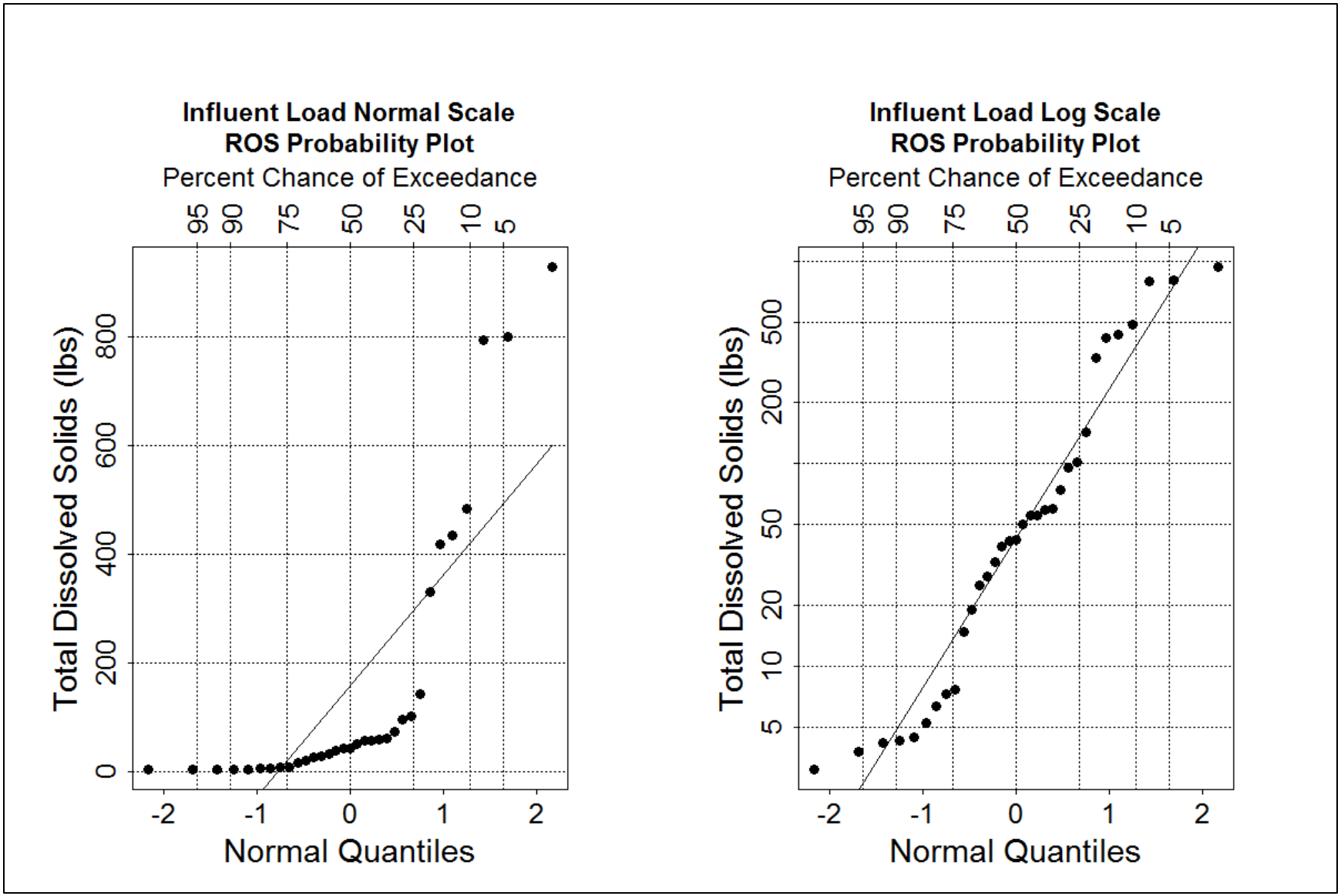

Figure E-5. Q-Q plots of influent loads for total dissolved solids.

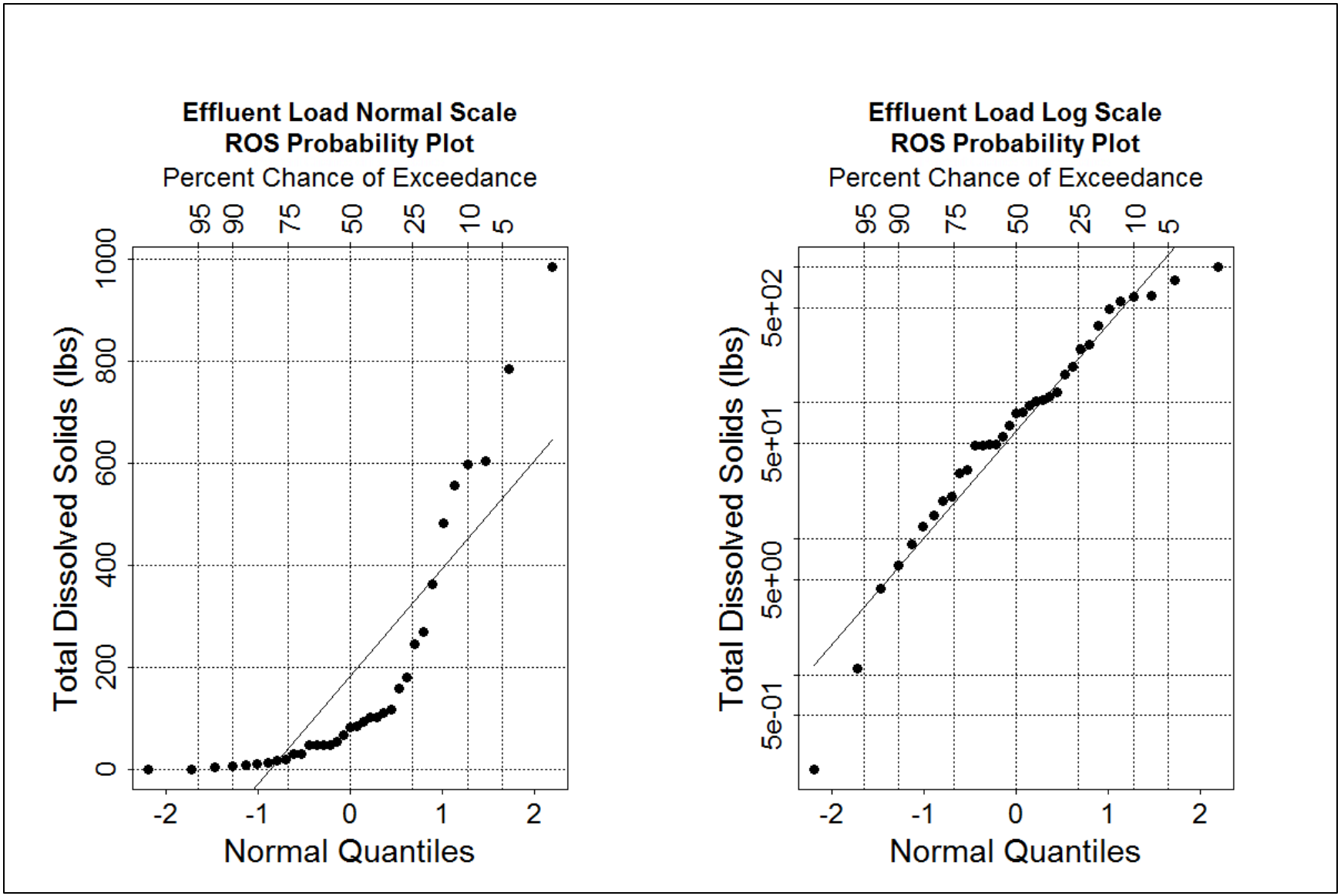

Figure E-6. Q-Q plots of effluent loads for total dissolved solids.

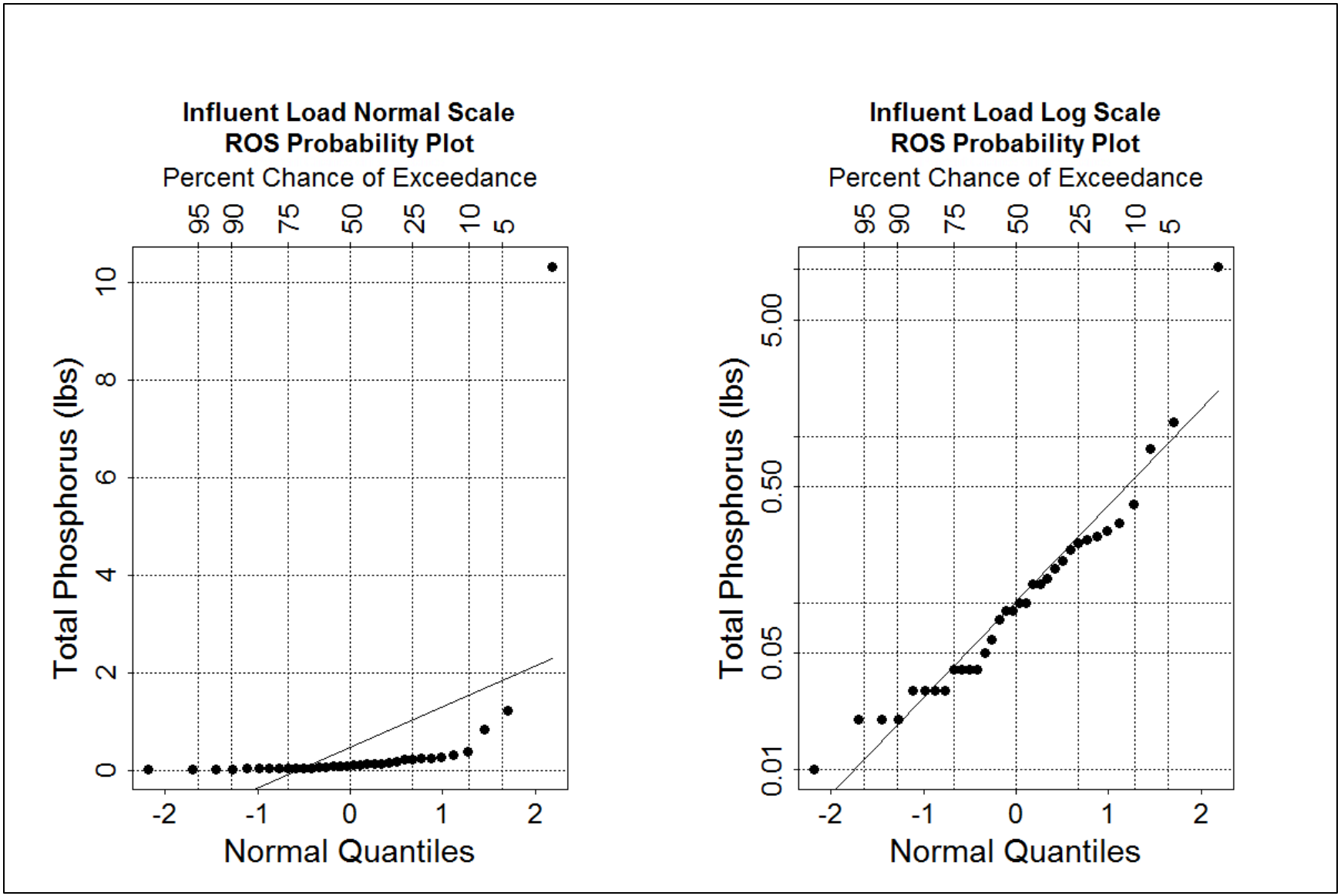

Figure E-7. Q-Q plots of influent loads for total phosphorus.

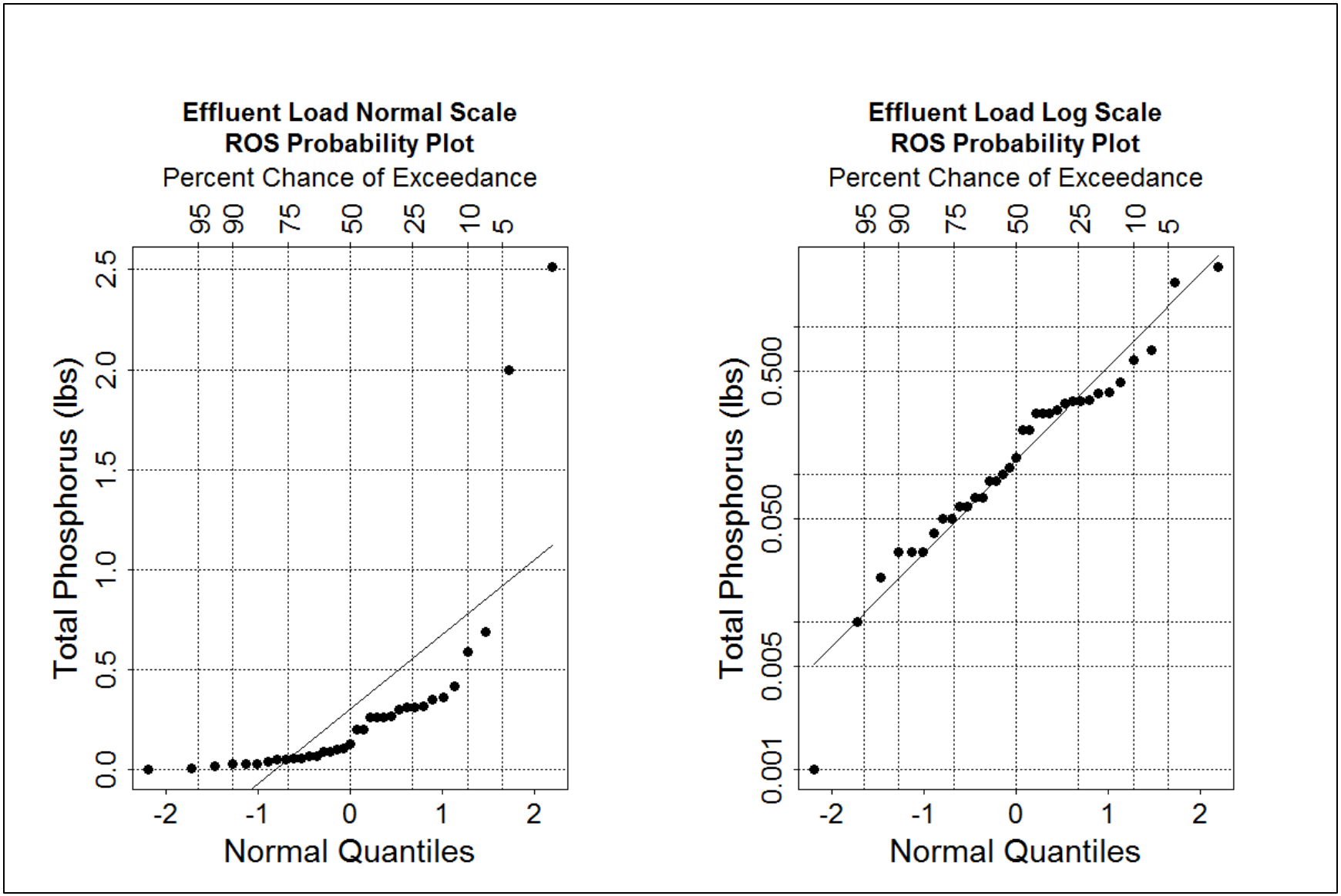

Figure E-8. Q-Q plots of effluent loads for total phosphorus.

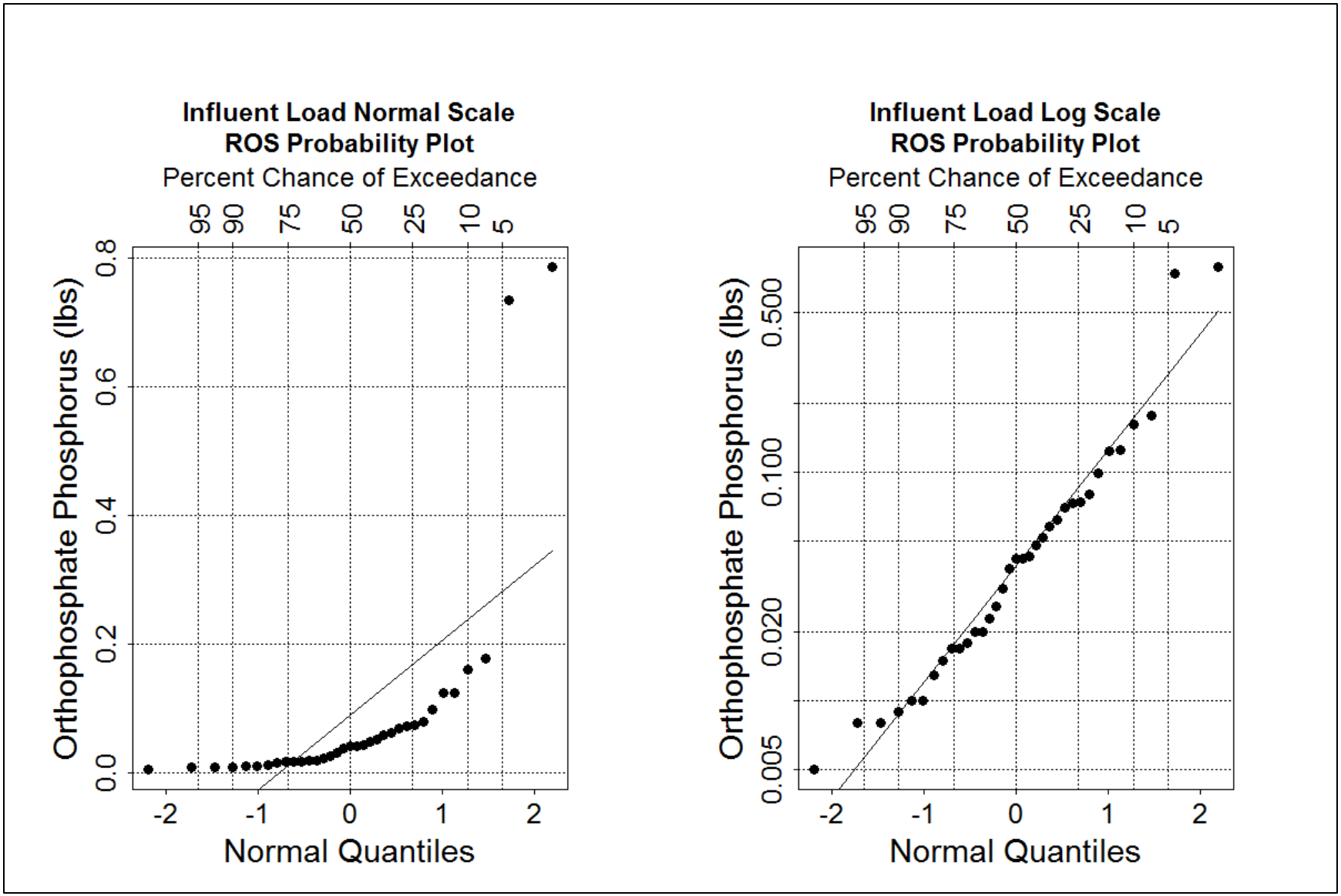

Figure E-9. Q-Q plots of influent loads for orthophosphate phosphorus.

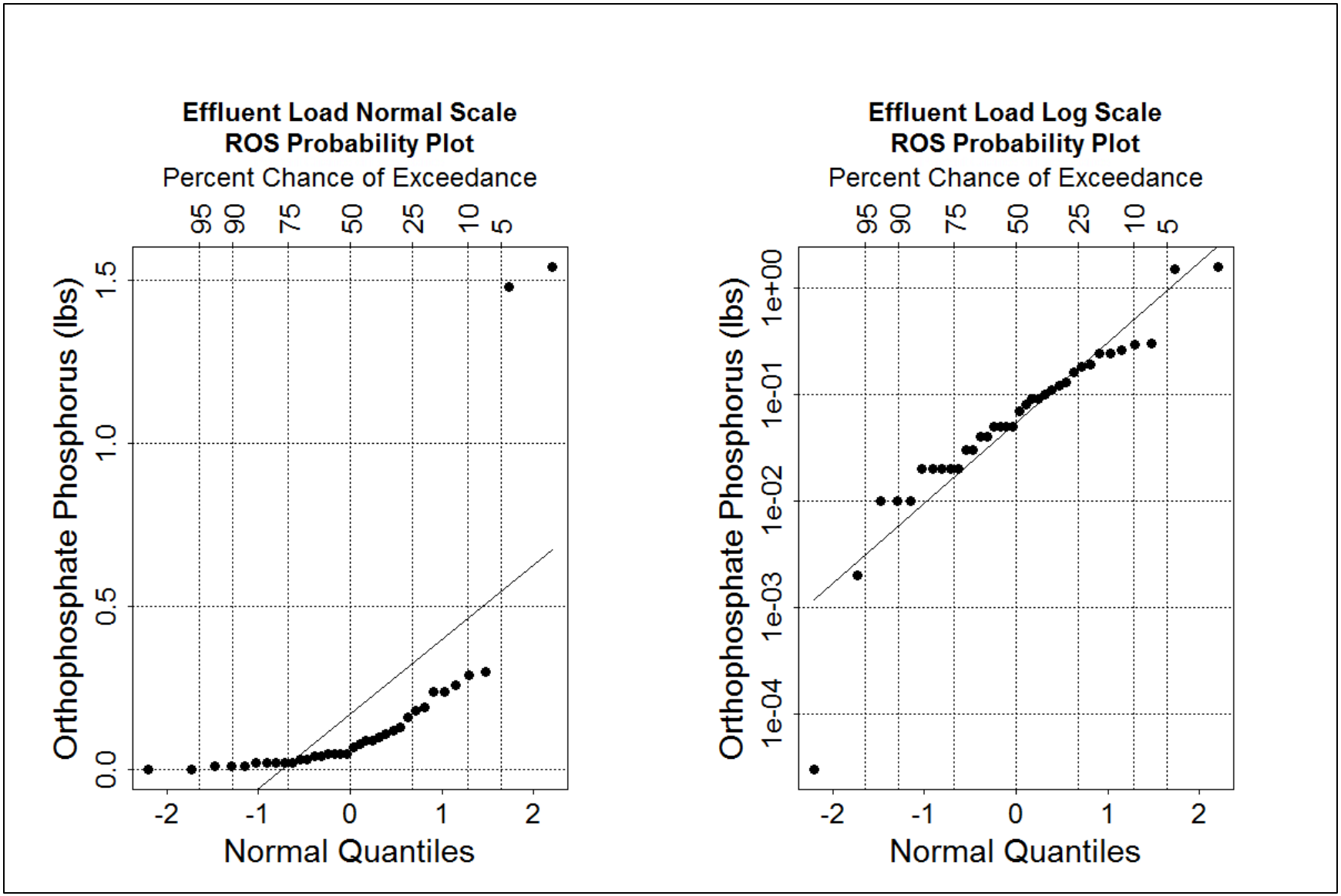

Figure E-10. Q-Q plots of effluent loads for orthophosphate phosphorus.

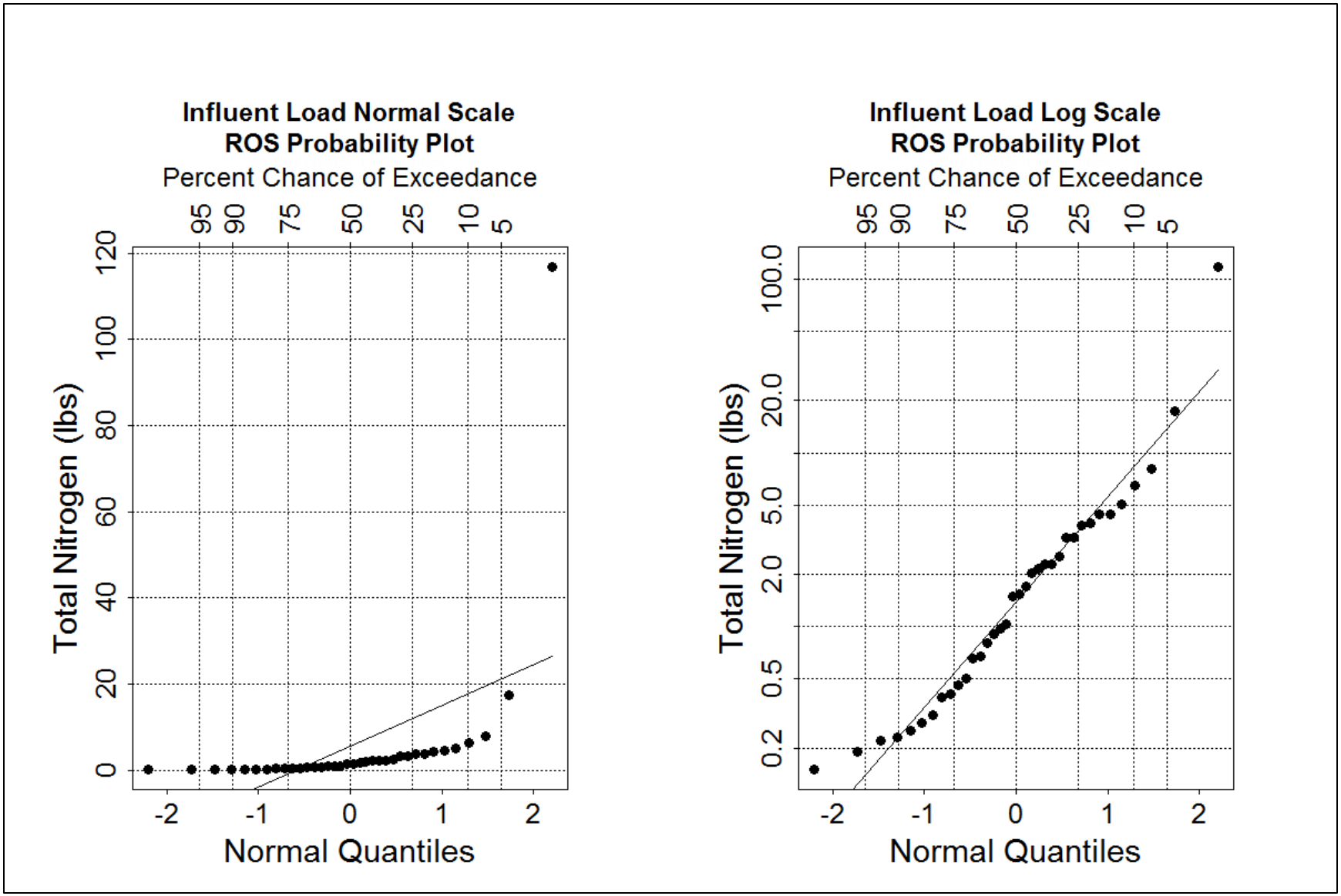

Figure E-11. Q-Q plots of influent loads for total nitrogen.

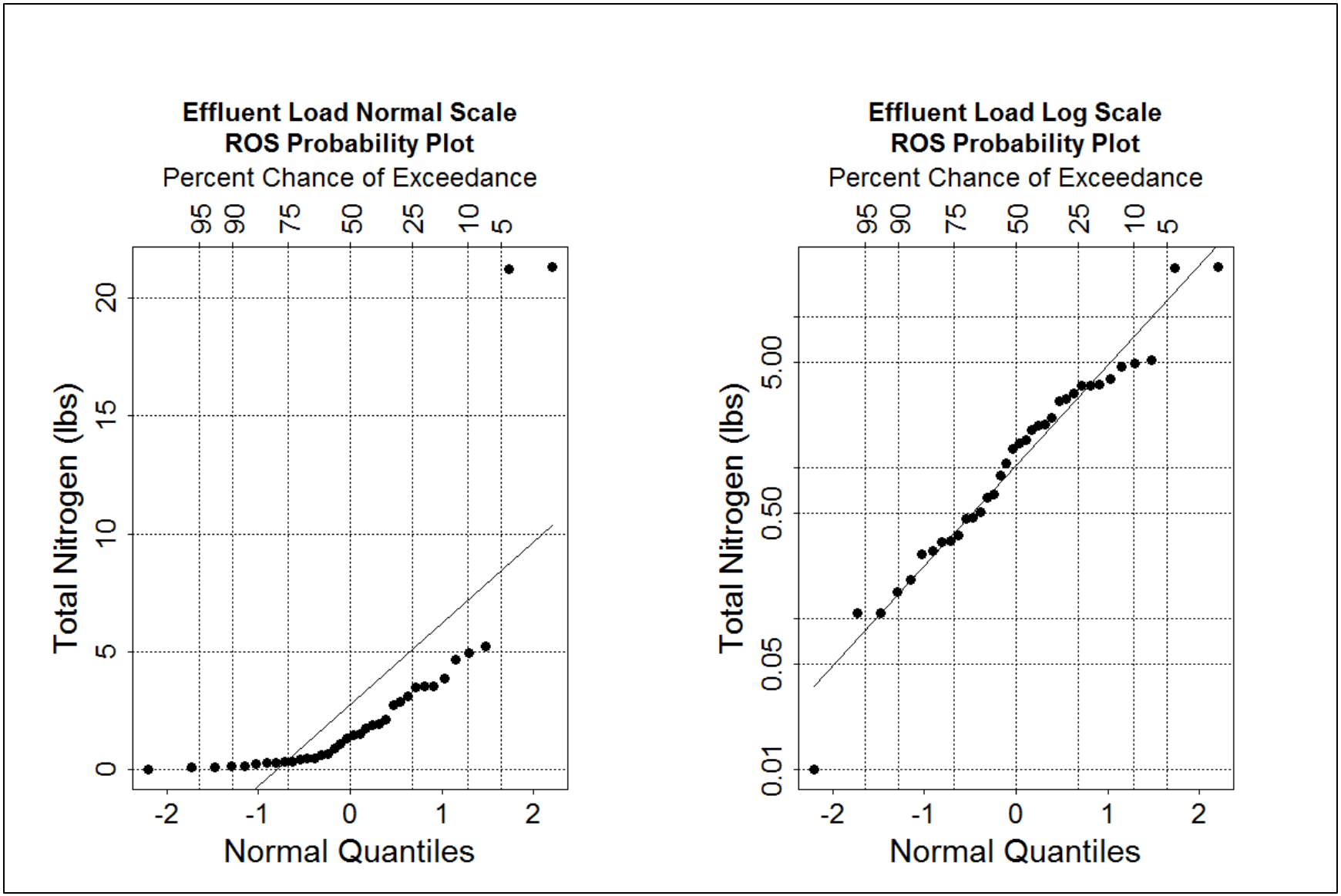

Figure E-12. Q-Q plots of effluent loads for total nitrogen.

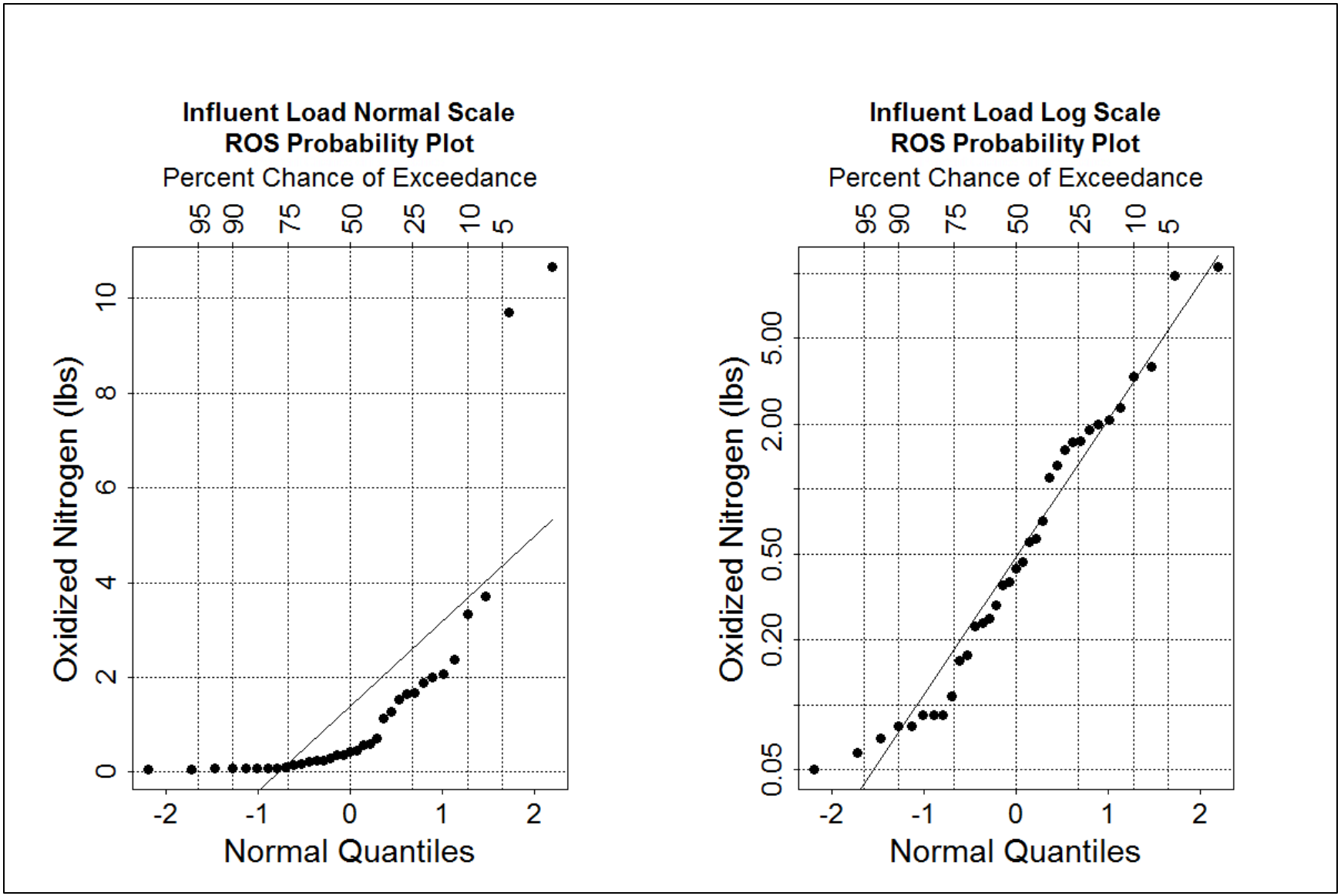

Figure E-13. Q-Q plots of influent loads for oxidized nitrogen.

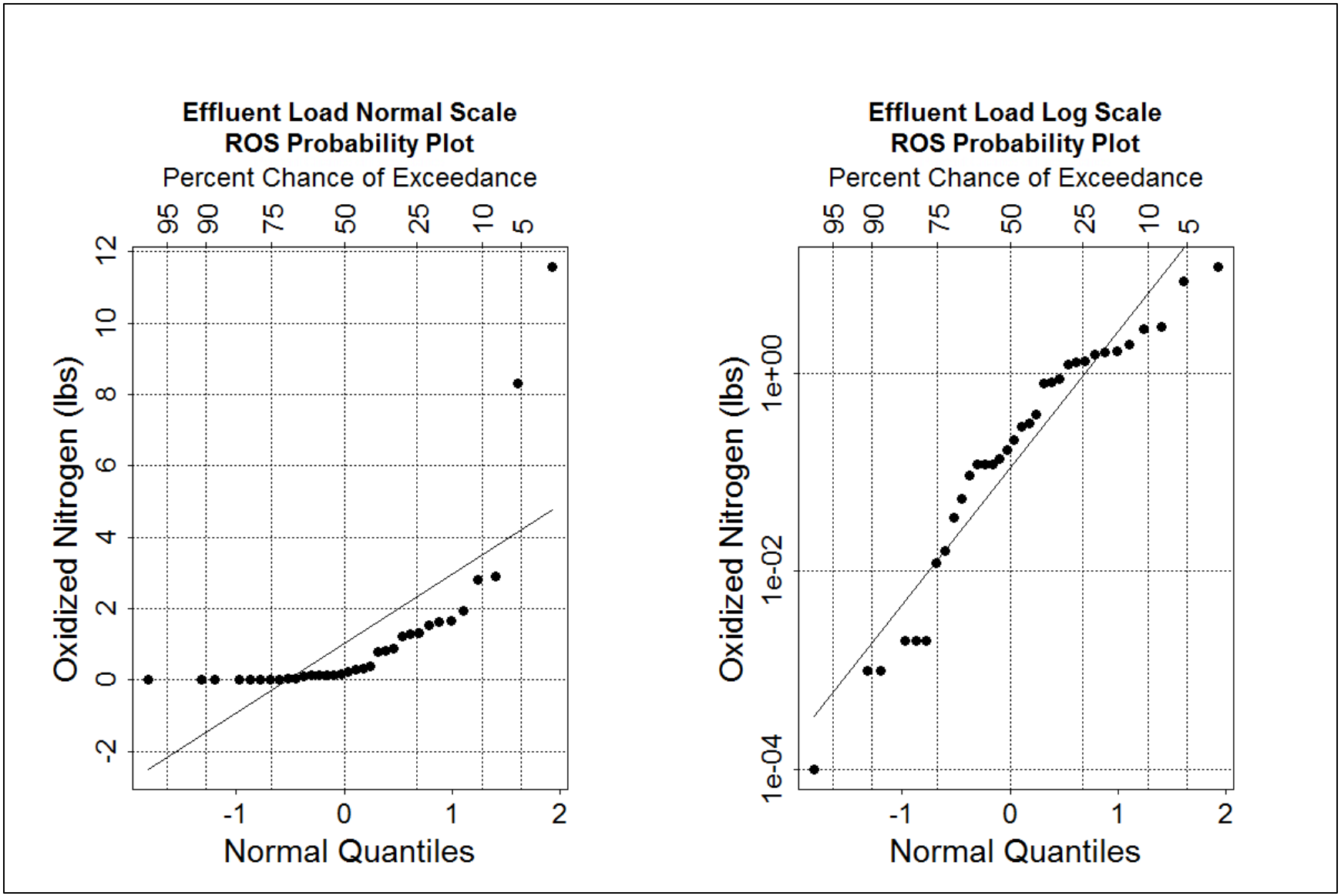

Figure E-14. Q-Q plots of effluent loads for oxidized nitrogen.

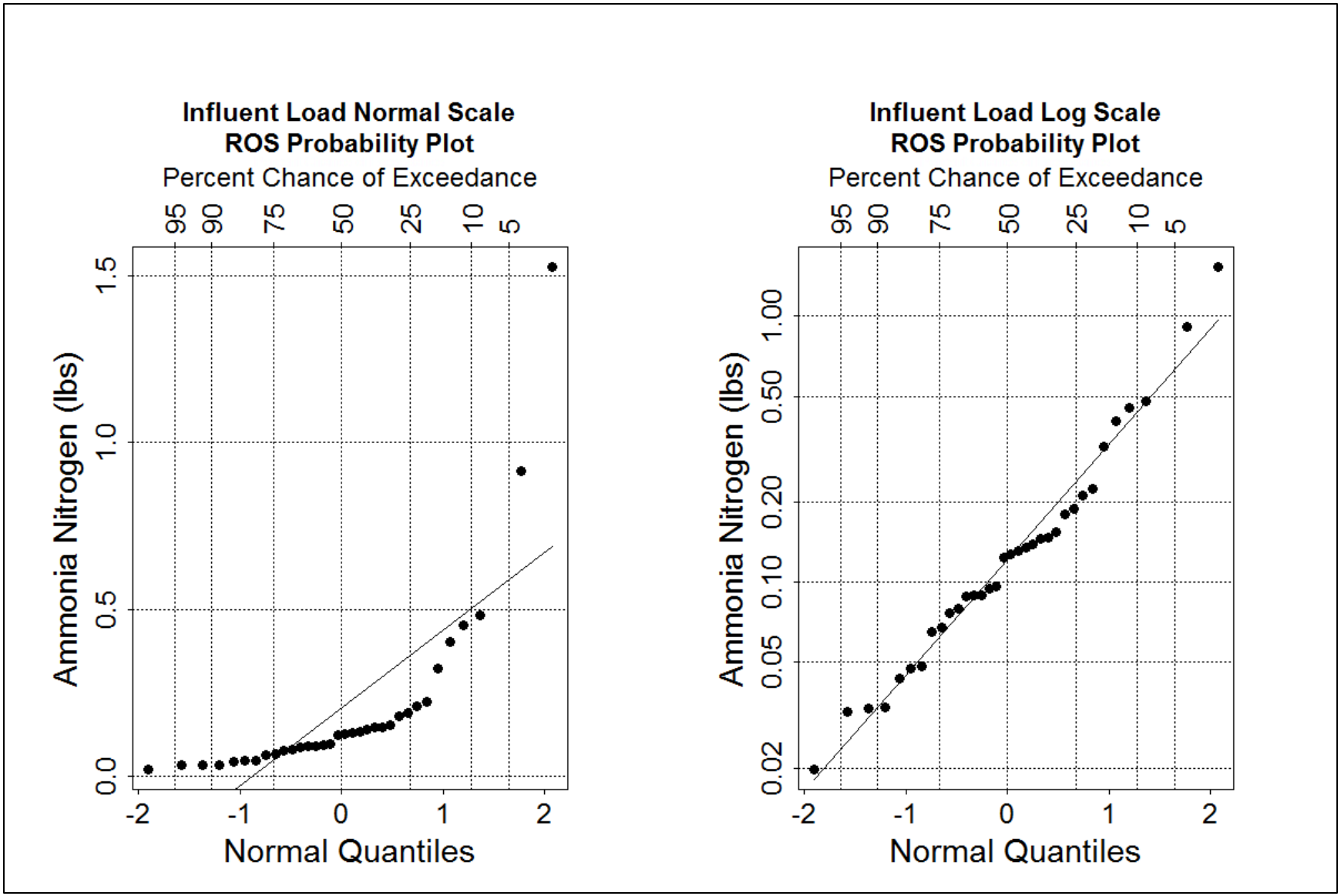

Figure E-15. Q-Q plots of influent loads for ammonia nitrogen.

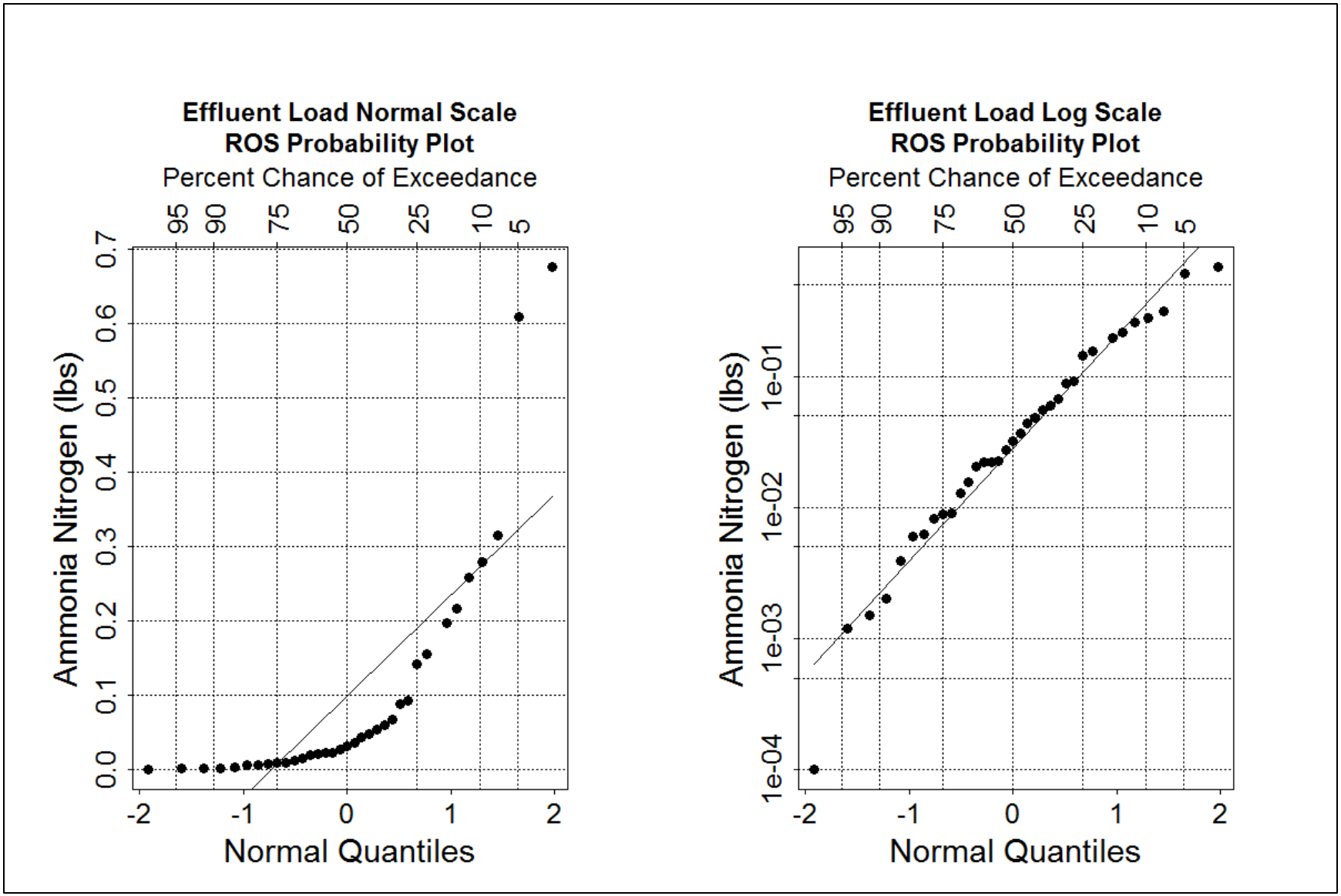

Figure E-16. Q-Q plots of effluent loads for ammonia nitrogen.

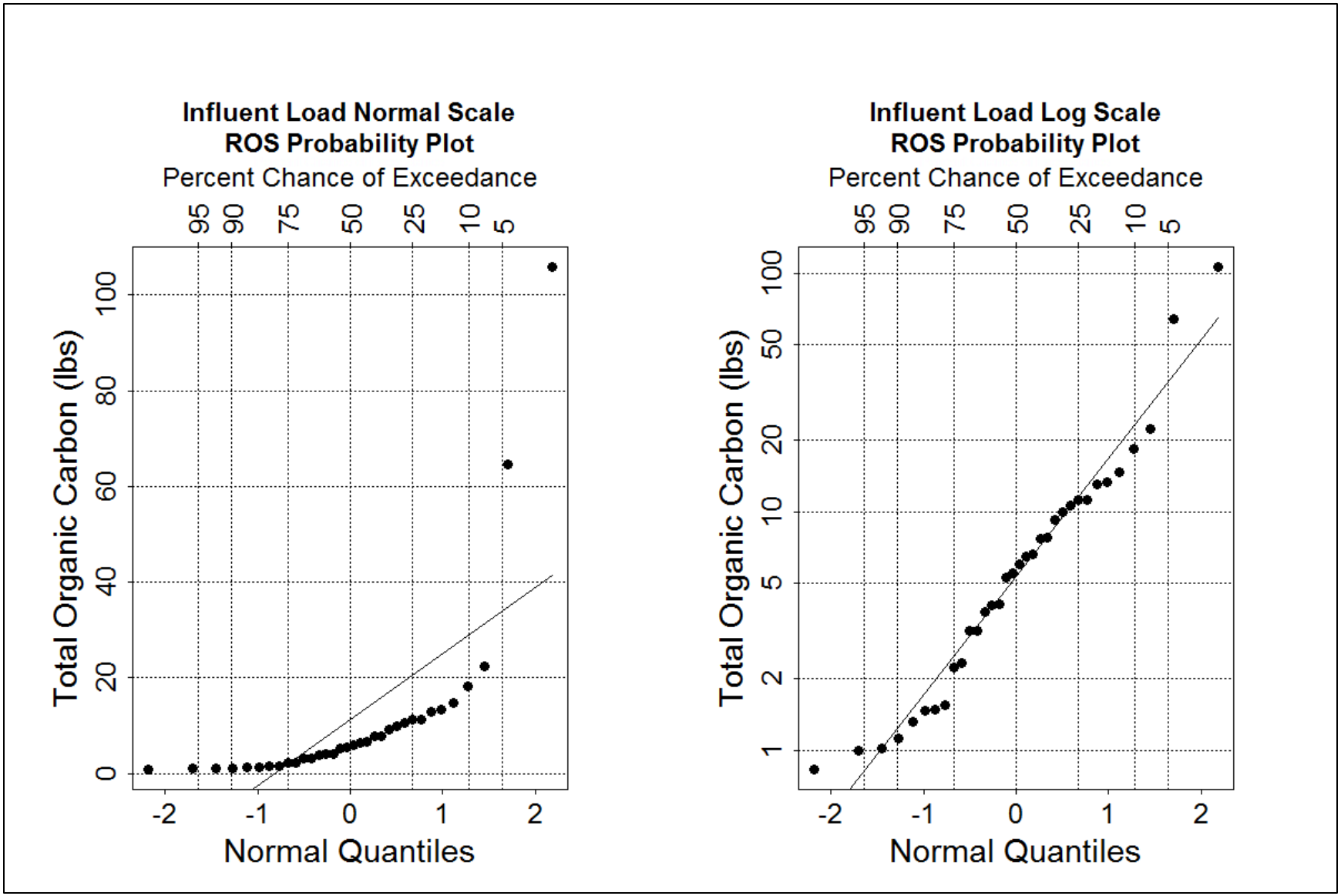

Figure E-17. Q-Q plots of influent loads for total organic carbon.

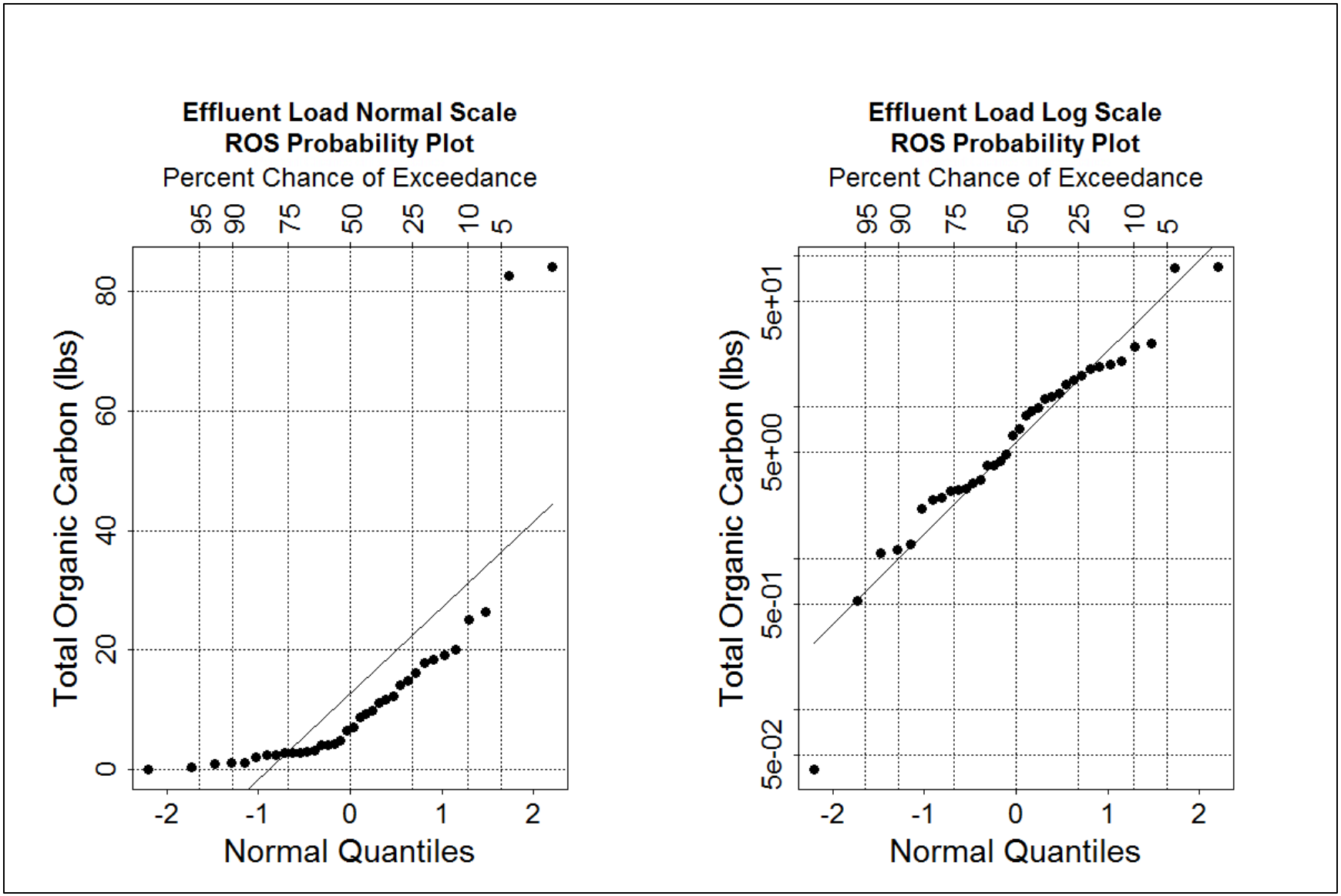

Figure E-18. Q-Q plots of effluent loads for total organic carbon.

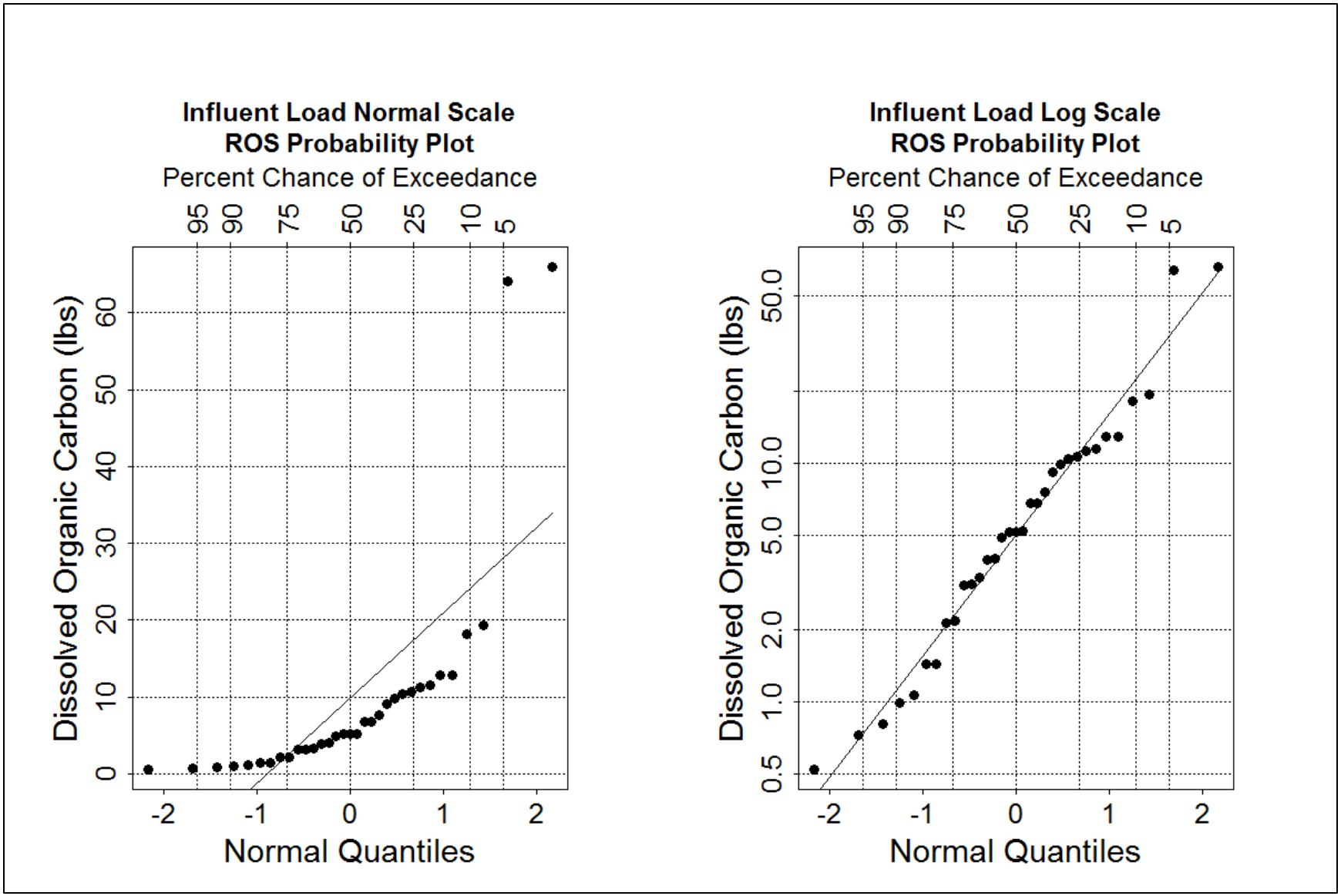

Figure E-19. Q-Q plots of influent loads for dissolved organic carbon.

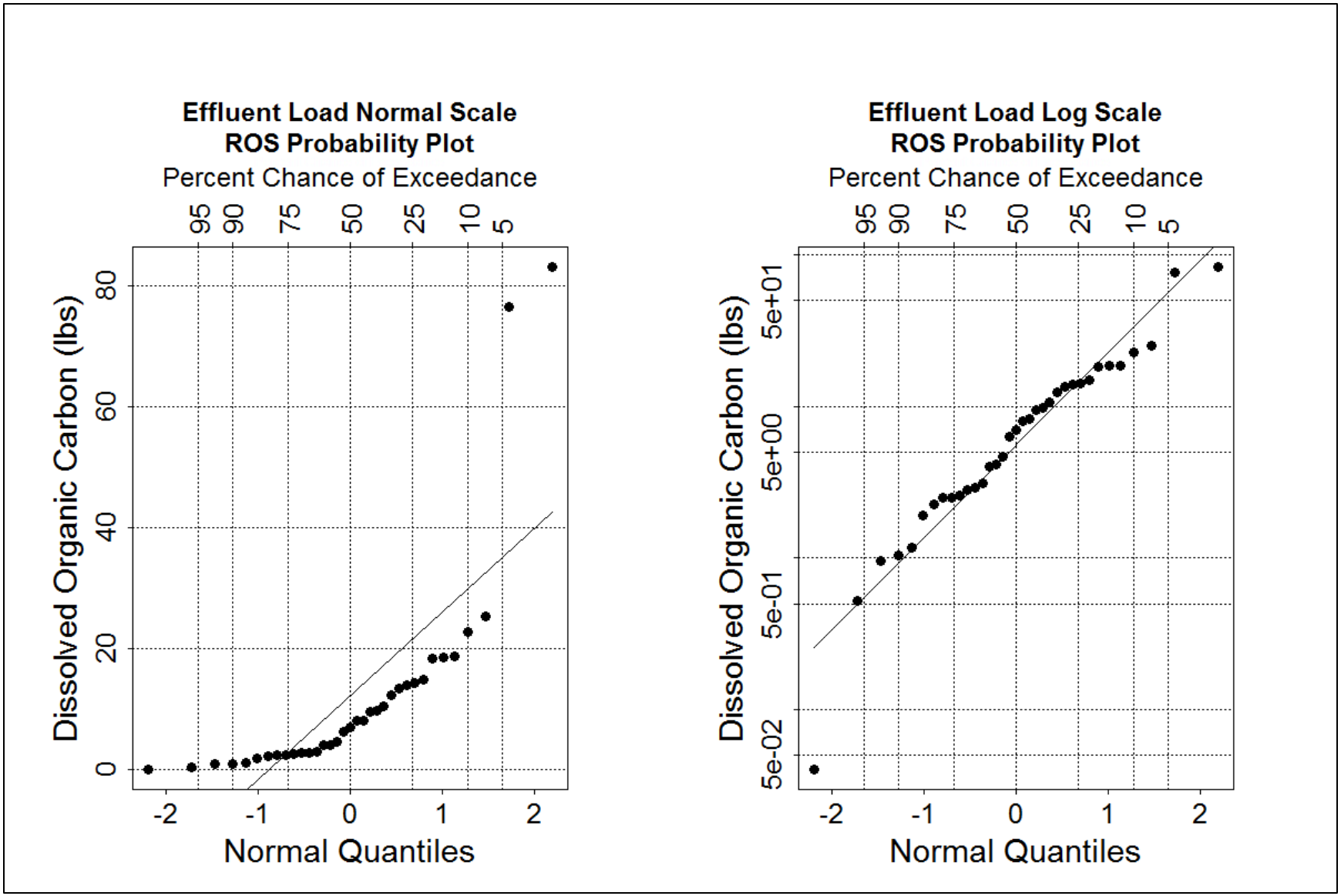

Figure E-20. Q-Q plots of effluent loads for dissolved organic carbon.

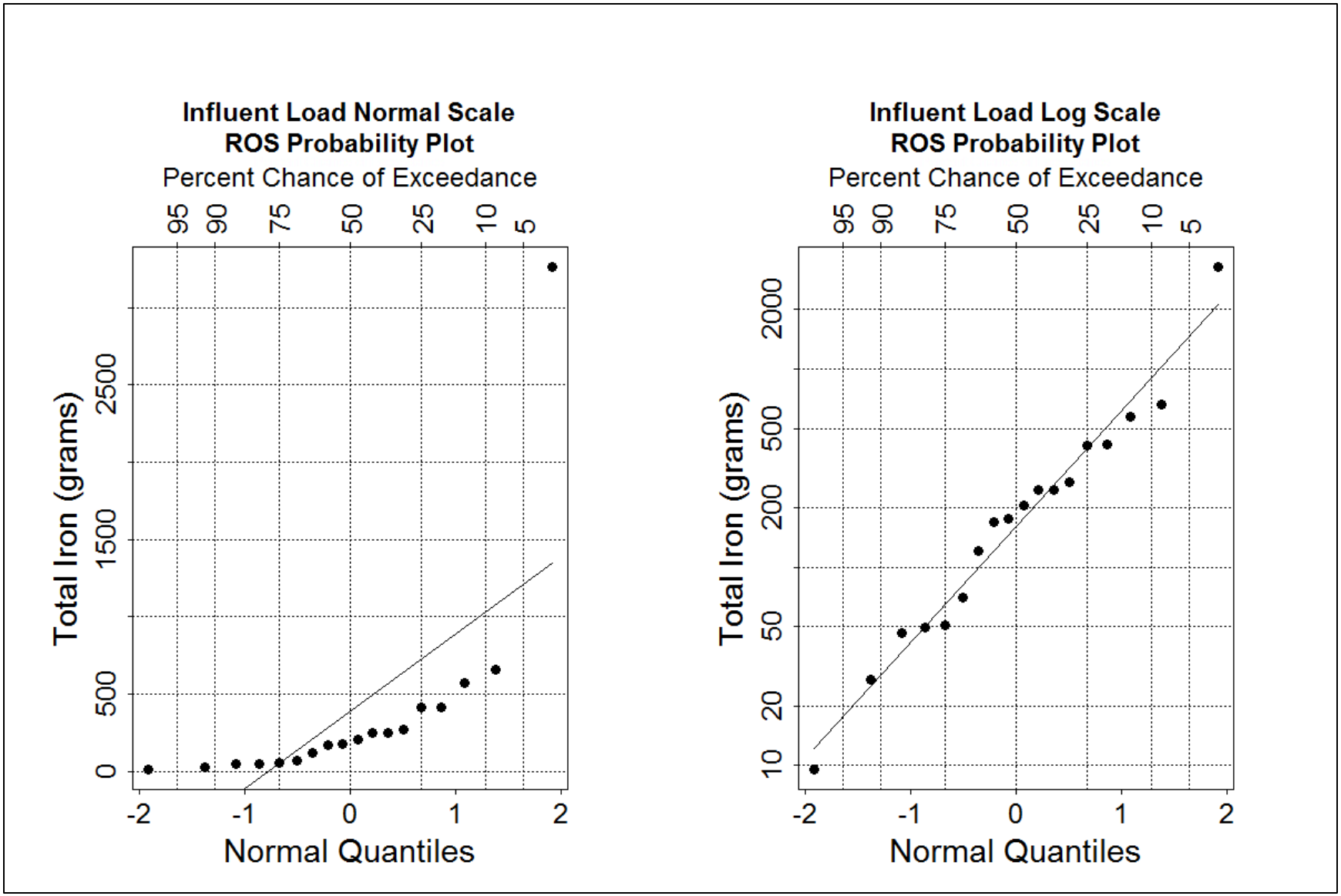

Figure E-21. Q-Q plots of influent loads for total iron.

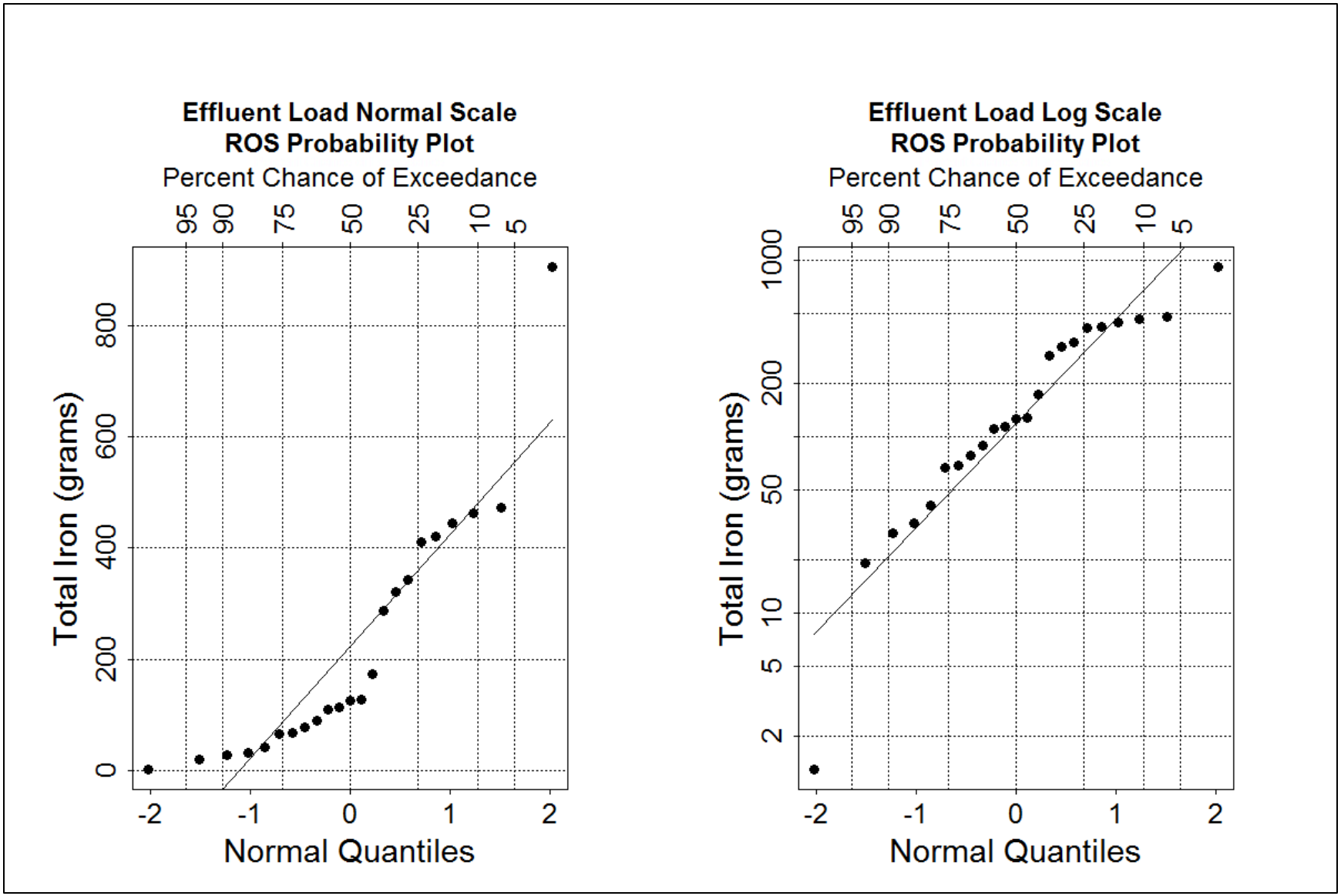

Figure E-22. Q-Q plots of effluent loads for total iron.

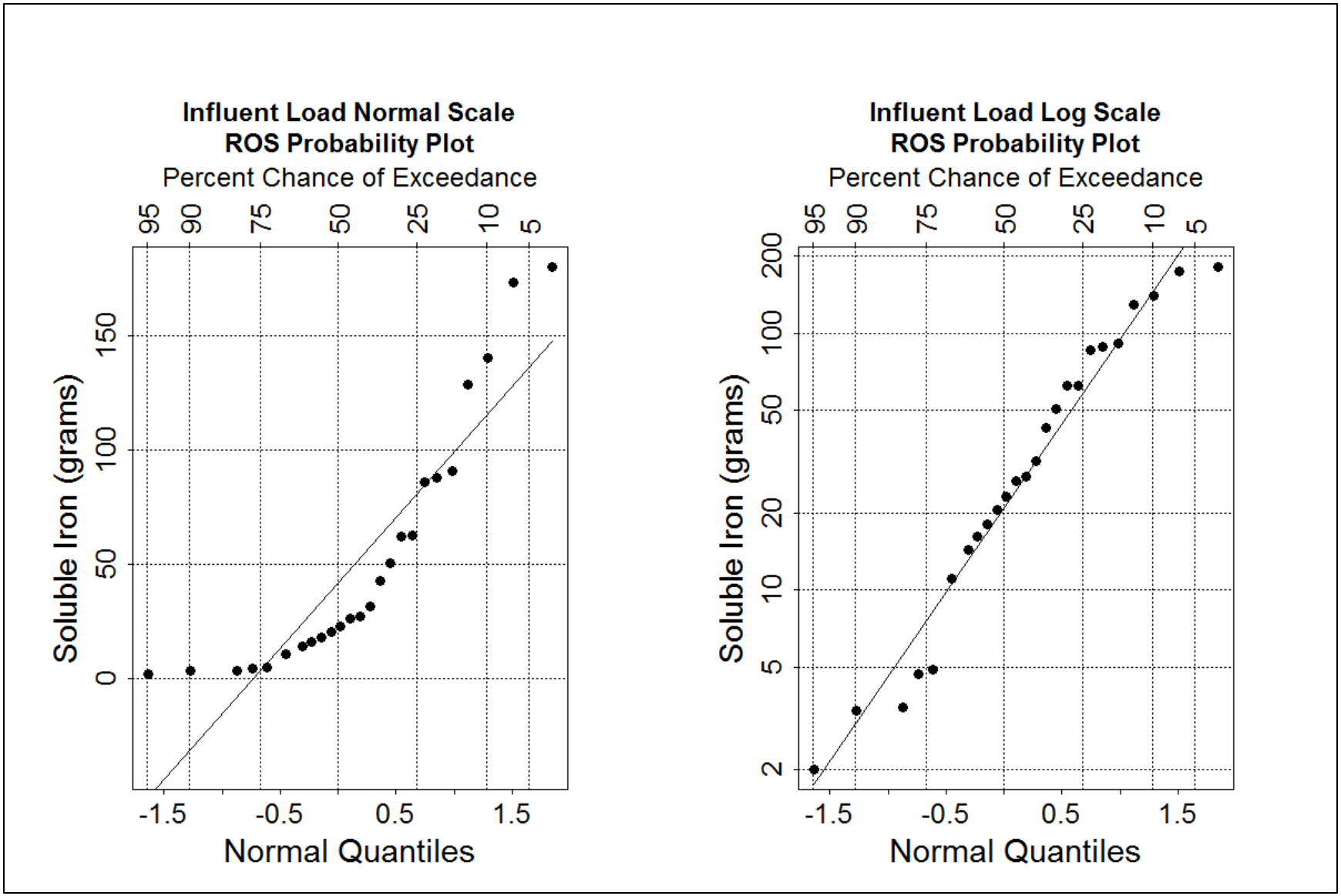

Figure E-23. Q-Q plots of influent loads for soluble iron.

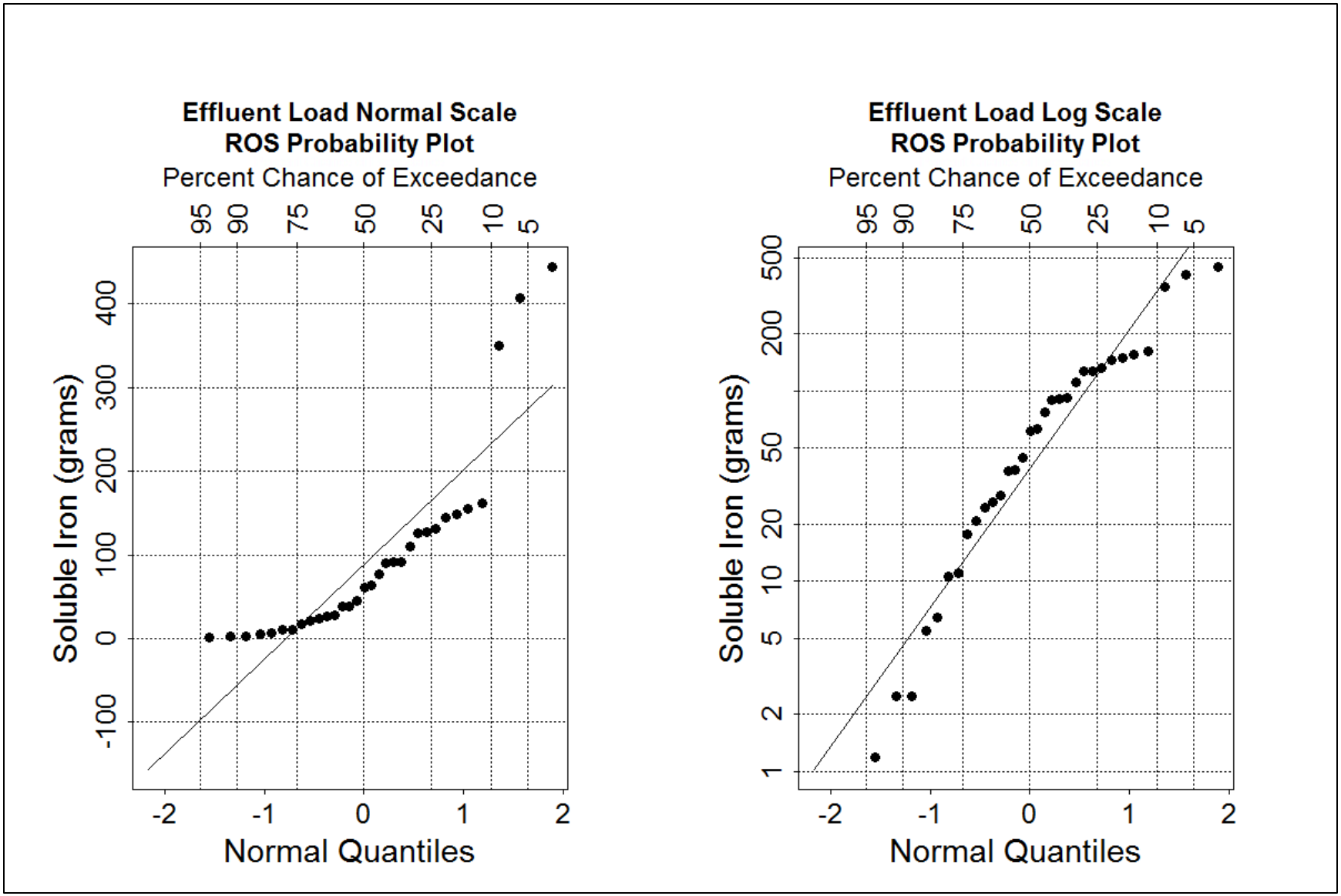

Figure E-24. Q-Q plots of effluent loads for soluble iron.

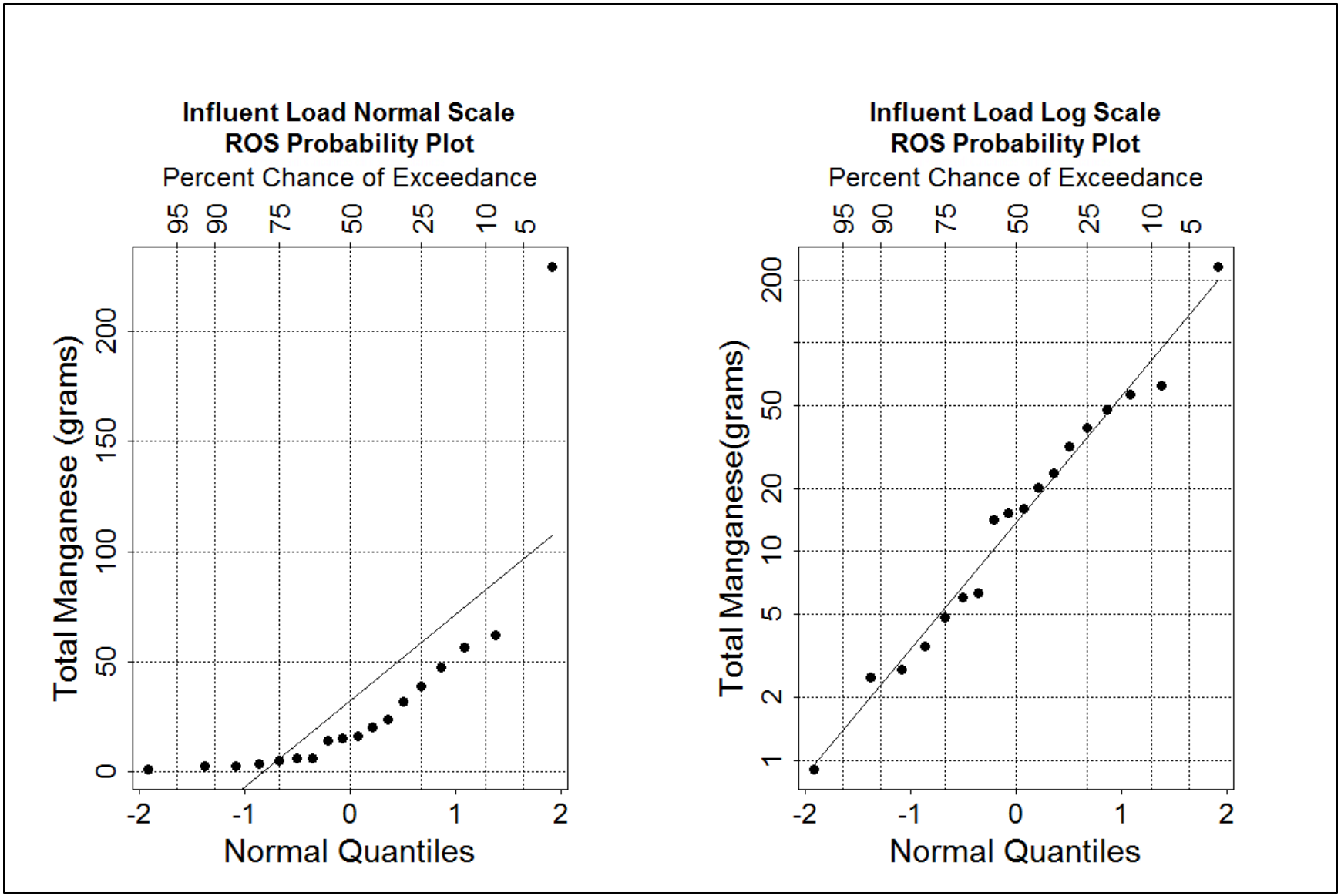

Figure E-25. Q-Q plots of influent loads for total manganese.

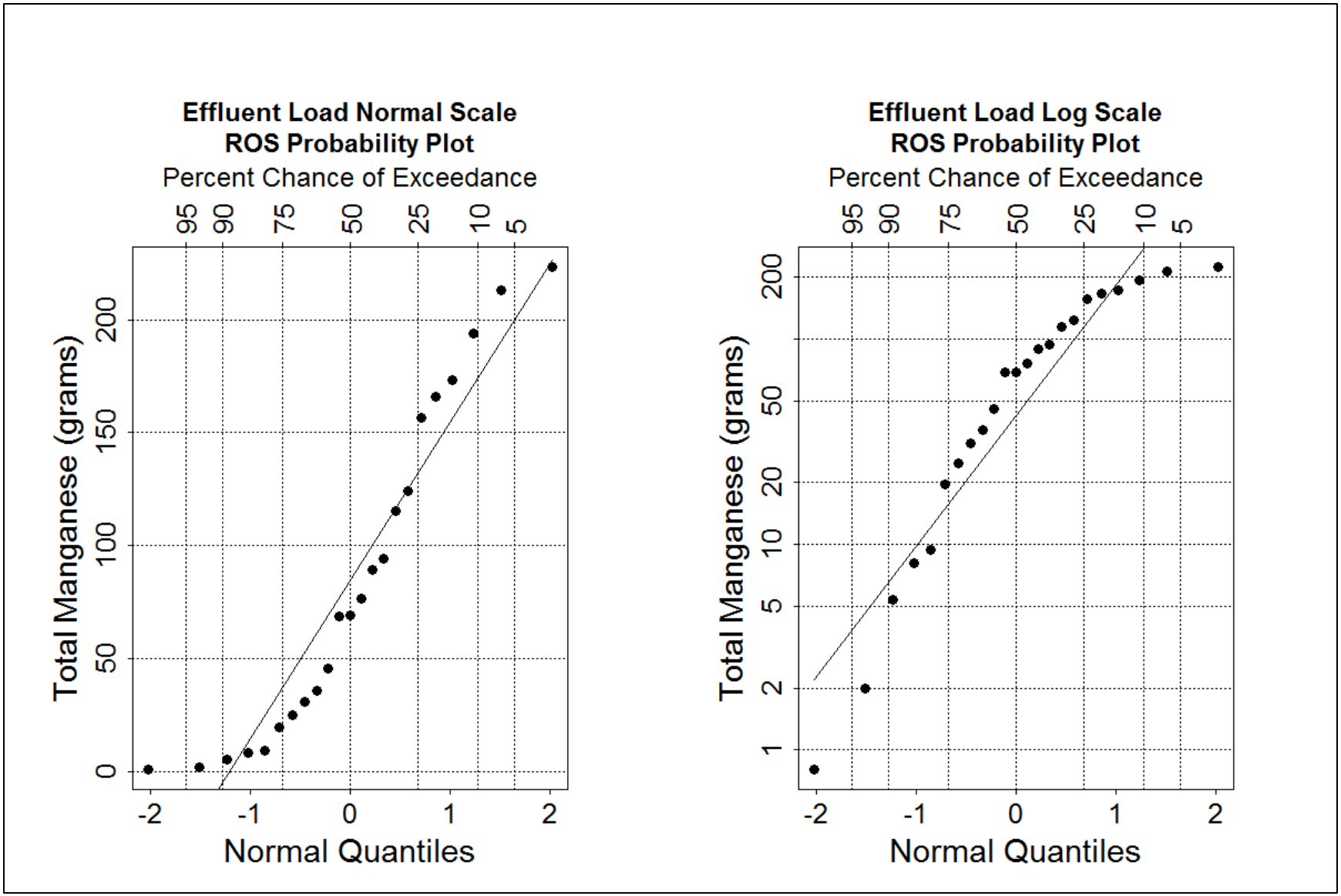

Figure E-26. Q-Q plots of influent loads for total manganese.

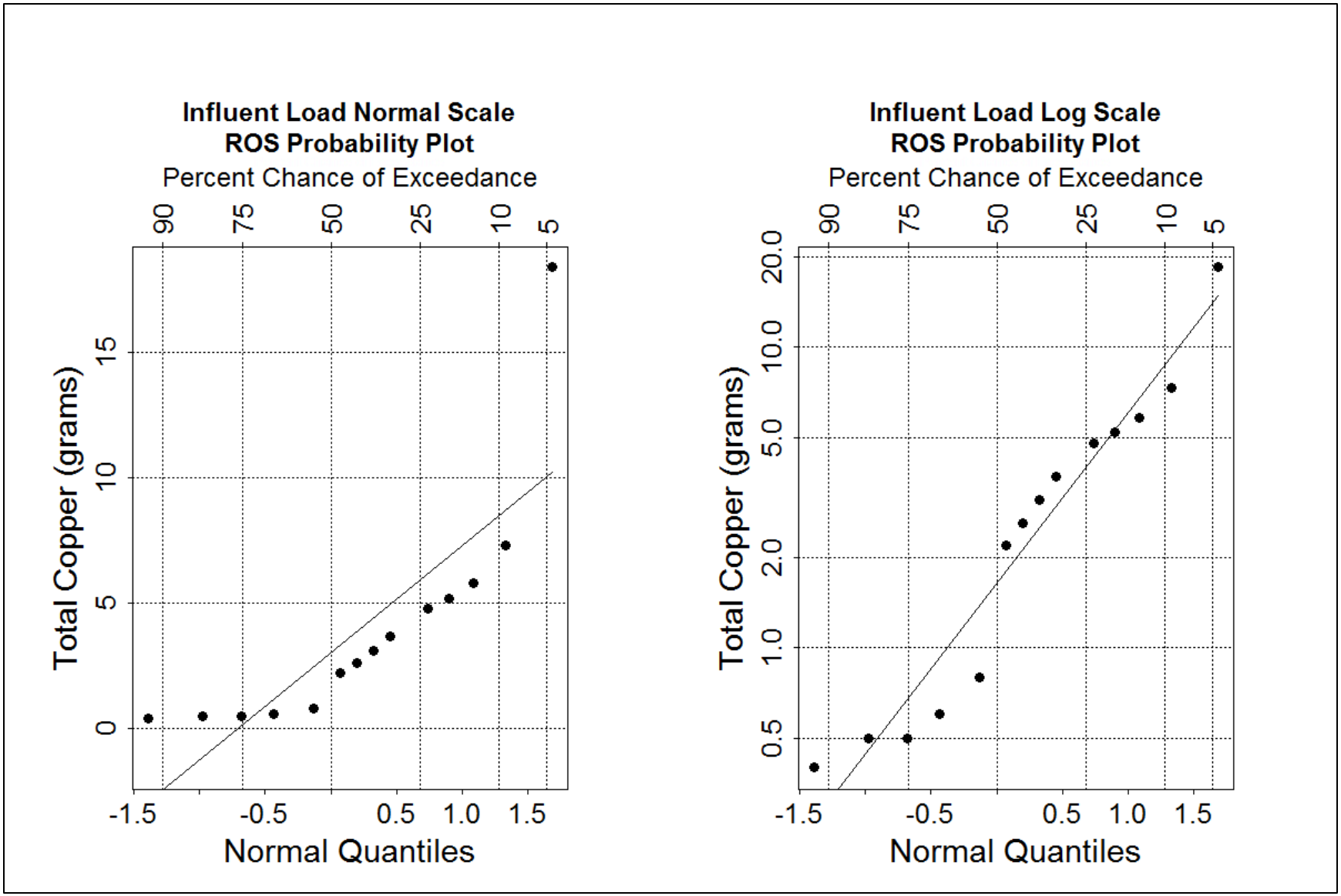

Figure E-27. Q-Q plots of influent loads for total copper.

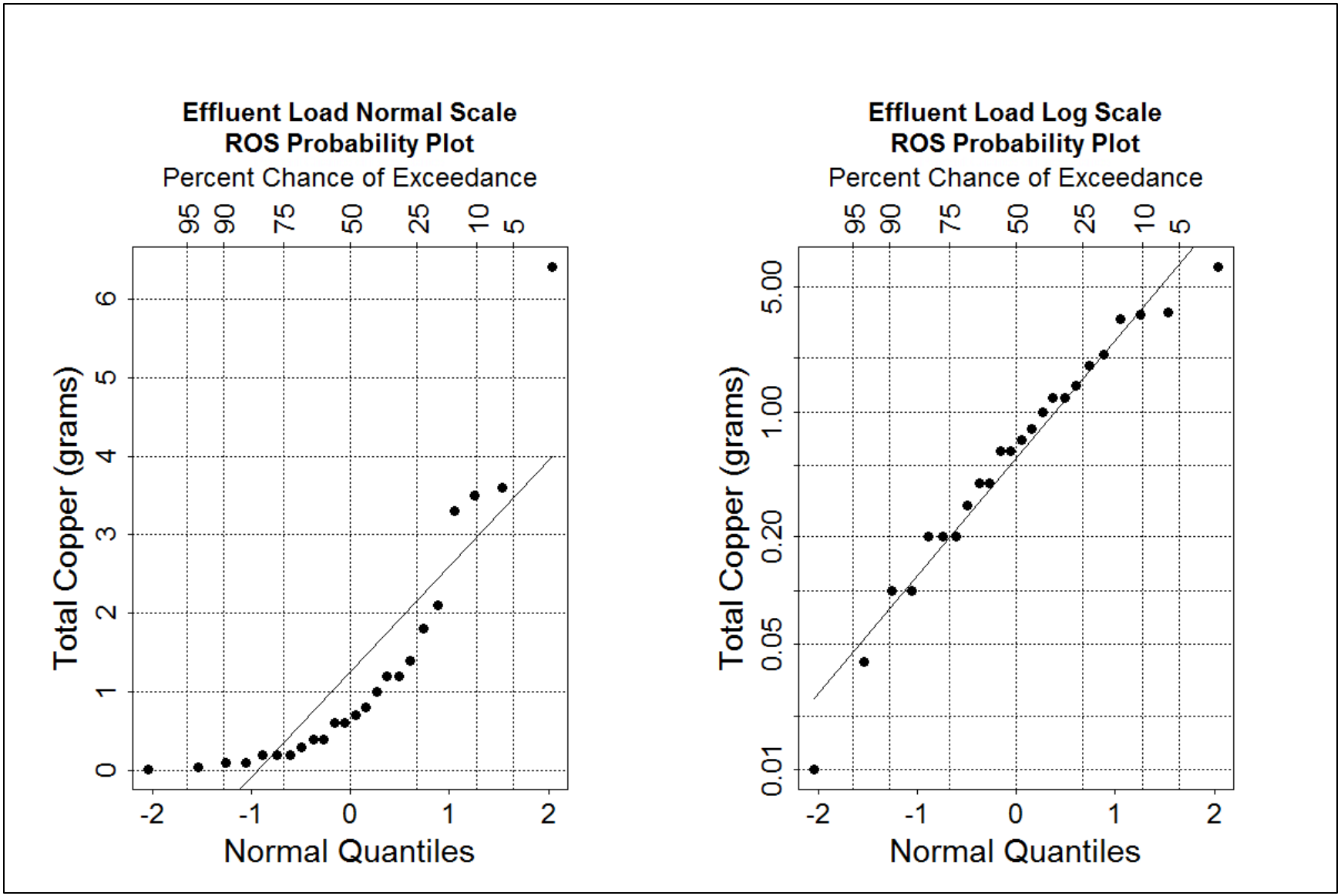

Figure E-28. Q-Q plots of effluent loads for total copper.

APPENDIX F EPA SWMM Hydrographs

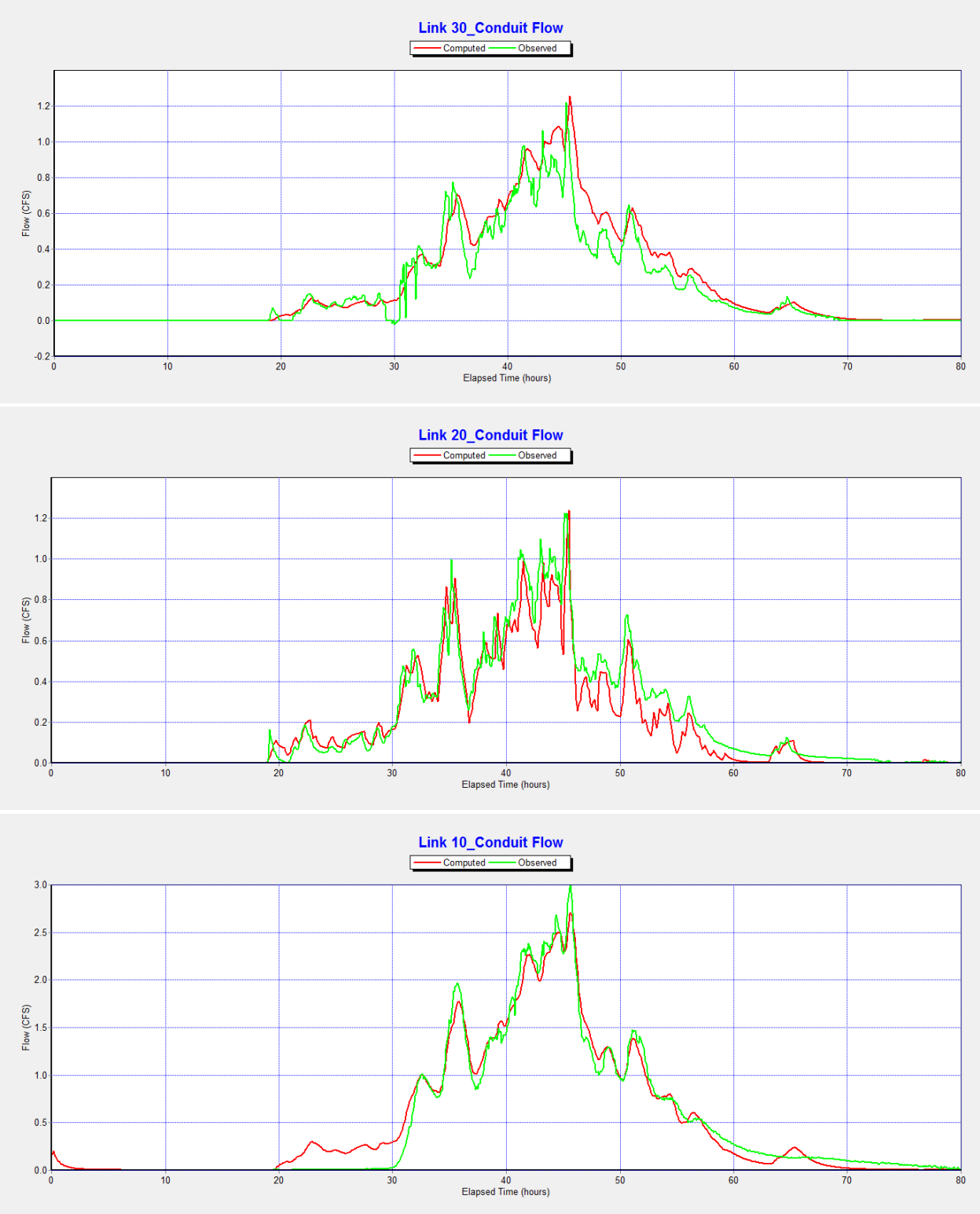

Figure F-1. EPA SWMM model hydrographs for October 28- November, 02, 2012.

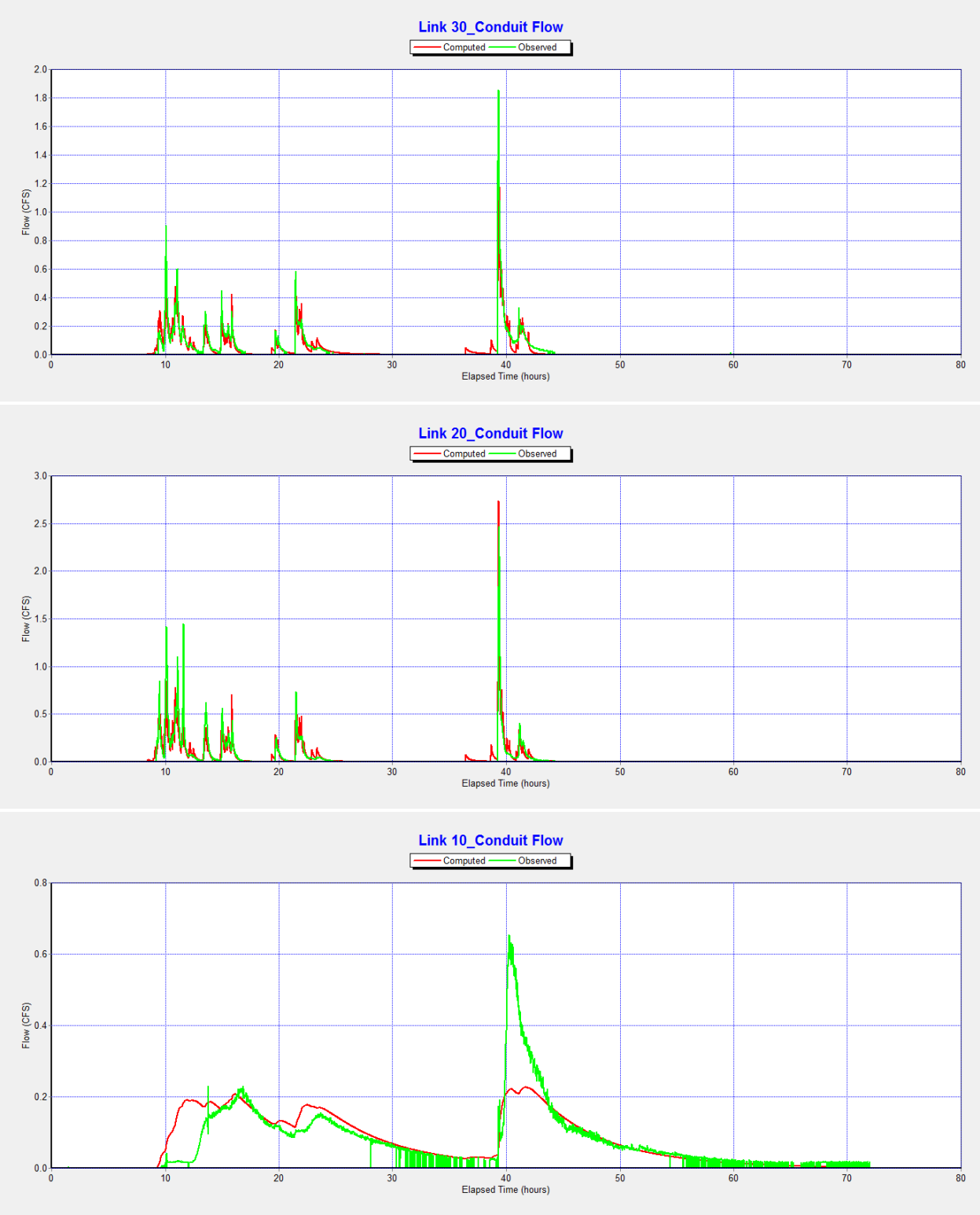

Figure F-2. EPA SWMM model hydrographs for May 07-10, 2013.

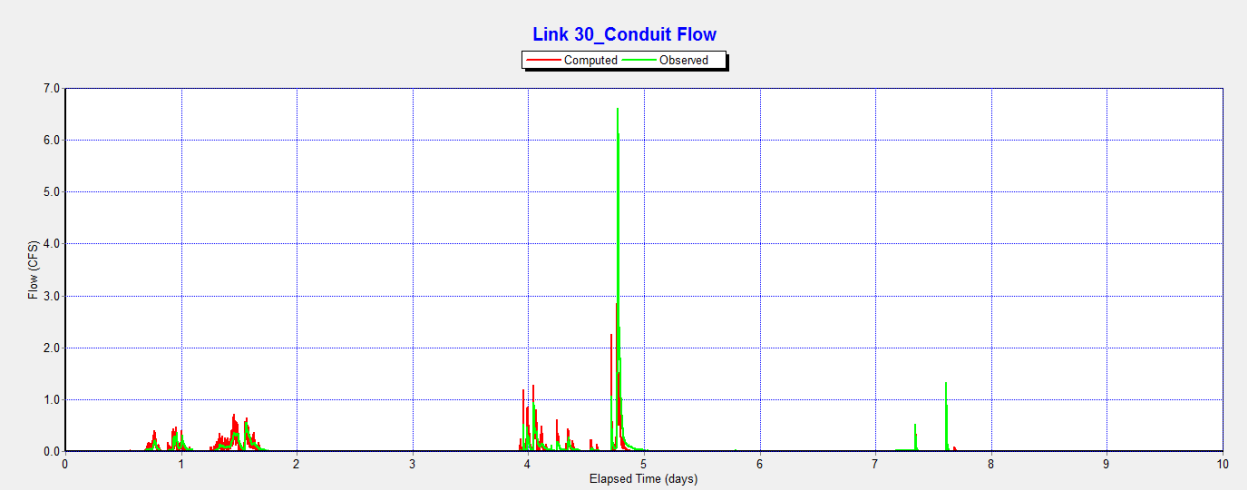

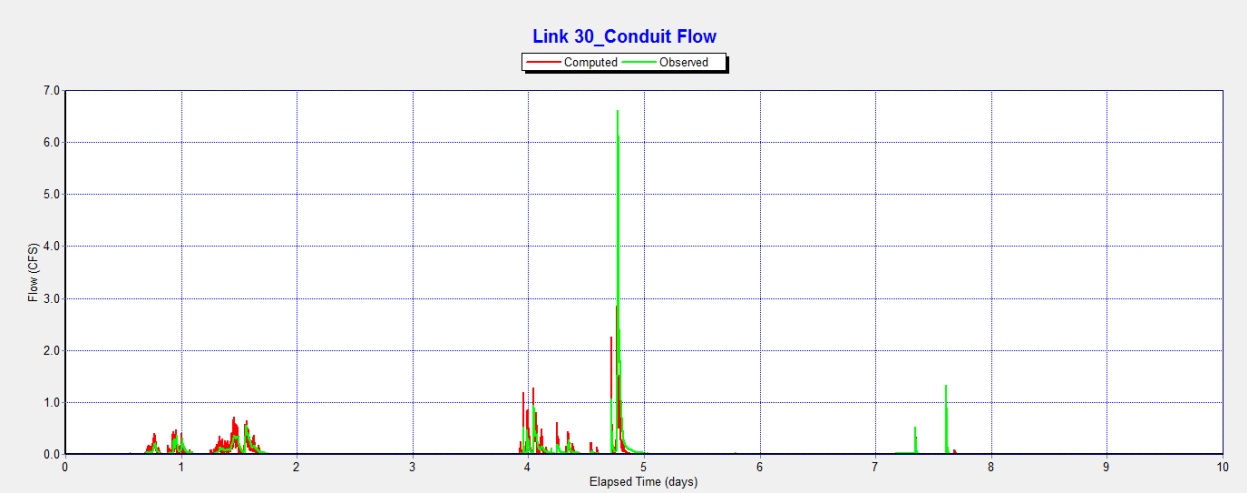

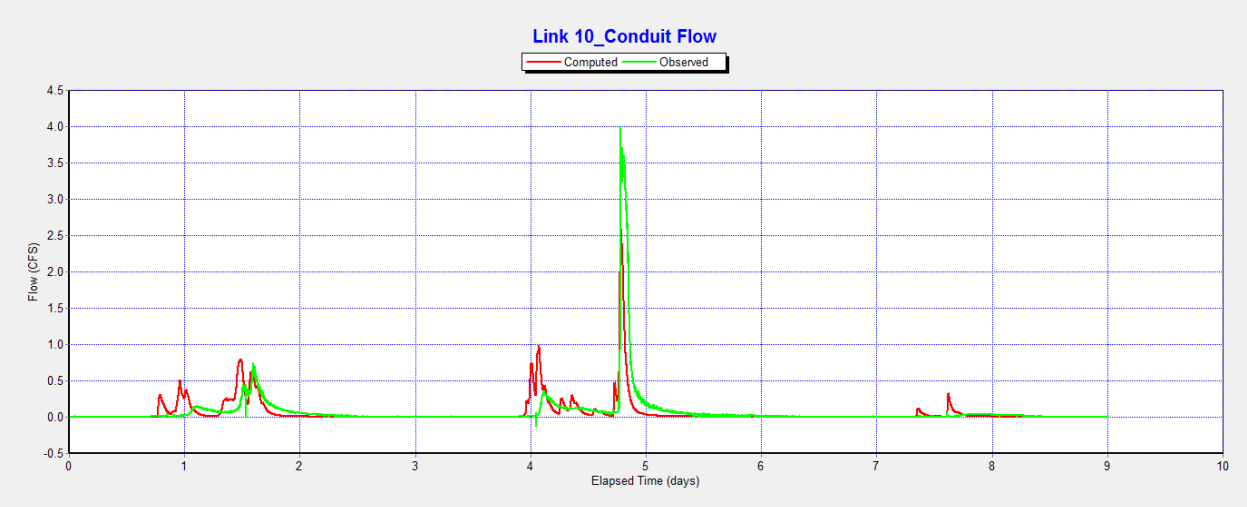

Figure F-3. EPA SWMM model hydrographs for June 06-15, 2013.

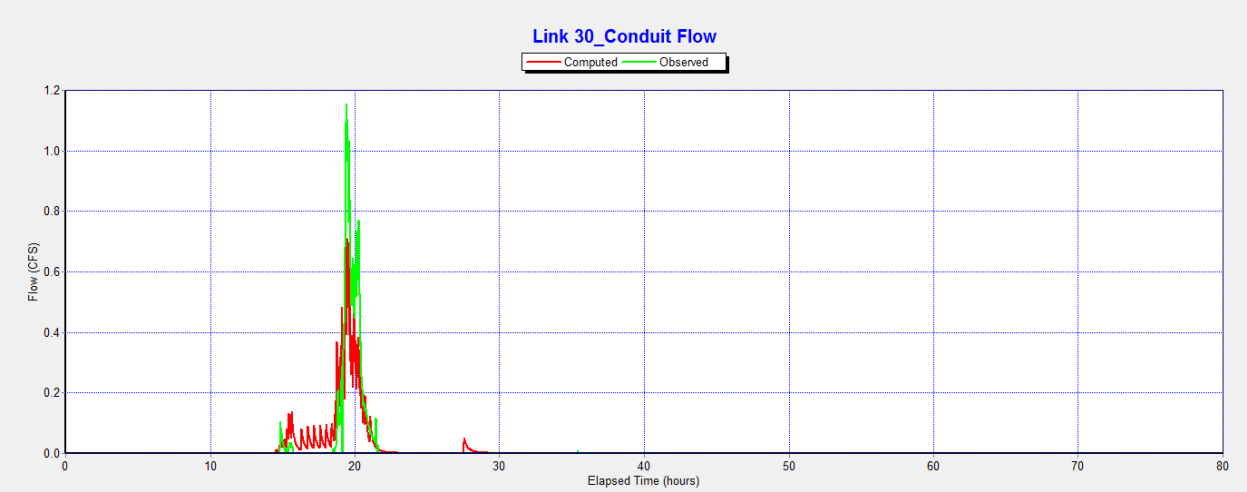

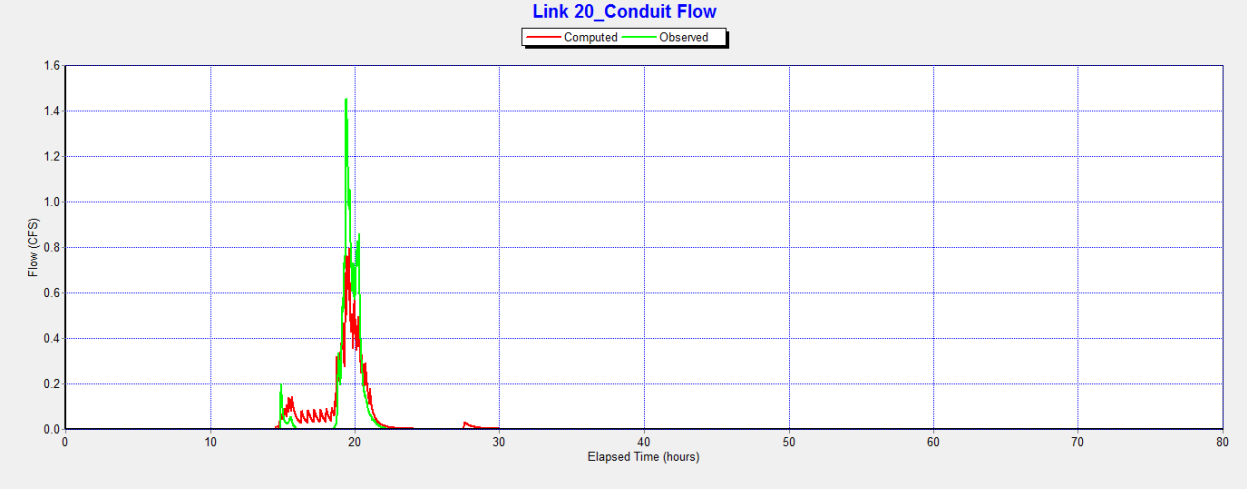

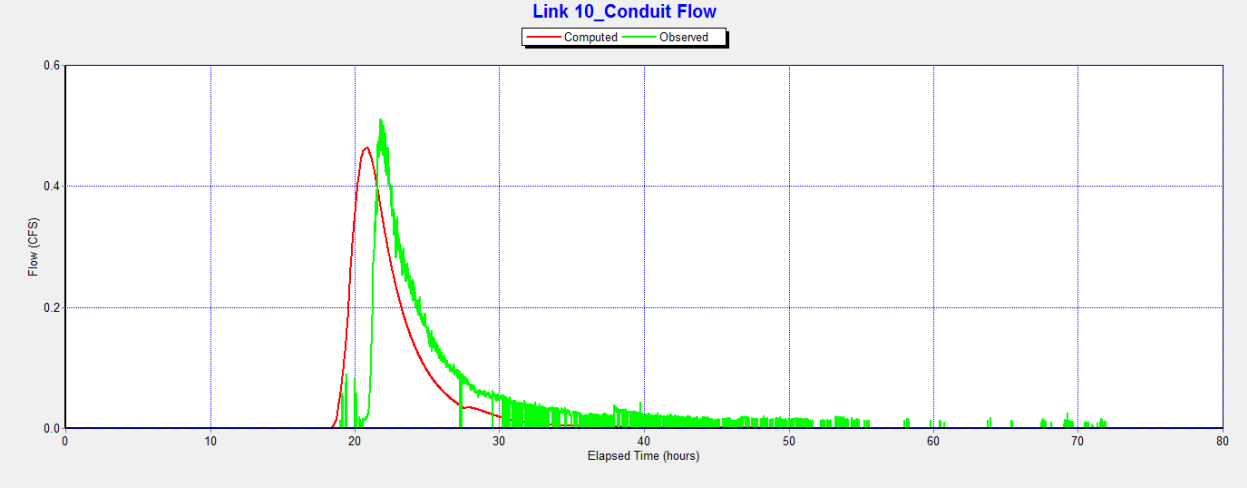

Figure F-4. EPA SWMM model hydrographs for September 21-24, 2013.